Osteology, Taxonomy, Phylogeny, and Body Shape Changes of Eocene Catostomid and Problematic Catostomid Fishes

by

Juan Liu

A thesis submitted in partial fulfillment of the requirements for the degree of

Doctor of Philosophy

in

Systematics and Evolution

Department of Biological Sciences

University of Alberta

Abstract

Extant catostomid fishes occupy diverse aquatic ecosystems and niches in North America (NA). Less than 3% of catostomid taxonomic richness, or two species, are found outside of NA in Asia. Such adjunct and unbalanced distribution pattern has been established since the late Oligocene, when catostomids disappeared from Asia and became common fishes in NA. Eocene catostomids, representing the oldest fossil records of this family, reached relatively high taxonomic richness in both NA and Asia, and thus are critical to understand evolution of catostomids.

This thesis is a study of about 3000 specimens of Eocene catostomids and problematic catostomids. Osteology of 33 extant catostomid species and 11 other otophysans are examined for comparison. Morphological characters are acquired through microscopic examination and CT scans. Cladistic analyses using the parsimony criterion are performed in PAUP 4b10 and TNT 1.5, and explored in MrBayes on XSEDE (3.2.6) using model-based Bayesian inferences through the CIPRES Science Gateway. Analyses of body shape changes and variations of Eocene catostomids are performed using the landmark-based geometric morphometric method. Body shapes of laterally preserved complete fish are captured using surface scanning and digitized with landmarks in TPS utility and TPS dig2, then analysed in MorphoJ 1.06C.

First, taxonomy is clarified for Eocene catostomids and problematic catostomids. Of the NA taxa,

Amyzon gosiutense, a previously hypothesized junior synonym of *A. aggregatum*, retains its specific status based on a suite of osteological features. "NewGenus" *brevipinne* is revised from the nominal *Amyzon brevipinne* and represents the first known shallow bodied, small sized, fluvial-sediment derived, and loach-like catostomid genus. Of the Asian taxa, *Jianghanichthys hubeiensis*, which was firstly assigned to *Osteochilus* of Cyprinidae and later Catostomidae, is suggested to be a stem cypriniform based on osteological comparison and phylogenetic analysis. The first fossil family of Cypriniformes, Jianghanichthyidae, is erected to contain the species. Additional problematic catostomids, which were described as Eocene *Osteochilus* from south China, are assigned to Jianghanichthyidae and combined into two species: *Jianghanichthys sanshuiensis* and *J. linliensis*. New species *Amyzon kishenehnicum* and *Jianghanichthys huachongensis* are described from NA and Asia, respectively.

Second, the systematic position and intrarelationships of Eocene catostomids were largely unresolved before this study, although they are critical to understand the evolution of the family and Cypriniformes. Three sets of phylogenetic analyses based on different character sets are performed. The first set vouches that *Jianghanichthys* doesn't belong to any known cypriniform family, but is a basal clade. The second set finds that *Amyzon* is a basal clade of Catostomidae instead of a member in the Ictiobinae. The third suite of analyses is optimized by maximally utilizing Eocene species and creating an osteological character list. These analyses suggest that most Eocene catostomids (except *Plesiomyxocyprinus*) were stem taxa of Catostomidae, and

"NewGenus" *brevipinne* represented the most basal clade. Also, known species of *Amyzon* are not monophyletic, with Asian *A. hunanense* and NA *A. commune* being distinctive basal clades. Another Asian genus *Plesiomyxocyprinus* is sister to all extant catostomids except ictiobines.

Third, Eocene catostomids possess similar general appearances and have highly overlapped meristic and morphometric characters, which caused had taxonomic confusion. Quantitative anatomical comparison in this study (geometric morphometrics) finds significant body shape differences between jianghanichthyids and sampled catostomids, *A. aggregatum* versus *A. gosiutense*, and *A. aggregatum* versus *A. kishenehnicum*. Regression analysis on Procrustes coordinates and centroid sizes shows that allometry does not significantly affect body shapes differences among well-sampled catostomids and jianghanichthyids. Phylogenetically mapped morphospace indicates evolutionary trajectories and trends of body shape changes are congruent to phylogenetic branches of Eocene catostomids and jianghanichthyids.

In sum, all unambiguous oldest cypriniforms are included for discussion (Catostomidae, and Jianghanichthyidae of this study plus Cyprinidae). The only area that all oldest cypriniforms are found is south Asia, which suggests that area is the hotspot of origin and cladogenesis of Cypriniformes. Central Asia, including north China, Mongolia, Kazakhstan, and Fareast Russia, where the last remains of catostomid fossils in Asia recorded cyprinids' dispersal route, is a gateway leading to the dispersal events eastward to NA through Beringia and westward to

Europe. The mosaic distribution of the Asian taxa across the phylogeny suggests multiple episodes of intercontinental dispersals during the early evolution of catostomids, probably through the freshwater connections of Beringia before the middle Eocene.

Preface

This thesis contains published journal articles. Except the introduction and conclusion chapters, Chapters 2 and 3 are published, and Chapters 4 through 7 are original research being prepared for submission to peer-reviewed journals. In addition, five refereed conference abstracts and presentations have derived from projects of this thesis.

Chapter 2 of this thesis has been published as *Liu, J., M.-M. Chang, M. V. H. Wilson, and A. M. Murray. 2015. A new family of Cypriniformes (Teleostei, Ostariophysi) based on a redescription of †*Jianghanichthys hubeiensis *(Lei, 1977) from the Eocene Yangxi Formation of China. Journal of Vertebrate Paleontology e1004073:23*. I collected the data, designed and performed the analyses, and wrote the paper. Wilson co-designed and discussed the analyses. Chang CT-scanned the specimen. Wilson and Chang provided funding support. All three co-authors (Chang, Wilson, and Murray) provided supervisory and editorial supports.

Chapter 3 has been published as *Liu, J., M. V. H. Wilson, and A. M. Murray. 2016. A new Catostomid fish (Ostariophysi, Cypriniformes) from the Eocene Kishenehn Formation and remarks on the North American species of †*Amyzon *Cope. Journal of Paleontology. FirstView: 1-17*. I was responsible for the data collection and analysis, as well as the manuscript

composition. Wilson helped with collecting data, co-designed analysis and provided funding support. The co-authors (Wilson and Murray) collected fossil materials and provided supervisory, editorial, and laboratory equipment supports.

The following published abstracts and presentations are derived from or partially from the thesis:

Liu J. and Mark V. H. Wilson, 2016. Eocene fossil record of catostomids (Teleostei: Cypriniformes) from North America and discovery of the first loach-like catostomid. Supplement to the online Journal of Vertebrate Paleontology. 76th Annual Meeting Society of Vertebrate Paleontology, Program and Abstracts. Salt Lake City, Oct., 2016: 175. (oral presentation)

Liu J., Mark V. H. Wilson, and Alison M. Murray, 2015. Growth rates during ontogeny of early Eocene catostomids from British Columbia, Canada. Supplement to the online Journal of Vertebrate Paleontology. 75th Annual Meeting Society of Vertebrate Paleontology, Program and Abstracts. Dallas, Oct., 2015: 165. (oral presentation)

Liu J., Mark V. H. Wilson, Alison M. Murray, and Z. Jack Tseng, 2014. A new sucker (Teleostei, Catostomidae) from the Eocene Kishenehn Formation of Montana and the systematic position of Amyzon*. Supplement to the online Journal of Vertebrate Paleontology. 74th Annual Meeting Society of Vertebrate Paleontology, Program and Abstracts. Berlin, Nov.,*

2014: 169. (poster presentation)

Liu J., M. V. H. Wilson, and A. M. Murray, 2013. North American Eocene suckers and their implications for the systematics of Catostomidae (Ostariophysi, Cypriniformes). Supplement to the online Journal of Vertebrate Paleontology. 73rd Annual Meeting Society of Vertebrate Paleontology, Program and Abstracts. Los Angeles, Oct., 2013: 163. (poster presentation)

Liu J., Z. J. Tseng, M. V. H. Wilson, and A. M. Murray, 2012. Body shape differences between North American and Asian fossil catostomids and ontogenetic change in early cypriniforms. Supplement to the online Journal of Vertebrate Paleontology. 72nd Annual Meeting Society of Vertebrate Paleontology, Program and Abstracts. Raleigh, Oct., 2012: 128. (poster presentation)

Liu J., M. V. H. Wilson, M-m. Chang, and A. M. Murray, 2011. The early diversity of non-cyprinid cypriniforms (Ostariophysi, Cypriniformes) in the Eocene of East Asia and North America. 71st Annual Meeting Society of Vertebrate Paleontology, Program and Abstracts. Las Vegas, Nov., 2011: 145. (oral presentation)

Liu J., M-m. Chang, M. V. H. Wilson, 2010. The fossil catostomid Jianghanichthys *from China and implications for the evolution of basal catostomids (Cypriniformes, Actinopterygii). 70th*

Anniversary Meeting Society of Vertebrate Paleontology, Program and Abstracts. Pittsburgh,

Oct., 2010: 123A. (oral presentation)

Acknowledgements

First of all, I would like to express my deepest gratitude to my PhD advisor, Dr. Mark V. H. Wilson, who guided me through research training, curriculum study, language barrier, and culture shock of living in a different country. His patience, kindness, generosity, and immense knowledge have continuously supported my research, study, and enthusiasm in ichthyology. I am very fortunate to have such a great advisor who gave me freedom to explore on my own but also generously advised me whenever I needed guidance.

My sincere gratitude also goes to my PhD co-advisor Dr. Alison M. Murray for her insightful guidance, constructive comments, and continuous support and encouragement. She is one of the most approachable people in the world, and she always responds request and answers questions sooner than anyone. She is my role model for woman scientists in this fast-paced world.

I am deeply grateful to Dr. Mee-Mann Chang, who was my MSc advisor but also a lifetime mentor. She helped with specimen arrangements, CT scan, and fieldwork plan for this PhD research. She is an exemplary mentor who always sets high standards and achieves the goals. Her thoughtful advice and continuous encouragement has also contributed to the direction and attitude of my study.

I am indebted to all those professors who have served on various committees for my PhD program. My supervisory committee member Dr. Bill M. Tonn provided constructive comments through committee meetings, candidacy exam, and final exam, which made me re-think about ecology aspects in my study. Drs. Phil J. Currie and John Acorn have generously advised on my candidacy exam. Drs. and Murray Gingras have kindly advised and guided me through the final exam. Dr. Ted Allison has served as the committee chair on the final exam.

I owe my gratitude to those people who have made this dissertation possible for help with collection and specimens. First of all, collection staff that directly helped me with collection access and specimen loans are: John Bruner (UALVP), Fang Zheng (IVPP), Binghe Geng (IVPP), Liwu Lu (GMC), Kelvin Seymour (ROM), Margret Currie (CMN), Andy Bentley (KU), Radford Arrindell (AMNH), Babara Brown (AMNH), and Zerina Johanson (NHM). I thank Drs. Gloria Arratia (KU) and Lance Grande (FMNH) for granting access to the collection in their care of; to Zhao Wang (IVPP) and Allan Lindoe (UA) for fossil preparation; to late Norman J. Constenius, Leona Constenius and Kurt Constenius for help towards Kishenehn specimens; to Betsy Kruk and Pengchu Tseng for specimen retrieval; to Bin Bai (IVPP) for loaning photographing equipment and geology discussion; to Gengjiao Chen and Ning Wang for photographing Russian specimens; and to Xinxin Hao and Yemao Hou (IVPP) for laboratory assistance. I am sincerely grateful to the IVPP fieldwork folks led by Dr. Jiangyong Zhang for

extended families for understanding and patience for what I study.

Table of Contents

List of Tables

List of Figures

Chapter 1 Introduction

Catostomids are freshwater fishes in the family Catostomidae (Order Cypriniformes) that currently are found in North America and East Asia but nowhere else in the world. The family name "Catostomidae" (Gill, 1861) is derived from the genus *Catostomus* and from the Greek κατά (*kata*, "down") and στόμα (*stoma*, "mouth"). Their usual common name is suckers in North America (Harris et al., 2014), and Rouge Fish (literally in Chinese) for the one endemic species in China (Meng et al., 1995). Whereas the English common name sucker is derived from the suction-feeding habit and ventrally directed mouth, "Rouge Fish" refers to the bright red color of the Chinese sucker when sexually mature.

In addition to the recently extinct species *Moxostoma lacerum* (Simon, 2006), the freshwater family Catostomidae consists of 13 genera with 78 extant species (Nelson et al., 2016). Whereas the majority of the family, 12 genera with 77 species (Nelson et al., 2016) is widely distributed from coast to coast in North America, including one widely distributed species *Catostomus catostomus* extending to the northeastern corner of Siberia, there is a single endemic genus with a single species, *Myxocyprinus asiaticus*, living in southern China (Meng et al., 1995). While North American catostomids are abundant and contribute about 7% of the North American ichthyofauna (Harris and Mayden, 2001), the only sucker in China is endangered and only found in the Yangtse

and Minjiang rivers. Thus, the taxonomic diversity and corresponding geographic distributions between North America and Asia are strongly unbalanced.

Except for endangered species, Catostomids are generally abundant freshwater fishes that occupy diverse aquatic systems and important niches in the freshwater ecosystem. They inhabit a range of environments from large rivers, such as the Mississippi, Missouri, and Yangtze rivers, to small tributaries, such as streams along the Rocky Mountains, from large lakes such as the Great Lakes to unnamed ponds, and from warm-water rivers to cold-water streams (Nelson and Paetz, 1992; Jenkins and Burkhead, 1994; Moyle, 2002; Hubbs et al., 2004). However, significant population declines (Cooke et al., 2005) and extinctions caused by anthropogenic effects (Simon, 2006) of suckers have caused concerns for these ecologically important fishes. Developing conservation strategies for suckers relies on basic natural history, and on taxonomic, ecological and evolutionary knowledge of the family.

Functionally, the specialized plicate or papillose fleshy lips (Nelson and Paetz, 1992) and protrusible premaxillary jaw augmented by the kinethmoid (Hernandez and Staab, 2015), contribute to the suction feeding of catostomids. Suckers are also equipped with typical sub-terminal to inferior mouths, distinctive toothed pharyngeal bones (Eastman, 1977), a palatal organ (Doosey and Bart, 2011), and functional support of the pectoral fin on the substrate (Lundberg and Marsh, 1976), all aiding catostomids in feeding on benthic algae and invertebrates

including aquatic insect larvae and mollusks. Consistent with their feeding capabilities and body form, they are basal consumers in the aquatic ecosystem. Given their abundance and wide geographic distribution, they often are a fundamental feature of a healthy freshwater ecosystem.

The economic value of catostomids is demonstrated by their importance in sport fishing, food resources, and commercial aquaculture and aquaria. Many suckers have become popular sport fishes in North America recently, whereas the juvenile Chinese sucker (*Myxocyprinus*) has been a feature of commercial aquaria in China, Canada, and the USA. Although the market value of suckers is not high, suckers are among the largest and tastiest fishes that are low in cholesterol, high in protein, and can be kept refrigerated for a relatively long time without deteriorating in quality (Becker, 1983). Suckers are usually consumed by sport fishers in North America, and they used to be important protein resources for Native Americans and for many Chinese. Aquaculture of the Chinese sucker (Zhou, 1995) and introduction of the North American species, Bigmouth Buffalo (*Ictiobus cyprinellus*) to China (Shen, 2000) has replaced the endangered wild Chinese sucker as a food source. Species of *Ictiobus* have also been introduced to Central Asia and Europe (Welcomme, 1988; http://www.fao.org/fishery/dias/en). Remains of catostomid fishes have been also found in paleoanthropology and archeology sites (Smith, 1985; Dombrosky et al., 2016), showing that they were consumed by prehistoric humans of North America.

The Catostomidae are therefore taxonomically, biogeographically, ecologically, and economically

3

important fishes. Fossil records of catostomids and related taxa are the basis to understand the evolution, diversification and radiation of these fishes and their living relatives. To draw a better picture of the evolution of catostomids, I will examine a large sample of all the Eocene catostomids, recently discovered fossil materials, and species that previously were thought to be allied with the group. To answer a variety of the questions such as taxonomy (Chapters 2 through 5), systematics (Chapter 6), ecomorphology (Chapter 7), and biogeography, each chapter will examine a different aspect of the fossil record of this group as noted below.

Fossil catostomids: taxonomy, diversity, distribution, and problems

Similar to the disjunct taxonomic and geographical distribution of extant catostomids, the Cenozoic fossil record of catostomids as currently known is also unbalanced across the continents, except for the Eocene. Prior to the Eocene, the oldest known catostomid-like cypriniform is known from disarticulated cleithra in Paleocene (66-56 Ma) sediments from a single locality in the Paskapoo Formation of Alberta, Canada (Wilson, 1980c). After the Eocene, catostomids disappeared from the Asian fossil record by the early Oligocene (Chang and Chen, 2008), while at the same time they were becoming common fishes in North America. Many fossil species from western North America have been attributed to modern genera (Smith et al., 1968; Smith, 1981; Smith et al., 2000).

During the Eocene, fossil catostomids reached a relatively high taxonomic diversity (Table 1.1; Fig. 1.1). Three fossil genera with 10 nominal species from this time period have been described from both North America and East Asia. This period of diversification of catostomids coincides with the Early Eocene Climate Optimum (EECO; Zachos et al., 2001; Zachos et al., 2008), which has been correlated with significant effects on faunal changes of land mammals (Woodburne et al., 2009). Thus the Eocene potentially represents a critical time for the evolution and divergence of this group of fishes because of the climate influences.

Cope (1872) reported the first fossil catostomid species, *Amyzon mentale*, from Osino, Nevada, USA. In North America, all Eocene catostomids have subsequently been assigned to the extinct genus *Amyzon*. Cope reported another four species of *Amyzon*, two of which are considered by later authors to be junior synonyms (Cope, 1874; 1875; 1893; Bruner, 1991). Based on a large collection of specimens, Wilson (1977a) comprehensively re-described *Amyzon brevipinne* Cope, 1894, and described a new species *A. aggregatum* from Horsefly, British Columbia, Canada. Grande (1981) described another species of *Amyzon*, *A. gosiutense*, from the Green River Formation, USA, but this species was suggested to be a junior synonym of *A. aggregatum* based on a comparison of meristic and morphometric characters (Bruner, 1991). However, the detailed osteological characters of *Amyzon* have not been well assessed yet, and the taxonomy of North American catostomids remains to be clarified.

In Asia, the first fossil catostomid record was recovered from Eocene sediments in Inner Mongolia, China, based on several opercles and disarticulated bones (Hussakof, 1932). One species of *Amyzon* and two new genera, *Plesiomyxocyprinus,* and *Vasnetzovia* have been reported from southern China (Chang et al., 2001), northeastern China (Liu et al., 2010), and Siberia (Sytchevskaya, 1986), respectively. The only Asian *Amyzon*, *A. hunanense*, was originally assigned to an extant genus *Osteochilus* (Cheng, 1962). Several additional Eocene species of *Osteochilus* were described from southern China (Tang, 1959; Wang et al., 1981). Chang and Chen (2008) and Liu et al. (2010) considered all the previously reported occurrences of Eocene *Osteochilus* in China to be identifiable as problematic catostomids. One particular problematic catostomid, *Jianghanichthys hubeiensis*, is reanalysed in this thesis and removed from the Catostomidae into its own family in Chapter 2. The remaining nominal Eocene *Osteochilus* species in China are revised to be species of *Jianghanichthys* in Chapter 5.

Among the known Eocene taxa, three species of *Amyzon* described by Wilson (1977) and Grande (1982) received detailed osteological descriptions, and thus greatly improved our knowledge of Eocene catostomids. However, the remaining species are not well understood or taxonomically clarified. One of the well-described species, *A. gosiutense*, was considered to be a junior synonym of *A. aggregatum* (Bruner, 1991), whereas some species of *Amyzon* described in the 19th Century lacked diagnosable characters.

To better understand the diversity of early catostomids, the taxonomy of Eocene catostomids must be clarified, and recently discovered materials must be studied and compared with nominal taxa (Table 1.1). Not only the synonymized *A. gosiutense* needs clarification, the rest of the North American *Amyzon* species including *A. brevipinne* which is represented by recently collected specimens, are pending further revision. A reanalysis of *A. brevipinne* is undertaken in Chapter 4. New catostomid materials from the Kishenehn Formation, Montana, USA, are well preserved and may potentially be a new species of *Amyzon*-like catostomid. This material is studied in detail in Chapter 3, and a new species is diagnosed. The problematic catostomids from Asia are also important for the evolution of Cypriniformes, since East Asia is so far the only region of the world from which has been recovered both Eocene cyprinids and catostomid that represent the oldest articulated cypriniforms (Fig. 1.1). The Asian catostomids are the subject of Chapter 5.

Systematics of the family: the role of fossil catostomids and problematic catostomids

Four subfamilies have been recognized in Catostomidae: Ictiobinae (*Ictiobus* + *Carpiodes*), Myxocyprininae (*Myxocyprinus*), Cycleptinae (*Cycleptus*), and Catostominae (the rest of the genera of the family; Nelson et al., 2016). The subfamily Catostominae contains more than 80% of the species in the family. Two speciose genera of Catostomidae, *Catostomus* (26 species) and

Moxostoma (22 species) of Catostominae representing two tribes Catostomini and Moxostomatini, contain recognized but undescribed species (Harris et al., 2014).

Prior to the prevalence of cladistics, when the family Catostomidae was recognized (Agassiz, 1850), Gill (1861) established three subfamilies, Catostominae, Cycleptinae, and Bubalichthyinae (type genus *Carpiodes*, based on the general appearance of the fish. In subsequent studies, three subfamilies, Ictiobinae (*Ictiobus + Carpiodes*), Cycleptinae (*Cycleptus + Myxocyprinus*), and Catostominae (the rest of the genera), were generally recognized and supported by phylogenetic studies based on morphology, biochemistry, ontogeny, and karyotypes (Smith, 1992). The separation of *Myxocyprinus* from Cycleptinae to form Myxocyprininae was proposed in a review (Fowler, 1958), and supported by morphology study (Nelson, 1948) and molecular phylogeny studies (Harris and Mayden, 2001; Sun et al., 2002; Doosey et al., 2010).

The phylogeny of Catostominae has been studied with a large array of character types. The first hypothetical scheme of relationships for the Catostomidae was depicted in a morphology review (Miller, 1959). So far, the most comprehensive phylogenetic analysis was conducted by Smith (1992) based on morphology and combined with biochemical data (Smith and Koehn, 1971), gene expression (Ferris and Whitt, 1978b), and larval characters (Fuiman, 1985). Along with the rise of molecular systematics, mitochondrial rDNA (Harris and Mayden, 2001), mitochondrial and nuclear DNA (Sun et al., 2007), mitochondrial protein coding genes (Doosey et al., 2010),

duplication growth hormone gene (Bart et al., 2010b), and nuclear DNA (Chen and Mayden, 2012) have been extensively used to explore the phylogeny of Catostomidae.

The Eocene genus *Amyzon* was included in phylogenetic studies of Miller (1959) and Smith (1992). Whereas the former suggested that *Amyzon* arose from the stem of Ictiobinae and close to Old World catostomids (basal clade of Miller's phylogeny), the latter suggested that *Amyzon* was a basal clade of the subfamily Ictiobinae. Not only is the systematic position of the Eocene catostomids uncertain, but also their evolutionary intrarelationships have never been studied.

Fossil taxa and their phylogenetic relationships are known to be critical to the understanding of the evolution of their living relatives (Donoghue et al., 1989; Novacek, 1992). The systematic position and intrarelationships of catostomids from the Eocene, a time critical to their divergence and diversification, are fundamental to our understanding of the evolution of catostomids, including divergence time and rate, and these fossils need to be added to the phylogenetic data set and evaluated along with extant catostomids. A comprehensive phylogeny based on osteological and other morphological characters is presented in Chapter 6.

Body shape changes and ecomorphology in fossil catostomids

Species of *Amyzon* resemble each other in general appearance, and in meristic and morphometric

characters. Because of the large size of the collections, continued field collecting and laboratory study (Wilson, 1977b; Wilson, 1984; Barton and Wilson, 1999), *A. aggregatum* are found to display high intraspecific variation that is much higher than any of the other known Eocene catostomids. The meristic and morphometric characters of *A. aggregatum* overlap greatly with those of *A. gosiutense*, *A. hunanense*, and the new species from the Kishenehn Formation (Chapter 3). One of the species, *A. gosiutense,* was thus suggested to be a junior synonym of *A. aggregatum* (Bruner, 1991). Quantitative morphology using geometric morphometrics to quantify body shape variation is potentially a powerful tool to detect interspecific discrimination if it exists (Zelditch et al., 2004). Various fields including ecomorphology have been explored in a variety of organisms including freshwater fishes (Rohlf, 1998; Tseng and Wang, 2011; Bower and Piller, 2015), but have been rarely applied to fossil fish.

The body shapes of all known catostomids ranges from extremely deep to very shallow. Catostomid body shape is strongly correlated with the environment they live in. Generally speaking, deep-bodied catostomid fishes inhabit large, low-gradient waters; slender catostomids live in medium-to-small tributaries of intermediate gradient (Nelson and Paetz, 1992; Smith, 1992; Becker, 1983), and small-sized shallow bodied fish live in small streams of mountain areas (Smith, 1966). This correlation can shed light on understand the paleoecology of Eocene catostomids after the body shape has been quantified. This is the goal of Chapter 7.

Fossil catostomids and problematic catostomids are commonly preserved in lateral view on slabs in the form of two-dimensional, complete fish. The large number of specimens of certain species, i.e., *A. aggregatum*, *A. gosiutense*, *A. hunanense*, the new species from the Kishenehn Formation, and the problematic catostomid from Yangxi Formation (Chapter 2), make Eocene catostomid and problematic catostomids ideal candidates to study with geometric morphometric methods to quantify body shapes and hypothesize on paleoecology. Also, mapping phylogeny (Chapter 6) to a morpho-space created by quantified body shapes of Eocene catostomids is potentially of use to understand the diverse pathways of variation and morphological transformation.

To sum up, the goals of this Ph.D. thesis are to understand the diversity of Eocene catostomids, provide fundamental knowledge on the systematic relationships within the family Catostomidae for both extant and extinct taxa, to draw a clearer picture of catostomid evolution, and shed light on the evolution of cypriniforms. Three major categories of study, taxonomy, systematics (phylogeny), and quantitifable morphology, are presented. Chapters 2 through 5 clarify the taxonomy of a problematic catostomid (Chapter 2), describe new materials (chapter 3), and reassess the fossil record of described catostomids and problematic catostomids from North America (Chapter 4) and Asia (Chapter 5). The phylogeny of catostomids, including extant and Eocene species, with descriptions of the osteological characters is presented in Chapter 6. The quantitative body shape changes of Eocene catostomids are the subject of Chapter 7. Therefore,

this thesis is an integrative study of taxonomy, systematics, and ecomorphology using comparative

morphology, cladistics, and geometric morphometrics.

Table 1. 1 Taxonomic status, locality, and collection availability of Eocene catostomids and problematic catostomids.

		Taxon (reference)	LOCALITY	LOCALITY LABEL IN FIG. 1.1	COLLECTIONS/REMARK
N O R T H A M E R I C A	**D E S C R I B E D T A X A**	†*Amyzon aggregatum* (Wilson, 1977)	Horsefly, British Columbia, Canada; Klondike Mountain Formation, Republic, Washington, USA	A; D	UALVP, ROM, CMN specimens (including holotype, over 1000 pieces)
		†*Amyzon brevipinne* (Cope, 1893; Wilson, 1977)	North Fork of the Smilkameen River (Cope), Princeton, and Tulameen (Wilson), British Columbia, Canada	C	UALVP, CMN (holotype), ROM
		†*Amyzon commune* (Cope, 1874, 1875; Cavender, 1986; Bruner, 1991.)	Tertiary shale, South Park (Florissant Formation), Colorado, USA	K	UALVP, AMNH. Junior synonym: †*Amyzon fusiforme* Cope, 1875 †*Amyzon pandatum* Cope, 1875
		†*Amyzon mentale* (Cope, 1872)	Tertiary shale, Osino, Nevada, USA	I	Images of holotype for comparison
		†*Amyzon gosiutense* (Grande et al., 1982)	Laney Member, Green River Formation, Lake Gosiute locality, Wyoming, USA	J	FMNH (paratype), AMNH (paratype), UALVP
	N E W M A T E R I A L S	——	Whipsaw Creek and Blakeburn Mine (near Princeton), British Columbia, Canada	B	438 specimens in UALVP collection, referred to *Amyzon brevipinne*.
		——	Republic, Washington state, USA	D	UALVP; Some specimens from that area were referred to *Amyzon aggregatum* (Wilson, 1996).
		——	Kishenehn Formation, Flathead River (Middle Fork), Montana, USA	E	217 specimens referred to †*Amyzon* in UALVP collection.
		——	Near the town of Grant, Montana, USA	F	Fragments

		——	Ruby, Montana, USA	G	Scales
		Catostomidae cf. *Amyzon* (Cavender, 1986)	Ochoco Pass, Mitchell, Oregon. U.S.A.	H	FMNH, disarticulated bones and teeth
E A S T A S I A	D E S C R I B E D T A X A	†*Amyzon hunanense* (Cheng 1962; Chang et al., 2001;)	Xiawanpu, Xiangxiang, Hunan, China	Q	IVPP
		†*Plesiomyxocyprinus arratiae* (Liu and Chang, 2009)	Hudian Basin, Northeastern China	M	IVPP
		†*Vasnetzovia artemica* (Sytchevskaya, 1986)	Southern Premorie, Russia	L	images
		Catostomus sp. (Hussakoff, 1932)	Ulan Shiren Formation, Inner Mongolia, China	N	AMNH
	N E W M A T E R I A L S	†*Jianghanichthys hubeiensis* (Lei, 1977;1987)	Songzi, Hubei, China	P	IVPP (problematic catostomids)
		Osteochilus sanshuiensis; *Osteochilus longipinnatus*; *Osteochilus laticorpus*. (Wang et al., 1981)	Sanshui Basin, Guangdong, China	S	IVPP (problematic catostomids)
		——	Wutu and Longkou, Shangdong Province	O	Fragments
		Osteochilus linliensis (Tang, 1959)	Xiajiashan, Linli, Hunan, China	T	missing (problematic catostomids)
		——	Qingjiang, Jiangxi, China	R	Fragments

Figure 1. 1 Fossil localities of Eocene catostomids and problematic catostomids.　Map is modified from Chang et al. (2001, fig.1b). Eocene cypriniforms other than catostomids are mapped for comparison. Letter A through T represent localities of Eocene catostomids and problematic catostomids that are listed in Table 1.
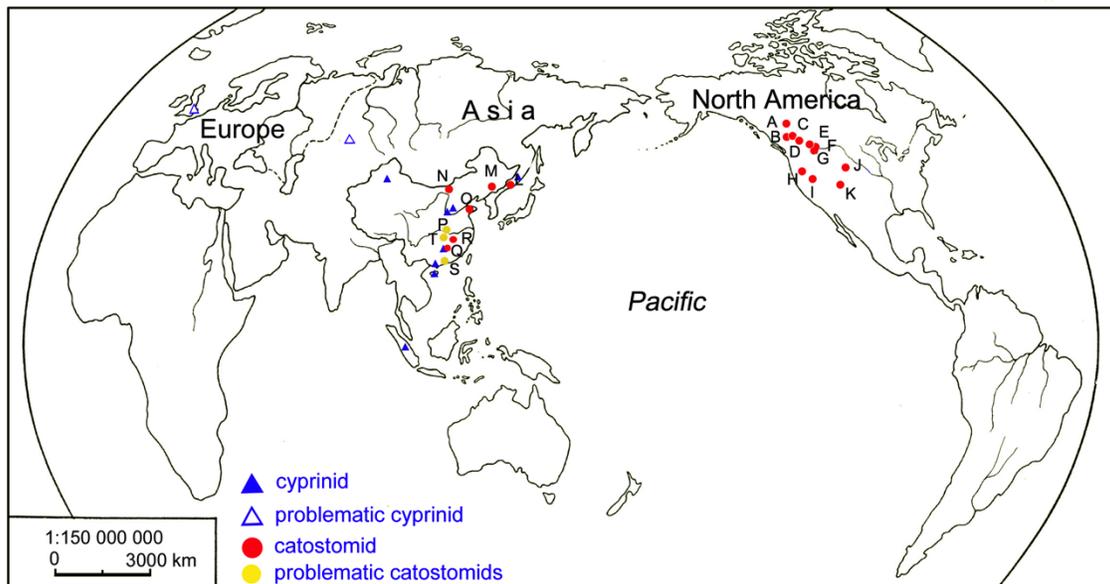
Chapter 2 Systematic position of a supposed catostomid from Asia

This chapter has been published as:

Liu, J., M.-M. Chang, M. V. H. Wilson, and A. M. Murray. 2015. A new family of Cypriniformes (Teleostei, Ostariophysi) based on a redescription of †*Jianghanichthys hubeiensis* (Lei, 1977) from the Eocene Yangxi Formation of China. Journal of Vertebrate Paleontology e1004073:23.

I collected the data, designed and performed the analyses, and wrote the paper. Co-authors' contributions see the Preface of this thesis (Page VI).

ABSTRACT—The fossil cypriniform fish †*Jianghanichthys hubeiensis* from Eocene mudstones in Songzi, Hubei, China, was originally assigned to the extant cyprinid genus *Osteochilus*, then later to the new genus †*Jianghanichthys* by its original author, but with its familial status uncertain. Other authors subsequently assigned it to the cypriniform family Catostomidae.

A detailed comparison of osteological characters shows that †*Jianghanichthys* is distinguished from all other cypriniforms by having: 1) first principal anal fin ray branched; 2) supraorbital sensory canal largely exposed in frontal but roofed by longitudinal flange; 3) supraorbital sensory canal meeting the temporal sensory canal within the parietal; 4) maxilla bearing three dorsal processes; 5) dorsal surface of anterior end of dentary triangular and broad; 6) the first centrum of †*Jianghanichthys* has a similar size and prominent posterior concavity to the second centrum. CT scan of a matrix-covered skull confirmed the aforesaid unique characters, as well as that the pharyngeal teeth are either absent, or not well formed.

A series of phylogenetic analysis, using parsimony criteria and morphological characters, consistently recovers †*Jianghanichthys* in a polytomy with the non-loach cypriniform families, but could not be placed within any recent family. Among osteological characters, few unique synapomorphies were shared by *Jianghanichthys* and recent families of Cypriniformes, whereas a large number of symplesiomorphies with the Catostomidae, Cyprinidae, and Gyrinocheilidae were obtained indicating that *Jianghanichthys* is a stem taxon of Cypriniformes. Therefore, the first family of Cypriniformes known only from fossils, †Jianghanichthyidae, is erected to contain this Eocene cypriniform fish.

Introduction

The order Cypriniformes, containing suckers, carps, loaches and relatives, is the most diverse and largest clade of freshwater fishes, containing 321 extant genera and over 3268 species (Nelson, 2006). Cypriniforms are specialized fishes with a kinethmoid bone functioning in jaw protrusion, a Weberian apparatus connecting the inner ear with the swim bladder (shared with other otophysans), and well-developed pharyngeal bones with ankylosed teeth (except in Gyrinocheilidae) (Fink and Fink, 1981). Within the order, both the number of species and their higher-level groupings have seen dramatic increases with recent discoveries (Eschmeyer and Fong, 2014). These fishes occupy a wide range of freshwater aquatic habitats in their native distributions around the world, but are absent from oceanic islands, Australia, South America, Antarctica, and parts of the far north (Nelson, 2006). Adult body size ranges from less than 9 mm in *Paedocypris* (Kottelat et al., 2006) to greater than 1720 mm in *Catlocarpio* (Mayden and Chen, 2010). Because of the wide geographic distribution, large number of taxa, and high diversity of morphological and molecular characters, the classification and phylogenetic relationships of Cypriniformes are complex and remain problematic (Simons and Gidmark, 2010). Presented here is a redescription of a highly unusual Eocene cypriniform fossil from China, †*Jianhanichthys hubeiensis* (Lei, 1977), which at first was assigned to the Cyprinidae (Lei, 1977), then later classified incertae sedis as to family (Lei, 1987), and still later assigned to the Catostomidae (Chang and Chen, 2008), but which

now appears to represent a new, extinct cypriniform family with profound implications for the phylogeny and classification of the order.

Traditional classifications of the Cypriniformes include five or six families (following Nelson, 2006): Cyprinidae (carps, minnows), Psilorhynchidae (mountain carps), Catostomidae (suckers), Gyrinocheilidae (algae eaters), Cobitidae (loaches), and Balitoridae (= Homalopteridae, river loaches). Psilorhynchidae have been classified as a subfamily of Cyprinidae, as a subgroup of Cobitidae, or as closer to non-cyprinids (non-Cyprinoidea) than to cyprinids (Hora, 1920; Chen, 1981; Conway and Mayden, 2007; He et al., 2008). They were recently placed as the sister group to Cyprinidae in a comprehensive phylogenetic study based on morphological characters, supporting their familial status (Conway, 2011). Four families, Nemacheilidae (Nalbant and Bianco, 1998), Botiidae (Nalbant, 2002), Vaillantellidae (Šlechtová et al., 2007), and Ellopostomatidae (Bohlen and Ŝlechtová, 2009), were created to be new families from the previous loach families (Cobitidae and Balitoridae) and further studied by other researchers (Kottelat, 2004; Tang et al., 2006; Mayden et al., 2009; Conway et al., 2010; Liu et al., 2012). Two mono-generic families, Barbuccidae and Serpenticobitidae, were also established from the loach clade recently (Kottelat, 2012). Another genus *Paedocypris*, which was considered as a miniature cyprinid (Kottelat et al., 2006), is elevated to the family level as Paedocyprididae by Mayden and Chen (2010). However, Tang et al. (2010) argued that Paedocyprididae should be a junior synonym of Danionae, whereas Britz et al. (2014) suggested that *Paedocypris* to be a basal clade of the Cypriniformes with other miniature cyprinids. Although debates on some family level

classification of Cypriniformes are ongoing, the recognition of high family level diversity has been firmly established in recent years.

In recent publications, Conway et al. (2010) and Simons and Gidmark (2010) extensively reviewed the systematics of Cypriniformes, giving a brief history of the development of our knowledge of these fishes. An early phylogenetic study was that of Wu et al. (1979), who used eight morphological characters. Two main sister groups were present, one being Catostomoidea, consisting of Catostomidae, Gyrinocheilidae, and Cobitidae, and the other Cyprinoidea, composed of Cyprinidae and Homalopteridae (= Balitoridae). Later, Siebert (1987) provided a more comprehensive phylogenetic analysis using considerably larger sample sizes and numbers of characters. He suggested Cypriniformes should be divided into the superfamilies Cobitoidea, consisting of all non-cyprinid families, and Cyprinoidea, consisting only of cyprinids. This concept has prevailed in cypriniform studies for the past few decades. The main difference between the results of Wu et al. (1979) and those of Siebert (1987) is that Cyprinidae were hypothesized to be the most advanced family in the former framework, but the sister group to the lineage containing the remaining cypriniforms in the latter. With the rising popularity and development of molecular systematics, the relationships among the families have been investigated further using both mitochondrial and nuclear DNA sequences (Harris and Mayden, 2001; Liu et al., 2002; Saitoh et al., 2006, 2011; Šlechtová et al., 2006; Tang et al., 2006; Mayden et al., 2009). Molecular phylogenetic analysis including cypriniforms in a broader context, such as the Otocephala and Otophysi, also shed light on the intra-relationships of Cypriniformes (Poulsen

et al., 2009; Chen et al., 2013). The molecular results agree with those of Siebert (1987) in that the Cypriniformes are divided into two clades, the Cyprinoidea containing only the Cyprinidae (including *Psilorhynchus*), and the Cobitoidea containing all the remaining families. The most comprehensive morphological phylogenetic investigation by Conway (2011) differed slightly in that Cyprinidae and Psilorhynchidae comprise Cyprinoidea, whereas Cobitoidea consist of all the loach families, plus the sister group consisting of Catostomidae and Gyrinocheilidae.

In stark contrast to the modern biodiversity of the cypriniforms, their early fossil record prior to the Eocene is relatively sparse, even though the origin of Cypriniformes was reconstructed as being 158.9Ma based on a molecular systematic study (Chen et al., 2013). The only skeleton fossil records prior to the Eocene are known from the Cretaceous of South America and the Paleocene of Canada (Wilson, 1980; Gayet, 1982). The Upper Cretaceous *Molinichthys inopinatus* from Bolivia was originally designated in the Family Cyprinidae, based on fragmentary bones and putative teeth (Gayet, 1982). But this was challenged by Fink et al. (1984), Gaudant (1993), and Arratia and Cione (1996). In a subsequent review, Gayet and Meunier (1998) considered *Molinichthys* to be a nomen nudum because no additional, more diagnostic material has been found, but it remains an available name under ICZN and thus it should more properly be termed a nomen dubium. The material of Paleocene *Amyzon* sp. from the Paskapoo Formation, Canada, included a complete cleithrum (Wilson, 1980). I examined the cleithrum, and agreed with its placement in the family Catostomidae. Unlike their poor older fossil record, cypriniforms diversified globally during the Eocene. Occurrences of this age have without exception been

assigned to either Cyprinidae or Catostomidae (Sytchevskaya, 1986; Cavender, 1991; Chang and Chen, 2008). Several Eocene taxa from southern China were assigned to a living genus of Cyprinidae, *Osteochilus*, by early researchers (Tang, 1959; Cheng, 1962; Lei, 1977; Wang et al., 1981; Lei, 1987), but one of these taxa has since been moved to Catostomidae (Chang et al., 2001), and the others are pending further study, which could provide significant evolutionary information about systematics of early cypriniform fishes.

The species redescribed herein is one of the problematic cypriniforms from southern China (Lei, 1977, 1987). Its taxonomic assignment has been uncertain for a long time. It was initially assigned to *Osteochilus*, as *O. hubeiensis* Lei, 1977, and subsequently made the type of the new genus †*Jianghanichthys* with uncertain family status (Lei, 1987). Later, this fish was considered to be closely related to the Catostomidae (Chang and Chen, 2008; Liu and Chang, 2009). However, new data indicate that this fish belongs neither in Cyprinidae nor in Catostomidae. Therefore, a major goal of the current study is to understand the systematic position of †*Jianghanichthys* and its implications for the early diversity and evolution of Cypriniformes.

Geology

The fossil specimens of †*Jianghanichthys* are from the early Eocene Yangxi Formation, which has a thickness of 100–150 m, underlying the Paomagang Formation and overlying the Pailoukou Formation (Editorial Committee of Stratigraphical Lexicon of China, 1999). The

freshwater Yangxi Formation consists of finely laminated mudstones and siltstones that contain vertebrate fossils. Along with the fossil cypriniform, the locality has produced the bony-tongued fish (Osteoglossiformes) †*Phareodus songziensis* (Zhang, 2003), two gruiform birds †*Songzia heidangkouensis* and †*S. acutunguis* (Hou, 1990; Wang et al., 2012), and a pantodont mammal †*Asiocoryphodon* cf. *A. conicus* (Chen and Gao, 1992). Most specimens from the formation listed by Hou (1990), Zhang (2003), and this paper were collected in 1987 by one of the authors, Mee-mann Chang, and her colleagues Yi Lu, Mei Shen, Yifeng Chen, and Yiyu Chen. The original field notes provided the locality information as "Heidangkou, Wangjiaqiao Area, Songzi County," which is now Wangjiaqiao Town, Songzi City, in Hubei Province, China. A small outcrop in farmland generated thousands of fishes in the 1980s. However, devastating excavations by commercial collectors had destroyed the fossil locality by the time Jiang-yong Zhang visited the locality in 2005. With further fieldwork, additional specimens were obtained by Jiang-yong Zhang in 2010. In a subsequent paper, Lei (1987) suggested that more specimens of †*Jianghanichthys* were collected from Laochengzhen in Songzi City, Paomagang in Dangyang City, and Laoyashan, Louzihe and Lijiaxi in Yidu City (Fig. 2.1).

Materials and Methods

Referred Specimens—Two specimens listed and collected by Lei (1977, 1987) and deposited in GMC were available for this study: GMC V1810-1 and GMC V1810-2. Additional

specimens collected in 1987 and 2010 are deposited in the collection with catalogue numbers IVPP V 12163.1− 65, and IVPP V 18858.1 − 2. All the above fossil specimens are preserved with the bone in place and articulated.

Materials for Comparison—Materials used for comparison include those listed in Liu and Chang (2009). Additional modern fish specimens are listed here, in three orders and 6 families (dried skeletons unless otherwise indicated, cleared and stained specimens indicated with C&S): (1), Gonorynchiformes: **Chanidae**: *Chanos chanos*, UAMZ F3523 (C&S), UAMZ F8463, AMNH I 30837, AMNH I 89719 through 89724, AMNH I 95424, AMNH I 95415, AMNH I 95573. (2), Cypriniformes: **Catostomidae**: *Carpiodes carpio*, KU 12732; *Carpiodes cyprinus*, UAMZ 4431 (C&S), CMN 77-0183; *Catostomus catostomus*, AMNH I 41156 (C&S); *Catostomus commersoni*, UAMZ F3835.6 (C&S), UAMZ F8422, UAMZ F7341; *Catostomus discobolus*, KU 11902; *Catostomus macrocheilus*, KU 11867; *Chasmistes liorus*, KU 12456; *Deltistes luxatus*, KU 12424; *Hypentelium nigricans*, ROM R 5871; *Ictiobus cyprinellus*, KU 15337; *Ictiobus niger*, KU 13047; *Minytrema melanops*, ROM R6701; *Moxostoma macrolepidotum*, UAMZ 6731 (C&S), ROM R7377, KU12718. **Cobitidae**: *Chromobotia macracanthus*, UAMZ F8748; *Cobitis taenia*, AMNH I 10412 (C&S). **Cyprinidae**: *Barbus* sp. AMNH I 21657; *Carassius auratus*, AMNH I 21689; *Cyprinus carpio*, UAMZ F8464, AMNH 10147, AMNH I 49088 (C&S); *Hypophthalmichthys nobilis*, UAMZ F8749; *Osteochilus sp.*, AMNH I 94472, AMNH I 94473. **Gyrinocheilidae**: *Gyrinocheilus aymonieri*, UAMZ 5109, AMNH I 77898 (C&S). (3) Characiformes: **Citharinidae**: *Citharinus congicus*, CMN 81-0190 (C&S); *Distichodus lusosso*,

ROM R6940.

In addition to the fossil specimens listed by Liu and Chang (2009), 1,973 specimens in the UALVP of †*Amyzon mentale* Cope (latex peel), †*A. commune* Cope, †*A. brevipinne* Cope, †*A. aggregatum* Wilson, and †*A. gosiutense* Grande, Eastman, and Cavender were also used for comparison (specimen numbers are available in the online database of the UALVP).

Preparation and Photography—The fossils were prepared by hand with needles. Some structures were coated with sublimated NH_4Cl to see details, and then photographed using a Nikon DXM 1200C digital camera mounted on a Zeiss Discovery V8 stereomicroscope.

Computerized Tomography—Fossil specimen was scanned using X-ray computerized topographically (CT) in the IVPP on a CT scanner 225KV ЄL produced by the IHEP. The specimen was scanned through the sagittal axis at 0.020 mm slice thickness/interslice distance, and reconstructed into 160 2048x2048 pixel RAW image files using IHEP-FBPCT developed by the IHEP. The complete image stack was examined in ImageJ and converted to TIFF files for creating figures.

Phylogenetic Analysis—All characters were coded in Mesquite V2.75 (Maddison and Maddison, 2011) and analysed in PAUP* 4beta10 (Swofford, 2002). Characters were run as unordered and unweighted. Heuristic searches were used. A "furthest" addition sequence was used, with no topological constraints enforced, no ancestral taxa identified, and "parsimony" as the optimality criterion. Character states were optimized with accelerated transformation (ACCTRAN). Character changes were traced over the resulting trees using Mesquite V2.75

(Maddison and Maddison, 2011). Bootstrap analyses were performed based on 10,000 replicates using fast heuristic search with the starting trees obtained via a stepwise addition with a random addition sequence. An additional independent heuristic search was enforced with a manually set-up constraint tree using the "backbone" option; in this analysis, only trees compatible with the constraint tree were retained. Finding specific topologies of trees in the obtained best trees, such as a clade formed by †*Jianghanichthys* and certain other taxa, used the "Filter Trees from other source" option in Mesquite.

Measurement and Fin Ray Counting—Fossil specimens were scanned for morphometric analysis using an Epson Perfection 3590 or Uniscan M800U scanner and measured using the computer program Image J. The measurements of neural spine length were all taken from the neural spine of the first caudal vertebra, which is the vertebra bearing a definite hemal spine. The length of the neural spine was measured from where the neural spine meets the neural arch, to the free, pointed tip.

For fin rays counts, I provide both principal fin ray number, as well as branched and unbranched fin ray numbers. In a fin formula, the unbranched fin ray number is represented by lowercase Roman numerals, whereas the branched fin ray number is represented by Arabic numerals. For the concept and counting of principal fin rays, I follow the definition from Hubbs and Lagler (1949), "In certain fishes, particularly the Cyprinidae and Catostomidae, ..., the principal rays include the branched rays plus one unbranched ray, since only one unbranched ray reaches to near the tip of the fin". That is to say, if the unbranched fin ray does not "reach to near

the tip of the fin", it is not counted towards the principal fin rays. The short unbranched fin rays preceding the principal rays are commonly and meaningful called rudimentary rays of dorsal and anal fins, and procurrent rays of the caudal fin. However, Arratia (2008) defined "rudimentary" rays differently, and all the small, unbranched fin rays of median fin were called procurrent rays. To avoid confusion in the usage of rudimentary ray, I use procurrent rays for all the small unbranched fin rays proceeding principal rays in the dorsal, anal, and caudal fin.

Anatomical Terminology—The terminology of the opercular series is from Nelson (1949), that of the Weberian apparatus is from Nelson (1948), that of the maxilla is from Miller and Smith (1981), and that of the caudal skeleton is from Grünbaum et al. (2003). The prefix 'auto-' has been introduced to several osteological terms in cypriniforms, i.e., 'autopalatine', 'autopterotic', and 'autosphenotic', because these are believed to be merely chondral bones. Fink and Fink (1981, 1996) have suggested that the dermal portion of palatine is absent in Ostariophysi. I agree the autopalatine is more precise and should be adopted. For the pterotic, although Cubbage and Mabee (1996) suggested that the pterotic is a chondral bone in *Danio*, it is apparent the pterotic bears a bone-enclosed sensory canal in many cypriniform fishes, for example *Psilorhynchus* (Conway, 2011) and *Cyprinus*, indicating it should have a dermal portion. The development of sphenotic is more complicated in cypriniforms, because it is largely overlapped by the frontal and infraorbitals in some cypriniforms (i.e. cyprinids), compared to mostly exposed on the surface in some others (i.e. catostomids). I favor classifying the sphenotic is a chondral bone in certain cyprinids as Cubbage and Mabee (1996) suggested, thus it is appropriated to use 'autosphenotic' for some

27

cyprinids. However, in catostomids, the sphenotic is associated with the supraorbital sensory canal by the evidence of the sensory canal running above the sphenotic and a few minute pores on the surface of the posteriodorsal sphenotic, both common conditions of the usually detached (not bone-enclosed) cranial sensory canal and associated bones of catostomids. Therefore, both the pterotic and the sphenotic, at least in certain cypriniforms, still possess dermal portion and should be a complex of dermal and chondral bone. The original forms "pterotic" and "sphenotic' should be retained.

Anatomical Abbreviations—**1par**, first principal anal fin ray; **aa**, anguloarticular; **ap**, auricular process of opercle; **apa**, autopalatine; **bop**, basioccipital; **brs**, branchiostegal rays; **c1–4**, first through fourth centrum; **cl**, cleithrum; **crp**, coronoid process of dentary; **den**, dentary; **em**, ethmoid; **epo**, epiotic; **epu**, epural; **ff**, frontal flange; **fr**, frontal; **gr**, gnathic ramus; **hy1–6**, hypurals 1 through 6; **hyo**, hyomandibular; **iob**, infraorbital; **ioc**, infraorbital sensory canal; **iop**, interopercle; **kem**, kinethmoid; **L.**, left; **lem**, lateral ethmoid; **max**, maxilla; **msc**, mandibular sensory canal; **mxb**, maxilla body; **mxn**, maxilla neck; **mxp**, premaxilla process of maxilla; **mxpd**, posterodorsal process of maxilla; **mxpn**, posterior process of the neck of maxilla; **nc**, neural complex; **ns**, neural spine; **oco**, opercular canal ossicle; **op**, opercle; **opf**, opercular fossa; **os**, opercular socket; **otc**, otic sensory canal; **oto**, otolith; **opc**, opercular sensory canal; **par**, parietal; **pcl**, postcleithrum; **pgt**, pharyngeal tooth/teeth; **phy**, parhypural; **pls**, pleurostyle; **pmx**, premaxilla; **poc**, preopercular sensory canal; **pop**, preopercle; **pr4**, fourth pleural rib; **ps**,

parasphenoid; **ptc**, posttemporal sensory canal; **pto**, pterotic; **ptt**, posttemporal; **pvp**, posteroventral process of dentary; **qua**, quadrate; **R.**, right; **ra**, retroarticular; **rna**, rudimentary neural arch; **SL**, standard length; **sco**, sensory canal opening; **soc**, supraorbital sensory canal; **sop**, subopercle; **spc**, supracleithrum; **sph**, sphenotic; **spo**, supraorbital; **stc**, supratemporal sensory commissure; **sym**, sympletic; **tc**, temporal sensory canal; **uhy**, urohyal; **vom**, vomer.

Institutional Abbreviations—AMNH, American Museum of Natural History, New York, USA; CMN, Canadian Museum of Nature, Ottawa, Canada; GMC, The Geological Museum of China, Beijing, China; IHEP, Institute of High Energy Physics, Chinese Academy of Sciences, Beijing, China; IVPP, Institute of Vertebrate Paleontology and Paleoanthropology, Chinese Academy of Sciences, Beijing, China; KU, University of Kansas, Kansas, USA; **LUC**, Loyola University Chicago, Chicago, USA; ROM, Royal Ontario Museum, Ontario, Canada; UALVP, University of Alberta Laboratory for Vertebrate Paleontology, Alberta, Canada; UAMZ, University of Alberta Museum of Zoology, Alberta, Canada.

Systematic Paleontology

Subdivision TELEOSTEI Müller, 1845

Superorder OSTARIOPHYSI Sagemehl, 1885

Order CYPRINIFORMES Bleeker, 1859/60

Family †JIANGHANICHTHYIDAE, fam. nov.

Type Genus—†*Jianghanichthys* Lei, 1987.

Diagnosis—Same as that for the only known genus and species.

†*JIANGHANICHTHYS HUBEIENSIS* (Lei, 1977)

Osteochilus hubeiensis Lei, 1977, p. 134, plate 49, figs. 3–4 (original description).

Jianghanichthys hubeiensis (Lei, 1977): Lei, 1987, p. 191 (new combination).

Designation of Lectotype—A holotype was not designated when the species and genus

were described (Lei, 1977), and Lei (1987) did not clarify the matter when he assigned the species

to his new genus. Specimen GMC V1810-1 (V 25404 in Lei, 1977; 1987) was considered the

holotype when it was transferred to GMC from Yichang Institute of Geology and Mineral

Resource in Hubei, whereas the rest of Lei's collection remained in Yichang. GMC V1810-1 is a

complete, articulated specimen, preserved in right lateral view (Fig. 2.2A; Lei, 1977: pl. 49 fig. 3;

Lei, 1987: pl. 23 fig. 1), which is part of the type series and was figured by Lei in his original

description of the species. This specimen is here designated as the lectotype.

Paralectotype—GMC V1810-2 (the specimen number was V 25405 in the original type

series of Lei, 1977; 1987).

Topotypes/Homeotypes—IVPP V 12163.1−65, IVPP V 18858.1, complete and incomplete articulated fishes from the type locality and identified by us as belonging to this species.

Locality and Horizon—Songzi City, Hubei Province, China; Yangxi Formation (early Eocene).

Etymology of Generic and Specific Names—Lei (1977) did not provide a derivation of the specific name when he named the species, nor did Lei (1987) provide one for his new generic name. According to its Chinese version, I interpret the names as follows. The locality of †*Jianghanichthys* is in the southwestern portion of the Jianghan Plain in central to southern Hubei Province. Jiang- refers to the Yangtze River that is also called Changjiang; han- refers to the Hanjiang River, which is also known as Hanshui. The Hanjiang River is north of the Yangtze River, and is one of the main tributaries flowing into the Yangtze. The alluvial plain around these two main rivers, before the Hanjiang flows into the Yangtze, has been known as the Jianghan area for thousands of years. Therefore, a number of places, institutions, mineral resources etc. from that area, such as the well-known Jianghan Oilfield, have been named after it. The word ichthys is Greek for fish. The specific name "hubei-" refers to Hubei Province, within which the fossil locality was found.

Emended Diagnosis—Cypriniform fish that are medium sized, with caudal fin forked to emarginate, dorsal and anal fins short and emarginate, first principal anal fin ray branched;

supraorbital sensory canal in frontal enclosed in bone posteriorly but for most of length, running ventrolateral to prominent, longitudinal flange; parietal portion of supraorbital sensory canal enclosed in parietal, and meeting the temporal canal within the parietal; maxilla dorsally with pointed anterior process, stout posterodorsal process, and with small posterior process on maxillary neck; dorsal surface of anterior end of dentary triangular and broad; first centrum amphicoelous. Differing from other cypriniform fishes also by the following combination of characters: smaller, younger individuals with shallow body and with straight ventral body margin; larger, older individuals with very deep body and convex ventral margin; shallowest portion of body in middle of caudal peduncle in juveniles, but at caudal fin base in adults; skull roof lacking frontoparietal fontanelle; frontal with broad anterior portion and narrow posterior portion; premaxilla broad, triangular and flat; mandibular sensory canal enclosed in dentary; preopercular sensory canal partly enclosed in bone; supratemporal sensory canal embedded in parietal; fourth pleural rib associated with Weberian apparatus short, rod-like, with hooked end; dorsal fin originating at mid-point of body, with 2–3 procurrent rays and 12–13 principal rays (iii/iv,11–12); anal fin originating below a point posterior to end of dorsal fin, with 2 procurrent rays and 7 principal rays (ii,7), all principal rays branched including first, leading-edge ray; caudal fin with 19 principal rays in formula i,9,8,i; 4 procurrent rays on upper and lower lobe of caudal fin.

Description

General Appearance—Known specimens of †*Jianghanichthys hubeiensis* are medium-sized, laterally compressed, and somewhat to very deep-bodied fish. All the specimens are preserved in lateral view as articulated skeletons. They range in standard length (SL) from 35.5 mm (IVPP V 12163.46) to 128.5 mm (IVPP V 12163.12). The head in all specimens is medium sized compared to that of other Eocene cypriniforms, but large compared to that of most extant cypriniforms, with a head length about 30% of SL (range 27–33%). The body of older individuals is deeper than those in the common, comparably sized Eocene catostomid genus †*Amyzon*. The young individuals (Fig. 2.2B) are usually less than 70 mm in SL, and slender, with body depth around 40% of SL (range 34−48%), whereas adults (Fig. 2.2A, 3A and 4A) are deeper with body depth about 50% of SL (range 40−63%). In addition, the ventral profile is straight in most young individuals (Fig. 2.2B), but markedly convex in large specimens (Fig. 2.2A). The slender body of young specimens is a common character of fossil suckers, such as †*Amyzon*. However, the adults probably had not only a deep body but also a rather broad body, judging by the fact that the ventral body margin of the compressed fossils, as preserved, is protruded between the insertion of the pelvic and anal fins. Individuals with SL between 60 mm and 80 mm are somewhat intermediate in body depth and ventral profile. The body depth of specimens in this size range varies from 31% to 54% of SL. Their ventral profiles are either straight or convex, and thus not as consistent as in smaller or larger specimens.

The lectotype, GMC V1810-1 (Fig. 2.2A), is very well preserved in lateral view, as are topotype specimens IVPP V 12163.14 (Fig. 2.4A), 15 (Fig. 2.3A), and 19, showing much detail to be described. The lectotype represents a small adult fish, of 78.8 mm SL. Its morphometric characters are in the aforesaid ranges. The following detailed descriptions apply to all the specimens in which they can be observed. A specimen number in parentheses follows some features that are especially well preserved in particular specimens. The cephalic sensory canal system reconstruction (Fig. 2.5A) is inferred from the broken or medially preserved bone-enclosed sensory canal and from canal openings on the surfaces of the bones. The individual portions of the sensory canal are described in conjunction with the descriptions of the associated bone(s).

Cranium—Orienting from anterior to posterior, medial to lateral, and dorsal to ventral, the visible and distinguishable cranial bones consist of: ethmoid complex, lateral ethmoid, frontal, sphenotic, parietal, pterotics, and epiotics (Fig. 2.3C).

The unpaired ethmoid complex is the compound bone formed by the ontogenetic fusion of the endochodral mesethmoid and the dermal supraethmoid, as in other cypriniform fishes (Harrington, 1955; Cubbage & Mabee, 1996; Conway, 2011). The supraethmoid portion (dorsal) of the ethmoid complex is large and rectangular, and thus visible on almost every specimen. The dorsal portion is short and wide with an anterior process in the middle (IVPP V 12163.2b and 3), as in catostomids. The anterior process descends slightly and is interdigitated with the porous mesethmoid portion (ventral) of the ethmoid complex, which articulates with the vomer and autopalatines. A small foramen is located at the base of the anterior process. The paired lateral

ethmoids, lateral to the ethmoid complex, are longitudinally elongated. Their surfaces have a porous appearance and they are larger in size than the ethmoid complex (Fig. 2.3). An anterolateral process of the lateral ethmoid is nearly parallel to the midline of the fish.

Parts of the vomer and of the anterior portion of the parasphenoid, ventral to the ethmoid, are visible through the orbit on most specimens (Fig. 2.3B, 3C, 4A). The anterior portion of the parasphenoid is flat and broad. A small, lateral, basipterygoid process can be found on the posterior part of the parasphenoid (IVPP V 12163.15).

The frontal has a broad anterior half with a prominent postorbital extension and a narrow posterior half, similar to that of various catostomids (Fig. 2.3A, 6A). The medial margin of the frontal is straight, indicating a frontoparietal fontanelle is absent. The anterior cranial fontanelle between frontal and ethmoid complex is also absent. The anterior and anterolateral margin of the frontal is slightly convex and fan-shaped, with striations on the surface, but lacks a prominent supraorbital notch. A prominent longitudinal flange extends dorsally along the anterior half and along the lateral edge of the posterior half of the frontal. The supraorbital sensory canal lies in a deep groove beneath and roofed by this flange. Several sensory canal openings are located medial to the frontal flange and directed anteriorly. In IVPP V 12163.14a, the flange was damaged, allowing observation of the groove (Fig. 2.4B). In contrast, a complete frontal (IVPP V 12163.15, Fig. 2.3C) shows the flange roofing and hiding the sensory canal. The sensory canal extends to the posterior end of the frontal where it enters the parietal in a bony tube (Fig. 2.3C, 6A).

The parietal is much smaller than the frontal, being similar in size to the posterior narrow

portion of the frontal. It is roughly rectangular with an elongated posterolateral process extended behind the pterotic (Fig. 2.3B, 3C, 6A). The right and left parietals probably met in the midline of the skull roof, given a lack of any evidence for a fontanelle. Two bone-enclosed sensory canals are found in the parietal (Fig. 2.6A). One is the temporal sensory canal (temporal portion of infraorbital canal, continues from the otic region and leads to the trunk lateral line) at the lateral margin of the parietal, running longitudinally and continuous with the infraorbital sensory canal at the otic region (otic sensory canal, Fig. 2.5, 6A) and the supraorbital sensory canal of the parietal. The other is the supratemporal commissure (sensory canal running across the skull roof and forming a connection between left and right temporal canals; 'supratemporal cross-commissure' in Allis (1889) and 'supratemporal canal' in Illick (1956)). The supratemporal commissure lies mediolaterally on the posterior margin of the parietal with an opening towards the epiotic (Fig 3B, 3C, 5A). Posterior to the ridge created by the posterior, enclosed supratemporal commissure sensory canal, the parietal extends slightly farther posteriorly (Fig. 2.3C). The supraorbital canal (parietal portion) and the temporal canal of †*Jianghanichthys* meet within the parietal (Fig. 2.6A, 5A), an unusual situation. In other teleost especially cyprinids, the supraorbital canal and infraorbital canal are commonly disjunct or connected in the otic or postorbital region (Allis, 1889; Illick, 1956; Gosline, 1974; Cavender and Coburn, 1992; Takeuchi et al., 2011).

The sphenotic is a prominent bone on the surface of the skull lateral to the frontal. Its wing-like anterolateral portion, the postorbital process, reaches the orbit (Fig. 2.3B, 3C, 4B). This is a common condition in catostomids, and considered to be a plesiomorphy observed in a few

cyprinids (Cavender and Coburn, 1992). The posterior portion of the sphenotic is depressed as a fossa with an uneven dorsal surface, where the dilator operculi muscles attach, as in *Catostomus* (Weisel, 1960). The anterior and medial borders are roughly perpendicular to each other and together fit into the lateral concavity of the frontal (Fig. 2.3C).

The pterotic attaches posterior to the sphenotic, lateral to the parietal, and anterior to the epiotic (3B, 3C, 4B). Its main portion is located dorsal to the concave margin of the opercle, with a sizeable posterolateral process directed posteriorly and partly overlain by the posttemporal (Fig. 2.3C, 4C). It has no smooth plate, but rather has a vertical ridge in the middle. The prominent ridge creates two fossae: the anterior one is composed of both the sphenotic and pterotic; the posterior one is small and surrounded by the ridge and a vertical process of the pterotic itself. These two fossae form a large lateral temporal fossa, which is more prominent on specimen IVPP V 12163.14a (Fig. 2.4B). Since there is no smooth lateral portion of the pterotic, it is not possible to have a bone enclosed sensory canal in the otic region. The otic sensory canal ("temporal canal" in some literature), which continues from the infraorbital canal and leads to the lateral line, is not associated with the pterotic. This condition resembles the temporal sensory canal that is detached from the otic bones in catostomids, but is unlike the bone enclosed otic canal in cyprinids.

The epiotic is similar to that of catostomids in its position posterolateral to the parietal, and unlike that in cyprinids, in which it is mostly posterior to the parietal (Fig. 2.3B, 3C, 4B). The superficial part contributing to the skull roof is small, triangular, and pointed ventrally.

The supraoccipital is not visible on most specimens, indicating it is not located on the

dorsal surface of the skull as it is in cyprinids. It more likely forms only the posterior skull wall, as in catostomids. Its size, including the supraoccipital process, is similar to that of the parietal (IVPP V 12163.2b).

A pair of large otoliths is found in several specimens (IVPP V 12163.1a, 2b, 3, 18b and 21b). They are located close to the opercular arm (anterodorsal condyle) and opercular fossa (the socket below the opercular arm for the hyomandibular) (Fig. 2.7A), and were probably enclosed in the otic chamber mainly by the sphenotic. They are ovoid, with a thicker dorsal portion. On IVPP V 12163.21b, a few otolith fragments are preserved posterior to, and not in contact with, the paired large otoliths (Fig. 2.7A). Since the asteriscus and saggita are both posteriorly situated, whereas the lapillus is anteriorly placed and large in cypriniforms (Adams, 1940), I interpret the large, paired otoliths as lapilli from the left and right utricular vestibuli.

Jaws, Palate, and Hyoid Arch—†*Jianghanichthys* has a terminal and edentulous mouth. The gape is bordered by both maxilla and premaxilla. In IVPP V 12163.2b, 16, and 17, the fish is preserved with its mouth agape, giving a good view of individual bones of the jaws (Fig. 2.5B-D, 6A, 7B).

The premaxilla is triangular and flat. Its alveolar process is a little longer than its ascending process (Fig. 2.6A, 7B). The dorsal end of the ascending process has a small projection, which serves as a site for ligament attachment (IVPP V 12163.2b). The medial margin of the ascending process, where left and right premaxillae meet in a symphysis, is long and straight. This indicates that the premaxilla extends dorsally to a point adjacent to the midline as is common in

cypriniforms, and unlike the condition in other ostariophysans, in which the dorsal-most point of

the premaxilla is more laterally located (Fink and Fink, 1981).

The ventral portion of the maxilla has the basic shape found in cypriniform fishes,

including a dorsal constriction (neck), a broad body, and a dentary process (Fig. 2.5B, 7B). The

dorsal portion has three dorsal processes: a premaxillary process extends to the ascending process

of the premaxilla, a posterodorsal process extends more posteriorly, towards the ethmoid region,

and the third process arises from the neck and projects posteriorly (Fig. 2.5B, 7B). The

premaxillary process is delicate and pointed, extending to the dorsal-most point of the premaxilla.

The posterodorsal process is large and robust, with a laterally compressed body and a knobbed end.

The posterior process from the neck is small and is situated right below the posterodorsal process.

Both the neck and the three dorsal processes are curved and inclined medially, a trait that is not

visible in lateral view of the preserved material, except for a laterally visible maxilla neck on IVPP

V 12163.14a. The body of the maxilla has a rounded ventral keel and a posterodorsally extended

dorsal keel. The dentary process (ventral strut directed to the dentary) is knob-shaped.

In lateral view, the autopalatine commonly consists of three rami: a dorsomedial one abuts

the ethmoid, an anterior one is directed anterodorsally to the maxilla, and a broad ventral one is

directed towards the endopterygoid and probably also contacts the ectoperygoid. These three rami

are short, blunt, and not fully developed. The dorsomedial ramus and the conjunction of the three

rami are usually visible in the specimens, but the anterior ramus is covered by the maxilla and the

ventral ramus is overlain by the lacrimal (Fig. 2.3B, 3C). The body of the autopalatine (the

conjunction of the three rami) is exceptionally robust and bears a lateral projection at its anterior and another at its posterior end. Compared with that of other cypriniforms, the ventral ramus is anteriorly directed, rather than posteriorly, indicating that the autopalatine is more posteriorly located.

The dentary is roughly the same general shape as those found in other cypriniform fishes bearing the anterior gnathic ramus, the posterodorsal coronoid process, and a posteroventral process (Fig. 2.5C, 5D). However, the dorsal surface of its anterior end is distinctly broad and triangular (Fig. 2.5C, 5D, 6A), rather than the typical narrow band shape. In lateral view, the gnathic ramus is short, and the coronoid process little developed, whereas the posteroventral process is elongated (Fig. 2.5C, 5D). The mandibular sensory canal is enclosed in bone along the ventromedial edge of the dentary. There are two sensory canal openings on the lateral surface; one is located at the angle of the bone just below the ridge, and the other one is in the middle of the posteroventral process (IVPP V12163.15 and 16, Fig.5D). A prominent longitudinal ridge extends from the anterior end of the gnathic ramus to the posterior end of the dentary, along the edge where the dorsomedial surface and lateral surface meet. In a cross-sectional view of a broken specimen, the ridge is hollow, supporting the inference that the sensory canal is enclosed in the bone (IVPP V 12163.19a). In medial view, there is a prominent depression between the dorsal end of the anguloarticular and the medial side of the dentary, indicating Meckel's cartilage and possible a coronomeckelian were present as in other cypriniforms (IVPP V 12163.16).

The anguloarticular is nearly rectangular, and is the same size as the posteroventral process

of the dentary (IVPP V 12163.15). In lateral view, it consists of an anterior lamina and a large posterior socket for the quadrate articulation. It is mostly visible where it is exposed dorsal to the posteroventral process of the dentary (Fig. 2.3C, 6A). A few sensory canal openings close to the ventral margin of the anguloarticular are present from the junction of the anguloarticular and retroarticular to the bottom of the socket. The preopercular sensory canal continues from there posteriorly. The retroarticular is a small rectangular and laterally flattened bone attached to the ventral surface of the anguloarticular and the posterior end of the dentary (Fig. 2.3C).

The quadrate (Fig. 2.3B, 3C, 6A) possesses an anterior condyle that articulates with the anguloarticular, a roughly square dorsal part, and an elongated ventral strut. The ventral strut, extending posteriorly, is short, robust and truncated compared to that of other cypriniforms. The condyle is large, fitting into the sizable socket of the anguloarticular. The unusually large symplectic (Fig. 2.3B, 3C) is rod-like, extending far beyond the end of the ventral strut of the quadrate. Anteriorly, the symplectic fits into the slot between the dorsal part and the ventral strut of the quadrate.

The urohyal consists of a broad vertical median plate and two lateral willow-leaf-like laminar plates. It thickens at the anterior end of the median plate where it articulates with the ventral hypohyals. The posterior part of the lateral lamina is free from the vertical plate (IVPP V 12163.15; Fig. 2.3B, C). The ceratohyal is only preserved and visible on a medially preserved specimen (IVPP V 12163.19a). The anterior ceratohyal is slender and its posterior process is well developed. The posterior ceratohyal is larger than the posterior process of the anterior ceratohyal.

The hyomandibular is complex in shape, but overall it is deep, slightly curved, triangular (IVPP V 12163.16, Fig. 2.3C, Fig. 2.6A), and robust, consisting of two prominent facets dorsally and a strut ventrally. The anterior dorsal facet that articulates with the pterotic and the sphenotic is broad and flat. The posterior facet, articulating with the opercular fossa, is large and ball-shaped. The ventral strut is truncated and curved, concave anteriorly. A narrow flange of bone is present anteriorly from the upper border of the ventral strut to its ventral end. The posterior edge of the hyomandibular is curved, convex posteriorly, and lacks projections.

Orbital Region—There are four infraorbital bones visible including the lacrimal. The sensory canal is partly bone-enclosed but for the most part extends in an open groove (Fig. 2.3C). It is possible that the canal was completely bone-enclosed or ossified like that of all other cypriniform fishes, but broken during preservation because of its raised position on the bone and the thinness of the infraorbital bones. The lacrimal (Fig. 2.3B) is not exceptionally enlarged compared to the more posterior infraorbitals 2–4, unlike the enlarged lacrimal of most cypriniforms. Infraorbitals 2–4 are robust and deeper.

The supraorbital is present, immediately above the orbit (Fig. 2.3, 4), anterior to the anterolateral wing of the sphenotic, and ventrolateral to the frontal. It is large and semicircular, resembling in this respect that of some catostomids and cyprinids, and differing from the small and lunate bone or the total absence of the bone in some other cypriniforms. Since the frontal is not part of the orbital margin, the supraorbital contacts the sphenotic, of which the anterolateral wing reaches the orbital margin. A large supraorbital, not greatly enlarged lacrimal, and a sphenotic

forming part of the orbital margin have been hypothesized as primitive conditions in cyprinids (Cavender and Coburn, 1992).

Opercular Series, Hyoid Elements, and Branchial Arches—The opercular series includes an opercle, preopercle, subopercle, and interopercle (Fig. 2.3B, 3C, 6A). The opercle resembles those of Catostomidae in having a broadly concave dorsal edge, a prominent opercular arm (Fig. 2.6A), and an auricular process (posterodorsal process; Fig. 2.6A). However, unlike that of all catostomids, the opercular arm is pointed and flat rather than rod-like and robust, and the auricular process is also pointed rather than rounded. Moreover, the opercular fossa (Fig. 2.6A), a medial socket where the hyomandibular articulates, is far below the concave dorsal edge, whereas it is almost at the same level as the edge in catostomids. Furthermore, the ventral border is nearly horizontal. Fine external striations radiate from the base of the opercular arm towards the periphery. A foramen is located at the base of the opercular arm. The remains of a small ossicle (Fig 3C) close to the foramen indicates there might be a short opercular sensory canal present (Fig. 2.5A) which, if true, would have transferred the preopercular sensory canal to the otic region as it does in most cyprinids, such as cyprinins and barbins (Cavender and Coburn, 1992).

The preopercle (Fig. 2.3B, 3C, 6A) has moderately broad vertical and horizontal arms that meet at an obtuse angle (IVPP V 12163.14a and 15). The vertical arm is almost equal in length to the horizontal arm. The preopercular sensory canal is partially enclosed in the bone. On the vertical arm, there is no evidence for a sensory canal opening or foramen, suggesting the sensory canal might be detached from the bone, whereas the sensory canal is completely enclosed in the bone

with a few openings along its length in the horizontal arm. A continuous ridge divides the vertical

arm into wider anterior and narrower posterior portions, and the horizontal arm into wider dorsal

and narrower ventral portions. In the horizontal arm, the openings of the sensory canal are along

the ridge, whereas the non-bone-enclosed sensory canal in the vertical arm might have been behind

the ridge.

The interopercle is largely covered by the opercle and preopercle (Fig. 2.3B, C). The

subopercle is broad; its dorsal edge is slightly overlapped laterally by the lower edge of the opercle.

The ventral edge is broadly rounded.

The three branchiostegal rays decrease in size anteroventrally (Fig. 2.3B, 3C, 6A). The first

(most dorsal) ray sits beneath the interopercle and subopercle and is attached to the posterior

ceratohyal. The other two originate more anteriorly on the anterior ceratohyal (IVPP V

12163.19a).

The branchial arches are positioned just medial to the opercular series. They are visible in

specimens that are preserved in medial view or split into part and counterpart. However the

branchial area is usually crushed, even in laterally preserved specimens that are covered by a

complete opercle. The bony branchial arches are slender and flat, with porous surfaces. The gill

rakers are long, slim and pointed, indicative of filter feeding.

A few unusual structures were found on the medial surface of the opercle of IVPP V

12163.16. These are tiny, pointed spines resembling gill rakers, but with enlarged and vertically

compressed bases (Fig. 2.6B and C). Each enlarged base has an enamel-like surface, which is

similar to that of the flat pharyngeal teeth of Catostomidae; it is probably the same structure referred to as a pharyngeal tooth of †*Jianghanichthys* by Liu and Chang (2009). Since IVPP V 12163.16 represents the only specimen with these unique structures consisting of a tooth-like base and gill raker-like spine, I hesitate to interpret them here as either gill rakers or pharyngeal teeth, and instead leave them as structures of doubtful homology.

It is noteworthy that no enlarged pharyngeal teeth were discovered in the original fossil sample, of which many opercular areas of complete specimens were prepared and exposed by technicians in the 1990s. I also tried to find a pharyngeal tooth in specimen IVPP V 18858.1 (Fig. 2.8A), which was well covered by matrix when collected, by opening and dissecting its opercular area, but could find no evidence of pharyngeal teeth. As a comparison, we performed the same preparation on specimen UALVP 40844, an incompletely exposed specimen of †*Amyzon aggregatum*, by opening and dissecting its opercular area (Fig. 2.8C). In the latter preparation, two small pharyngeal teeth were easily found (Fig. 2.8B). I conclude that either †*Jianghanichthys* has no pharyngeal teeth, or else it bears very fine teeth resembling the aforementioned raker-like structures.

Vertebral Column—There are 32 or 33 vertebrae in total, with about 20 in the abdominal and 12–13 in the caudal region. The first four are modified as the Weberian apparatus (IVPP 12163.15, Fig. 2.3A, 3C, and 7D). The first centrum has a prominent posterior concavity and is about the same size as the second centrum. It is unlike the condition in known cypriniforms, in which the first centrum is thin and disc-like, because of strong modification for the Weberian

apparatus. The second and third vertebrae are not fused together (Fig. 2.3B, 3C; IVPP V 12163.15). It is difficult to trace the outline of the neural complex of these two vertebrae, but clearly it is small, with its length only half that of the neural spine of a non-Weberian vertebra. The neural spine on the fourth vertebra is short, and about half the size of more posterior ones. The fourth pleural rib (that on the fourth vertebra) is noticeably short, slender, rod-like, projects anteroventrally, and has a hooked end. It is less than half the length of normal ribs (IVPP V 12163.20, Fig. 2.7D). The fourth pleural rib articulates with centrum 4 by means of a pyramidal root fitting into an enlarged ventrolateral pit. The root has a triangular fenestra at the proximal end, resulting in a bifurcated appearance (Fig. 2.3B, 3C; IVPP V 12163.15). The posterior branch of the root projects medially and contributes to the os suspensorium.

Neural spines of non-Weberian and non-ural vertebrae are visually short, although the body of †*Jianghanichthys* is very deep. To determine whether the short neural spine is a false impression given by the relatively deep body, I compared the neural spine length of †*Jianghanichthys* with that of two deep-bodied Eocene catostomids, †*Amyzon aggregatum* and †*A. hunanense*. I graphed the regression of the neural spine length against standard length to remove any effect of size. To be consistent, the lengths of neural spines were all measured on the first caudal vertebra. †*Jianghanichthys* has a clearly shorter neural spine length in both juvenile and adult fish (Fig. 2.9), despite the extremely deep body of many of its adult specimens.

The intermuscular bones are rarely observed in adult specimens, perhaps because of the thick covering of scales, but can be seen in younger specimens. They extend at a shallow angle to

the vertebrae, from the anterior end of the trunk to the caudal skeleton dorsally, and in the caudal region ventrally. It is hard to tell where these fragile and delicate bones attach, but they are probably of the epineural and epipleural series, respectively, as in other cypriniforms (Patterson and Johnson, 1995).

Paired Fins and Girdles—The pectoral fin is short (Fig. 2.3A) compared to that of the Eocene catostomid †*Amyzon*, in which the end of the longest pectoral fin ray is close to the origin of pelvic fin. The pectoral fin of †*Jianghanichthys* is composed of 15 principal rays, of which the first one is not branched and the rest are branched (i,12–13). The first branched fin ray is the longest. Four pectoral radials support the fin rays: lateromedially the first one (counting from dorsal to ventral) is elongated, the second one triangular, the third squarish and the ventral-most one is sesamoid (IVPP V 12163.15 and 19b).

The posttemporal (Fig. 2.3C) is a small, slender, flat bone sitting vertically behind the parietal and above the supratemporal. It bears the sensory canal that extends from the posterior edge of the parietal (IVPP V 12163.14a).

The supracleithrum (Fig. 2.3B, C) is long, slender, and tapered dorso-ventrally with a deep groove along the midline of its lateral side. Its ventral portion overlaps the cleithrum laterally behind the anterolateral flange of the cleithrum.

The cleithrum (Figs. 3A, 3C, 6A) is gently curved, and bears a medially expanded and curved flange. It has a vertical ramus and an anteroventral ramus in lateral view. The vertical ramus has a groove created by an anterolateral flange. The groove is continuous with that of the

supracleithrum.

The postcleithrum (Fig. 2.6A) is a thick, rod-like bone consisting of a dorsal ramus and a ventral ramus. The dorsal ramus is straight, vertical and attached to the cleithrum. It is slightly shorter than the ventral ramus. The ventral ramus is slightly curved, and has a free end. Both left and right postcleithra are usually visible on laterally preserved specimens.

The pelvic fin consists of five principal rays, of which four of them are branched (i,4). The pelvic splint preceeding the pelvic fin rays is short, less than 20% the length of the longest pelvic fin ray. The basipterygium (Fig. 2.2B) is long and flat, anteriorly reaching a point below the fifth pleural rib (IVPP 12163.2a and 19a). Although the bone is partly preserved on some specimens, there is no evidence as to whether it is bifurcated or not.

Dorsal and Anal Fins— The dorsal fin is triangular and emarginate, with a high leading edge (by comparison, that of †*Amyzon* is much longer and not as high, but also emarginate). The origin of the dorsal fin is slightly posterior to the middle of the body, with a predorsal length of about 52% of SL (range 50–52%). The dorsal fin is composed of 12 or more, usually 13, principal rays and two or three procurrent rays, supported by 12 or usually 13 pterygiophores. The first principal ray is segmented but not branched, whereas the rest are segmented and branched (iii–iv, 11–12). The last two small rays both articulate with a single pterygiophore and are supported by a small element known as a "stay" (Weitzman, 1962) as is common in other cypriniforms (see description of anal fin below), and so they are counted as one (doubled) principal ray.

The origin of the anal fin is below a point posterior to the end of dorsal fin and has a similar

48

high, triangular, slightly emarginate shape. The anal fin consists of 7 principal and two procurrent rays (ii,7), supported by 7 pterygiophores. Principal rays 2–7 are segmented and branched, as in other cypriniform fishes. The last (doubled) principal ray is comprised of two independent but articulated rays, as is typical in cypriniforms. However, the longest and most anterior ray, forming much of the leading edge of the fin and interpreted here as the first principal ray is, unlike that in any other cypriniform, branched (Fig. 2.4C, D). The first principal ray in cypriniforms is normally the leading-edge ray, and is usually the longest, segmented (soft) ray (Hubbs and Lagler, 1947; 2004). But in some cyprinids, specifically members of the subfamily Cyprininae, the first principal ray is modified into a short and robust (unsegmented) pseudospine with posterior serrations. Arratia (2008) defined principal rays as including only one segmented, unbranched ray (the posteriormost unbranched ray) plus the following branched rays of the fin, as is typical of other cypriniforms (Hubbs and Lagler, 1947). Both definitions apply to the condition of the dorsal fin in †*Jianghanichthys* very well. However, although the latter definition is applicable to most actinopterygian fishes, it does not describe the situation in †*Jianghanichthys*. The last unbranched ray in the anal fin of †*Jianghanichthys* is much too short to reach near the tip of the fin and is only segmented near its tip, and thus is better interpreted as a procurrent ray. The main leading-edge ray of the anal fin is the long and stout first branched ray, and I interpret it here as the first principal ray. This unusual feature has been found in all our specimens that preserve a good view of the anal fin, and I conclude that it is a true feature of the species, and different from that in all other cypriniforms.

If we were to apply the definition of the first principal fin ray from Arratia (2008) to the anal fin of †*Jianghanichthys*, there would be a very short first principal anal fin ray, i.e., the last unbranched ray. In that case, the anal fin ray that forms the leading edge of the fin would be identified as the second principal ray. Even so, the anal fin of †*Jianghanichthys* would still differ from that of all other cypriniform fishes in having a very short first principal anal fin ray and a second principal fin ray forming the leading edge of the fin.

Pterygiophores supporting both dorsal and anal fins are thick and medially broad. It is probable that the muscular arrangement in †*Jianghanichthys* was similar to that of most teleosts (e.g., salmonids: Greene and Greene, 1914), including cypriniforms such as zebra fish (Schneider and Sulner, 2006). Thus, †*Jianghanichthys* probably had thick, antagonistic erector and depressor muscles (erector dorsalis and depressor dorsalis for the dorsal fin and erector analis and depressor analis for the anal fin) attached to the anterolateral and posterolateral sides of the pterygiophores. These two groups of muscles functioned to erect and depress the fin rays and, together with more laterally placed inclinator muscles on each side, worked to stabilize the body in an upright position. The robust size of the pterygiophores suggests relatively stronger fin muscles than in most cypriniforms, helping to stabilize this deep-bodied fish even with its low number of median fin rays.

The posterior-most element supporting the last (doubled) anal-fin ray is very small and has no spinous portion, resembling that in modern cypriniforms. It has been called a "stay" or "end-piece" by Weitzman (1962) in a study of the osteology of *Brycon*. The last (doubled) fin ray,

which is supported by the stay, actually is in series with the last pterygiophore, which supports the next-to-last fin ray. Therefore, the stay was not counted as a pterygiophore in the counts given above.

Caudal Skeleton and Fin—The caudal skeleton includes a compound centrum, which in cypriniforms is conventionally considered to represent a phylogenetic fusion of the first preural and two ural centra (as also supported by the ontogenetic work of Grünbaum et al., 2003 on the catostomid *Moxostoma hubbsi*), though in some teleosts corresponding elements can develop from fewer or more ural-centrum primordia (Schultze & Arratia, 2013). The caudal skeleton also contains a pleurostyle, which at least in catostomids is formed from a pair of modified anterior uroneurals (Grünbaum et al., 2003). In addition, the caudal skeleton of †*Jianghanichthys* (Fig. 2.7C) includes one parhypural, six hypurals, one epural, a rudimentary neural arch on the compound centrum, and paired, posterior, free uroneurals that are only occasionally seen. The neural arch of the parhypural bears paired hypurapophyses, processes that are important sites of muscle insertion (Nursall, 1963). Hypural 1 and the parhypural are very likely fused with each other at their proximal ends (as in other cypriniforms, e.g., Moxostoma: Grünbaum et al., 2003), and the two elements articulate proximally with the compound centrum, which is considered a synapomorphy of Cypriniformes (Conway, 2011). Hypural 2 is fused proximally to the compound centrum, whereas the proximal parts of hypurals 3−6 abut but do not fuse with the pleurostyle of the compound centrum. Hypural 6 is small and may be absent from some specimens (IVPP V 12163.1b). There appears to be a small gap, wider distally, between hypurals 2 and 3 (the caudal

diastema, e.g., Schultze & Arratia, 2013).

The caudal fin is deeply forked in small individuals but only slightly forked or broadly emarginate in large individuals (Figs. 2, 3A, 4A, 7A). There are 19 principal rays; of these, nine segmented and branched rays support the dorsal lobe, and eight support the ventral lobe; each lobe has one segmented but unbranched ray at its leading margin, included in the principal ray count. There are four, or occasionally five, dorsal procurrent rays, whereas there are four, or rarely three, ventral ones.

Scales—The scales of †*Jianghanichthys* are cycloid, large, thick, and ovate. There are about 35 lateral-line scales. The focus is closer to the anterior than to the posterior margin. Posterior radii are very strong and numerous (range 6–14), whereas the anterior radii are comparatively weaker and fewer (1–9). The strong radii, especially longitudinal ones in the center of the scales, are aligned with those from adjacent anterior and posterior scales. This results in the appearance of strong, longitudinal, parallel lines on bodies of the fossil specimens (Figs. 2, 3). The lateral line, which pierced the scales, is complete and arched.

Discussion

Comparison with Other Cypriniforms

†*Jianghanichthys* undoubtedly belongs to the order Cypriniformes, an assignment based on the morphology of the first four vertebrae contributing to the Weberian apparatus, the autopalatine consisting of a dorsomedial process abutting the ethmoid, the premaxillae meeting at the dorsalmost point close to the midline, and presence of three branchiostegal rays (Fink and Fink, 1981; Conway et al., 2010). Lei (1987) also mentioned that the second centrum bore both transverse and pleural parapophyses. Although I cannot confirm the presence of these parapophyses, or the presence of particular Weberian ossicles, the first four vertebrae are unambiguously modified such that the fourth centrum bears short modified pleural ribs and neural spine. Moreover, the dorsal portion of the maxilla is divided into premaxillary and robust posterodorsal processes. It is possible that the space between the processes where they met their counterpart in the midline housed a cartilaginous structure, the kinethmoid, which is ossified in many cypriniforms and functioned in jaw protrusion (Staab and Hernandez, 2010), but I can only infer its presence from the processes on the maxillae.

Unlike the strong support for a cypriniform assignment based on synapomorphic features, the familial assignment of †*Jianghanichthys* has been uncertain since its original description (Lei, 1977, 1987; Chang and Chen, 2008; Liu and Chang, 2009). It is excluded from Gyrinocheilidae, Psilorhynchidae, Cobitidae, Bottidae, Balitoridae, Nemacheilidae, and Vaillantellidae, because it lacks an inhalant aperture dorsal to the opercle (present in gyrinocheilids), it retains a posttemporal

and postcleithrum (absent in psilorhychids), it lacks an erectile spine below the eye (present in cobitids and bottids), and the lateral process of its second vertebral centrum does not reach or fuse to the fourth pleural rib (fused in balitorids and nemanchelids, in contact in vaillantellids) (Conway, 2011; Bird and Hernandez, 2007). Comparison with cyprinids and catostomids also did not yield a straightforward assignment. Shared features of †*Jianghanichthys* and cyprinids include presence of 19 principal caudal fin rays and sensory canals enclosed in the bone. Upon comparison with other cypriniform fishes, characters shared between †*Jianghanichthys* and cyprinids were determined to be symplesiomorphies. In addition, based on some uniquely shared characters, we also initially assigned †*Jianghanichthys* to Catostomidae (Liu et al., 2010). However, in subsequent analyses, we realized that †*Jianghanichthys* does not share several key synapomorphies of the Catostomidae, such as superficial cephalic sensory canal (not enclosed in bone), presence of descending ventral process of the second vertebral centrum that is fused to the fourth pleural rib, and reduction to 18 principal caudal fin rays. Thus, †*Jianghanichthys* cannot be considered a catostomid.

Several significant autopomorphies also distinguish †*Jianghanichthys* from any recognized family. Firstly, the first principal anal fin ray is branched. In cypriniform fishes, the first principal dorsal or anal fin ray is usually the leading-edge ray, which is segmented (except for cyprinids with a pseudospine) but unbranched. A branched first principal anal fin ray (Fig. 2.4C, D) has never been seen in cypriniform fishes (pers. oberv.; pers. comm., G. Arratia). This condition is similar only to that in some of the primitive teleosteomorphs (the Mesozoic pachycormiforms,

aspidorhynchiforms and pholidophoriforms), in which the main leading marginal dorsal and anal ray is segmented and branched (Arratia, 2008), but the condition in †*Jianghanichthys* is undoubtedly a convergence with the condition in those groups.

Second, the supraorbital sensory canal is largely exposed in frontal but roofed by a longitudinal flange. The supraorbital sensory canal is detached from the frontal in catostomids and loach families, but enclosed well within the bone in cyprinids and gyrinochelids. The sensory canal ossicles of catostomids extend laterally to the longitudinal ridge of the frontal. In †*Jianghanichthys*, the sensory canal extends under a longitudinal flange (Fig. 2.3C, 4B) similar to that of catostomids, but it is enclosed or at least partially enclosed in the frontal with a few openings, somewhat resembling the condition in cyprinids.

Third, the supraorbital sensory canal is unusual in that it meets the otic sensory canal within the parietal, and continues as the temporal sensory canal to meet the supratemporal commissure (Fig. 2.5A, 6A). Among cypriniforms, gyrinochelids possesses the most similar distribution of skull roof sensory canal to *Jianghanichthys*. They both have the supraorbital sensory canal extending posteriorly to join the otic canal, and then towards the supratemporal commissure. However, the supraorbital sensory canal meets the otic sensory canal on the sphenotic and continually through the otic region in gyrinochelids, instead of meeting in the parietal as in the *Jianghanichthys*.

Fourth, the maxilla of †*Jianghanichthys* bears three independent dorsal processes (Fig. 2.5B), a condition that is found in neither catostomids nor cyprinids. The broad dorsal surface of

the anteromedial part of the dentary is also very different from the slim and narrow dorsal surface commonly observed in cypriniforms.

Lastly, the first centrum of †*Jianghanichthys* has a similar size and prominent posterior concavity to the second centrum. The first centrum is usually antero-posteriorly foreshortened in fishes with a Weberian apparatus, such as cypriniforms, siluriforms, and characiforms. Compared to the second centrum, the first one in †*Jianghanichthys* is not highly reduced as it is in other otophysans.

In addition to these unique characters, †*Jianghanichthys* also has a suite of osteological characters that contribute to difficulties in its taxonomic assignment. Because it appears to be intermediate between Catostomidae and Cyprinidae, the following comparisons are made mainly with regard to those two cypriniform families.

Skull Roof—The shape of the frontal in †*Jianghanichthys* is similar to that of catostomids in consisting of a broad, fan-shaped anterior part and a rectangular posterior part. The posterior margin of the fan is straight. Some cyprinids also have a broader anterior than posterior part; however, the difference between them is never as distinct as in catostomids.

The sphenotic in †*Jianghanichthys* is prominently exposed and has a fan-shaped anterior process reaching the margin of the orbit, resembling that of catostomids. In contrast, most cyprinids have the sphenotic overlain by the frontal, with or without a small part exposed laterally. A few cyprinids have the sphenotic reaching the orbit, but much less so. This difference between the two families was noted a long time ago (Weisel, 1960), and is also consistent with my

observations.

The absence of a frontoparietal fontanelle in †*Jianghanichthys* resembles more closely the condition in cyprinids than in catostomids. In fossil and modern catostomids, except *Cycleptus*, the two parietals are almost always separated at their anterior end by a prominent frontoparietal fontanelle and at their posterior ends by the supraoccipital. The fontanelle also separates the posterior portions of the frontals.

Also unlike most catostomids, in †*Jianghanichthys*, two bone-enclosed sensory canals are present in the laterally elongated parietal. Such an elongated parietal has also been observed in the catostomid *Carpiodes*, but not in any of the other catostomids examined.

The main external part of the pterotic of †*Jianghanichthys* has no smooth lateral surface and has an elongated posterolateral process directed posteriorly with a vertical ridge on top of it creating a lateral temporal fossa. In catostomids, the presence of one or two fossae dorsal to the long process of the pterotic is also very common. However, most have a smooth plate externally at the anterior part, except in *Carpiodes* and *Myxocyprinus*. Some catostomids, such as *Minytrema*, *Moxostoma*, and *Hypentelium*, have one vertical ridge on the long process of the pterotic, whereas others have two vertical ridges (e.g., *Catostomus*). The pterotic of cyprinids, unlike that of †*Jianghanichthys* and catostomids, usually has a large, smooth plate laterally, and there is no fossa created by its posterolateral process. The pterotic of †*Jianghanichthys* is thus more similar to but not identical to the pterotic of catostomids.

The epiotic of †*Jianghanichthys* is more lateral to the parietal, also resembling that of

catostomids. In cyprinids, it is usually found posterior to the parietal and composes the posterior skull wall. In †*Jianghanichthys*, the parietal is extended posteriorly and probably contributed to the posterior skull wall.

Jaws, Hyomandibular, and Opercular Series—The premaxilla of †*Jianghanichthys* is broad and triangular, with the alveolar limb slightly longer than the ascending process (3B), a condition far different from that of cyprinids, which have a long, slender and curved alveolar process forming the whole upper mouth margin. This is also different from the common "L" shape in catostomids. In modern Catostominae, the alveolar process is slightly shorter to much shorter than the ascending process, and in Ictiobinae, Myxocyprininae, and Cycleptinae it is equal in length to or slightly longer than the ascending process. The fossil catostomid †*Amyzon* also has a slightly longer alveolar process than does †*Jianghanichthys*.

The gnathic ramus of the dentary in †*Jianghanichthys* is short, contributing to a 'short mouth' (Fig. 2.5C, D). Catostomids usually have a shorter mouth than cyprinids, associated with their benthic suction-feeding habits. The weakly developed coronoid process of the dentary of †*Jianghanichthys* is also similar to that of some catostomids such as *Myxocyprinus*, whereas the elongate posteroventral process resembles that of some other catostomids, for instance *Catostomus* and *Moxostoma*. However, the mandibular sensory canal is enclosed in the dentary of †*Jianghanichthys*, a feature shared with cyprinids but never observed in catostomids, including fossil taxa.

The hyomandibular of †*Jianghanichthys* is robust overall (6A), resembling more that of

cyprinids than that of catostomids, in which it is slender. The condyle articulating with the opercular fossa is large (Fig. 2.6A). In cyprinids and †*Jianghanichthys*, the posterior side of the hyomandibular has a sloped facet that is tightly connected to the preopercle; the anterior margin is slightly curved; the dorsal condyle articulating with the cranium is anteroposteriorly broad; and the ventral strut of the hyomandibular is short, truncated, and stout. In contrast, the hyomandibular in all catostomids has a groove along the posterior side that braces the preopercle, a roughly "S"-shaped anterior margin, a narrower dorsal condyle, and a slender ventral strut.

Catostomids can be distinguished from cyprinids in the shape of the opercular bone (Hussakof, 1932; Cavender, 1968), because the opercular arm and auricular process are differently developed. The opercular arm in catostomids is usually rod-like, though sometimes elongated and flattened (*Myxocyprinus*). Meanwhile, the auricular process is variable in size and somewhat in shape, but generally rounded at the posterodorsal corner of the bone (Nelson, 1949). The opercle of †*Jianghanichthys* also bears an opercular arm and a well-developed auricular process. However, both the opercular arm and auricular process are tapered and pointed at their ends, a condition never observed in catostomids (Fig. 2.6A).

The preopercle in cyprinids usually bears a well-developed, bone-enclosed sensory canal. In contrast, in the majority of catostomids, such as *Catostomus*, *Moxostoma*, *Deltistes*, *Chasmistes*, *Minytrema*, and *Hypentelium*, the sensory canal is completely detached from the preopercle, with a few small holes piercing the preopercle. Several catostomids, including *Carpiodes*, *Ictiobus* and the fossil genus †*Plesiomyxocyprinus*, have a ridge along the midline of the preopercle creating a

wider anterior half and narrower posterior half of the bone. Sensory canals are positioned along the ridge, and probably only loosely attached. For the other catostomids, e.g., *Myxocyprinus* and the Eocene †*Amyzon*, a partially bone-enclosed sensory canal is present in the preopercle. The canal is exposed on the vertical limb of the preopercle, but enclosed on the horizontal limb with an anteroventrally directed sensory opening. In †*Jianghanichthys*, the canal is also partly enclosed in the preopercle, resembling more the condition found in primitive catostomids such as *Myxocyprinus* and †*Amyzon*.

Abdominal and Caudal Region—The fourth pleural rib articulating with the fourth centrum is the only rib contributing to the Weberian apparatus. It is generally shorter and thicker than other pleural ribs. It is also a sizeable element easily observed in all cypriniforms, but has a different shape and size depending on the family. Catostomids have the most robust and longest fourth pleural rib among cypriniforms. The rib is fused with the descending process of centrum 2, much expanded laterally, and extends far ventrally, over half the length of the normal thoracic ribs (Nelson, 1948; Bird and Hernandez, 2007). Even in the Eocene †*Amyzon*, such a robust fourth rib is already present. Members of the loach families usually have their 4th pleural rib modified in variable shapes or reduced, and the overall shape of the os suspension is complicated. Cyprinids have the most variable fourth rib: some are robust, one-half abdominal rib length; some are short and broad, about one-third abdominal rib length; some are thick, short, and quickly taper to a distal point; and others are bifurcated distally (Bird and Hernandez, 2007). Even so, the fourth rib of cyprinids can be distinguished from those of catostomids, cobitids, and balitorids in its medium or

small size, in not being fused to the process from centrum 2, and in having a rod-like or other simple shape with little modification. In gyrinocheilids, the fourth rib is also large, bifurcated distally, very close to the process of centrum 2, but not fused. In †*Jianghanichthys*, the fourth pleural rib is slender, with a posteriorly hooked distal end, and short, with a length less than one-half that of the thoracic ribs. The lateral process of centrum 2 gives no evidence of contact or fusion with the fourth pleural rib, a condition more similar to that in cyprinids. Thus, a somewhat similar morphology to that in †*Jianghanichthys* may occur in some cyprinids, but not in other cypriniforms.

†*Jianghanichthys* has a shorter caudal region. First, its caudal peduncle is shorter than in the contemporaneous catostomid genus †*Amyzon*. Second, †*Jianghanichthys* also has a smaller number of caudal vertebrae, just 11–12, compared to 14–18 in †*Amyzon aggregatum*, 14–17 in †*A. brevipinne*, 14–15 in †*A. hunanense*, and ~20 in †*Plesiomyxocyprinus arratiae* (Wilson, 1977; Chang et al., 2001; Liu and Chang, 2009). Hubbs et al. (2004) stated that cyprinids generally have a longer caudal peduncle than catostomids. Therefore, †*Jianghanichthys* probably has a relatively short caudal peduncle compared to both cyprinids and catostomids.

Critical Characters of *Jianghanichthys* from CT scan

To clarify critical characters of *Jianghanichthys* identified through the course of this study, we CT scanned the skull region of a complete and matrix covered specimen (IVPP V 18858.2, SL 88.63 mm, head length 19 mm). The reconstructed CT slices confirmed the previous inference on

the absence of pharyngeal tooth in *Jianghanichthys*. Moreover, the delicate or medial structures that were not available from direct observation, such as the kinethmoid, the distribution of cranial sensory canal, and the delicate structures of Weberian apparatus are visible and traceable through CT slices (Fig. 2.10).

First, gill arches and filaments are preserved in situ; however, there is no evidence for developed tooth-like structure in gill area (Fig. 2.10A, B). It is possible a higher resolution CT scan will generate more precise details of the gill arches in the future. To the best of my knowledge, the pharyngeal tooth is either absent or not well formed, in *Jianghanichthys*, sharing the symplesiomorphy with gyrinochelids.

Second, the presence of the kinethmoid was previously inferred by the space between posterodorsal processes of right and left maxillae. The CT scan images confirmed that a delicate kinethmoid is bilaterally housed by the posterodorsal processes of the both maxillae (Fig. 2.10B). The kinethmoid is slender and rod-like, much smaller than the nearby processes of the maxillae. It is simple in shape and small in size compared to the other cypriniforms (Hernandez et al., 2007, p.633, Fig. 2.4).

Third, the bone-enclosed cranial sensory canal are traced and visualized through CT slices (Fig 10A, C), which confirmed the inferences based on the remains and opening of sensory canals. The temporal canal, continued from the supraorbital canal and probably the infraorbital canal, is enclosed within the parietal as reconstructed in Figure 5 (Fig.10 A). The opercular sensory canal, transferring the preopercular sensory canal to the otic region, is present as well (Fig. 2.10C).

Lastly, the Weberian apparatus shows a more complete view in the virtual slices complimenting the previous description. A small tripus is traceable, although none of the slices grant it a complete view (the scan did not provide good enough contrast to permit objective 3D reconstruction of the anatomy). The neural complex is thin and so it is hard to trace the margin, as in hand-prepared specimens. The neural spine of the centrum 4 is short, half the size of those on non-Weberian vertebrae. The 4th pleural rib is short, and ventral end is slightly hooked as in Figure 7. A medial groove, along the midline of 4th pleural rib, is about half-length of the rib (Fig. 2.10B). The centrum 2 and centrum 3 are not fused.

Summary of Osteological Characters and Taxonomy

To clarify the characteristics of *Jianghanichthys*, I herein combine and sum up the taxonomic informative characters obtained from observation, comparison, and CT scan images (Table 2.1). There is little doubt that *Jianghanichthys* is a distinctive cypriniform fish. A suite of synapomorphies shared with Cypriniformes secure the order assignment (Table 2.1). The series of unique apomorphies differentiate the *Jianghanichthys* from all known cypriniforms (Table 2.1). With such amount of significant difference, an attempt of designation to any known families of Cypriniformes would be denied, especially by comparing to the establishment of the recently recognized families of extant cypriniforms (Bohlen and Ŝlechtová, 2009; Kottelat, 2012).

Because the differences between *Jianghanichthys* and loach families (non-catostomid

cobitoids) are apparent, I searched for synapomorphies of *Jianghanichthys* within the basal, non-loach cypriniform families, i.e. Gyrinochelidae, Cyprinidae, and Catostomidae. Unfortunately, few synapomorphies have been found, whereas most of the shared morphology characters are considered plesiomorphies (Table 2.1). *Jianghanichthys* uniquely share the opercular sensory canal (Cavender and Coburn, 1992) with Cyprinidae, whereas share the dorsally concaved opercle created by developed opercular arm and auricular process with Catostomidae. *Jianghanichthys* and *Gyrinocheilus* are the only two known cypriniforms to lack pharyngeal teeth on ceratobranchial 5. This character is listed as a synapomorphy of Gyrinochelidae in Conway et al. (2010). Within the scope of ostariophysian, it is arguable the absence of pharyngeal teeth is a plesiomorphic character, since the sister group of otophysians, i.e. gonorynchiforms, have no teeth on ceratobranchial 5 (Grande and Poyato-Ariza, 2010).

The large number of unique symplesiomorphies shared by *Jianghanichthys* and aforesaid cypriniform families are not phylogenetically informative for its taxonomic assignment. However, those characters demonstrate that *Jianghanichthys* is a stem cypriniform, which does not belong to any recent family.

Phylogenetic Analysis

The most comprehensive and most recent morphological phylogenetic analysis of the Cypriniformes is that of Conway (2011). That author described 127 informative morphological characters, some of which were adopted and modified from previous phylogenetic studies, such as

64

those of Fink and Fink (1981), Sawada (1982), Siebert (1987), Smith (1992), and Johnson and

Patterson (1997). Two parsimony analyses were conducted, including species from nine families

of cypriniforms as the ingroup, and using basal members of characiforms, clupeiforms,

osteoglossiforms and elopiforms as four outgroups. Analysis 2 of Conway (2011) included 53

cypriniform species, whereas Analysis 1 excluded one taxon, *Psilorhynchus homaloptera*, which

was missing a large amount of data. As the first step of the analysis, I repeated these analyses using

the methods as in Conway (2011), with the only exception that I assembled the data matrix in

Mesquite v2.75 (Maddison and Maddison, 2011). The results are consistent with those of Conway

(2011), except that 100 equally parsimonious cladograms, rather than 98, were found.

Relationships among families were well resolved by both analyses (Fig. 2.11A). Conway (2011)

recognized two superfamilies, as is the prevalent classification, and nine families. The superfamily

Cyprinoidea includes Cyprinidae and Psilorhynchidae, whereas the superfamily Cobitoidea

contains Gyrinocheilidae, Catostomidae, and the loach families (Botiidae, Vaillantellidae,

Cobitidae, Balitoridae and Nemacheilidae). Two subfamilies of Cyprinidae, Cyprininae and

Leuciscinae, were also recovered. Within the Cobitoidea, the clade Gyrinocheilidae plus

Catostomidae was recovered as the sister group to the loach clade (Fig. 2.11A).

In a subsequent series of analyses, I performed two sub-analyses for each analysis: one

excludes *Psilorhynchus homaloptera* (A1, as Conway's "analysis 1"), and the other one includes it

(A2, as Conway's "analysis 2"). Both A1 and A2 generate the same step length, consistency

indices (CI) and retention indices (RI) for equally parsimonious trees, and the same topology for

the strict consensus cladogram in each analysis. The only prominent difference between A1 and A2 is that A2 usually generated more equally shortest trees. Therefore, the strict consensus trees described below and in figures are generated from both A1 and A2 for each analysis.

Our second analysis was conducted by simply adding the data for †*Jianghanichthys* to the unmodified data matrix of Conway (2011) (Fig. 2.11B). This changed the topology of Conway's consensus cladogram. In the strict consensus cladogram of 116 (A1) and 651 (A2) equally parsimonious trees, †*Jianghanichthys* was resolved in a polytomy with Catostomidae, Gyrinocheilidae, Cyprinoidea and the loach clade (Fig. 2.11B). This change probably results from the fact that †*Jianghanichthys* shares a large number of characters with both cyprinids and catostomids.

In the third analysis, I edited the data matrix and repeated Conway's analysis. Based on new observations, I modified seven characters for catostomids from Conway's data matrix: For Character 7 [anterolateral process of lateral ethmoid absent (0) or present (1)], the state for *Carpiodes*, *Myxocyprinus* and *Cycleptus* changed from '1' to '0'. The lateral ethmoid of catostomids is porous, concave and rounded in dorsal view. Only when the lateral ethmoid is detached from the ethmoid complex anteriorly, e.g., in *Catostomus*, does the anterior end of the lateral ethmoid look like an anterolateral process paralleling the median edge of the infraorbital 1. For Character 15 [postepiphysial fontanelle absent (0) or present (1)], the state for *Cycleptus* changed from '1' to '0'. All catostomids, including *Myxocyprinus* but with the exception of *Cycleptus*, possess a frontoparietal fontanelle (postepiphysial fontanelle). For Character 16

[supraorbital and otic sensory canals connected to one another (0) or disjunct from one another (1)], the state for *Catostomus* changed from '0' to '1' and that for *Carpiodes* and *Cycleptus* changed from '1' to '0'. According to new observation of catostomid specimens, only *Catostomus* shows the disjunction between the supraorbital sensory canal and the temporal sensory canal (otic sensory canal). Although I am not sure whether or not this condition of discontinuous sensory canal changes through ontogeny, the cleared and stained specimens show a state different from the coding of Conway (2011). For Character 32 [infraorbital series excluding first infraorbital comprised of four, roughly plate-like bones (0), or by variable number of small tubular ossifications around infraorbital canal (1)], the state for all catostomids changed from '1' to '0'. In juvenile catostomids, the infraorbital series posterior to infraorbital 1 is represented by small tubular ossifications around the infraorbital. Adult catostomids have the large, roughly plate-like infraorbital bones. For Character 45 [symplectic formed by simple dorsal lamina near metapterygoid (0) or with dorsal flanges forming suture with metapterygoid (1)], the state for Cycleptus changed from '1' to '0'. The dorsal surface of the symplectic of *Cycleptus* exhibits simple contacts and is not sutured with the metapterygoid. For Character 52 [anterodorsal head of opercle absent/short (0), or greatly elongate (1)], the state for *Cycleptus* and *Myxocyprinus* changed from '0' to '1'. The opercular arm (anterodorsal head of opercle in Conway (2011)) is greatly elongated in all catostomids. The criterion used in Conway (2011) is that of comparing the opercular arm to the auricular process (posterodorsal process). All catostomids have such an auricular process. However, the auricular process is well developed in some catostomids, but less so in others. The

opercular arm in catostomids is not only extended dorsally, but also rod-like and not laminar as in

other cypriniforms. For Character 123 [proximal tip of third hypural separate from associated

centrum (0) or fused with it (1)], the state for *Catostomus* changed from '1' to '0'. In certain

members of Catostomidae, such as *Carpiodes*, *Ictiobus*, *Myxocyprinus*, *Minytrema*, and *Cycleptus*,

the third hypural is fused with the compound centrum. The third hypural is tightly articulated

tightly in some other catostomids, such as *Catostomus* and *Moxostoma* (Liu and Chang, 2009).

With these additions and modifications, I repeated Conway's (2011) analyses. Some 14 and 106

equally shortest trees were found for analyses A1 and A2 respectively with identical step length of

288, CI 0.49, and RI 0.88. The strict consensus cladogram from both A1 and A2 shows

Gyrinocheilidae as the most basal clade of Cypriniformes, whereas Catostomidae are sister to

Cyprinidae plus Psilorhynchidae (Fig. 2.11C). These results differ from the consensus cladograms

of Conway (2011), which show the Gyrinochelidae as a sister group to Catostomidae. The

placement of Catostomidae with Cyprinoidea is also different from that of Conway (2011), in

which Catostomidae are basal to the loach clade (Fig. 2.11A). However, the clade of

Gyrinochelidae plus Catostomidae is not strongly supported with low value of Bremer (Decay

Index = 1) and Bootstrap support (0%) in the repeated analysis on Conway's original data.

Subsequently, I added data on †*Jianghanichthys* to the modified Conway data matrix and

performed the fourth and the main analysis (Table 2.2). The parsimony analysis generated 84

equally parsimonious trees for A1 and 596 for A2 with step length 292, CI 0.48, and RI 0.88.The

addition of †*Jianghanichthys* to the modified matrix resulted in a strict consensus cladogram with

a large polytomy among †*Jianghanichthys*, Gyrinocheilidae, Catostomidae, Psilorhynchidae, the

loach clade, and Cyprinidae (Fig. 2.11D). Among the equally shortest trees, †*Jianghanichthys* is

sister to the rest of the cypriniforms in 14/84 and 98/596 trees, sister to Catostomidae in 28/84 and

202/596 trees, sister to Catostomidae plus Gyrinocheilidae plus loach families in 14/84 and 98/596

trees, and sister to Cyprinidae or in a polytomy with the two subfamilies of Cyprinidae in 28/84

and 198/596 trees.

In an additional analysis, I set up a backbone constraint cladogram for the data matrix,

which includes †*Jianghanichthys* and uses the modified dataset from Conway (2011). The

constraint tree is extracted from a proposed phylogeny of otophysans by Chen et al. (2013) that is

the most recent molecular phylogenetic study of cypriniforms in a broad context. I constrain the

family interrelationships according to Chen et al. (2013:Fig. 2.2). Family Cyprinidae is sister to

Psilorhynchidae, and then together these are sister to the clade including the rest of the families, in

which Catostomidae are sister to Gyrinocheilidae plus the loach families (Fig. 2.11E). The

relationships among species within each family are not constrained because the taxa at the specific

level of Chen et al. (2013) are not compatible with ours. The families Cyprinidae and

Psilorhynchidae are not defined as monophyletic groups in the constraint tree, since Cyprinidae

are not monophyletic if one excludes the clade of psilorhynchids in the Chen et al. (2013) study.

One of the loach families, Nemacheilidae, is constrained as monophyletic as there was only one

representative of the family in Chen et al. (2013), whereas it was paraphyletic in Conway (2011).

An heuristic search on the data matrix enforced with the constraint tree generated 168 and 1176

best trees for A1 and A2 respectively with step length 302, CI 0.46, and RI 0.87. †*Jianghanichthys* is resolved in a polytomy with (Cyprinidae + Psilorhynchidae), Catostomidae, and (Gyrinocheilidae + loach families) in both strict and 50% majority rule consensus trees (Fig. 2.11F). Among the equally shortest trees, †*Jianghanichthys* is sister to the rest of the cypriniforms in 28/168 and 196/1176 trees, sister to Catostomidae + (Gyrinocheilidae + loach families) in 56/168 and 392/1176 trees, sister to Gyrinocheilidae + loach families in 28/168 and 196/1176 trees, and sister to Catostomidae in 56/168 and 392/1176 trees. It is interesting that none of the trees suggests †*Jianghanichthys* is sister to the Cyprinidae or to the Cyprinoidea clade.

One of the exploratory analyses was conducted by adding the Eocene fossil catostomid †*Amyzon*, which is consistently recovered within the Catostomidae throughout all the analyses. Another series of exploratory analyses was conducted by adding the basal ostariophysian *Chanos chanos* (Gonorynchiformes) as the fifth outgroup. The result through repeated analyses was nearly identical to that of the original analysis, excepting slight differences in the number and scores of the shortest tree from each analysis and the topography of the majority consensus cladogram of A2 using the revised data matrix with the data for †*Jianghanichthys* added. The character list and morphological data matrix, which was slightly modified from Conway (2011) and with additional data for †*Jianghanichthys hubeiensis*, †*Amyzon aggregatum*, and *Chanos chanos*, has been made available online at Morphobank (Project ID: 1104).

Thus, the addition of †*Jianghanichthys* significantly alters the results of Conway's (2011) morphological analysis, suggesting that much remains to be learned about the evolution of

morphological features in the Cypriniformes. Through the various analyses, the phylogenetic position of †*Jianghanichthys* has four possibilities: the most basal clade of Cypriniformes (about 1/6 of trees), the most basal clade of Cobitoidea (1/6), the sister group of Catostomidae (1/3), and the sister group (or in unresolved position) of Cyprinidae (1/3). †*Jianghanichthys* is equally as likely to be grouped with Cyprinidae as it is to be grouped with Catostomidae. These results, coupled with the absence in †*Jianghanichthys* of the defining synapomorphies of those groups, lead to the conclusion that †*Jianghanichthys* cannot be assigned to either Cyprinidae or Catostomidae under our current knowledge of cypriniforms. Thus, the Eocene of China was home to the first known fossil cypriniform that does not belong to any of the extant families of Cypriniformes.

Early Diversity and Biogeography of Cypriniforms

Cypriniform diversity as seen in the fossil record dramatically increased during the Eocene, though Eocene occurrences were until now without exception assigned to either Cyprinidae or Catostomidae. Whereas undoubted Eocene cyprinids have been reported only from Asia, catostomids were found in both East Asia and North America (Cavender, 1991; Chen et al., 2005; Chang and Chen, 2008).

There are three Eocene catostomid genera known so far: †*Amyzon*, †*Plesiomyxocyprinus*, and †*Vasnetzovia*. All of the Paleogene occurrences of catostomids in North America have been assigned to †*Amyzon* (Cope, 1872, 1874, 1875, 1893; Wilson, 1977; Grande et al., 1982). At least

four species of †*Amyzon* were distributed widely in western North America. Three of the five

species described by Cope have been considered valid (Bruner, 1991). One of these, †*A.*

brevipinne, was restudied in detail with additional materials (Wilson, 1977). Two additional North

American species, †*A. aggregatum* and †*A. gosiutense*, were also described more thoroughly

(Wilson, 1977; Grande et al., 1982). However, based on new observations, there might be more

than one genus occurring in North America in the Eocene, because fossils currently identified as

†*A. brevipinne* exhibit strong morphological disparity.

On the other side of the Pacific, one species of †*Amyzon* was also reported from Xiawanpu,

Hunan, southern China (Chang et al., 2001). Another genus, †*Plesiomyxocyprinus*, was reported

from Huadian, Jilin, northeastern China (Liu and Chang, 2009). A Siberian genus, †*Vasnetzovia*, if

valid, would be the third genus in East Asia (Sytchevskaya, 1986). As it currently stands, the

Eocene catostomid record presents a higher diversity at the generic level in East Asia than in North

America, pending further research on both continents.

In this context, the recognition of the new family †Jianghanichthyidae herein increases the

higher-level taxonomic diversity in East Asia. The significant morphological differences between

†jianghanichthyids and previously recognized families of cypriniforms points to a

morphologically diverse but still mostly undocumented radiation of cypriniforms in Asia.

The growing diversity of fossil catostomids and now †jianghanichthyids also coincides

with the relatively rich Eocene cyprinid record in East Asia (Cavender, 1991; Chang and Chen,

2008). Early fossil occurrences of cyprinids overlap the present day distributions of almost all the

major groups and subgroups of the family. Moreover, the existing collection of problematic early cypriniform fossils and the ongoing field discoveries in China promise that an even higher diversity of early cypriniforms will soon be recognized. Therefore, East Asia can be expected to play a vital and increasingly important role in our understanding of cypriniform evolution.

Table 2. 1 Osteological character summary of †*Jianghanichthys hubeiensis*. The determinations of apomorphic or plesiomorphic characters are based on comparison to other ostariophysians unless otherwise indicated.

Character type	Character status
Unique automorphies of †*Jianghanichthys*	● the first principal anal fin ray branched; ● the supraorbital sensory canal unusually meeting the temporal sensory canal within the parietal; ● the maxilla of †*Jianghanichthys* bearing three independent dorsal processes; ● dorsal surface of anterior end of dentary triangular and broad; ● the first centrum of †*Jianghanichthys* has a similar size and prominent posterior concavity to the second centrum;
Synapomorphies with Cypriniformes	● kinethmoid present (Fink and Fink, 1981); ● the autopalatine consisting of a dorsomedial process abutting the ethmoid (Fink and Fink, 1981); ● the premaxillae meeting at the dorsalmost point close to the midline, (Fink and Fink, 1981); ● three branchiostegal rays (Conway et al., 2010); ● hypural 1 and parhypural fused at proximal end (Conway, 2011);
Synapomorphies with Cyprinidae	● opercular canal present (Cavender and Coburn, 1992);
Symplesiomorphies with Cyprinidae	● cephalic sensory canal mostly enclosed in bones; ● fontanelle absent; ● 19 principal caudal fin rays (i,9,8,i);
Synapomorphies with Catostomidae	● both opercular arm and auricular process well developed creating a concave dorsal edge (modified from Smith, 1992);
Symplesiomorphies with Catostomidae	● mouth gape consist of both premaxilla and maxilla; ● sphenotic exposed with anterior wing reaching the orbit; ● centrum 2 and 3 not fused;
Symplesiomorphies with Gyrinochelidae	● pharyngeal tooth absent.

Table 2. 2 Character states for †*Jianghanichthys* hubeiensis. Descriptions and states of characters for the rest of ingroup and outgroup taxa can be found in Conway (2011), with modifications discussed in text.

Characters	1–10	11–20	21–30	31–40	41–50	51–60
States	???0001000	0???00010?	??????00?1	000111??0?	?000000?0?	0111000011

61–70	71–80	81–90	91–100	101–110	111–120	121–127
12100?????	??????0???	???????10?	???00?00?0	00??00???0	100??00011	200000?

Figure 2. 1 Map showing the location of the fossil locality for †*Jianghanichthys hubeiensis* at Songzi, Hubei Province, China (labelled with a star) and the other two possible localities Dangyang and Yidu. Numerous tributaries of the Yangtze and Hanshui rivers are omitted due to layout constraints.
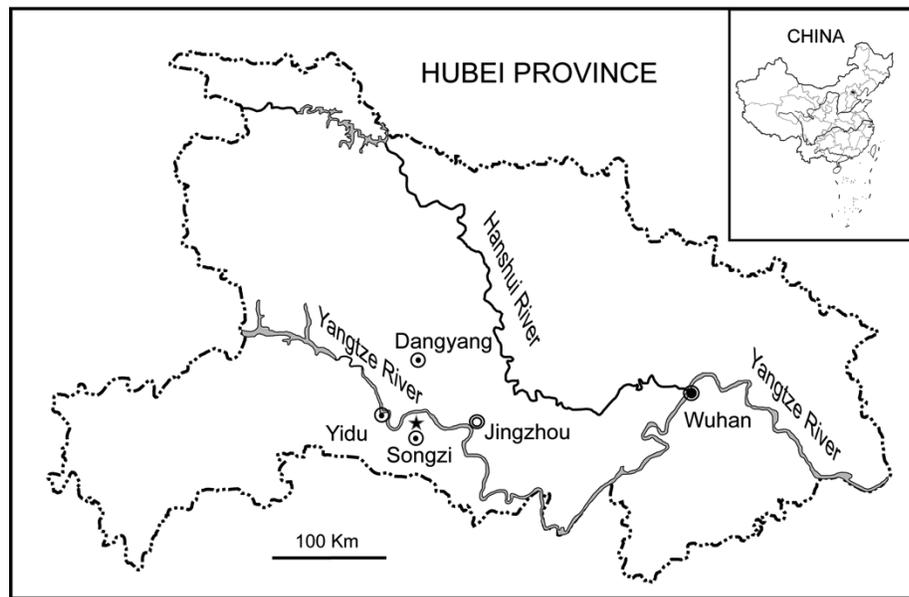
Figure 2. 2 †*Jianghanichthys hubeiensis* in right lateral view. A, lectotype, GMC V1810-1; B, a juvenile, IVPP V 12163.17. Scale bar equals 1 cm.
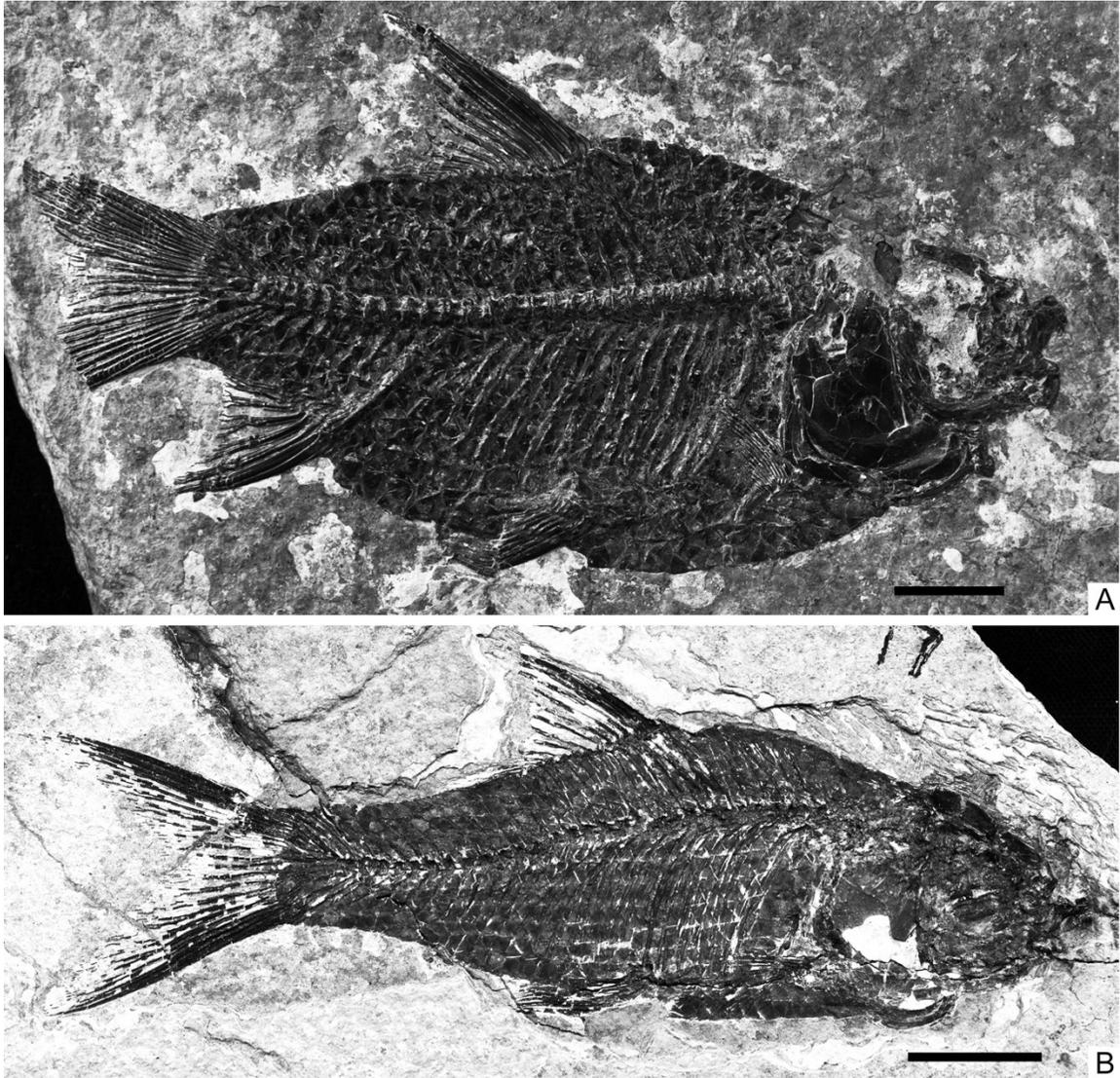
Figure 2. 3 Well-preserved specimen of †*Jianghanichthys hubeiensis* showing osteological features (IVPP V 12163.15). A, photographed complete fish in right lateral view, scale bar equals 1 cm; B, interpretive drawing of skull including pectoral girdle and Weberian apparatus; **C**, photograph of head region of A coated with ammonium chloride sublimate.
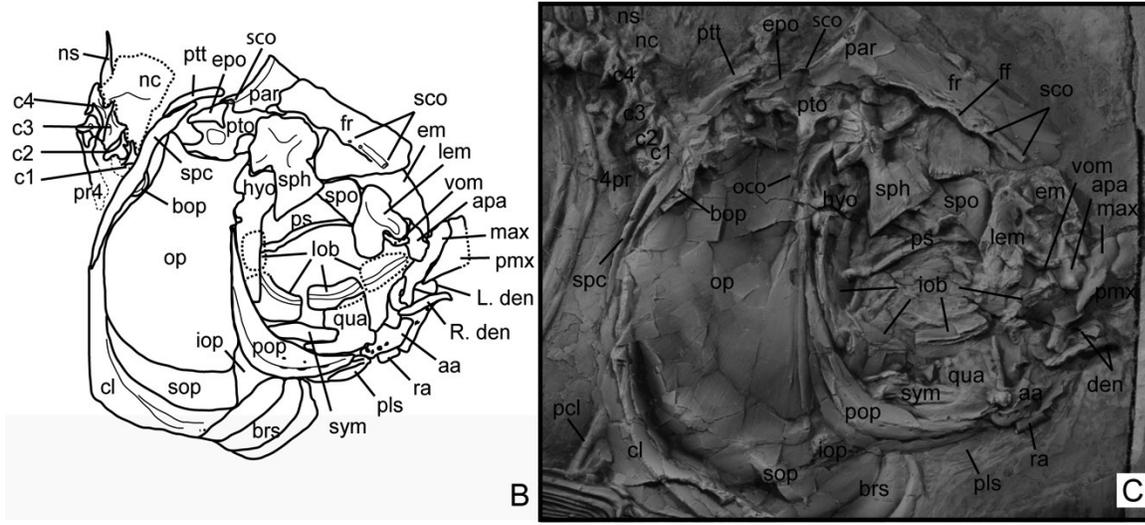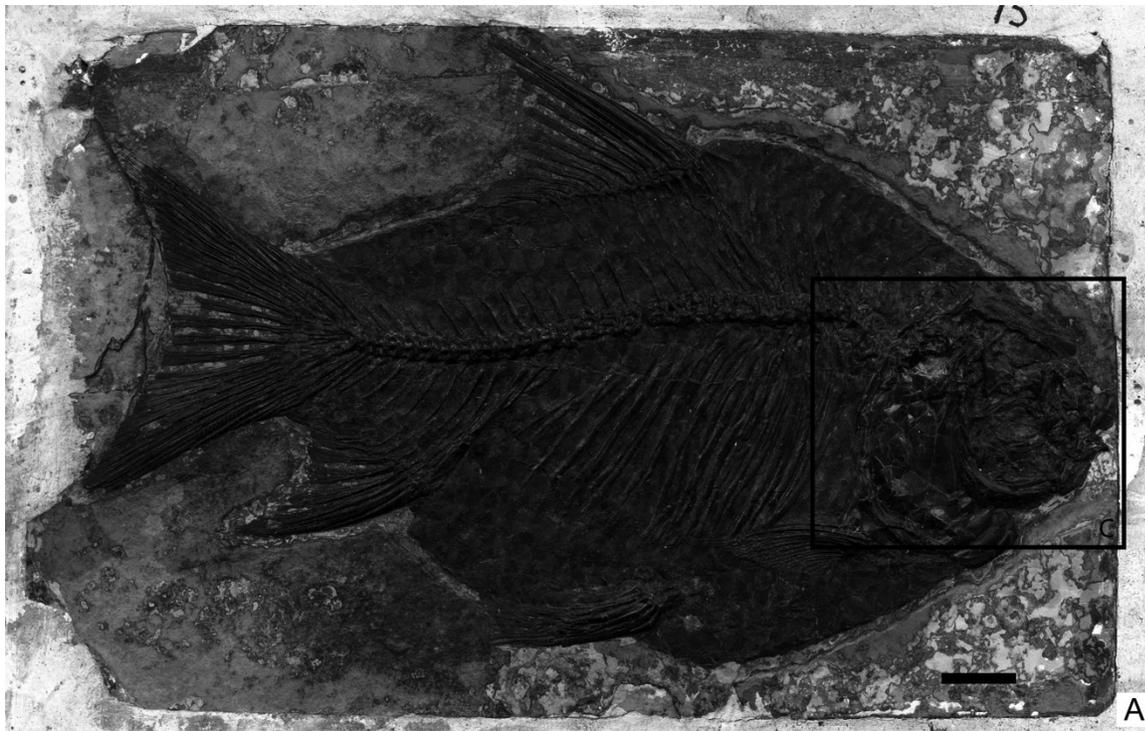
Figure 2. 4 Photographs of adult specimens of †*Jianghanichthys hubeiensis* showing osteological features. A, adult fish IVPP V 12163.14a in left lateral view; B, slightly damaged frontal of IVPP V 12163.14a showing the sensory canal opening and the groove for the sensory canal; C, anal region of IVPP V 12163.14a showing the first principal anal fin ray; D, anal region of IVPP V 12163.15 showing the first principal anal fin ray. B, C, and D coated with ammonium chloride sublimate. Scale bars equal 1 cm.
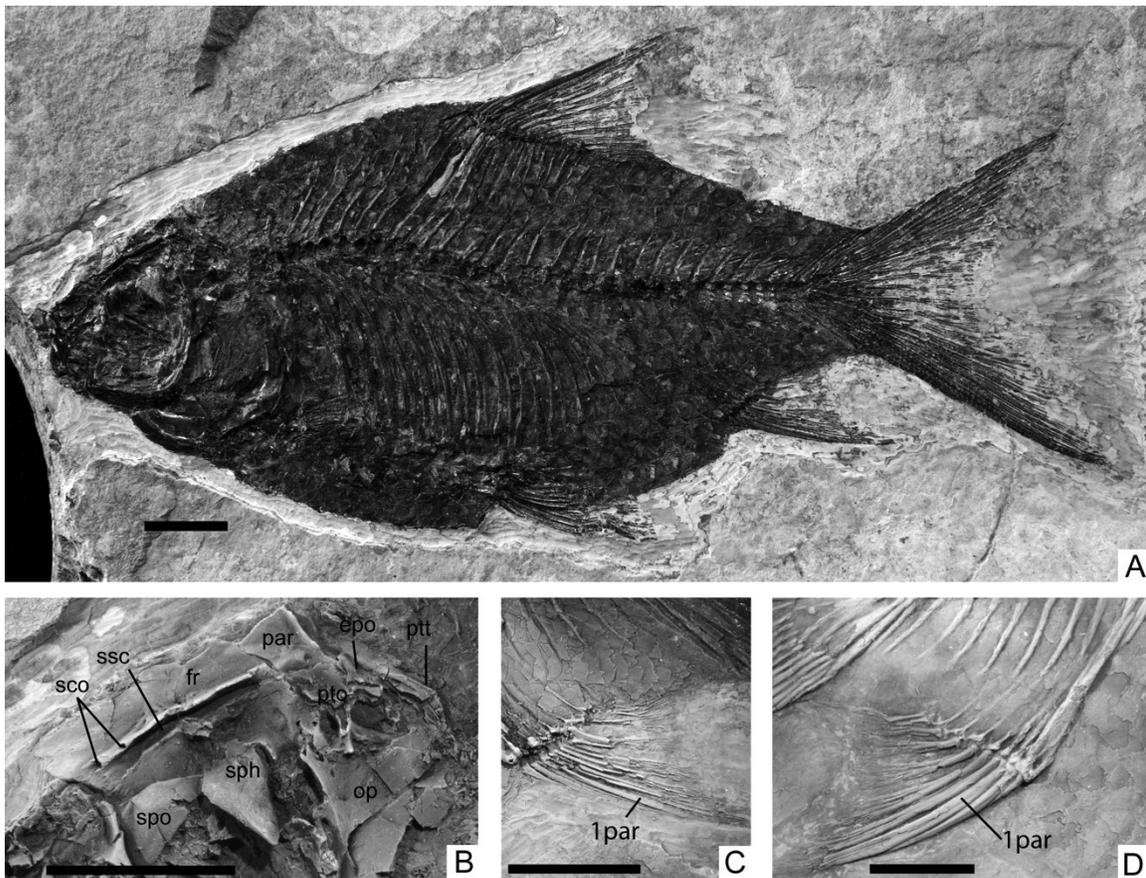
Figure 2. 5 Reconstruction of cephalic sensory canal, maxilla, and dentary of †*Jianghanichthys hubeiensis*, anterior to right. Reconstruction was based on all specimens in which at least part of the structure was visible, such as the sensory canal enclosed by bones and the processes of the maxilla. **A**, reconstruction of the cephalic sensory canal system showing the distribution of canals. As in most teleosts, there are four main sensory canal lines: supraorbital, infraorbital, preopercular, and the supratemporal commissure. The supraorbital canal extends from the anterior part of the frontal to the parietal. The infraorbital line originates from the infraorbital bones, and is continued by the otic and temporal canals. The preopercular canal begins with the mandibular canal, extends into the preopercular, and then is continued by an opercular canal. The supratemporal commissure runs mediolaterally to connect the left and right sensory canals, is continued bilaterally as posttemporal sensory canals, and then led to the lateral line. **B**, reconstruction of a left maxilla in medial view showing the processes discussed in text. **C**, reconstruction of a left dentary in medial view. **D**, reconstruction of a right dentary in lateral view.
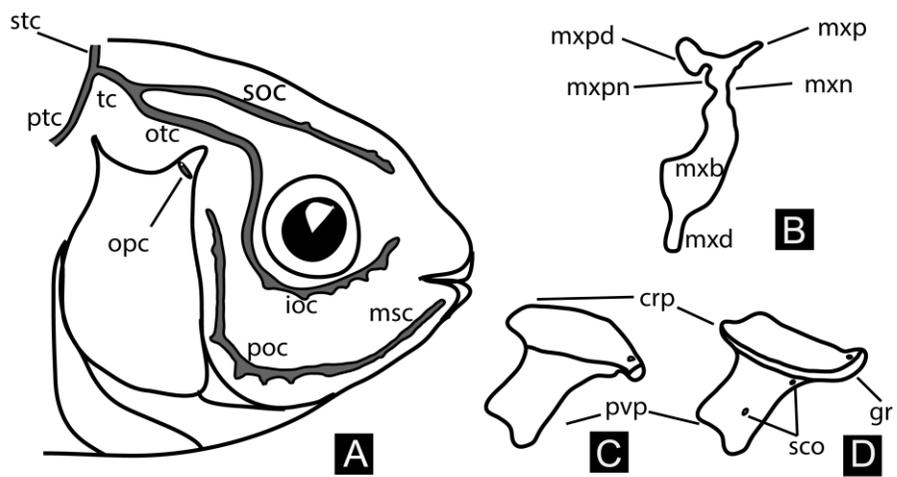
Figure 2. 6 Medial view of †*Jianghanichthys hubeiensis*, IVPP 12163.16. A, medial view of the

skull showing complete shape of individual bones, coated with ammonium chloride sublimate; B,

C, enlargements of opercular areas in **A**. Scale bar equals 1 cm.
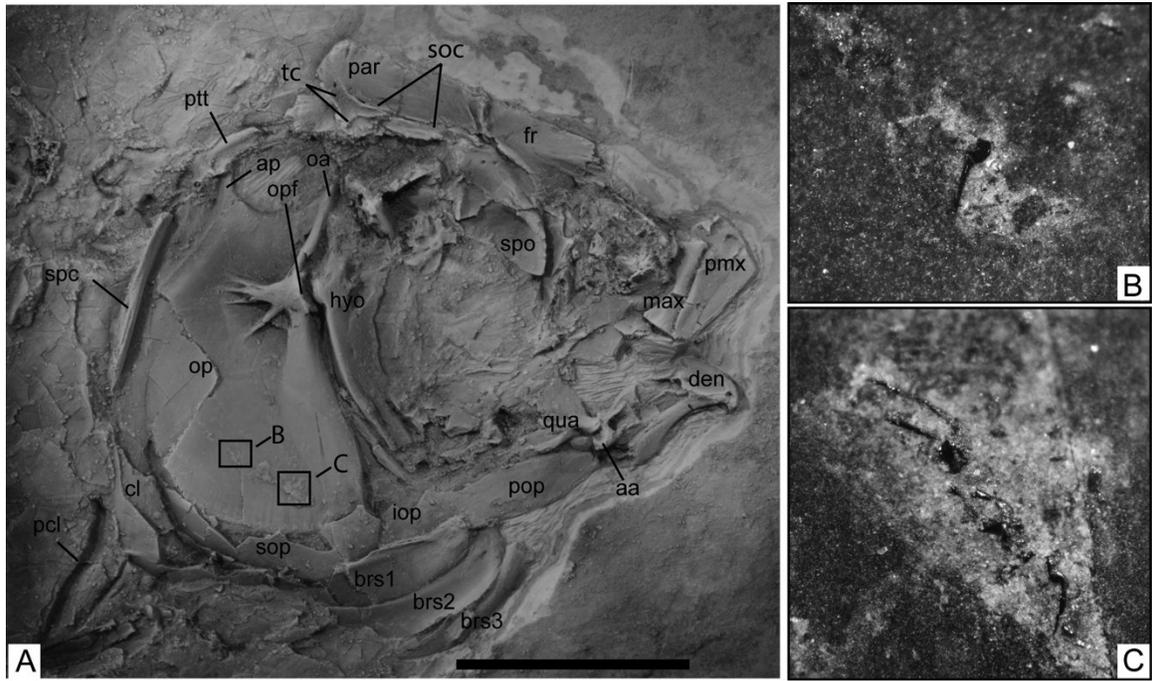
Figure 2. 7 Photographs of †*Jianghanichthys hubeiensis*, coated with ammonium chloride sublimate. A, the lapillus otolith and fragments posterior to them in IVPP V 12163.21b; B, mandible area of IVPP V 12163.17 showing the dorsal processes of the maxilla; C, caudal region of IVPP V 12163.1a showing the caudal skeleton; D, Weberian apparatus region of IVPP V 12163.20 showing the shape and size of a complete 4th pleural rib. Scale bars equal 0.5 cm.
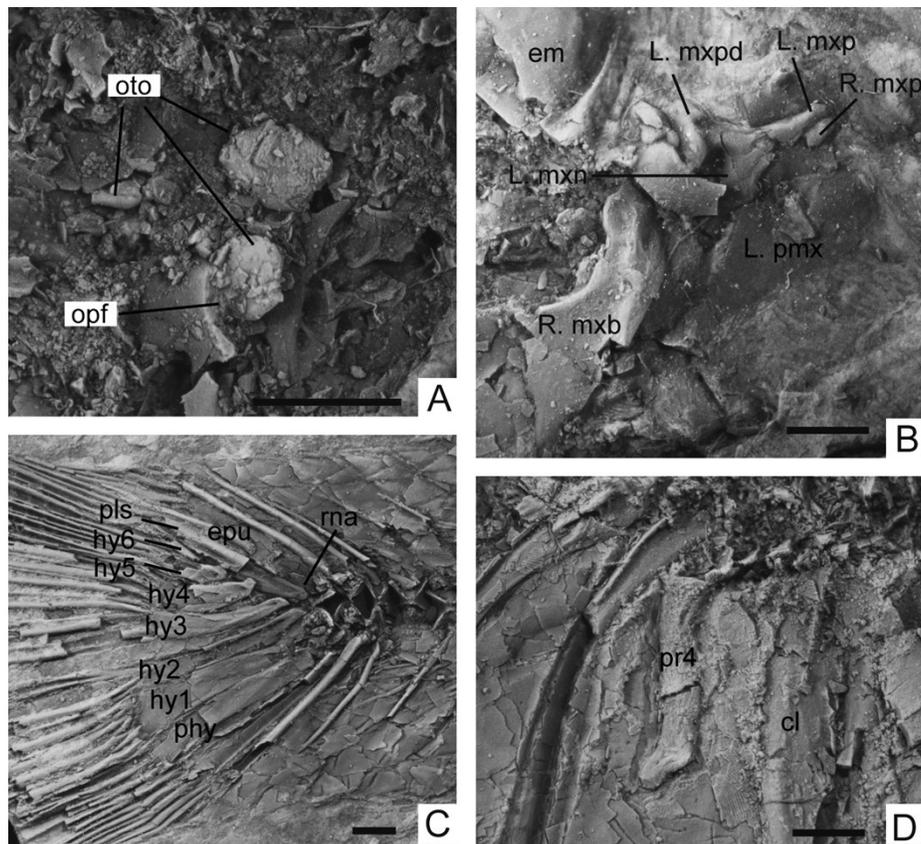
Figure 2. 8 Photographs of specimens of †*Jianghanichthys hubeiensis* and †*Amyzon aggregatum*
dissected to reveal the pharyngeal region. A, †*Jianghanichthys hubeiensis* IVPP V 18858.1; B, **C**,
†*Amyzon aggregatum* (UALVP 40844), showing pharyngeal region with pharyngeal teeth (**B**)
and complete specimen (**C**). The left opercle of each specimen was removed using needles, but
enlarged pharyngeal teeth were only found in the specimen of †*Amyzon*. Scale bars equal 1 cm.
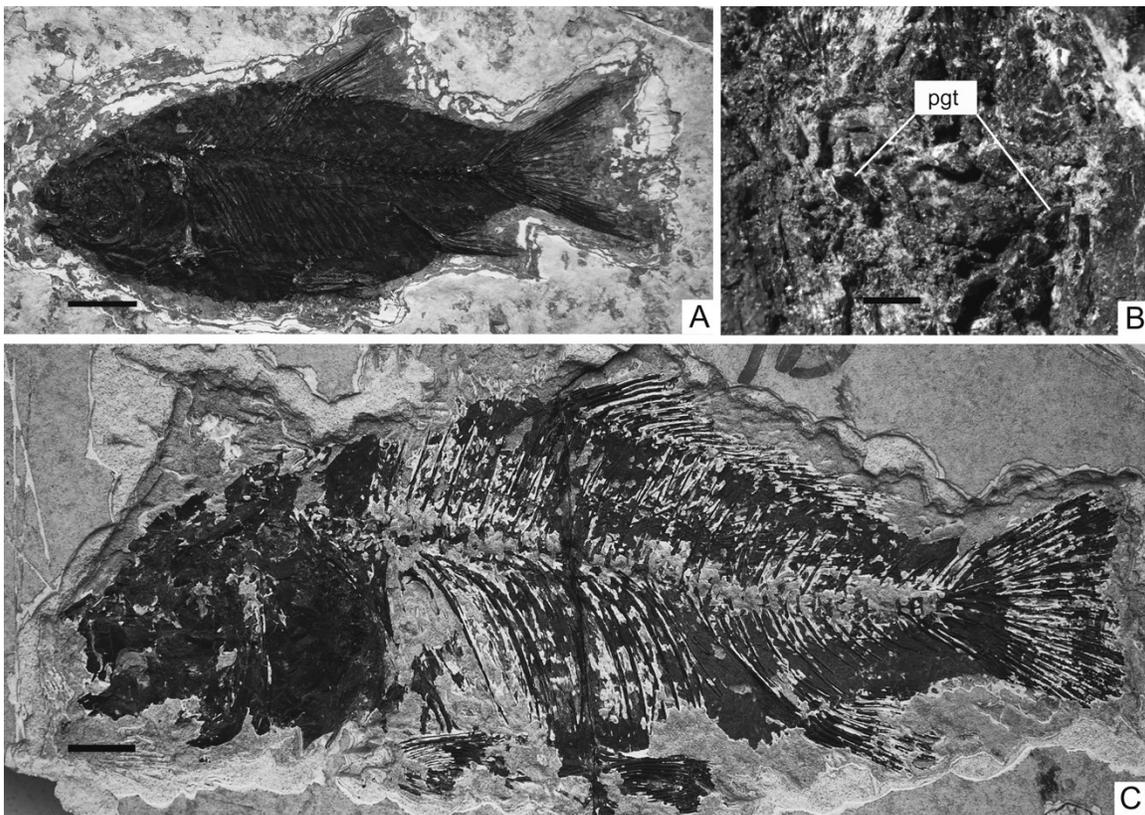
Figure 2. 9 Scatter diagram and regression of neural spine length against standard length in †*Jianghanichthys* and two species of †*Amyzon*. The neural spine in †*Jianghanichthys* is significantly shorter than that in species of †*Amyzon*.
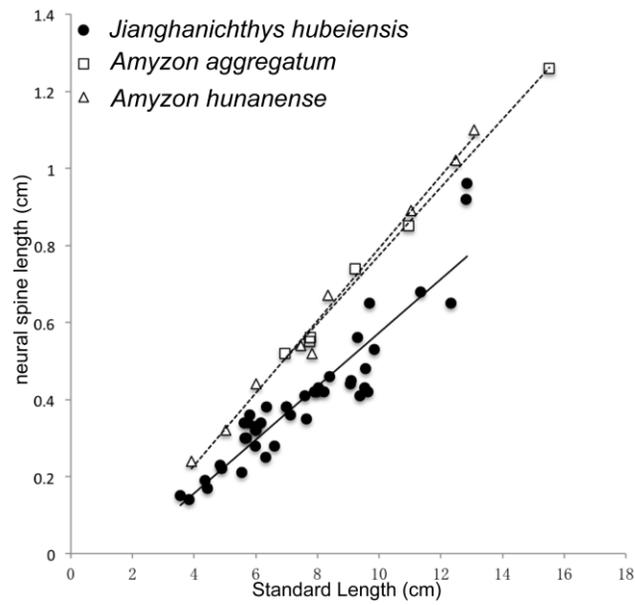
Figure 2. 10 Cross-section images from CT scan of †*Jianghanichthys hubeiensis* (IVPP V. 18858.2) in sagittal plane. The virtual slices **A**, **B**, and **C** are selected from No. 51, 59, and 79 out of 160 from left to right of the laterally preserved fossil fish to show structures of interest.
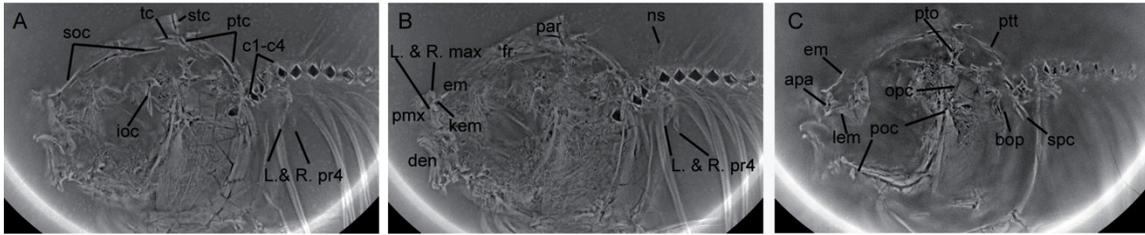
Figure 2. 11 The interrelationships of Cypriniformes: simplified strict consensus cladograms of equally parsimonious trees resulting from phylogenetic analysis of 127 morphological characters and 57 taxa (sub-analysis A1) or 58 taxa (sub-analysis A2) using MP (the maximum parsimony criterion), of which 4 taxa are outgroups (see the full taxon list in the online data matrix at Morphobank, project ID 1104). Sub-analyses A1 and A2 generate the same topology of strict consensus cladogram with the same step length, CI, and RI. **A**, repeat of the original analysis and data matrix of Conway (2011), with resulting shortest trees of 289 steps, CI 0.48, RI 0.88; **B**, analysis with addition of data for †*Jianghanichthys* to the original data matrix of Conway (2011): 295 steps, CI 0.48, RI 0.88; **C**, analysis of modified data matrix of Conway (2011): 288 steps, CI 0.49, RI 0.88; **D**, analysis with addition of data for †*Jianghanichthys* to the modified data matrix of Conway (2011): 292 steps, CI 0.48, RI 0.88; **E**, cladogram modified from Figure 2 of Chen et al. (2013); **F**, analysis with addition of †*Jianghanichthys* to the modified data matrix of Conway (2011) enforced with the backbone constraint tree shown in **E**: 302 steps, CI 0.46, RI 0.87.

A

Outgroup
Cyprinidae
Psilorhynchidae
Gyrinocheilidae
Catostomidae
Botiidae
Vaillantellidae
Cobitidae
Balitoridae
Nemacheilidae

B

Outgroup
Gyrinocheilidae
Catostomidae
Jianghanichthys
Cyprinidae
Psilorhynchidae
Botiidae
Vaillantellidae
Cobitidae
Balitoridae
Nemacheilidae

C

Outgroup
Gyrinocheilidae
Catostomidae
Cyprinidae
Psilorhynchidae
Botiidae
Vaillantellidae
Cobitidae
Balitoridae
Nemacheilidae

D

Outgroup
Cyprinidae
Gyrinocheilidae
Catostomidae
Psilorhynchidae
Jianghanichthys
Botiidae
Vaillantellidae
Cobitidae
Balitoridae
Nemacheilidae

E

Outgroup
Cyprinidae
Psilorhynchidae
Catostomidae
Gyrinocheilidae
Botiidae
Vaillantellidae
Cobitidae
Balitoridae
Nemacheilidae

F

Outgroup
Cyprinidae
Psilorhynchidae
Catostomidae
Jianghanichthys
Gyrinocheilidae
Botiidae
Vaillantellidae
Balitoridae
Cobitidae
Nemacheilidae

Chapter 3 Remarks on the North American species of *Amyzon* and description of new materials

This chapter has been published as:

I collected the data, performed the analyses, and wrote the paper. Co-authors' contributions see the Preface of this thesis (Page VI).

ABSTRACT—Fossil catostomids were very rare prior to the Eocene, and decreased in diversity suddenly in Asia after the Eocene, while becoming common fishes in the North American fauna. Knowledge of the taxonomy, diversity, and distribution of Eocene catostomids is critical to understanding the evolution of this fish group. I herein describe a new catostomid species of the genus †*Amyzon* from the Eocene Kishenehn Formation in Montana, USA. The new species differs from known species of †*Amyzon* in having hypurals 2 and 3 consistently fused to the compound centrum proximally, and differs from other Eocene catostomids in that the pelvic bone is intermediately forked. All of the phylogenetic analyses suggest that the new species is the sister group of †*A. aggregatum*, and that †*Amyzon* is the most basal clade of the Catostomidae. I reassessed the osteological characters of the North American species of †*Amyzon* based on a large number of well-preserved specimens of the new species, as well as †*A. gosiutense* and †*A. aggregatum*. Osteological characters newly discovered indicate that †*A. gosiutense* is not a junior synonym of †*A. aggregatum*, but should be retained as a distinct species.

Introduction

Catostomid fishes (Family Catostomidae) belong to the largest, most diversified, and most widely distributed order of freshwater fishes, the Cypriniformes (carp-like fishes; Nelson, 2006). The cypriniform fishes consist of over 4000 species, including a large number of commercially

important species in Eurasia, many aquarium fishes, and the zebrafish (*Danio rerio*), which is a model organism for bony fishes. Cypriniforms are characterized by toothless oral jaws with a protrusible premaxilla, enlarged ascending premaxillary process, kinethmoid bone, enlarged pharyngeal bone with ankylosed pharyngeal teeth, and three branchiostegal rays. Like other otophysans, they have a well-developed Weberian apparatus that connects the inner ear with the swim bladder as an adaptation for improved hearing.

Catostomids are commonly known as suckers, as they have protrusible, fleshy lipped, subterminal mouths used in food suction. They inhabit a wide range of environments from large rivers, such as the Mississippi (USA) and Yangtze (China), to small tributaries, such as streams along the Rocky Mountains, and from large lakes such as the Great Lakes of North America to small ponds. Their body shapes range from extremely deep to very shallow, and also change through ontogeny (Nelson and Paetz, 1992; Meng et al., 1995). Modern catostomids consist of thirteen genera with 72 species. One of 71 North American species, *Catostomus catostomus* (Forster, 1773), extends its range to northeastern Siberia. Only one extant species*, Myxocyprinus asiaticus* (Bleeker, 1865), is found solely outside North America, as an endemic form in the Yangtze River of China (Meng et al., 1995; Nelson, 2006).

In contrast to the family's modern disjunct distribution, catostomid occurrences in the Eocene (56–34 Ma - million years ago) were abundant in both North America and East Asia. Prior to the Eocene, the oldest catostomids are represented by a disarticulated cleithrum in Paleocene (66–56 Ma) sediments from a single locality in the Paskapoo Formation of Alberta, Canada (Wilson,

1980b). During the Eocene, fossil catostomids reached relatively high taxonomic diversity. Three fossil genera with 10 nominal species from this time period have been described from both North America and East Asia (Cope, 1872, 1874, 1875, 1893; Wilson, 1977; Grande et al., 1982; Chang et al., 2001). After the Eocene, catostomids disappeared from the Asian fossil record by the early Oligocene, at the same time becoming common fishes in North America. Many fossil species from western North America have been attributed to modern genera (Smith, 1981).

From a coalmine near Osino, Nevada, USA, Cope (1872) reported the first arguably Eocene catostomid species †*Amyzon mentale* Cope, 1872. In North America, all Eocene catostomids were subsequently assigned to the extinct genus †*Amyzon*. Cope (1874, 1875, 1893) reported another four species of †*Amyzon*, two of which were suggested as junior synonyms by Bruner (1991). Based on a large collection of specimens, Wilson (1977) comprehensively re-described †*Amyzon brevipinne* Cope, 1894, by re-examining the holotype and studying new specimens, and described a new Eocene species, †*Amyzon aggregatum* Wilson, 1977, from Horsefly, British Columbia, Canada. Later, Grande et al. (1982) described another species, †*Amyzon gosiutense* Grande, Eastman, and Cavender, 1982, from the Eocene Green River Formation, USA. In Asia, the first catostomid fossil was recovered from Eocene sediments in Inner Mongolia, China, based on several diagnosable opercles and disarticulated bones (Hussakof, 1932). One species of †*Amyzon*, †*A. hunanense* (Cheng, 1962), and two new genera with new species, †*Plesiomyxocyprinus arratiae* Liu and Chang, 2009, and †*Vasnetzovia artemica* Sytchevskaya, 1986, were reported from southern China, northeastern China, and Siberia, respectively (Sytchevskaya, 1986; Chang et

al., 2001; Liu and Chang, 2009). Among the known Eocene taxa, Wilson (1977) and Grande (1982) gave detailed osteological descriptions of three species of †*Amyzon*, thus improving our knowledge of their morphologies. However, the remaining species are not well understood or taxonomically clarified. One of the well-described species, †*A. gosiutense*, was concluded to be a junior synonym of †*A. aggregatum* by Bruner (1991), whereas some species of †*Amyzon* described in the 19th Century lacked diagnosable characters and thus require clarification.

As evident from this short summary of the catostomid fossil record, the Eocene represents a critical time for the evolution and divergence of this group of fishes. To better understand the diversity of early catostomids, recently discovered materials, such as those from the Eocene Kishenehn Formation described here, are taxonomically, systematically, and paleogeographically important. Early catostomid fossil records, together with cyprinid records (Family Cyprinidae), represent the oldest known cypriniforms (Chang and Chen, 2008) and thus are also important for understanding the origin and evolution of the order Cypriniformes.

Not only is the taxonomy of the Eocene catostomids unclear, but also the evolutionary relationships of their species have never been studied. In recent works, phylogenetic analyses of modern catostomids have been performed using a variety of data, especially osteology and molecular sequences (Smith, 1992; Doosey et al., 2010; Chen and Mayden, 2012). Of those studies, Smith (1992) performed the most comprehensive morphological phylogenetic analysis on the family Catostomidae. He included 62 extant and one recently extinct catostomid species as well as the fossil genus †*Amyzon*, using 157 morphological, biochemical, developmental, and genetic

95

characters. That analysis suggested that †*Amyzon* is the sister group to the modern genera *Carpiodes* and *Ictiobus*. However, the relationships of the other Eocene genera with the modern genera, and the relationships among the Eocene genera and species remain poorly known. The aim here is to improve our understanding of the interrelationships of the species of †*Amyzon* and the systematic position of the genera †*Amyzon* and †*Plesiomyxocyprinus* by performing a series of phylogenetic analyses that include those fossil species with well-preserved specimens, based on the characters and data matrix of Smith (1992).

Methods and Materials

Methods.—The fossil specimens were prepared manually and mechanically. Fossil specimens were scanned for morphometric analysis using an Epson Perfection 3590 scanner and measured using the computer program Image J. Details of structures were photographed using a Nikon DXM 1200C digital camera mounted on a Zeiss Discovery V8 stereo microscope at the University of Alberta, and a Nikon SMZ-U mounted on a stereo microscope in the Division of Paleontology, AMNH.

For the phylogenetic analyses, all characters were coded in Mesquite V 3.03 (Maddison and Maddison, 2011) and analysed in PAUP* 4beta10 for Macintosh computers (Swofford, 2003) and TNT (Goloboff et al., 2000). In PAUP, all characters were run as unordered and unweighted. Heuristic searches used a "furthest" addition sequence, with no topological constraints enforced,

no ancestral taxa identified, and "parsimony" as the optimality criterion. Character changes were optimized onto the resulting trees using Mesquite V3.03 (Maddison and Maddison, 2011). In TNT, both traditional heuristic searches and a 'new technology' search were used.

The terminology of the anatomical characters follows various significant studies with or without a few modifications: that of the pharyngeal bone and teeth is from Chu (1935); that of the opercular series is from Nelson (1949); that of the Weberian apparatus is from Nelson (1948); that of the maxilla is from Miller and Smith (1981); and that of the caudal skeleton is from Grunbaum et al. (2003).

Institutional Abbreviations.—AMNH, American Museum of Natural History, New York, USA; CMN, Canadian Museum of Nature, Ottawa, Canada; GMC, The Geological Museum of China Beijing, China; IVPP, Institute of Vertebrate Paleontology and Paleoanthropology, Chinese Academy of Sciences, Beijing, China; KU, University of Kansas, Lawrence, USA; ROM, Royal Ontario Museum, Toronto, Canada; UALVP, University of Alberta Laboratory for Vertebrate Paleontology, Edmonton, Canada; UAMZ, University of Alberta Museum of Zoology, Edmonton, Canada.

Materials.—The majority of the fossil specimens included in this study were collected by one of the authors (MVHW) and his field teams in 1984 and 1992. The Constenius family, John, Leona, and Kurt, also joined the field trip and collected many useful specimens. The family also conducted fieldwork independently, and donated their fish specimens to the UALVP.

Fossil and extant fishes used for comparison are listed in Liu et al. (2016). In addition to those,

the holotypes of †*Amyzon brevipinne* (CMN 6189) and †*Amyzon aggregatum* (ROM 11019a,b), and the paratype of †*Amyzon gosiutense* (AMNH FF 10460) were also available for comparison. †*Amyzon* specimens deposited in the ROM and CMN and listed in Wilson (1974, 1977) were examined by JL. The important specimens of catostomids in the AMNH were also added for comparison, e.g., †*Amyzon gosiutense* AMNH FF 10401, and †*Amyzon commune* Cope, 1874 AMNH FF 2579 and 8069. Modern comparative fish specimens from the Ichthyology collection of AMNH were also used; these are dry skeletons unless otherwise indicated: *Carpiodes cyprinus* (Lesueur, 1817) AMNH I-90212; *Carpiodes sp*. AMNH I-21694; *Catostomus catostomus*, AMNH I-I-47712, AMNH I-41156 (cleared and stained); *Catostomus commersonii* (Lacépède, 1803), AMNH I-55944; *Chasmistes brevirostris* (Cope, 1879), AMNH I- 47030; *Deltistes luxatus* (Cope, 1879), AMNH I-46205; *Cycleptus elongatus* (Lesueur, 1817), AMNH I-94810, AMNH I-77906; *Erimyzon oblongus* (Mitchill, 1814), AMNH I-88732; *Ictiobus cyprinellus* (Valenciennes, 1844), AMNH I-56459; *Ictiobus bubalus* (Rafinesque, 1818), AMNH I-88699; *Ictiobus meridionalis* (Günther, 1868), AMNH I-28077; *Moxostoma poecilurum* (Jordan, 1877), AMNH I-94811; *Myxocyprinus asiaticus*, AMNH I-22437.

Geology

The fossil specimens of †*Amyzon* from Montana were collected from oil shales of the Kishenehn Formation. The Kishenehn strata are located in the Kishenehn Basin and the South Fork Basin, and are exposed along the cut bank of the Flathead River system, which extends north

to the North Fork Flathead River in British Columbia, Canada, and south to the South Fork

Flathead River in Montana, USA (Constenius et al., 1989). The lacustrine Kishenehn Formation

has been dated as Eocene and Oligocene (Whipple, 1992). All the middle Eocene fossil sites in the

Kishenehn are along the Middle Fork of the Flathead River which is in the southern part of the

Kishenehn basin (pers. comm., Kurt Constenius, 2016), whereas all of the fossils of †*Amyzon*

reported here were collected from the area of Disbrow Creek and Tunnel Creek, small tributaries

of the Middle Fork Flathead River, Montana. They were collected from an interval about 20–25

meters thick (pers. comm., Kurt Constenius, 2013), and along the cut bank of the creeks. The

sediments from the fossil fish locality belong to the middle part of the Coal Creek Member,

consisting of an interbedded sequence of oil shale, marlstone, litharenite, and siltstone, and lesser

amounts of lignite, sapropelic coal, tuff, claystone, and mudstone (Pierce and Constenius, 2014).

The age of the middle part of the Coal Creeek Member is suggested to be the middle Eocene age of

at 46.2 +/- 0.4 Ma dated by Ar/Ar biotite (Constenius, 1996), equivalent to the Lutetian stage of

Eocene.

Among the vertebrates recovered from Kishenehn Formation, Russell (1954) reported a

Kishenehn mammalian fauna from the area of the North Fork Flathead River in British Columbia,

whereas Li and Wilson (1994) studied the bony-tongue fish †*Hiodon consteniorum*

(Osteoglossomorpha: Hiodontidae). The fossils of †*Amyzon* were mostly collected from the

exposures near Tunnel Creek and Disbrow Creek. They are the most abundant vertebrates from the

Kishenehn Formation, and are preserved as complete, articulated specimens or with only slight

disarticulation of the skeleton.

Species of †*Amyzon* from various Eocene localities are often the most abundant fishes found at a given site (Cope, 1874; Wilson, 1977, 1980a, 1984; Grande, 1980; Chang et al., 2001). The specimens of †*Amyzon* are also dominant in the two Kishenehn sites where they were collected, Tunnel Creek and Disbrow Creek. Most of the specimens represent articulated juveniles, and very few are large adults. This extremely unbalanced combination of juveniles and adults suggests that the new species partitioned its habitat based on size, as do most extant catostomids, possibly because of differences between juveniles and adults in avoidance of predation or food resource utilization. The fish assemblages from these two sites also include small individuals of *Hiodon* and †*Eohiodon* (Li and Wilson, 1994; Hilton and Grande, 2008), along with disarticulated bones of amiids. By comparison with fossil-fish assemblages in British Columbia of a similar age and faunal composition (Wilson, 1980a), the presence of mostly small individuals of †*Amyzon* and †*Eohiodon* with disarticulated amiids suggests that the Disbrow and Tunnel creek sites were deposited in a near-shore region of the Eocene lake; however, the nearly uniform excellent articulation and preservation of the small fishes would suggest deeper water. Also relevant to conclusions about the paleoenvironment are the numerous very well-preserved fossil plants and invertebrates (mainly insects) that have been discovered at the same localities (Constenius et al., 1989). A series of studies on the Kishenehn invertebrates is underway, and some have been published. The Kishenehn Formation in the South Fork area has been claimed as an emerging Konservat Lagerstätte of middle Eocene insects (Huber and Greenwalt, 2011; Harbach and

Greenwalt, 2012; Greenwalt et al., 2013; Shockley and Greenwalt, 2013; Greenwalt and Labandeira, 2014; Greenwalt and Rust, 2014; Greenwalt et al., 2015).

Systematic Paleontology

Subdivision TELEOSTEI Müller, 1845

Superorder OSTARIOPHYSI Sagemehl, 1885

Order CYPRINIFORMES Bleeker, 1860

Family Catostomidae Agassiz, 1850

Genus †*Amyzon* Cope 1872

Type species.—†*Amyzon mentale* Cope, 1872 from the Osino shale, Nevada, USA, by original designation.

Included species.—†*A. commune* Cope, †*A. aggregatum* Wilson, †*A. gosiutense* Grande, Eastman and Cavender, and †*A. hunanense* (Cheng).

Emended diagnosis.—Large-sized Eocene catostomid fish with terminal mouth, elongate and emarginate dorsal fin with 19 to 33 principal rays, anal fin with 7 to 10 (rarely 11) principal rays originated approximately opposite the posterior end of the dorsal fin base, caudal fin slightly forked with 18 (occasionally 19) principal rays, body deep with ratio of body depth to standard length 0.34 to 0.52 in adults and 0.25 to 0.30 in juveniles and larvae, posteroventral process of dentary moderately elongate, suborbital 2 through 5 thin and deep, sensory canal on preopercle

partly superficial and partly embedded, autopterotic ridge intermediate (neither broad nor sharp), predorsal bones 4 to 6 large.

Occurrence.—Eocene, North America and East Asia.

†*Amyzon kishenehnicum*, new species

Figure 1, 2, 4.1–4.5

Holotype.—UALVP 55260, a complete adult fish preserved on the slab in left lateral view (Fig. 3.1).

Paratypes.—UALVP 24137, 24140, 24147, 24148, 24149, 24152, and 24154, complete and nearly complete juvenile fishes.

Diagnosis.—A species of †*Amyzon* differing from all other species in having the following combination of characters: body depth/standard length (SL) 0.21–0.42, of which juveniles have 0.21–0.32 and adults 0.36–0.43; vertebrae (exclusive of Weberian apparatus) 31–36 (most 31–32), of which 15–18 (most 16) are precaudal and 15–18 (most 15) are caudal; D i–iv, 22–25; A i–iv,7–9; P 9–12; V 7–11; C iv–vii, 9, 9, iv–vi; both ethmo-frontal and fronto-parietal fontanelles present; frontal ridge thick and robust with projections; lateral margin of parietal bow-shaped; second infraorbital (IO2) enlarged and curved composing the ventral orbit; preopercular sensory canal partially enclosed in bone; anteromedial corner of premaxilla angled ninety degrees; dentary

process of maxilla bent anteriorly; fork length of pelvic bone about half total length of pelvic bone; both hypurals two and three (hyp2 and hyp3) fused to the compound centrum.

Age and horizon.—43.5±4.9Ma, middle Eocene (Lutetian), Kishenehn Formation, Coal Creek Member.

Type locality.—Tunnel Creek of Middle Fork Flathead River, east of Whitefish, Montana.

Referred specimens.—UALVP 23943, 24131–24134, 24138, 24139, 24141–24146, 24150, 24151, 24153, 24155–24199, 24226, 38728–38788, 38792–38807, 38876, 38877, 38881–38920, 38922–38958, 38962–39039, 52373, in total 295 specimens.

Etymology.—The specific epithet *kishenehnicum* is a combination of the name of the Kishenehn Formation name and the Latin suffix *–icum* (neuter) meaning "belonging to" or "pertaining to."

General Appearance.—The new species is elongated and fusiform, with a deep and laterally compressed body in adults (Fig. 3.1), a shallow body in juveniles (Fig. 3.2.1), and nearly straight ventral outline in most individuals. The body size of the specimens ranges from 3.08cm (UALVP 24143) to around 40cm (UALVP 55515, and 55156) in standard length (SL; Fig. 3.3; Table 3.1). The ratio of body depth to SL ranges from 0.21 to 0.42 (Table 3.1), with the juveniles possessing a shallower body with a ratio range of 0.21–0.32, and adults having a deeper body with a ratio range of 0.36–0.43. The head length-to-SL ratio is around 0.30 with the range 0.23 to 0.34 (Table 3.1). The fish has a terminal to subterminal mouth and the jaw would have been protrusible, based on the shape of the mandibular bones and the presence of the kinethmoid. The dorsal fin is

emarginate and the dorsal fin base is long (around one third of SL) with over 20 principal rays. The caudal fin is slightly forked in adults and forked in juveniles.

Skull roof.—Skull-roof bones include the frontal and parietal. As in all catostomids, sensory canals are entirely detached from the roofing bones. Both anterior (ethmo-frontal) and posterior (fronto-parietal) fontanelles are present in †*Amyzon kishenehnicum*.

The frontal (Fig. 3.4.1, 5.1–5.2) resembles that of most catostomids in that it is, overall, broad anteriorly and narrow posteriorly, because of the laterally expanded orbital process of the frontal in the anterior part and the medially notched longitudinal margin (given the presence of the fronto-parietal fontanelle) in the posterior part. Both anterior and posterior ends are truncated. Two notches are found along the medial margin of the frontal. One is small, located at the antero-medial corner and open to the ethmoid, indicating there is an ethmo-frontal fontanelle. The other one is prominent and longitudinally elongated along the medial margin of the posterior part of the frontal, representing the fronto-parietal fontanelle. The posterior medial margin of the frontal surrounding the fronto-parietal fontanelle is not parallel to the medial line; it angles closer to the midline more posteriorly. This indicates that the fronto-parietal fontanelle is broader anteriorly and narrower posteriorly, resembling an elongated wedge. The ethmo-frontal fontanelle is restricted in the ethmoid and bordered by the frontal posteriorly (ROM 11041).

Laterally, the frontal bears a supraorbital notch (Fig. 3.4.6), which houses the supraorbital, and a supraorbital process (Fig. 3.4.6) that contacts the sphenoid (Fig. 3.4.1) posteriorly and reaches the orbit with its tip. The supraorbital notch is shallow and small.

Dorsally, the frontal bears a prominent longitudinal ridge extending from near the anterior margin to the posterior end (Fig. 3.4.1, 5.1). The ridge is ornamented with sturdy and dorsally pointed projections.

The parietal is very small, about the size of the posterior narrow part of the frontal (Fig. 3.4.2). Laterally, the margin is concave and smooth, which gives the parietal a bow shape in dorsal view, instead of triangular, rectangular, or square as in most catostomids. The bow-shaped parietal is also seen in *Myxocyprinus* and †*A. aggregatum* (Fig. 3.4.7). However, the other closely related species †*A. gosiutense* possesses a slightly convex lateral margin and thus displays a roughly rectangular shape (Fig. 3.4.11).

The supraoccipital (Fig. 3.5) is sutured to the parietal posteriorly, forming the dorsal and posteromedial cranial wall. The supraoccipital crest, extending posteriorly towards the neural complex of the Weberian apparatus, is intermediately developed as in *Ictiobus, Catostomus,* and *Moxostoma*, less robust than that in *Cycleptus, Myxocyprinus,* and *Erimyzon,* and more developed than that in *Carpiodes*.

Ethmoid region.—Both kinethmoid and ethmoid are present in †*A. kishenehnicum*, but are not completely visible in any specimen. Combining the appearance from several specimens, the kinethmoid is rod-like, narrow, and curved dorsally in the middle. Both anterior and posterior ends are enlarged. The ethmoid is domed anteriorly, with an elongated anterior process. It encloses the ethmo-frontal fontanelle posteriorly.

The paired lateral ethmoids, located on either side of the ethmoid, are "Q"-shaped (Fig. 3.5.1). The circular part of the lateral ethmoid is not porous as in many catostomids, but instead is concave laterally like a bowl with a hollow in the middle. The ventral process is prominent and posteriorly pointed towards the orbit, resembling the condition in †*A. aggregatum*. In the other catostomids, the ventral process is pointed anteriorly, ventrally, or reduced.

Orbital region.—A supraorbital (Fig. 3.5.1) is present as in the other species of †*Amyzon*. It is small and rounded. The first infraorbital (IO1, lacrimal; Fig. 3.5.1) is large and elliptical. IO2 is also large and semi-lunate, but much more elongated and curved than IO1, and crosses the ventral orbit. IO3 is much smaller, and the possible IO4 is reduced with only the associated sensory canal present along the posterior margin of the orbit. The sensory canal on IO1 is detached because of preservation, whereas on IO2 it is completely attached and tube-like, running along the lateral surface and closer to the dorsal edge.

Otic region.—The sphenotic (Fig. 3.4.1, 5.1) is bordered both anteriorly and dorsally by the frontal and posteriorly by the autopterotic, as in other catostomids. The wing-shaped postorbital process, produced from the anterolateral sphenotic and forming the posterodorsal margin of the orbit, is nearly the same size as, but less broad than, the central region of the sphenotic. The ventral end of the postorbital process lacks the extended pointed tip, which is also absent in *Carpiodes, Cycleptus,* certain species of *Ictiobus*, and in *Catostomus.* The surface of the sphenotic is slightly depressed for the attachment of opercular muscles (Weisel, 1960). The sphenotic of †*A. kishenehnicum* is similar to that of other species of †*Amyzon*, where known.

The autopterotic (Fig. 3.2.3) is a main component of the posterolateral cranium, posterior to the sphenotic and ventral to the parietal. As in most catostomids, the autopterotic ridge (Smith, 1992), which is the outer surficial part and sutured to the sphenotic and parietal, is small, with a depression formed by ridges at the anterior and posterior margins. A sizeable posteroventral process of the autopterotic extends towards the shoulder girdle. The opening of lateral temporal fossa, surrounded by the concave lateral margins of the parietal, autopterotic, and epiotic, is large, as in *Ictiobus*, *Cycleptus*, and *Myxocyprinus*. The epiotic is a robust bone situated at the posteroventral corner of the cranium and slightly exposed in lateral view.

The arrangement of the otoliths (Fig. 3.2.2) is like that of other ostariophysan fishes, i.e., the sagitta is delicate and smaller than the other two otoliths (Adams, 1940). The sagitta is anteroposteriorly elongated with both ends pointed (Fig. 3.2.2). The asteriscus is below the sagitta, rounded, and is the largest of the three. The lapillus is small and rounded, and anterior to the other two.

Opercular series.—The opercle (Fig. 3.1, 5.1) has an opercular arm, a concave dorsal margin, and an auricular process as in typical catostomids (Nelson, 1949). The opercular arm is stout, with striations on the outer surface and a truncated dorsal end. The dorsal concave margin is broad and shallow. The auricular process is well developed, with a pointed dorsal tip. The peripheral striations are moderately developed, neither as deep and numerous as in *Ictiobus* and *Carpiodes*, nor totally absent as in some *Catostomus*, *Moxostoma*, and *Cycleptus*. The anterior

border of the opercle is straight, and the angle of the inferior (ventral) border more than 30°, thus resembling Nelson's "OP1" group (Nelson, 1949).

The preopercle (Fig. 3.5.1) consists of a vertical and a horizontal arm and resembles that of all catostomids except for *Myxocyprinus* and *Cycleptus*, in which the horizontal arm is reduced. In †*A. kishenehnicum*, the height of the vertical arm nearly equals the length of the horizontal arm, resembling that of other species of †*Amyzon* and some species of *Ictiobus*. These two arms form a right angle as in other species of †*Amyzon*, *Erimyzon*, and some *Carpiodes*. The preopercular sensory canal runs along the axis of the preopercle. The sensory canal is in an open groove at both ends of the preopercle, whereas there is a thin layer of bone covering the canal in the middle region, thus partially enclosing the canal. There is no evidence of a prominent ridge, as seen in the primitive cypriniform †*Jianghanichthys*, in †*A. kishenehnicum.*

The interopercle (Fig. 3.5.1) has the general form of that in most catostomids, which is roughly lunate in shape and tapered anteriorly in depth. It is situated at the corner of the opercle, overlapped by the preopercle anteriorly and overlapping the subopercle posteriorly. It resembles Nelson's "IOP1" (Nelson, 1949). The subopercle is similar to that in other species of †*Amyzon* in having a nearly straight dorsal margin and more curved ventral margin.

Jaw and suspensorium.—As in all catostomids, the mouth gape is formed by the premaxilla, maxilla, and dentary (Fig. 3.4.3, 5.1). The premaxilla in †*A. kishenehnicum* is L-shaped. The ascending process is nearly as long as the alveolar process. The ascending process is narrow and tapered towards the dorsal pointed end, whereas the alveolar process is broad and

slightly curved. The anteromedial corner of the premaxilla forms a sharp right angle as in †*A. gosiutense,* unlike the rounded-off corner in †*A. aggregatum.*

The maxilla of †*A. kishenehnicum* bears two dorsal processes, a narrow neck, a broad body, and a dentary process, as in most catostomids. The neck is short and narrow (Fig. 3.4.3, 5.1). The process posterodorsal to the neck is at an obtuse angle. A ridge along the anterior margin of the neck, which is for the insertion of the palatomaxillary ligament (Miller and Smith, 1967), is prominent. The ventral (anterior) keel of the body of the maxilla is round, whereas the dorsal (posterior) keel is expanded posterodorsally as a projection. All the features noted above for the maxilla are also visible in †*A. aggregatum* and †*A. gosiutense.* However, the robust, knob-like dentary process is bent forward in †*A. kishenehnicum,* resembling that in †*A. aggregatum,* and unlike the truncated and straight process of †*A. gosiutense.*

The dentary (Fig. 3.5.1) consists of a ventrally pointed gnathic ramus, a developed coronoid process, and an elongate posteroventral process. A lateral ridge along the gnathic ramus extends from the anterior point to nearly the root of the ramus.

The anguloarticular (Fig. 3.5.1) is much shorter and narrower than the posteroventral process of the dentary, and is overlapped anteriorly by part of it. Posteriorly, the anguloarticular possesses a large socket to articulate with the quadrate. The retroarticular is a prominent and laminar bone ventral to the anguloarticular. The size of the retroarticular is similar to that in *Ictiobus,* and larger than that in *Catostomus.* The quadrate, resembling that of most cypriniforms, possesses an anterior condyle that articulates with the anguloarticular, a flat dorsal part, an elongated, slender ventral

part, and a wedge-shaped slot in between the dorsal and ventral parts. In †*A. kishenehnicum*, the condyle is large, corresponding to the sizable socket of the anguloarticular. The flat dorsal part is roughly square, whereas the ventral slender part is rod-like and extends far posteriorly. The wedge-shaped sympletic fits into the slot of the quadrate.

Pharyngeal tooth.—A single tooth was found in situ along with several tooth sockets on UALVP 24152 (Fig. 3.2.4). The tooth is compressed as in all catostomids. The overall triangular shape resembles those of the other species of †*Amyzon* (Grande et al., 1982; Sytchevskaya, 1986; Liu et al., 2010). However, unlike in the other species of †*Amyzon*, the tooth is short and lacking a hooked conical tip, which may be because it is immature or has been truncated by abrasive wear.

Paired girdles and fin.—The posttemporal is overall a flat, vertically elongate bone attaching the shoulder girdle to the skull as in other catostomids (Fig. 3.2.3, 5.1). A prominent ridge extends along the midline of the upper half of the posttemporal, and merges with the posterior edge of the lower half. The upper half of the bone is narrow, with a pointed superior end, whereas the lower half is broad with a round ventral end. An anteromedial process at the midpoint of the bone at the bottom of the upper half indicates the area of contact with the extremely elongate posteroventral process of the autopterotic. The supracleithrum (Fig. 3.2.3, 5.1) is also a flat bone overlapping with the posttemporal in its upper part and with the cleithrum in its lower part. It is slightly broader than, and about twice as high as, the posttemporal. The cleithrum is spoon-shaped (Fig. 3.2.3, 5.1). In lateral view, a ridge along the anterior margin is followed by a deep, narrow groove. The postcleithrum attaches to the posterior side of the cleithrum and has a slightly curved

ventral limb. There are 9 to 12 (usually 12, Table 3.1) pectoral fin rays with the longest one nearly reaching the insertion of the pelvic fin.

The pelvic bone is bifurcated anteriorly into a rod-like lateral strut and a flat medial splint (Fig. 3.4.4, 5.4). The strut length, measured from the anterior tip of the strut to the posterior end of the pelvic bone excluding the ischial process and thus representative of the pelvic bone length (PL), is slightly longer than the splint length measured in the same manner. The fork length (PFL), from the anterior point of the strut to the posteriormost point of the fork, is about half of the pelvic bone length (PFL/PL 0.448). The posteromedial ischial process is compressed and tapered to a posterior point. The length of the ischial process (posterior end of splint to posteriormost point of ischial process) compared to PL is about 1/2 (ratio 0.444). There are 7 to 11 (usually 7 to 9, Table 3.1) pelvic fin rays attached to the pelvic bone.

Median fins.—The dorsal fin base is long with a length to SL ratio of 0.22–0.40 (0.22–0.32 found in juveniles and 0.40 in the single adult measured). There are 22 to 25 principal dorsal fin rays (Table 3.1) preceded by 1 to 4 rudimentary rays. The first principal ray is unbranched and leads the fin web, and the rest are shorter and branched. They are all segmented distally. The last two rays are frequently articulated to the same pterygiophore and thus counted as one principal ray. There are 22–25 pterygiophores supporting the fin rays. The vertical ramus of the first dorsal pterygiophore is thick and robust, indicating it would have supported a large muscle volume, and thus probably strong *erector dorsalis* and *depressor dorsalis* muscles to control the dorsal fin.

The ratio of anal fin base length to SL is 0.06 to 0.08 for the juveniles, and 0.1 for the single sampled adult specimen (UALVP 55260). There are 7 to 9 principal anal fin rays (Table 3.1), of which the count 9 only occurred in the adult specimen. The first principal anal fin ray is unbranched, and the rest of the fin rays are branched. They are all segmented distally, and preceded by 1 to 4 rudimentary rays. The anal fin is supported by 7 to 10 pterygiophores. Similar to the condition in the dorsal fin, the last principal anal fin ray usually consists of two small rays sharing one support, and the thick first pterygiophore indicates strong *erector analis* and *depressor analis* muscles.

Vertebral column.—Exclusive of the Weberian apparatus, there are 31 to 36 (mostly 31 or 32) vertebrae, of which 15 to 18 (mostly 16) are precaudal and 15 to 18 (mostly 15) are caudal (Table 3.1). Two of the four Weberian ossicles are visible: a small triangular tripus and a thin flake-like scaphium (Fig. 3.2.3). The Weberian apparatus has an exceptionally robust and long fourth pleural rib (Fig. 3.2.3), as in all other catostomids (Nelson, 1948; Bird and Hernandez, 2007). The fourth pleural rib tapers ventrally. In lateral view, the anterior and posterior edges of this rib are slightly elevated and ridge-like, whereas a deep, vertical groove in the middle extends from the bifurcated root to the ventral end. The shape of the neural complex (Fig. 3.5.1) is roughly a parallelogram, resembling that in †*A. aggregatum* and †*A. gosiutense*. The superior margin is slightly convex. The fourth neural spine nearly reaches the superior margin of the neural complex (Fig. 3.5.1). There are 4 to 5 triangular predorsal bones between the fourth neural spine and the ninth or tenth neural spine anterior to the dorsal fin.

Two series of intermuscular bones, the epineural and epipleural (Patterson and Johnson, 1995), parallel the vertebral column. The epineural series, dorsal to the vertebral column, spans the length of the column, whereas the epipleural series is restricted to the caudal region ventral to the vertebral column. Both epineural and epipleural bones are forked proximally.

Caudal skeleton and fin.—The caudal fin is slightly forked in the adult and forked in the juvenile, with 18 principal fin rays, all of them segmented, of which nine form each of the upper and lower caudal fin lobes. The dorsal-most and the ventral-most principal fin rays are unbranched, whereas the rest are branched. There are three to six upper procurrent rays and three to five lower ones preceding the caudal fin. The count of the lower procurrent rays is usually equal to or less than that of the upper procurrent rays in the same individuals.

The caudal skeleton (Fig. 3.4.5, 5.5) consists of all the elements in other catostomids (Eastman, 1980). The compound centrum, formed by the union of the first preural and first ural centra, bears the posterodorsally extended pleurostyle that is formed by the fused anterior uroneurals (Eastman, 1980; Grünbaum et al., 2003). There are six hypurals (hyp1 to hyp6) and one parhypural below the pleurostyle, and the hypurals decrease in size dorsally in the series. The parhypural is fused with hyp1 proximally, and then articulated to the compound centrum as in almost all other catostomids (Eastman, 1980). The gap between hyp2 and hyp3, also called the caudal diastema, is narrow. Both hyp2 and hyp3 are fused to the compound centrum (Fig. 3.4.5, 5.5) in all specimens that present a good view of the caudal skeleton (UALVP 24137, 24140, 24146, 24154, and 24157). The rudimentary first preural neural arch is small, whereas the epural is

113

corresponding long. A free uroneural is posterolateral to the pleurostyle in specimens preserved in both left and right lateral view, suggesting that a pair of free posterior uroneurals was present (UALVP 24139, 24146, 24147, and 24157).

Discussion

Phylogenetic Analysis Including Fossil Catostomids

The systematic relationships of catostomid fishes have been studied for decades; for example, Hubbs (1930) reviewed the classification of eastern North America catostomids, and provided some characters used in his key, which are applicable to the whole family. Among the valuable systematic studies, external morphology of the brain and lips (Miller and Evans, 1965), morphological characters for the tribe Moxostomatini (Jenkins, 1970), morphological and biochemical characters in *Catostomus* (Smith and Koehn, 1971), genetic information (Ferris and Whitt, 1978), and developmental characters (Fuiman, 1985), have all been used to hypothesize evolutionary intrarelationships of the Catostomidae. Nelson (1948; 1949), Eastman (1977; 1980), and Doosey and Bart (2011) comprehensively studied certain anatomical features among the members of the family Catostomidae, many of which are systematically valuable and informative. As a result, catostomids are among the best-known freshwater fishes.

However, our understanding of their relationships is still undergoing improvement, with more in-depth study and new technology applied to systematic ichthyology. Smith (1992) combined the non-molecular characters from earlier publications and also compiled a series of

morphological characters to perform the most comprehensive phylogenetic analysis of catostomid fishes to date. More recently, molecular sequences, including both mitochondrial and nuclear DNA, have been used to hypothesize catostomid systematic relationships (Harris and Mayden, 2001; Harris et al., 2002; Doosey et al., 2010; Chen and Mayden, 2012; Unmack et al., 2014).

Three subfamilies were recognized and in widespread use before the 1990s (Gill, 1861; Nelson, 1948; Smith, 1992). These are: Ictiobinae, consisting of *Ictiobus* and *Carpiodes,* Cycleptinae with the American *Cycleptus* and East Asian *Myxocyprinus*, and Catostominae containing the rest, comprising nine genera and more than 60 species. A fourth subfamily, Myxocyprininae, with only the monotypic *Myxocyprinus*, was proposed by Miller (1959), and is widely recognized and accepted in recent studies (Miller, 1959; Harris and Mayden, 2001; Nelson, 2006; Doosey et al., 2010). The Myxocyprininae were separated from Cycleptinae, which were left also with a single genus, *Cycleptus*. Unless otherwise designated, Cycleptinae and Myxocyprininae in the following discussion represent the extant members only. The fossil members †*Amyzon* and †*Plesiomyxocyprinus* have been suggested to be closely related to Ictiobinae and Myxocyprininae, respectively (Smith, 1992; Liu and Chang, 2009). However, Smith's (1992) cladistic analysis on 63 post-Pleistocene species plus †*Amyzon* and using *Cyprinus* and *Leptobotia* as outgroups was the only one to include †*Amyzon* in a systematic study.

To explore the systematic position of †*A. kishenehnicum* within the genus †*Amyzon*, as well as to further understand the evolutionary relationships among extant and Eocene catostomids, I added data for †*Plesiomyxocyprinus* to Smith's (1992) data matrix, and replaced his codings for

†*Amyzon* with codings for three species of the genus, i.e., †*A. aggregatum*, †*A. gosiutense*, and †*A. kishenehnicum*. I then subjected the data matrix to a series of phylogenetic analyses.

Our first analysis used Smith's (1992) original data matrix, with its 64 ingroup taxa and 2 outgroups coded for 157 characters, of which most were ordered and polarized. His analysis was performed in HENNIG86 (Farris, 1989) using the parsimony criterion and generated two equally parsimonious trees of 853 steps, a consistency index (CI) of 0.35, and a retention index (RI) of 0.80. The re-analysis of Smith's unchanged complete data matrix used PAUP (Swofford, 2003) using heuristic search algorithms and the parsimony criterion, but with all characters unweighted and unordered. In this repeated analysis, 233 equally parsimonious cladograms were found with tree length 778 steps, CI 0.393, and RI 0.783. A strict consensus of the 233 trees suggests that †*Amyzon* is sister to modern ictiobines, identical to Smith's (1992) hypothesis. Ictiobinae are sister to Catostominae, rather than the most basal clade in the preferred tree of Smith (1992). Meanwhile, *Cycleptus* is the most basal clade of the catostomid family, whereas *Myxocyprinus* is sister to the rest of the catostomids instead of sister to *Cycleptus*.

Although the preferred tree of Smith (1992) suggested that Cycleptinae are the sister group to Catostominae, the author noticed that the number of characters supporting such a topology was not overwhelming and that the Ictiobinae might be the sister group to the Catostominae (Smith, 1992: p797). That the topology is changed by using a different computer program and algorithms is entirely reasonable.

In the second analysis, I coded character states of †*Jianghanichthys,* †*Plesiomyxocyprinus,*

†*Amyzon aggregatum,* †*Amyzon gosiutense,* and †*A. kishenehnicum* (Table 3.2) for the characters

from Smith's (1992) data matrix, and I also removed the genus "†*Amyzon*" from the data matrix as

a separate taxon. The complete data matrix can be found in Morphobank (Project 1277,

http://www.morphobank.org/). The genus †*Jianghanichthys* is a basal cypriniform fish from the

early Eocene of China, and represents an extinct family of Cypriniformes (Liu et al., 2015). This

fish shares a series of symplesiomorphies with both catostomids and cyprinids, and thus is an ideal

fossil outgroup member for this study. With the addition of the above taxa, the analyses include

three outgroups and 67 ingroup taxa. An analysis in PAUP of the modified data matrix, using the

same search algorithm and criteria as used in the first analysis, generated 1238 equally

parsimonious cladograms with 804 steps, CI 0.381, and RI 0.781. The strict consensus cladogram

(Fig. 3.6) suggests that the genus †*Amyzon*, rather than the subfamily Ictiobinae, is the most basal

clade within the family Catostomidae, whereas †*Plesiomyxocyprinus* is sister to Myxocyprininae

plus Cycleptinae. The Ictiobinae are found to be the sister group of the Catostominae as in the

previous analysis.

Our third analysis was performed in TNT (Goloboff et al., 2000) using both traditional search

and "new technology search" methods on the same data matrix as the second analysis. Only one

taxon, †*Jianghanichthys*, was designated as an outgroup, rather than three taxa as in the previous

analysis. The sub-analysis using the traditional search quickly generated 73 equally parsimonious

cladograms with 803 steps, CI 0.380, and RI 0.781. Although the matrix had fewer outgroup taxa,

these trees are only one step shorter than the equally parsimonious cladograms generated in the

PAUP analysis. Nevertheless, the strict consensus cladogram of the TNT analysis is identical to the one from the PAUP analysis (Fig. 3.6). The other sub-analysis, using "new technology search," was even faster but only generated five equally parsimonious cladograms with the same length as those from the traditional search. The strict consensus cladogram is also identical to the one from the PAUP analysis (Fig. 3.6).

All of the analyses with the modified data matrix found †*Amyzon* to be the most basal clade, possibly because of the inclusion of †*Jianghanichthys* as an additional outgroup. Within †*Amyzon*, †*A. kishenehnicum* is recovered as the sister to †*A. aggregatum*. Character 97 from the data matrix that united †*A. kishenehnicum* and †*A. aggregatum* is the number of post-Weberian vertebrae, of which †*A. gosiutense* possesses character state '0' with 30–31 vertebrae, whereas the other two species have character state '1' with 32–37 and 31–36 respectively. There are also other osteological characters that support †*A. kishenehnicum* and †*A. aggregatum* as sister to each other. The parietal of †*A. kishenehnicum* and †*A. aggregatum* is laterally concave and smooth, giving the parietal a bow shape in dorsal view, whereas in †*A. gosiutense* it is slightly convex laterally and rectangular in dorsal view. Second, but not least, the dentary process of †*A. kishenehnicum* and †*A. aggregatum* is knob-like, bent, and directed anteriorly, whereas the knob-like dentary process of †*A. gosiutense* is straight and downwardly directed.

Remarks on North American †*Amyzon*

Since Cope (1872) reported the first fossil catostomid species †*Amyzon mentale* from Osino,

Nevada, USA (syntype: USNM V 4074/4075), all Eocene–Oligocene catostomids from North America have been assigned to the extinct genus †*Amyzon*. Cope reported four additional nominal species of †*Amyzon* in subsequent studies: †*A. commune* Cope, 1874, †*A. fusiforme* Cope, 1875, †*A. pandatum* Cope, 1875, and †*A. brevipinne* Cope, 1893. Two more Eocene species, †*A. aggregatum* Wilson, 1977, and †*A. gosiutense* Grande et al., 1982, were more recently described in greater detail. Based on a large collection of specimens, Wilson (1977) also re-described †*Amyzon brevipinne* and emended the specific diagnosis after re-examining the holotype and additional materials. At the species, this taxon is well established by Wilson (1977). However, according to an ongoing project, the generic designation of †*A. brevipinne* needs revision as well.

Bruner (1991) reviewed the genus †*Amyzon* from North America and summarized the fossil localities and museum catalogues, as well as presented a bibliography of the genus. He pointed out that †*A. pandatum* and †*A. fusiforme* should both be junior synonyms of †*A. commune* for a number of reasons. First, according to Cope's original descriptions (Cope, 1874, 1875), there is no significant morphological difference between †*A. commune* and †*A. pandatum*, whereas †*A. fusiforme* seems to be a juvenile form of †*A. commune*. Second, the type specimens resemble each other in that the dorsal fin originates posterior to the origin of the pelvic fin, and the end of dorsal fin base is opposite to or posterior to the insertion of the last anal fin ray. This condition has not been seen in any other species of †*Amyzon*. Third, all three nominal species were recovered from the Florissant Formation, South Park, Colorado, which improves the possibility that they are the same species. While I expect to undertake further examination of the syntypes of those nominal

119

species, I agree with Bruner (1991) on the synonymy of †*A. pandatum* and †*A. fusiforme* with †*A. commune* based on the available evidence.

Bruner (1991) also suggested †*A. gosiutense* was a synonym of †*A. aggregatum* based on meristic and metric characters. It is true that the measurements and counts of most morphological structures of these two species overlap, and some characteristics of †*A. gosiutense* fall within the range seen in †*A. aggregatum*. However, one reason that the data for †*A. gosiutense* are within the range of those for †*A. aggregatum* could be that †*A. aggregatum* is represented by a much larger number of specimens (Grande et al., 1982, Table 3.1). Meanwhile, †*A. kishenehnicum* described here is represented also by a large collection and thus also shows high meristic and morphometric similarity to †*A. aggregatum*, as well as †*A. gosiutense* (Table 3.1). However, of even more significance, by comparing the osteology of these three species, I find that they differ from each other in a number of non-meristic osteological characters (Fig. 3.4, 5).

First, the anterior fontanelle (also known as ethmo-frontal, or preepiphysial fontanelle) is present in †*A. kishenehnicum* (Fig. 3.4.1, 5.1, 5.2) and †*A. gosiutense* (Fig. 3.4.11, 5.11), but absent in †*A. aggregatum* (Fig. 3.4.6, 5.6). All catostomids, including the fossil forms, have at least one fontanelle present. The fronto-parietal fontanelle is a notable synapomorphy, distinguishing them from the closely related cyprinids. All catostomid species possess the fronto-parietal fontanelle, with the exception of two members of the genus *Cycleptus*, in which only an ethmo-frontal fontanelle is present. Some catostomids, such as *Carpiodes, Myxocyprinus,* and some species of *Ictiobus,* have both the ethmo-frontal and fronto-parietal fontanelles. In the

Eocene †*Plesiomyxocyprinus,* a prominent anteriomedial notch was preserved very well in a disarticulated frontal, clearly showing the presence of an ethmo-frontal fontanelle in addition to the fronto-parietal fontanelle. In †*A. gosiutense,* an anteriomedial notch on the frontal is also visible in the examined specimen (Fig. 3.4.11, 5.11; AMNH FF 10460), which suggests an ethmo-frontal fontanelle exists. However, there is no anteriomedial notch on the frontal of †*A. aggregatum* (Fig. 3.4.6, 5.6). The ethmo-frontal fontanelle, occasionally present, is restricted in the ethmoid and bordered by the frontal posteriorly (ROM 11041).

Second, the frontal ridge is strong in †*A. kishenehnicum* (Fig. 3.4.1, 5.1) and †*A. aggregatum,* whereas it is weak in †*A. gosiutense.* The longitudinal ridge of the frontal is a synapomorphy for both fossil and extant catostomids, but varies in the length, strength, and ornamental pattern of the ridge. The frontal ridge in most catostomids extends from the middle of the frontal, at a level between where the postorbital processes of the frontal ends and the fronto-parietal fontanelle begins, to the posterior end of the frontal. However, some catostomids have a longer ridge, which extends nearly to the anterior end of the frontal, such as in †*A. kishenehnicum and* †*A. aggregatum.*

In terms of the strength of the ridge, the frontal ridge in some catostomids is weak and slightly raised, but in others it is strong and thick with thick dorsal projections, a thick dorsal flange, or with a laminated, laterally extended, roofing flange. The dorsal projection and flange of the frontal are common in many modern catostomids, as for example in *Ictiobus, Carpiodes, Myxocyprinus, Erimyzon,* and *Moxostoma,* whereas the lateral roofing flange is usually found in *Catostomus, Cycleptus,* and *Chasmistes.* In the fossil forms, †*A. kishenehnicum* and †*A. aggregatum* present

similar frontal ridges, i.e., a strong, thick ridge with projections, whereas †*A. gosiutense* and

†*Plesiomyxocyprinus* have a weak and slightly raised frontal ridge.

Nevertheless, the supraorbital notch of frontal is shallow and small in all of †*A. kishenehnicum*, †*A. aggregatum*, and †*A. gosiutense*. In catostomids, the supraorbital notch only exists in those that have a supraorbital bone. For example, the supraorbital bone is absent in *Catostomus* and *Moxostoma*, and there is no supraorbital notch; the lateral margin of the anterior part of the frontal forms the dorsal rim of the orbit and is usually truncated. Alternatively, the supraorbital process of the frontal is excluded entirely from the orbit, instead serving as a wedge between the supraorbital and the postorbital process of the sphenoid, for example, in *Ictiobus* and *Carpiodes*. The same condition of the lateral margin as in †*Amyzon kishenehnicum* also appears in the fossil forms †*A. aggregatum* and †*A. gosiutense* and in extant representatives *Myxocyprinus* and *Chasmistes*. Also, all of †*A. kishenehnicum*, †*A. aggregatum,* and† *A. gosiutense,* possess the truncated posterior margin of the frontal. The posterior margin of the frontal in catostomids is either truncated, oblique, zigzagged, or bears an elongated projection. The truncated margin is common in *Myxocyprinus* and some species of *Catostomus*.

Third, the parietal of *A. gosiutense* is roughly rectangular instead of bow-shaped as in †*A. aggregatum* and †*A. kishenehnicum* (Fig. 3.4.2, 4.7, 4.11). Most modern catostomids have the roughly rectangular shape of the parietal, whereas the laterally bow-shaped parietal is seen in *Myxocyprinus*.

Fourth, the anteromedial corner of the premaxilla of †*A. gosiutense* and †*A. kishenehnicum*

forms a sharp right angle, whereas it is rounded off in †*A. aggregatum* (Fig. 3.5.3, 5.7, 5.12). In the sampled extant catostomids, the rounded-off corner of the premaxillae is restricted to *Ictiobus*, *Carpiodes*, and *Myxocyprinus*, whereas the sharp-angled corner of the premaxillae occurs in the rest.

Fifth, the dentary process of the maxilla of †*A. gosiutense* is straight and truncated resembling that of *Cycleptus*, whereas the process is bent forward in †*A. aggregatum* and †*A. kishenehnicum*, which is a common condition in extant catostomids (Fig. 3.5.1).

Sixth, the size and arrangement of IO2 and IO3 of †*A. kishenehnicum* are different from those in †*A. aggregatum* and †*A. gosiutense*. In the latter species, IO3 is larger than IO2 and both of them form the ventral margin of the orbit, resembling in this respect the condition in *Ictiobus* and *Moxostoma*. In contrast, in †*A. kishenehnicum*, the elongated IO2 crosses the bottom of the orbit, resembling the condition in catostomids such as *Catostomus*.

Seventh, the preopercular sensory canal is partially enclosed in the bone in †*A. kishenehnicum*, whereas it is attached along a ridge on the middle line of the bone in †*A. aggregatum* and †*A. gosiutense*. In most Eocene catostomids, such as †*Plesiomyxocyprinus,* †*A. aggregatum* (UALVP 33041)*,* and †*A. gosiutense,* the sensory canal runs along a ridge that is created by thickening anterior or dorsal to the axis in comparison to the thin posterior lamina of the preopercle (Liu and Chang, 2009, Fig. 3.4e–f). The primitive cypriniforms †*Jianghanichthys* also possesses such a ridge, while the sensory canal is along the ridge on the upper half, but enclosed in the lower half.

Eighth, the pelvic bone fork is shallow in †*A. aggregatum* (UALVP 24147.2), medium depth in †*A. kishenehnicum* (Fig. 3.4.4, 5.4), and deep in †*A. gosiutense* (Fig. 3.4.13, 5.13). The variation in pelvic fork length of catostomids has been noted by Liu and Chang (2009). Three categories of catostomids according to PFL can be recognized: 1) fork shallow, PFL/PL equal to or less than 1/3, e.g., *Myxocyprinus, Carpiodes, Ictiobus,* †*Plesiomyxocyprinus*, and †*A. aggregatum*; 2) fork intermediate, PFL/FL around 1/2, e.g., *Cycleptus* and †*Amyzon* including †*A. kishenehnicum*; 3) fork deep, PFL/PL equal or more than 2/3, e.g., *Catostomus, Moxostoma, Erimyzon, Chasmistes*, and †*A. gosiutense*.

Last, the gap between hyp2 and hyp3 (caudal diastema) in †*A. gosiutense* (Fig. 3.4.14, 5.14) is consistently and visibly broader than that in †*A. aggregatum* (Fig. 3.4.9, 4.10, 5.9, 5.10). The gap is even narrower in †*A. kishenehnicum*. Moreover, both hyp2 and hyp3 are fused to the compound centrum proximally in †*A. kishenehnicum*, whereas only hyp2 is found to be fused to the compound in †*A. gosiutense*. In †*A. aggregatum*, hyp3 is occasionally fused to the compound in addition to hyp2. This condition with both hypurals fused to the compound centrum has also been found in †*Plesiomyxocyprinus* (Liu and Chang, 2009), *Minytrema, Myxocyprinus, Ictiobus, Carpiodes, Cycleptus* and *Erimyzon*, whereas the remaining catostomids have only hyp2 fused to the compound centrum.

As evident from the osteological characters, †*A. kishenehnicum*, †*A. aggregatum*, and †*A. gosiutense* are significantly different from each other. Therefore, I support the validity of †*A. gosiutense* as a distinct species.

Kinethmoid, Weberian Apparatus, and Pharyngeal Teeth of the North American †*Amyzon*

Compared to their Asian relatives, North American species of †*Amyzon* are much better known. However, because of the nature of fossil preservation, some key characteristics of †*Amyzon* have been unknown since the genus was first studied in 1872 (Cope, 1872). As more specimens have been discovered to give us a better understanding of these fishes, more features have become available for study. These account for our revised understanding of the evolutionary morphological traits of the family Catostomidae and even the order Cypriniformes.

The presence of the kinethmoid is a unique and universal synapomorphy of cypriniform fishes (Fink and Fink, 1981). The previous report of a "kinethmoid" in non-cypriniforms is that of a bone articulated with the maxilla distally and with the vomer and mesethmoid proximally in †*Chanoides*, which has been suggested to be not homologous with that of cypriniforms (Patterson, 1984). The other putative "kinethmoid" in non-cypriniforms was suggested to be in present in the gonorynchiform †*Ramallichthys* (Gayet, 1986), but neither observed nor agreed by Grande (1996) and Grande and Poyato-Ariza (1999). The kinethmoid is an endochondral bone connecting the premaxillary ascending processes and the ethmoid complex via ligaments, and contributing to the independently evolved protrusible jaw of cypriniforms (Hernandez et al., 2007; Staab and Hernandez, 2010; Staab et al., 2012). The kinethmoid is believed to have originated de novo in the ancestor of the Cypriniformes. However, it is rarely preserved in early cypriniform fossils (Cope, 1872, 1874, 1875, 1893; Liu, 1957; Wilson, 1977, 1980c; Grande et al., 1982; Sytchevskaya, 1986;

Zhou, 1990; Chang et al., 2001; Liu and Chang, 2009). The only description of the kinethmoid in a fossil was that of Wilson (1977) for †*A. aggregatum* using the term "rostral". As more specimens are collected and examined, the morphology and diversification of the kinethmoid in †*Amyzon*, represented by †*A. aggregatum*, †*A. gosiutense*, and †*A. kishenehnicum*, has become available. Overall, the kinethmoid in these three species has a rod-like shape resembling that of modern catostomids, and a very low aspect ratio (width/length) that probably correlated with the generation of great suction (Staab et al., 2012). The kinethmoid differs among species in shape, width, and presence of ridges on the dorsal end (the anterior end when protruded). In †*A. aggregatum*, the kinethmoid (Fig. 3.4.8) is long and thin, resembling that of *Moxostoma poecilurum*. Its length equals that of the ascending process of the premaxilla (Fig. 3.4.8). Both ends of the kinethmoid are rounded, whereas the middle is narrow. On the dorsal (anterior) end, only a few longitudinal ridges are present. In †*A. gosiutense*, the kinethmoid is laterally compressed, with rough ridges on the dorsal end (Fig. 3.4.12), similar to the condition in *Ictiobus* and *Catostomus*. Finally, in †*A. kishenehnicum*, the kinethmoid is present, but in no specimen is the whole element clearly visible. Inferred from the remains on several specimens, it is probably curved, with both ends rounded, and weak ridges on the dorsal (anterior) end; a similar shape can be found in *Cycleptus*. In summary, the kinethmoid of †*Amyzon* is variable, resembling that of different subfamilies of modern catostomids except Myxocyprininae.

The well-developed Weberian apparatus is another significant synapomorphy of ostariophysans including cypriniforms. The Weberian apparatus comprises four paired Weberian

ossicles and associated vertebral elements, modified from the first four or five vertebrae to transmit sound from the swim/gas bladder to the inner ear sensory cells. The Weberian apparatus of †*A. aggregatum* has been described by Wilson (1977), whereas that of †*A. gosiutense* has been described by Grande et al. (1982). The Weberian apparatus preseved in specimens of both taxa are revisited here. Together with †*A. kishenehnicum*, the Weberian apparatus of North American †*Amyzon* resembles that of Ictiobinae in general (Nelson, 1948). It is characterized by: a high neural complex with a lateral ridge and higher posterodorsal corner than anterodorsal corner; the neural spine of vertebra 4 nearly as high as the neural complex; a pair of parallel deep pleural ribs (rib 4) pointing ventrally with a very narrow and deep groove along the posterior margin; and a deep transverse plate with two prominent projections (Fig. 3.2.3). The deep neural complex and deep pleural rib 4 are probably correlated with the deep and compressed body of †*Amyzon* as discovered by Nelson (1948). Remarkably, an exceptionally preserved anterior view of a Weberian apparatus of †*A. aggregatum* shows that pleural rib 4 (fused with rib 2) is tightly sutured to vertebra 2 shortly below the elongated transverse process of vertebra 2 (UALVP 19540), resembling that in modern catostomids. Among modern cypriniform fishes, only in catostomids do the pleural ribs of vertebra 4 and 2 fuse into a robust pleural rib 4 and form a transverse plate. Apparently, this unique feature of catostomids was already present in the Eocene †*Amyzon* of North America.

A slender pharyngeal bone with one row of 16 or more compressed teeth with a comb-like arrangement is a key synapomorphy of catostomids (Eastman, 1977; Nelson, 2006). Grande et al.

(1982) estimated that †*A. gosiutense* had 50–60 pharyngeal teeth of conical shape. We have found a complete pharyngeal bone with teeth in posterior (ventral) view that belongs to †*A. aggregatum*. It bears 32 complete and broken teeth excluding the spaces for missing teeth (UALVP 24217a, ~37 including missing teeth). The teeth become gradually smaller as the pharyngeal bone tapers dorsally, and overall are laterally compressed with an apical projection. More precisely, the first few teeth have obliquely truncated tops probably because of wear, the teeth in the middle part of the bone are compressed with a hooked tip, and the remaining teeth on the dorsal end are very delicate (UALVP 24217 and 32931). According to the description of the pharyngeal teeth of †*A. gosiutense*, neither the number nor the shape is close to those of †*A. aggregatum*. One of the Asian Eocene catostomids, †*Plesiomyxocyprinus*, has a known pharyngeal bone and the teeth are similar in size and shape to those of †*A. aggregatum*. †*Plesiomyxocyprinus* has an estimated pharyngeal tooth number of "50+" based on one pharyngeal bone with 40 teeth preserved (IVPP V 12572.2). However, another pharyngeal bone with 14 teeth preserved on its ventral half suggests the total number of teeth was probably about 35, implying high intraspecific variation in the monotypic †*Plesiomyxocyprinus* (Liu and Chang, 2009, Fig. 3.5). Given this amount of variation, the 50 to 60 pharyngeal teeth suggested for †*A. gosiutense* vs. about 37 for †*A. aggregatum* are also reasonable in light of possible interspecific and intraspecific variation (Eastman, 1977) in †*Amyzon*. In summary, the number of pharyngeal teeth of Eocene catostomids is probably 35–60 and probably exhibits similar intraspecific and interspecific variation to that seen in modern catostomids (Eastman, 1977; Table 3.1).

Conclusions

In this study, I describe a new species, †*Amyzon kishenehnicum*, founded on 303 specimens from the Eocene Kishenehn Formation, Montana, USA. Based on the characters and data matrix of Smith (1992), a series of phylogenetic analyses are performed, suggesting that †*A. kishenehnicum* is sister to †*A. aggregatum*, and these together with †*A. gosiutense* form the most basal clade of Catostomidae. Meanwhile, the Asian genus †*Plesiomyxocyprinus* is closely related to the subfamily Myxocyprininae, supporting the hypothesis that was formulated by Liu and Chang (2009) without a phylogenetic analysis. I also reviewed the taxonomy of the North American species of †*Amyzon* by comparing the osteology. The osteological variations demonstrate that †*A. gosiutense* is a distinct species, although it had been considered to be a junior synonym of †*A. aggregatum*. Lastly, I summarized some key characteristics of the North American species of †*Amyzon*, such as the kinethmoid, Weberian apparatus, and pharyngeal teeth, which are critical to understanding the systematic evolution of the family Catostomidae, as well as the order Cypriniformes.

Table 3. 1 Meristic and morphometric data for North American species of †*Amyzon*, including †*A. kishenehnicum* sp. nov., †*A mentale*, †*A. commune*, †*A. aggregatum*, and †*A. gosiutense*. Values within () are observed from the specimens listed in the Methods and Materials section of this study. For those not otherwise designated, values for each species were obtained from the original descriptions. Standard length is in mm. Number of vertebrae does not include the Weberian apparatus.

Variable	*A. mentale*	*A. commune*	*A. aggregatum*	*A. gosiutense*	*A. kishenehnicum*
Number of dorsal fin principal rays	iii, 26 ii, 23	33 (31)	21—27; (21—27)	22—24; (20—21)	22—25
Number of anal fin principal rays	ii, 7	12	7—11; (7-10)	7—8; (7)	7—9
Number of pectoral fin rays	—	14	12—20; (11–16)	16	6—12
Number of pelvic fin rays	—	12—13	7—15; (7–14)	9—10; (9)	7—11
Number of vertebrae	—	38 or 39	32—37; (32—38)	30—31; (29)	31—36

Number of thoracic vertebrae	—	14 or 15	16—19; (16—24)	—; (15)	15—18
Number of caudal vertebrae	—	14 or 15	14—18; (14—17)	—; (14)	15—18
Standard length (SL)	—	260.3	39—242	?—240	30.8—370
Ratio of body depth to SL	—	0.38	0.41	0.36—0.44	0.21—0.43
Ratio of head length to SL	—	0.31	0.30	0.29—0.33	0.23—0.34
Ratio of caudal peduncle length to SL	—	—	—	0.16—0.22	0.14—0.21
Ratio of dorsal fin base length to SL	—	—	0.35	0.32—0.37	0.22—0.40
Ratio of anal fin base length to SL	—	—	0.09	0.08—0.09	0.06—0.10

Table 3. 2 Character states for fossil taxa †*Amyzon kishenehnicum* sp. nov., †*A. aggregatum*, †*A. gosiutense*, †*Plesiomyxocyprinus arratiae*, and †*Jianghanichthys hubeiensis*. See Smith (1992) for the character description and data matrix of extant taxa. Complete data matrix can be found in Morphobank (Project 1277, http://www.morphobank.org/).

Taxon	1–10	11–20	21–30	31–40	41–50	51–60	61–70
Jianghanichthys hubeiensis	???????100	0?0?0004??	???1?0?120	0?1???????	??????????	?????1?1??	?211002??-
Amyzon aggregatum	???00?1100	1?00?0001?	0??1?0??1?	0?0???????	??????????	???????1?0	?002120??0
Amyzon gosiutense	??????1100	1?00?0001?	???1?0??1?	0?0???????	??????????	???????1??	?002120??-
Amyzon kishenehnicum	??????1100	1?00?00?1?	???1?0??1?	0?0???????	??????????	???????1??	?003120??0
Plesiomyxocyprinus arratiae	???????10?	??10?00???	???1????1?	??????????	??????????	??????????	?????20??0

71–80	81–90	91–100	101–110	111–120	121–130	131–140	141–150	151–157
00??????2	01????????	???0000?0?	??????????	??????????	??????0???	??10140401	?0?11?0000	???1??1
00??????1	10????????	??011?101?	??????????	??????????	????200???	?11111?2?1	?1211?0001	20?????
00??????1	10????????	??011?0?1?	??????????	??????????	????2?0???	?11111??2?1	?1211?0001	?0?????
00??????1	11????????	??011?1?1?	??????????	??????????	????2?0???	?1110??2?1	?1211?0001	?0?????
????????1	2?????????	???1??203?	??????????	??????????	????200???	?11????1?1	?1?1??????	2??????

Figure 3. 1 †*Amyzon kishenehnicum*, sp. nov., photograph of the holotype specimen UALVP 55260

from the Kishenehn Formation. Scale bar represents 50 mm.
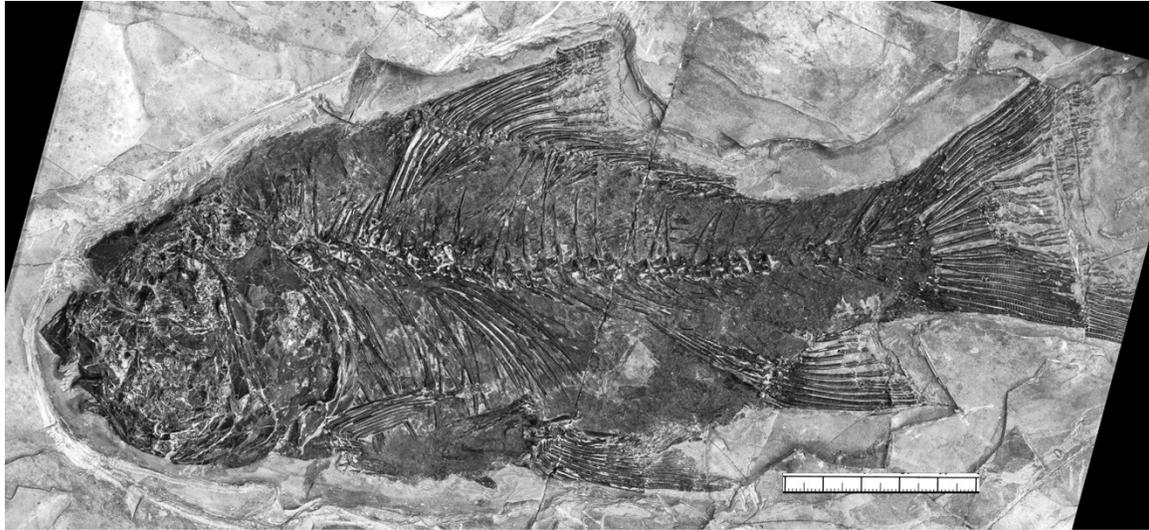
Figure 3. 2 †*Amyzon kishenehnicum*, sp. nov., photographs of juveniles from the Kishenehn Formation and osteological structures. (**1**), complete fish in left lateral view UALVP 24137; (**2**), otic region of UALVP 24152 showing the otoliths; (**3**), Weberian apparatus region of UALVP 24137; (**4**), gill region of UALVP 24152 showing the pharyngeal tooth and tooth socket. Scale bars represent 5 mm. Fish anterior of (**1**) and (**3**) facing left; of (**2**) and (**4**) facing right. Abbreviations: **cl**, cleithrum; **L. &. R. ast**, left and right asteriscus; **lap**, lapillus; **nc**, neural complex; **ns**, neural spine; **op**, opercle; **par**, parietal; **pr4**, the 4th pleural rib; **ptp**, posttemporal; **ptr**, autopterotic; **sag**, saggita; **scl**, supracleitrum; **scp**, scaphium; **trp**, tripus.
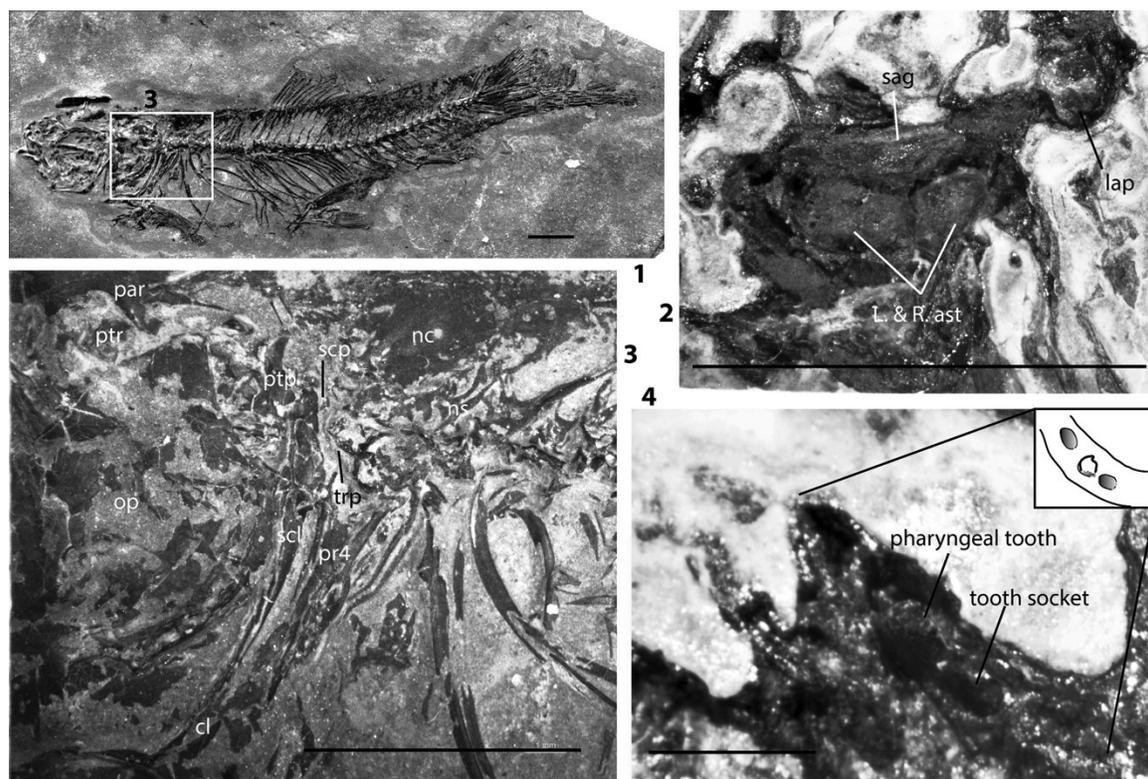
Figure 3. 3 Standard-length frequency distributions **(1)** and scatter diagram of body depth vs. standard length **(2)** in †*Amyzon kishenehnicum*, sp. nov., from the Kishenehn Formation.
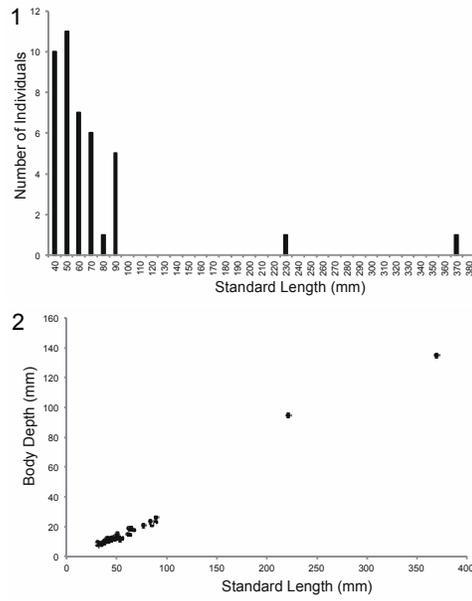
Figure 3. 4 Photographs of †*Amyzon kishenehnicum*, sp. nov., from the Kishenehn Formation, †*Amyzon aggregatum*, and †*Amyzon gosiutense* showing osteological differences. **(1)** through **(5)**, specimens of †*Amyzon kishenehnicum*, sp. nov.: **(1)**, skull roof of UALVP 55260 showing the frontal with the concave margin for the anterior fontanelle and posterior fontanelle; **(2)**, parietal of UALVP 24137; **(3)**, snout region of UALVP 24137; **(4)**, pelvic bone of UALVP 24137; **(5)**, caudal skeleton of UALVP 24154. **(6)** through **(10)**, specimens of †*A. aggregatum*; **(6)** & **(7)**, frontal and parietal of UALVP 32931; **(8)**, snout region of UALVP 31125; **(9)** & **(10)**, caudal skeleton of UALVP 31958 & 40931. **(11)** through **(14)**, specimens of †*A. gosiutense* AMNH FF 10460 showing **(11)**, skull roof, **(12)**, snout region, **(13)**, pelvic bone, and **(14)**, caudal skeleton. Black scale bars represent 5 mm; scale photographed with specimens is in mm. Fish anterior of **(1)** through **(5)**, **(8),** and **(9)** facing left; of **(6)** and **(7)** facing up; of **(10)** through **(14)** facing right. Abbreviations: **afn**, anterior fontanelle (ethmo-frontal); **cc**, caudal centrum compound; **den**, dentary; **emd**, ethmoid; **fr**, frontal; **frd**, frontal ridge; **hyp**, hypural; **kem**, kinethmoid; **max**, maxilla; **mxn**, neck of maxilla; **par**, parietal; **pfn**, posterior fontanelle (fronto-pariental); **phy**, parhypural; **pls**, pleurostyle; **pmx**, premaxilla; **psp**, pelvic splint; **psr**, pelvic strut; **ptr**, autopterotic; **rna**, rudimentary arch; **son**, supraorbital notch of frontal; **sop**, supraorbital process of frontal; **sph**, sphenotic.
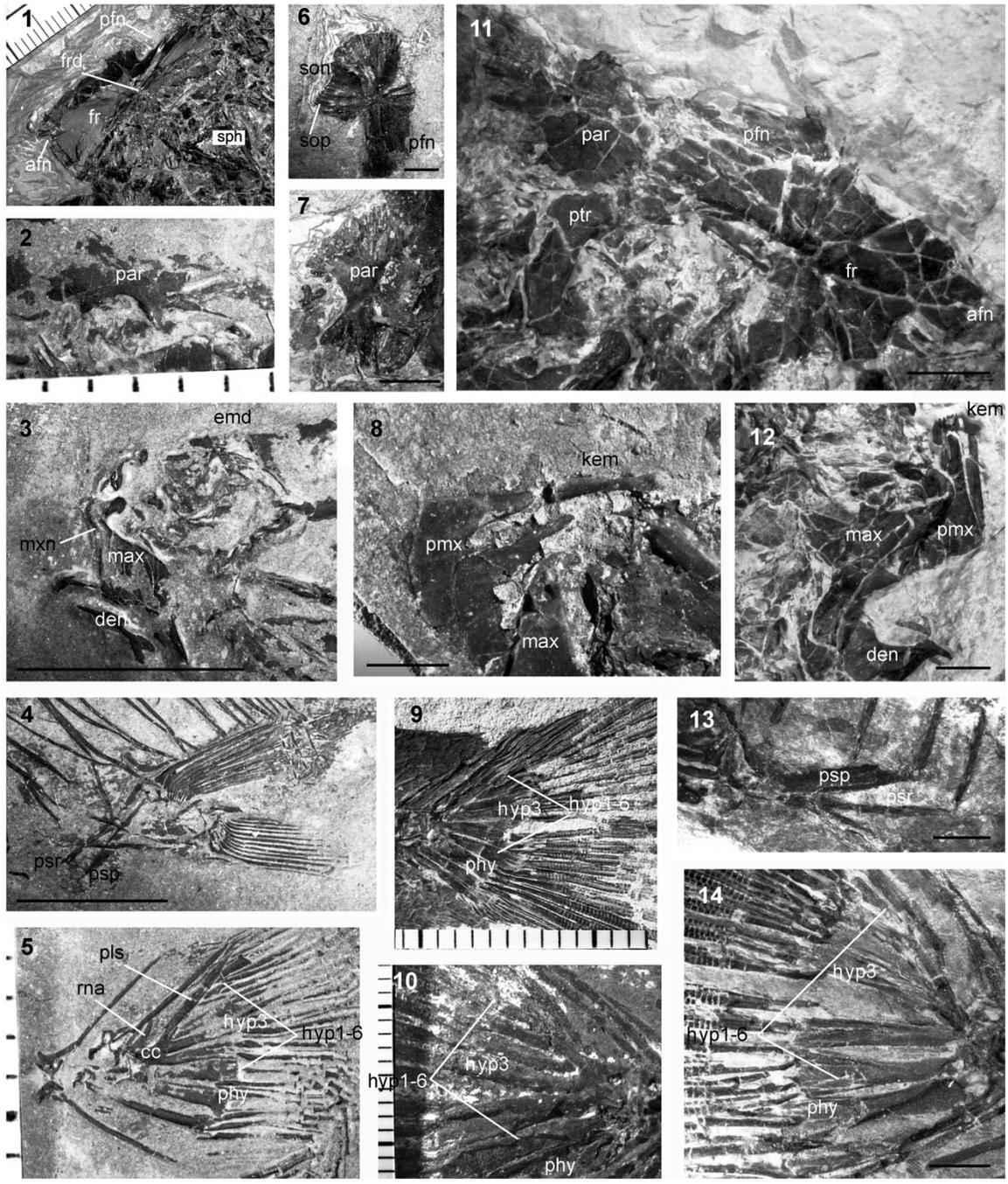
Figure 3. 5 Reconstructive drawing of †*Amyzon kishenehnicum*, sp. nov., from the Kishenehn Formation, †*Amyzon aggregatum*, and †*Amyzon gosiutense*. **(1)**. head region drawing of †*Amyzon kishenehnicum*, sp. nov. based on the holotype specimen UALVP 55260; **(2)** through **(5)**, reconstructive drawing of †*Amyzon kishenehnicum*, sp. nov.; **(6)** through **(10)**, †*Amyzon aggregatum*; **(11)** through **(14)**, †*Amyzon gosiutense*. **(2), (6)**, and **(11),** left frontal; **(3)**, **(7)**, and **(12)**, left premaxilla; **(4)**, **(8)** and **(13)**, left pelvic bone; **(5)**, **(9)**, **(10)**, and **(14)**, caudal skeleton. Reconstructions of **(2)** through **(14)** are based on the respective images of Figure 4. Anterior in all drawings faces left. Abbreviations: **aa**, anguloarticular; **afn**, anterior fontanelle (ethmo-frontal); **bh**, basihyal; **br**, branchiostegal; **cl**, cleithrum; **den**, dentary; **ect**, ectopterygoid; **emd**, ethmoid; **ent**, endopterygoid; **fr**, frontal; **frd**, frontal ridge; **hym**, hyomandibular; **hyp**, hypural; **io**, infraorbital; **iop**, interopercle; **lem**, lateral ethmoid; **lhh**, lower hypohyal; **max**, maxilla; **mpt**, metapterygoid; **mxn**, neck of maxilla; **nc**, neural complex; **ns**, neural spine; **op**, opercle; **par**, parietal; **pfn**, posterior fontanelle (fronto-pariental); **pmx**, premaxilla; **pop**, preopercle; **psp**, pelvic splint; **psr**, pelvic strut; **ptp**, posttemporal; **ptr**, autopterotic; **qua**, quadrate; **soc**, supraoccipital; **ra**, retroarticular; **scl**, supracleithrum; **so**, supraorbital; **sop**, subopercle; **sph**, sphenotic; **sym**, sympletic; **uhh**, upper hypohyal.
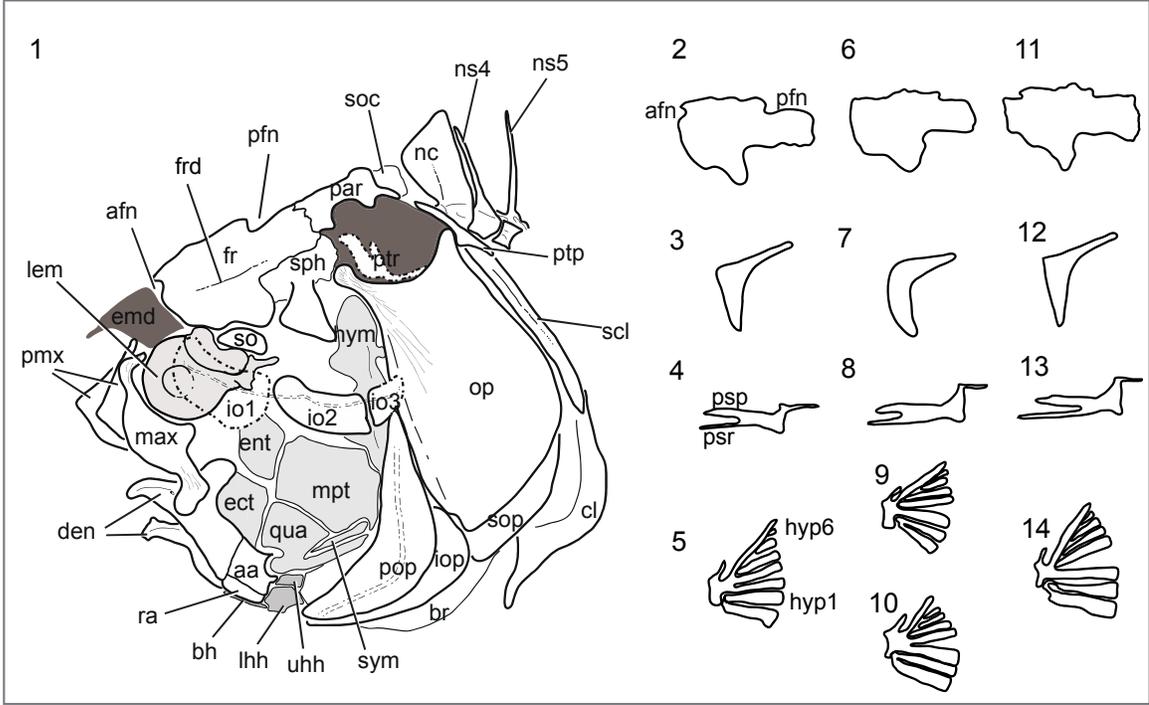
Figure 3. 6 Strict consensus cladogram of catostomids based on Smith (1992) with the addition of †*Amyzon kishenehnicum*, sp. nov. from the Kishenehn Formation, †*A. aggregatum*, †*A. gosiutense*, †*Plesiomyxocyprinus arratiae*, and †*Jianghanichthys hubeiensis*. Three analyses involving three outgroups and 67 ingroups, performed in PAUP and TNT, and using parsimony criteria, generated the same strict consensus cladogram; CI 0.38, RI 0.78.

Outgroup

Amyzon

Myxocyprininae
+ Cycleptinae

Ictiobinae
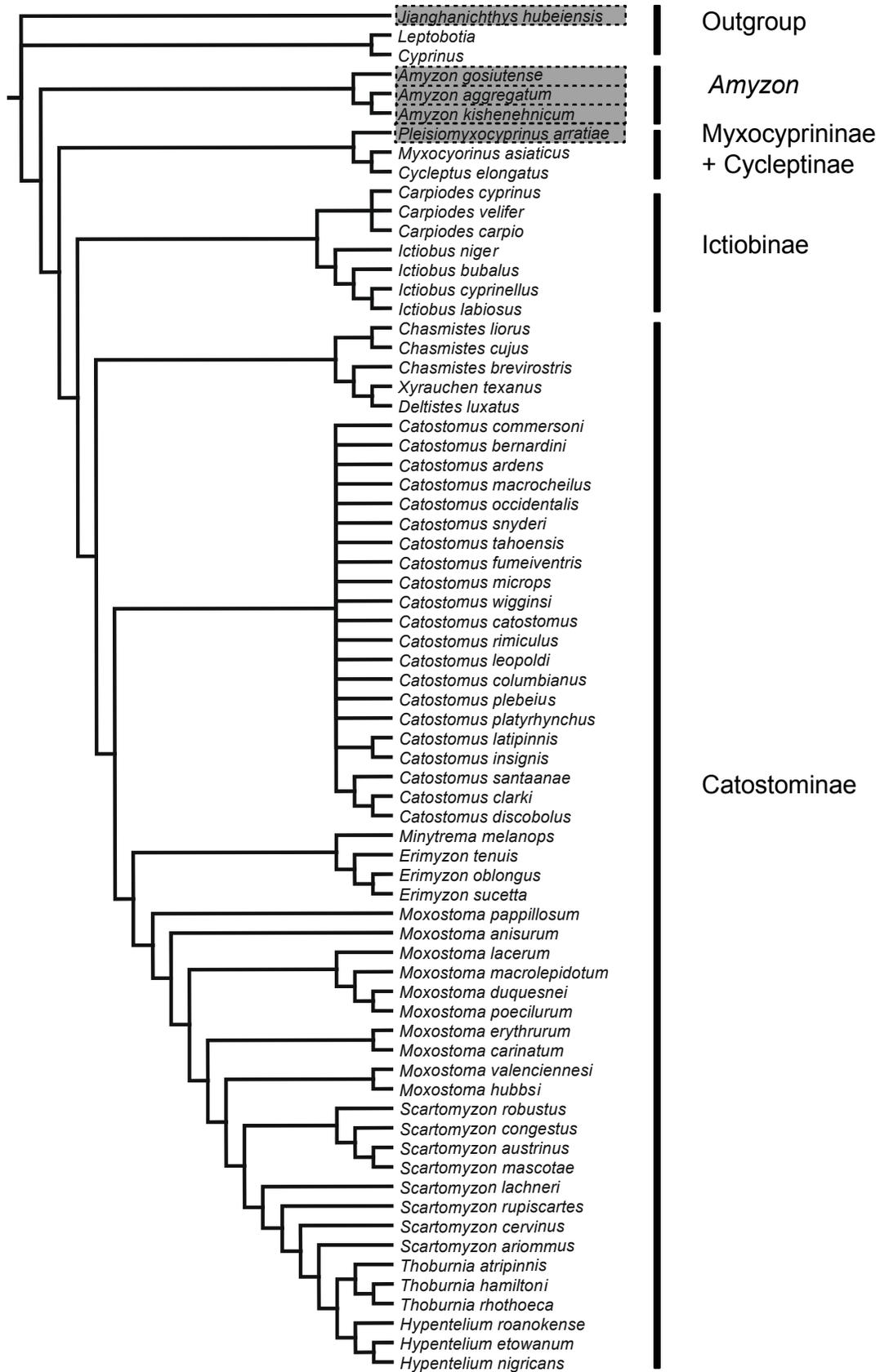
Catostominae

Chapter 4 Restudy of *"Amyzon" brevipinne* and the first discovery of loach-like catostomids from the Eocene Allenby Formation, British Columbia, Canada

Abstract

The Eocene catostomid fish (Cypriniformes, Catostomidae) from the Allenby Formation, British Columbia, Canada, is reviewed based on recently collected specimens. The fish was originally recognized as a catostomid by Cope in 1893 and described as *Amyzon brevipinne*. Wilson comprehensively re-described the species in 1977 based on a large collection. More specimens collected recently brought the need for a systematic revision of this fish to light. The fish is different from all known *Amyzon* species in having a narrow frontal with elongated orbital notch, shallow and slender infraorbital series, broad opercle, and a short and slender rib 4. However, the species also lacks synapomorphies of *Amyzon*, and herein is assigned to a new genus as "NewGenus" *brevipinne*. "NewGenus" resembles loaches in having the elongated orbital notch, whereas it resembles gyrinocheilids in the shallow and slender infraorbital series and moderately robust rib 4. It is the first loach-like catostomid known and as such fills the gap among the main clades of the superfamily Cobitoidea (Catostomidae, Gyrinocheilidae, and the clade of loach families).

Keywords

Eocene, Allenby Formation, Catostomidae, Cobitoidea, Cypriniformes

Introduction

Catostomid fishes (Ostariophysi, Cypriniformes, Catostomidae), with the common name of suckers, are widely distributed in North America with over 70 species, while only two species are known from East Asia (Nelson, 2006). They have diversified in North America since the Eocene, which is a critical geological age to the early evolution of catostomid fishes when they diversified globally and diverged into many species. Eight nominal species have been described from the Eocene of North America; however, they were without exception assigned to the genus *Amyzon* when described (Cope, 1872; Cope, 1874; 1875; 1893; Wilson, 1977a; Grande et al., 1982; Liu et al., 2016).

The type species of *Amyzon*, *A. mentale* was described from a coalmine near Osino, Nevada, USA (Cope, 1872). In subsequent studies, Cope (1874; 1875; 1893) reported four species of *Amyzon*. Wilson (1977a) described *Amyzon aggregatum* from the Horsefly Beds, British Columbia based on a large collection and comprehensive comparison and examination. Further new materials of *Amyzon* were discovered and subsequently described from the ancient Lake Gosiute of the Green River Fm., Wyoming (Grande et al., 1982) and the Kishenehn Fm., Montana, USA (Liu et al., 2016; Chapter 3).

Of the nominal species of *Amyzon* named by Cope excluding the type species, Bruner (1991) suggested only two of them, *A. brevipinne* and *A. commune*, should be considered valid species. This opinion was supported by Liu et al. (2016) in an overview of *Amyzon* (Chapter 3). Meanwhile, Liu et al. (2016) also questioned the generic designation of *A. brevipinne*. The species *A. brevipinne* was described (Cope, 1893) based on the single holotype specimen collected by G.

M. Dawson in 1888. Later on, Eocene fishes from British Columbia were generously sent to L. M. Lambe and described as *A. brevipinne* (Lambe, 1906). Wilson (1977a) clarified the taxonomic assignment for Eocene British Columbia fish by re-description of *A. brevipinne* and species recognition of *A. aggregatum* based on a large number of specimens. Wilson's description established the species status of *A. brevipinne*. Osteology based on skeletons of fossil catostomids was comprehensively described. Also, more specimens from multiple fossil localities in British Columbia were referred to the species. However, as new materials have been collected in recent years, even more osteological characters became available. Significant differences between *A. brevipinne* and other *Amyzon* species had been noticed, potentially contributing to our understanding of the systematic position of *A. brevipinne*.

This study aims to complement the known osteology of the nominal *A. brevipinne* with new characters discovered from recently collected specimens, hypothesize the systematic position of that fish, and understand the early evolution of the family. An overview of the Paleogene catostomids of North America will be presented.

Materials and Methods

Fossil specimens of the nominal "*Amyzon brevipinne*" were collected from the Princeton, and Tulameen areas of British Columbia, Canada. The fossil localities are Pleasant Valley of the Canadian Museum of Nature (CMN), Pleasant Valley L90, L92, L93, and L94, Whipsaw Creek L91, and Blakeburn Mine L95 of the Royal Ontario Museum (ROM) (Wilson, 1977a), and Whipsaw Creek and Blakeburn Mine of the University of Alberta Laboratory for Vertebrate Palaeontology (UALVP). Comparative fossil and extant fish specimens are listed in General

Appendix II.

Opercular measurement: The opercle height (OPH) is the vertical distance from the opercular fossa to the anteroventral corner of the opercle. The opercle width (OPW) is the widest measurement of the opercle measured perpendicular to the opercle height. The angle of the anteroventral corner is measured or estimated as that formed by the anterior vertical margin and the ventral margin of the opercle. In the case of the anterior margin of the opercle not being straight, a line that passes through both the opercular fossa and the anteroventral corner substitutes for it in this measurement.

Pharyngeal arch: The terminology of the pharyngeal bone and its teeth is based on Chu (1935). Since the pharyngeal bone is more dorso-ventrally directed than anteroposteriorly placed (unlike that of cyprinids), the Anterior and Posterior Edentulous Processes of Chu (1935) are revised to be the Anteroventral and Posterodorsal Edentulous Processes respectively. The Dorsal and Pitted Surface is combined into the Dorsolateral Surface since is more laterally directed and usually porous in catostomids rather than pitted as in cyprinids.

Pelvic girdle: The terminology of the pelvic girdle is as follows (Liu et al., 2016). The pelvic bone length (PL) is represented by the pelvic strut length, which is measured from the anterior tip of the strut to the posterior end of the pelvic bone excluding the ischial process. The pelvic fork length (PFL) is measured from the anterior point of the strut to the posteriormost point of the fork. The pelvic splint length (PSL) is measured from the anterior-most end of the splint to the posterior end of the pelvic bone excluding the ischial process. The PSL may or may not be equal to the PL in

catostomids.

Additional anatomical abbreviations used in text are: BD, body depth; HD, head length; hyp, hypural; SL, standard length.

Institution abbreviations: CMN, Canadian Museum of Nature, Ottawa, Canada; ROM, Royal Ontario Museum, Toronto, Canada; UALVP, Laboratory of Vertebrate Paleontology, University of Alberta, Edmonton, Canada; USNM, National Museum of Natural History, Washington D.C., USA.

Systematic Paleontology

<div align="center">

Subdivision TELEOSTEI Müller, 1845

Superorder OSTARIOPHYSI Sagemehl, 1885

Order CYPRINIFORMES Bleeker, 1860

Family CATOSTOMIDAE Agassiz, 1850

Genus †"NewGenus" gen. nov.

</div>

Type species: *Amyzon brevipinne* Cope, 1893

Included species: "NewGenus" *brevipinne* (Cope), 1893

Diagnosis: Same as that for the type and only known species.

"NewGenus" *brevipinne* **(Cope), 1893**

Synonyms: *Amyzon brevipinne* Cope, 1893, p. 402 (original description).

Amyzon brevipinne Cope: Lambe, 1906, p. 154.

Amyzon brevipinne Cope: Wilson, 1977, p. 23–32, fig. 8.

Holotype: CMNFV 6189, a fish lacking the tail (Fig. 4.1).

Referred materials:

Well-preserved specimens: UALVP 12159, a nearly complete fish; UALVP 12658, a nearly complete fish lacking the tail; UALVP 12610, a complete right frontal; UALVP 31585, a right pharyngeal bone with teeth; ROM 11160, a pharyngeal bone with teeth; ROM 11163, a nearly complete fish.

CMN collection: CMNFV 2042, 2046, 2050, 2054, 2055, 2057, 2066, 2068, 2069, 2071–2074, 2090, 2092, 2097, 2099, 2104, 34480–34492, 34509, 34820, 34821, 348883, 34885, 34888, 34891, 34893–34899, 41745, and 41746. Specimens listed together under NMC 3132 in Wilson (1977) are re-catalogued within CMNFV 34480–34899. CMNFV 6195(a, b) and 25266 from Tranquille area are recognized to be "NewGenus".

UALVP collection: UALVP 12104, 12133, 12462–12464, 12480, 12481, 12483, 12487, 12496, 12509, 12512, 12514–12517, 12519–12521, 12525–12529, 12532–12534, 12537–12539, 12541, 12542, 12545–12547, 12549, 12553–12556, 12558, 12561, 12563–12566, 12568–12570, 12572–12577, 12580, 12583, 12584, 12586–12589, 12591, 12593, 12595, 12597–12599, 12601,

12602, 12605, 12606, 12611–12613, 12616, 12617, 12619, 12621–112626, 126311–12636,12638, 12639, 12641–12645, 12647, 12651–12654, 12661–12680, 12682–12684, 12686–12689, 12691– 12698, 12700–12708, 12710, 12711, 12714–12716, 12719–12729, 12731, 12733–12736, 12743– 12746, 12750, 12754, 12757, 12762, 12763, 12767, 12768, 12770–12772, 12775, 12777–12779, 12783–12785, 12787–12790, 12794–12798, 12800–12804, 12806, 12807, 12810, 12812, 12813, 12819, 12820, 12825–12828, 12830, 12831, 12835, 12837–12843, 12845–12847, 12850, 12854– 12858, 12850–12864, 12866, 12867, 12869, 12878, 12879, 12884, 12888, 12889, 12893–12904, 12906, 12907, 12910, 12912–12921, 12923, 12957, 12969, 12978, 12981, 12987, 12989, 12991, 12992, 13006, 13008, 13012, 13019, 13021, 13037, 13054, 13071, 13072, 13078, 13085, 13089, 13097, 13114–13126, 13129, 13131–13135, 13137–13144, 13146, 13147, 13149, 13150, 13152– 13174, 13177, 13182, 13184, 13187, 13435, 14730, 14731, 14735, 14737, 14738, 14745–14748, 14754, 14755, 14759, 14760, 15912–15915, 17836, 21262–21339, and 27140.

ROM collection: ROM 11161, 11162, 11164, 11166, 11167, 11169–11171, 11179, 11182, 11370, 11377, 11379, 11382, 11387, 11389, 11461, 11468, and 19420.

Age and Horizon: Allenby Formation, early Eocene.

Type locality: North Fork of the Similkameen River (Tulameen Rivers), probably in Pleasant Valley (Princeton area), British Columbia, Canada (Wilson, 1977a).

Additional localities: Whipsaw Creek, Blakeburn Mine areas, and Tulameen, British Columbia, Canada.

Revised Diagnosis: Small-sized and shallow-bodied Eocene catostomid, BD/SL 0.20–0.32, HD/SL 0.30–0.40,   D 12–18, A 7–10, pharyngeal teeth about 20, frontal nearly rectangular with elongated orbital notch, supraorbital present, infraorbital series including lacrimal shallow and

slender, posteroventral process of dentary short, opercle broad with OPW slightly larger than OPH, neural complex oval in shape, rib 4 not very robust with length shorter than half the regular rib, PFL about 1/2 PL, PSL sub-equal to PL, hyp 3 not fused to compound centrum.

Description

Wilson (1977a) described this species in detail including the intraspecific variation of meristic and morphometric characters. However, as new specimens and new perspectives provide more information for understanding this fish, new characters have been discovered. The re-description below is intended to complement the earlier description and to emphasize the morphological traits that contribute to our understanding of its evolutionary position.

General Appearance

This is a small-sized and loach-like catostomid fish, with maximum standard length among the specimens being 84 mm (UALVP 27140). The holotype (Fig. 4.1) is one of the largest individuals with an estimated SL around 80 mm. The body is shallow (Fig. 4.1 and 4.2) with the ratio BD/SL ranging from 0.20 to 0.32. The ratio HD/SL ranges from 0.30 to 0.40.

Skull

Skull roof: the frontal (Fig. 4.3A, UALVP 12610) is antero-posteriorly elongated and roughly rectangular in shape with the anterior two-thirds broad and the posterior one-third narrow. The anterior margin, suturing to the ethmoid complex and possibly also to the lateral ethmoid, is convex.

Whereas the medial margin of the anterior portion is nearly straight, the lateral margin consists of an elongated orbital notch and a short pointed orbital process (Fig. 4.3A). The posterior portion has straight medial, lateral and posterior margins. The medial margin of the posterior portion surrounds the fronto-parietal fontanelle. The dorsal surface of the skull is slightly longitudinally domed, resembling the appearance of the frontal ridge. No sensory canal is enclosed by the frontal. The frontal is usually preserved in articulated specimens with the domed frontal ridge and elongated orbital notch visible, as in the holotype (CMN 6189) and UALVP 12159.

The parietal is roughly square with the width sub-equal to the width of the posterior portion of the frontal (UALVP 12658). It surrounds the fronto-parietal fontanelle medially. Left and right parietals may not contact each other at the posteromedial corner.

The anterior portion of the parasphenoid is usually visible in the orbit. It is slightly broad and flat as shown by *in situ* and undisturbed preservation (UVALP 12698, 12807). In some specimens it may show a vertical expansion due to the rotation of the bone in lateral preservation.

Infraorbital series: The orbit is large; this may correspond to large eyes in the living fish. A supraorbital and five infraorbitals (UALVP 12658) are present. The supraorbital is deep and semi-circular in shape (CMN 34893). The lacrimal (infraorbital 1, IOB 1) is an elongated oval shape. It is not significantly enlarged as in other catostomids. Also, unlike the lacrimal usually being horizontal in catostomids, the longitudinal axis of the lacrimal is more vertically placed and angled to the horizontal. IOB 2–5 are generally thin and slender. IOB 3 is positioned at the posteroventral corner of the orbit. Sensory canal remains are observed associated with the

infraorbitals and most likely were enclosed by bone (UALVP 11161).

Opercular Series

The preopercle consists of a vertical arm and horizontal arm that form an obtuse angle. It is moderately broad compared to other catostomids. The horizontal arm is shorter than the vertical arm. The preopercular sensory canal is enclosed in bone (ROM 11161).

The opercle (Fig. 4.4B) is the same general shape as in other catostomids in having an opercular arm, an auricular process, and a dorsal concavity (Nelson, 1949). The opercular arm is short and flat, whereas the auricular process is well developed with a dorsal projection. The opercle height is sub-equal to or slightly shorter than the opercle width. The angle of the anteroventral corner is broad and more than 60°.

The interopercle (Fig. 4.4C, UALVP 12616) is semi-lunate in shape with the anteroventral process well-developed and pointed. The subopercle is shaped roughly like a willow leaf. The anterodorsal process is well developed. Overall, the bone is broader than that of *Amyzon*.   Three branchiostegals are present.

Mandibular, Hyoid, and Gill Arches

The premaxilla is "L" shaped with the angle rounded. The ascending process and labial process are nearly equal in length. The ascending process is tapered posteriorly to a point, whereas the labial

process is broad and rounded at the end. The maxilla has two dorsal processes, of which the anterodorsal process toward the premaxilla and the posterodorsal process arise from the same point. Whereas the anterodorsal process is directed somewhat upward, the posterodorsal process is directed posteriorly at roughly a right angle to the maxilla body. The maxilla body is broad, with the anterior margin rounded and posterior margin protruding dorsally. The ventral process of the maxilla is slightly curved anteriorly.

The dentary (Fig. 4.4G, ROM 11161, UALVP 12666) is roughly triangular. The gnathic ramus is moderately long, only slightly longer than the base of the coronoid process. The anterior end of the gnathic ramus is slightly ventrally deflected. The coronoid process is well developed and semi-circular in shape. The posteroventral process is not elongated. A lateral ridge extends along the gnathic ramus to reach the far end of the dentary. The anteroventral margin between the anterior end of the gnathic ramus and the ventral point of the posteroventral process is nearly straight. The symphysis between left and right dentaries is short. No mandibular sensory canal is observed.

A small anguloarticular (Fig. 4.4G, ROM 11161) is sutured to the posteroventral process of the dentary. It is about the same size as the coronoid process of the dentary and smaller than the posteroventral process. A fossa is present posterodorsally to articulate with the quadrate. The retroarticular (Fig. 4.4G, ROM 11161) is very small and ovoid. The quadrate has a flat, diamond-shaped dorsal portion and a rod-like ventral strut that tapers posteriorly. The anterodorsal corner of the flat portion projects past the point of articulation between the quadrate and anguloarticular.

The endopterygoid (ROM 11161), positioned dorsal to the quadrate, is rounded. The anterodorsal fossa that articulates with the autopalatine is large.

The urohyal (Fig. 4.4D, ROM 11161a) is roughly diamond shaped. The hypohyal processes are adjacent to one another at the anterior end. The horizontal lamina is expanded to its greatest width just behind the anterior end, and then tapers gradually to the posterior point. It has a longitudinal deep groove in the middle.

Pharyngeal Arch

Two disarticulated pharyngeal bones are preserved with teeth (Fig. 4.4A; ROM 11160, UALVP 31585). The pharyngeal bone is slightly arched. Both dorsal dentigerous and ventral porous surfaces are narrow. Also, the dorsal and ventral edentulous processes are both short. Whereas 17 teeth or tooth impressions are preserved in UALVP 31585, 16 teeth are preserved in ROM 11160. Taking the spaces for missing teeth into account, the estimated pharyngeal tooth number is 20. Pharyngeal teeth are compressed, slender, and tall. Teeth become gradually smaller from ventral to dorsal edge of the pharyngeal bone. The first two ventral-most teeth are thick with rounded crowns, whereas the rest of the teeth are pointed.

Paired and Median fins

The shoulder girdle and fin consists of the posttemporal, supracleithrum, cleithrum, postcleithrum, and 11 to 15 (usually 11 or 12) pectoral fin rays. The posttemporal is prominent (UALVP 12698). It

is a flat, band-like bone vertically placed above the supracleithrum and cleithrum and it connects them to the cranium. The supracleithrum is also flat and band-like, but broader, longer and straighter than the posttemporal. The cleithrum (ROM 11468) is spoon shaped with the medial lamina much broader than the lateral surface. The postcleithrum dorsal ramus is attached posteriorly on the cleithrum, and the ventral ramus is elongated, more than two times the dorsal ramus in length (holotype CMN 6189), with a free end. There is no prominent projection at the angle where the two rami meet.

The pelvic fin contains 6 to 10 (usually 8) rays. The pelvic bone is bifurcated anteriorly with a pelvic fork that divides the pelvic bone into the lateral, rod-like pelvic strut and the medial lamina of the pelvic splint. The pelvic bone is intermedially forked with the fork length sub-equal to half of the pelvic bone length. The pelvic splint length is sub-equal to the pelvic length, so that the pelvic strut and pelvic splint nearly reach the same point anteriorly.

There are 12–18 (usually 12–14) principal dorsal fin rays. The principal anal fin ray number range 7–10, with most specimens having 8–9 and only one specimen having 10. There are consistently 2–3 procurrent rays preceding the principal dorsal and anal fin rays. The dorsal and anal fins are supported by the pterygiophores that number the same as the number of principal fin rays. Whereas the first pterygiophore supports all the procurrent rays, the usually doubled last median fin ray connects to a tiny and incomplete pterygiophore element that doesn't have a spinous structure and thus is not always counted. In the case of the anal fin, this is known as the anal fin stay (Weitzman, 1962). The first pterygiophore is relatively large and medially broad consisting of a broad median sheet of bone anteriorly and a spine-like posterior part.

Vertebral Column and Caudal Fin

Exclusive of the Weberian apparatus, there are 28 to 32 vertebrae, of which 13 to 16 (usually 14–16, only one specimen having 13) are caudal. The Weberian apparatus (UALVP 12658, 12698b and 12807) involves the first four vertebrae and associated elements. The neural complex (Fig. 4.4F) is roughly oval in shape with the dorsal and anterior margins convex. A vertical ridge is present in the lower middle portion of the neural complex. Neural spine 4 (Fig. 4.4F) at its greatest height reaches the dorsal edge of the neural complex. The fourth rib (Fig. 4.4F), including contributions from the pleural process of centra 2 and 4, is moderately robust and short in comparison to all other catostomids. It is less than half the length of the regular ribs on centrum 5, and narrower than that of extant catostomids that have a rib 4 of similar length. A vertical groove may be present on the lateral surface of rib 4. Rib 4 is generally thinner and more slender than that of *Amyzon* and extant catostomids, resembling more that of gyrinocheilids.

The caudal skeleton (Fig. 4.4E, ROM 11161a) consists of a compound centrum with fused pleurostyle and hypural 2, an epural, five to six hypurals, a parhypural, and a free uroneural. As in all other catostomids, hypural 1 and the parhypural are fused proximally (ROM 11161a) then attached to the compound centrum. Hypurals 3 to 5 or 6 are attached under the pleurostyle. A free uroneural is present along the distal half of the pleurostyle. There are 18 principal caudal fin rays (i, 8, 8, i) with 4–7 dorsal and 4–7 ventral procurrent rays.

Discussion

Characters contributing to the systematic position of "NewGenus"

The familial assignment of "NewGenus" *brevipinne* to Catostomidae is confirmed by the morphology of the pharyngeal arch. The pharyngeal bone of catostomids is falcate (Eastman, 1977), with the dentigerous side and the posterolateral side gradually tapered towards the dorsal end. These two sides in cyprinids are roughly triangular or rectangular (Chu, 1935; Zeng and Liu, 2009), whereas those of loaches are enlarged in the middle and roughly triangular although very delicate (Sawada, 1982). The compressed pharyngeal tooth is another unique synapomorphy of catostomids. While the shape and size of the pharyngeal teeth are varied in cyprinids (Chu, 1935; Zeng and Liu, 2009), no extremely compressed teeth as in catostomids have been seen. Pharyngeal teeth of loaches, if well formed, are fewer in number than those of catostomids, and generally conical in shape (Sawada, 1982; and pers. obs.).

Different from that of all known catostomids, the frontal of "NewGenus" is elongated antero-posteriorly and roughly rectangular in shape. It lacks the common fan-shaped anterior half of the frontal seen in both extant and extinct catostomids (Weisel, 1960; Branley, 1962; Wilson, 1977a; Lo and Wu, 1979; Liu and Chang, 2009). Furthermore, the frontal of "NewGenus" possesses a shallow and elongate orbital notch, which has not been seen in a catostomid before, let alone in other Eocene catostomids (Fig. 4.2B and C). In comparison to that of other cypriniforms, the frontal of "NewGenus" resembles that of loaches (Ramaswami, 1953; Sawada, 1982) in having such an orbital notch. The distinctive shape of the frontal has been seen consistently in the holotype and specimens of "NewGenus" from different localities (Fig. 4.1 and 4.2).

Another autapomorphy of "NewGenus" occurs in the infraorbital series. In extant catostomids and the Eocene *Amyzon*, the lacrimal is significantly enlarged, and infraorbitals 2 and 3 (IOB2 and 3) are thin and deep. The infraorbitals beyond IOB 3 in extant catostomids are string-like. However, in that of "NewGenus", neither thin and deep, nor string-like infraorbitals were observed. In addtion, the lacrimal is not as large as in other catostomids. All the infraorbitals of "NewGenus" are generally thin and slender, resembling more those of gyrinocheilids.

A plesiomorphic character of cypriniforms, which is seen in "NewGenus" but no other catostomid, is that the preopercular sensory canal is enclosed in the preopercle. In catostomids, three types of association of the preopercular sensory canal and the bone have been observed: partially enclosed, attached to a ridge, and completely detached (Chapter 6). The preopercular sensory canal is superficial (detached from the bone) in most extant catostomids, for instance, *Catostomus* and *Moxostoma*. In some catostomids, e.g., *Cycleptus*, *Myxocyprinus*, and *Plesiomyxocyprinus*, the sensory canal is attached tightly behind a bony ridge running through the midline of the preopercle. In some other catostomids, such as *Amyzon*, the sensory canal is enclosed in the middle of the bone and exposed at both ends. "NewGenus" is so far the only known catostomid possessing a completely enclosed preopercular sensory canal.

"NewGenus" differs from all other Eocene catostomids including the Asian members in the pharyngeal tooth number. The pharyngeal tooth number of "NewGenus" (about 20) is far less than the 50 to 60 pharyngeal teeth suggested for †*A. gosiutense* (Grande et al., 1982), about 37 for †*A. aggregatum* (Liu et al., 2015), and 35 to 50 for *Plesiomyxocyprinus* (Liu et al., 2015).

"NewGenus" differs from all the species of *Amyzon* except the Asian *A. hunanense* in having a shorter posteroventral process of the dentary. As an adaptation to subterminal suction feeding in catostomids, the gnathic ramus of the dentary is short and deflected, whereas the posteroventral process of the dentary is elongated. Short, moderately elongated, and elongated posteroventral processes of the dentary are distributed across genera and higher groups in the family (see Chapter 6). While the posteroventral process of the dentary is moderately elongated in *Amyzon*, it is short (about the size of its coronoid process) in "NewGenus". "NewGenus" is also different from all known species of *Amyzon* in having a greater width of the opercle. Generally, the opercle height is greater than opercle width in *Amyzon*, as well as most other catostomids. The height is sub-equal or shorter than the width in "NewGenus".

To sum up, "NewGenus" possesses a suite of characters that are different from other catostomids, as well as from the genus to which it was originally assigned, *Amyzon*. It is most likely a basal clade of Catostomidae, and thus it is here removed from *Amyzon*, and assigned to a new genus.

Distribution of "NewGenus"

Specimens of "NewGenus" are now known from localities in the Pleasant Valley, Whipsaw Creek, and Blakeburn Mine areas, British Columbia, Canada. In a previous study, Lambe (1906) assigned specimens recovered from another fossil locality of "NewGenus", Horsefly, to the nominal *Amyzon brevipinne*, which has since been demonstrated to be *Amyzon aggregatum* (Wilson, 1977a). In another early study, Eastman (1917) suggested that catostomid fishes from Republic, Washington, USA were nominal *Amyzon brevipinne* as well, based on comparison to the

illustration and description of Lambe (1906). In an overview of the Eocene Republic locality fossil fishes, Wilson (1996) suggested that the Republic catostomids belonged to *Amyzon aggregatum*.

Since then, more specimens have become available that contribute to a better understanding the Republic materials. Two latex peels of the original specimens of Eastman (1917) and held in the collection of USNM, served as the basis for comparison (peel UALVP 14932 from specimen USNM V 8117, peel UALVP 14933 from specimen USNM V 8378). Together with recently collected specimens housed in the UALVP, these specimens (Fig. 4.5) are determined to be *Amyzon* by having a large size, deep body, and more median fin rays than that of "NewGenus". In the caudal skeleton of the Republic catostomid, hypural 3 is consistently fused with the compound centrum. This is a character that is consistently seen in *Amyzon kishenehnicum* and occasionally found in *A. aggregatum*. At present, the Republic catostomids belong in *Amyzon*, but cannot be assigned to a known species based on anatomical characters.

North America catostomids of the Paleogene

Possible catostomids occurred as early as in the Paleocene, based on material from a single locality in the Paskapoo Fm., Alberta, Canada in the form of disarticulated bones (Wilson, 1980c). All the other Paleogene catostomids have been recovered from Eocene or arguably Eocene sedimentary rocks of western North America (Table 4.1, Fig. 4.6). While "NewGenus" is established to contain a nominal species of *Amyzon* here, all the other occurrences are either species of *Amyzon* or *Amyzon*-like fish (Table 4.1).

The only specimens from the Paleocene Paskapoo Formation are disarticulated cleithra and centra. The shape of the cleithrum is spoon-like, resembling that of catostomids. The vertical ramus of a complete cleithrum (UALVP 15051) is about 10 mm, which suggests it belonged to a small fish.

Liu et al. (2016; Chapter 3) had reviewed the species status and generic characters of *Amyzon*. Species of *Amyzon*, all extinct, include *Amyzon mentale* (Cope, 1872), *A. commune* (Cope, 1874), *A. aggregatum* (Wilson, 1977a), *A. gosiutense* (Grande et al., 1982), *A. hunanense* (Chang et al., 2001), and *A. kishenehnicum* (Liu et al., 2016). The species of *Amyzon* are characterized by large size, deep body, 19 to 33 principal dorsal fin rays, 7 to 10 anal fin rays, terminal mouth with the posteroventral process of the dentary moderately elongated, and hypural 3 fused in some species to the compound centrum. Undescribed catostomid fossils from the Klondike Mountain Fm., Renova Fm. and Clarno Fm, are *Amyzon*-like (Table 4.1).

"NewGenus" is the most loach-like catostomid known so far. The family Catostomidae has frequently been resolved as closely related to gyrinocheilids and the clade of loach families, known as the Superfamily Cobitoidea (Siebert, 1987; Saitoh et al., 2006; Tang et al., 2006; Šlechtová et al., 2007; Mayden et al., 2009; Chen et al., 2013). "NewGenus" resembles loaches in the shape of the frontal with an elongated orbital notch, in the shallow and thin infraorbital series, and in the short and moderately robust rib 4.

Not only catostomids but also some other cypriniforms had diverged and diversified in the Eocene based on the oldest skeleton-based specimens. Catostomids (Cope, 1872; Cope, 1874; Cope, 1875; Cope, 1893; Wilson, 1977a; Grande et al., 1982; Chang et al., 2001; Liu and Chang, 2009),

cyprinids (Su, 2011; Chen et al., 2015a), and jianghanichthyids (Liu et al., 2015; Chapter 2) have been recovered from East Asia and North America. However, the oldest known loaches are only known from Oligocene deposits in China (Chen et al., 2015b) and Germany (Böhme, 2008). The discovery of a catostomid with loach-like traits sheds further light on the origin and evolution of catostomids, which catostomids and loach were either closely related or convergent in the early history of the their clades.

Conclusion

Based on a character revision and new character descriptions, the Eocene *Amyzon brevipinne* is now removed from the genus *Amyzon*, and assigned to "NewGenus" *brevipinne* (Cope, 1893). Being the first catostomid with several loach-like traits, it not only illustrates the early divergence of Catostomidae in North America, but also sheds light on the origin of loaches, which have a rare fossil record. The shallow, loach-like body form and skull bones reveal the features of the oldest fluvial catostomid.

Table 4. 1 Eocene North American catostomid fossil record. Fossil localities and site information is

from the collection record associated with each specimen. "Fm." is short for Formation.

Locality #	Locality	Sites/Additional localities	Formation	Age	Taxon
A	Horsefly, British Columbia, Canada	Horsefly Mine, bank of Horsefly River		middle Eocene	*Amyzon aggregatum* Wilson, 1977
B	Princeton, British Columbia, Canada	Pleasant Valley, Whipsaw Creek, Blakeburn Mine，Tulameen	Allenby Fm.	middle Eocene	"NewGenus" *brevipinne* (Cope, 1893)
C	Republic, Washington, USA	Tom Thumb Mine	Klondike Mountain Fm.	early Eocene	*Amyzon sp.*
D	Flathead River (middle fork), Montana, USA	Tunnel Creek and Disbrow Creek	Kishenehn Fm.	middle Eocene	*Amyzon kishenehnicum* Liu et al., 2016
E	Grant, Montana, USA		Renova Fm.	Eocene	
F	Weiser, Idaho, USA			Eocene	Catostomidae sp.
G	Ochoco Pass, Mitchell, Oregon. USA		Clarno Fm.		*Amyzon sp.*
H	Osino, Nevada, USA			Eocene	*Amyzon mentale* Cope, 1872
I	Lake Gosiute locality, Wyoming, USA		Green River Fm.	middle Eocene	*Amyzon gosiutense* Grande et al., 1982
J	South Park, Colorado, USA		Florissant Fm.	late Eocene	*Amyzon commune* Cope, 1874

Figure 4. 1 The holotype (CMN 6189) of "NewGenus" *brevipinne* from the Eocene Allenby

Formation and probably from the Pleasant Valley locality, British Columbia, Canada. Scale bar

represents10 mm. Arrow indicates for the frontal.

Figure 4. 2 A juvenile or young adult and skulls of "NewGenus" *brevipinne* from the Eocene Allenby Formation, Blakeburn Mine, British Columbia, Canada. A. juvenile or young adult, UALVP 12159 ; B, skull of UALVP 12658; C, enlarged head area of A. Arrows indicate the frontals. Scale of A is in mm, scale bars of B and C represent 5 mm.
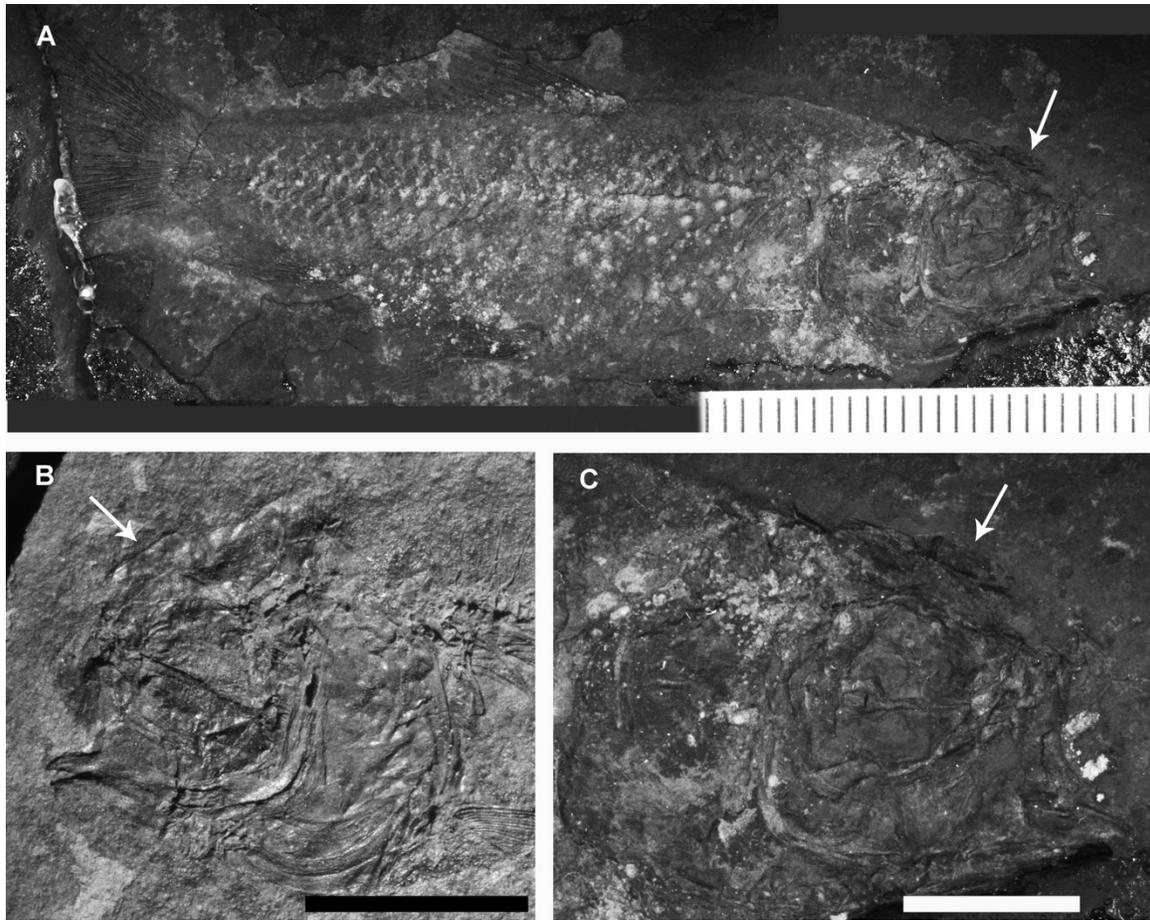
Figure 4. 3 Comparison of the frontals of "NewGenus", *Amyzon*, and *Plesiomyxocyprinus*.   A.

frontal of "NewGenus" *brevipinne* from the Eocene Allenby Formation, Blakeburn Mine, British

Columbia, Canada, UALVP 12610; B, frontal of *Amyzon aggregatum* from the Eocene of Horsefly,

British Columbia, Canada, UALVP 32931; C, frontal of *Plesiomyxocyprinus arratiae* from the

Eocene Huadian Fm, Huadian, Jilin, China, IVPP V 15711.29 (Liu and Chang, 2009, fig. 2a, b).

Abbreviations: **fpf**, fronto-parietal fontanelle; **obp**, orbital process of frontal; **on**, orbital notch of

frontal. Anterior of fish toward top of page. Scale bars represent 5 mm.
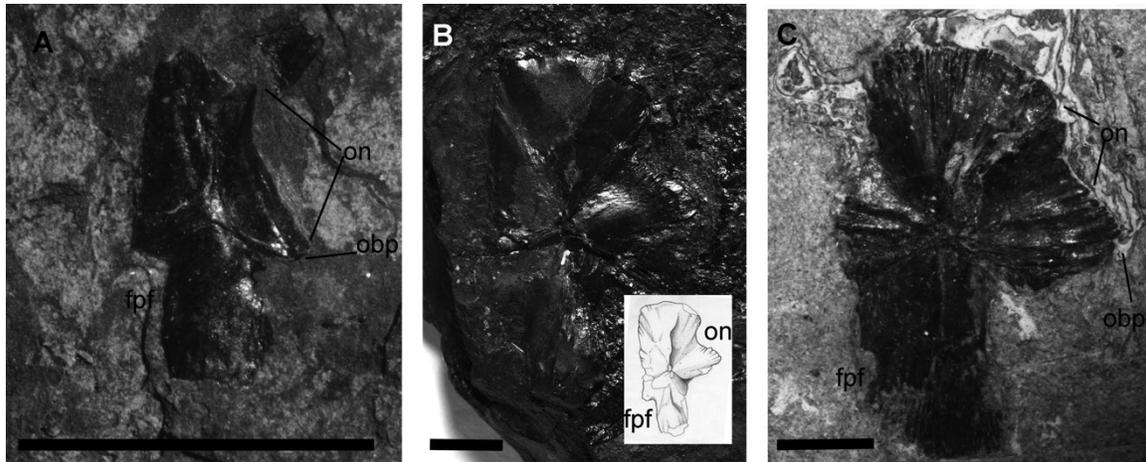
Figure 4. 4 Disarticulated bones and reconstructions of "NewGenus" *brevipinne* from the Eocene Allenby Formation. A, pharyngeal bone and teeth, UALVP 31585a; B, opercle, UALVP 12796; C, interopercle, UALVP 12616; D, urohyal, ROM 11161a; E, caudal skeleton, ROM 11161a; F, reconstruction of the Weberian apparatus based on UALVP 12658, 12698b and 12807; G, mandible, ROM 11161. Abbreviations: **aa**, anguloarticular; **aaf**, anguloarticular fossa for articulation with the quadrate; **aep**, anteroventral edentulous processes; **arp**, auricular process of opercle; **avp**, anteroventral process; **cc**, compound centrum of caudal skeleton; **cp**, coronoid process of dentary; **den**, dentary; **ep**, epural; **gr**, gnathic ramus of dentary; **hhp**, hypohyal processes of urohyal; **hyp** 1-4, hypural 1 through 4; **nc**, neural complex; **ns**, neural spine; **opa**, opercular arm; **opf**, opercular fossa; **pep**, Posterodorsal Edentulous Processes; **pls**, pleurostyle; **pt**, pharyngeal teeth; **r4**, rib 4; **ra**, retroarticular; **trp**, tripus. Anterior of fishes of A, C, and F faces left, whereas that of the rest faces right. Scale bars represent 5 mm.

168
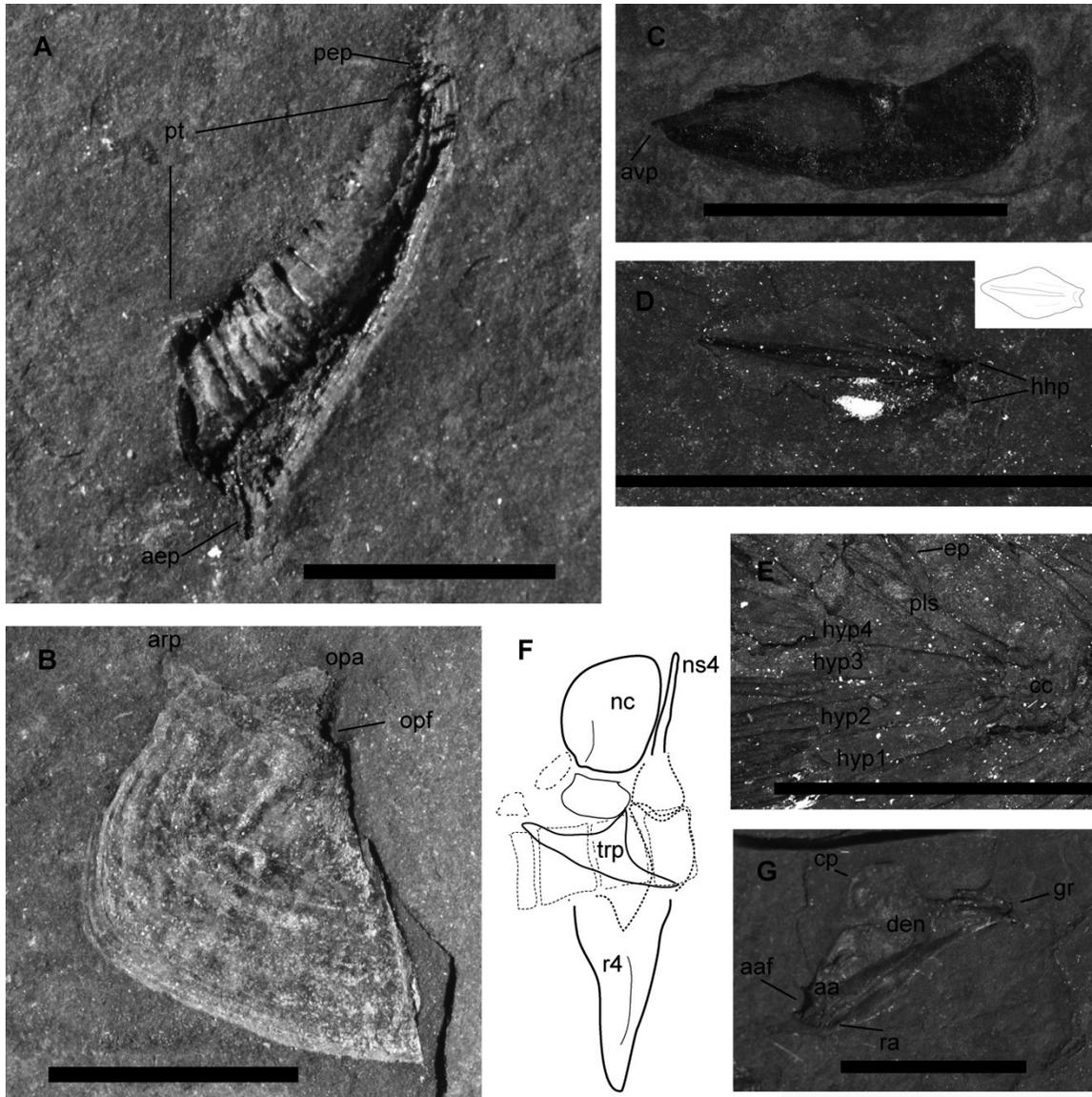
Figure 4. 5 *Amyzon* sp. from the Eocene Klondike Mountain Formation, Republic, Washington, USA.   (UALVP 14932 , latex peel of USNM V 8117).
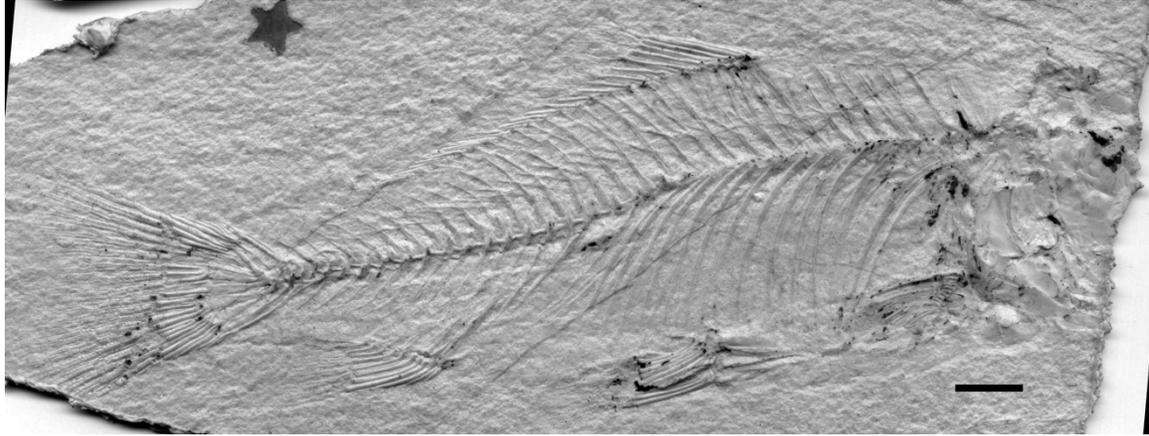
Figure 4. 6 Distribution of localities of skeleton-based Eocene catostomid fossils.   A–J represent the fossil localities listed in Table 4.1.

Chapter 5 Revision of the Catostomids and Problematic Catostomids from the Paleogene of Asia

Abstract: This study reviews the fossil record of catostomids and jianghanichthyids from Asia, systematically revises the position of problematic catostomids, and describes new materials of Paleogene non-cyprinid cypriniforms of Asia. Brief osteological comparisons are also made between extant *Osteochilus* and the nominal members. Three genera (*Amyzon*, *Plesiomyxocyprinus*, *Vasnetzovia*) each represented by a single species, have been identified from skeletal remains in the Eocene of Asia. Disarticulated bones and pharyngeal teeth extend their occurrence to the early Oligocene in Central Asia. The nominal taxa "*Osteochilus linliensis*", "*O. sanshuiensis*", "*O. longipinnatus*", and "*O. laticorpus*" are referred here to *Jianghanichthys*. Three of these nominal species from the Paleocene–Eocene Buxin Formation are considered here to be ontogenetic/allometric variations of *Jianghanichthys sanshuiensis*. The new species *Jianghanichthys huachongensis* sp. nov., is described from the Eocene Huachong Formation of Foshan, Guangdong, China. This revision shows that Asian fossil catostomids occur in China, Russian, Mongolia, and Kazakhstan from the early Eocene to the early Oligocene, whereas jianghanichthyids are restricted to the late Paleocene–middle Eocene of South China.

Key words: Cypriniformes, Catostomidae, Jianghanichthyidae, Paleogene, Asia

Introduction

Unambiguous cypriniform (Teleostei, Ostariophysi, Cypriniformes) fossils prior to the Eocene have been recovered only from Asia and North America. All of these forms were without exception assigned to modern families either Cyprinidae (carp) or Catostomidae (suckers), until the extinct family Jianghanichthyidae was erected to contain the basal cypriniform *Jianghanichthys hubeiensis* (Liu et al., 2015; Chapter 2), a taxon that had previously been assigned either to Cyprinidae (Lei, 1977) or Catostomidae (Chang and Chen, 2008). While all Eocene and Paleocene cypriniforms of North America appear to be catostomids, coeval Asian forms are more diverse and represent members of Cyprinidae, Catostomidae, and Jianghanichthyidae. In Asia the cyprinids and catostomids survived to the present day, while jianghanichthyids are extinct. Extant Asian catostomids are sparsely distributed, with only one Asian endemic species *Myxocyprinus asiaticus* and one species shared with North American, *Catostomus catostomus*.

The first Eocene catostomid records to be reported were disarticulated opercles and vertebral centra from the Ulan Shireh Formation of Inner Mongolia, China (Hussakof, 1932) although that assignment was questioned (Nelson, 1949). The first more complete skeletal material was described as the new genus and species *Vasnetzovia artemica* from the Eocene of Uglov Svita, Primorskyi Territory (Premorie), Russia (Sytchevskaya, 1986). Sytchevskaya (1986) also described nine new nominal species of catostomid and a supposed record of the North American taxon *Amyzon gosiutense* Grande et al., 1981 based on disarticulated pharyngeal teeth from

various localities in Central Asia. These nominal species assignments have all been questioned (Smith, 1992; Chang and Chen, 2008).

Two catostomids have been described on the basis of skeletal material from the Eocene of China: *Amyzon hunanense* and *Plesiomyxocyprinus arratiae*. The supposed cyprinid "*Osteochilus hunanensis*" (Cheng, 1962) was transferred to the Catostomidae (Chang et al., 2001), while Chang and Chen (2008) suggested that all the other nominal Eocene *Osteochilus* from China were also catostomids, a view that is retained here.

Among the nominal Eocene *Osteochilus* from China, "*Osteochilus hubeiensis*" was revised to *Jianghanichthys hubeiensis* (Lei, 1987). In a more recent study, based on a large number of specimens, comprehensive morphological comparison, and phylogenetic analysis, *Jianghanichthys hubeiensis* was given its own family status Jianghanichthyidae (Liu et al., 2015; Chapter 2). The remaining nominal fossil species of "*Osteochilus*", including "*O.*" *linliensis* from Linli, Hunan (Tang, 1959), and "*O.*" *sanshuiensis*, "*O.*" *longipinnatus*, and "*O.*" *laticorpus* from Sanshui Basin of Guangdong have remained systematically problematic.

This study aims to clarify the taxonomic assignments, geographic distribution, and geological age of catostomids (including the problematic forms) from Asia (Fig. 1). New material recently collected from Eocene Huachong Formation, Foshan, Guangdong will also be described.

Materials and Methods

Type specimens and referred materials of *Amyzon hunanense*, *Jianghanichthys hubeiensis*, *Plesiomyxocyprinus arratiae*, new materials from Huachong Formation, Guangdong, China, and catostomids specimens collected by the AMNH Central Asia Expedition in the 1920s are available for this study. For a complete list of specimens see General Appendix II.

General features, osteology, and meristic and morphometric data for other fossil taxa (including *Vasnetzovia artemica*, and the nominal taxa *'Osteochilus' linliensis*, *'O.' sanshuiensis*, *'O.' longipinnatus*, and *'O.' laticorpus*), are examined on the photographs of holotype and referred specimens. Photos of *Vasnetzovia artemica* holotype PIN N3882/1 and specimen PIN N3882/2 were taken by Drs. Ning Wang and Gengjiao Chen from the PIN. The specimens of *"Osteochilus" sanshuiensis*, *"Osteochilus" longipinnatus*, and *"Osteochilus" laticorpus* are "at unknown place" according to the first author who originally described these species (*pers. comm.* through Mee-Mann Chang and Gengjiao Chen in October, 2015), whereas the specimen of *"Osteochilus" linliensis* has not been found either. Comments on these nominal *"Osteochilus"* species are therefore based on the original description and published photographs.

Extant cypriniform fishes used for comparison, including catostomids and *Osteochilus*, are listed in General Appendix II.

Anatomical abbreviations used in the text: A. anal fin rays, BD, body depth; C., caudal fin rays; CPD, caudal peduncle depth; CPL, caudal peduncle length; D., dorsal fin rays; SL, standard length.

Institutional abbreviations see the General Appendix I.

Eocene Catostomids from Asia

Fossil and extant catostomids are only known from North America and Asia. Catostomids radiated in North America from the Eocene and are diverse today, with over 70 species. By contrast, Asian catostomids are known from the Eocene, but have apparently declined since the early Oligocene. The following section examines the fossil record of Asian catostomids, with comments on their morphology, systematics paleontology, and geological ages.

Amyzon hunanense (Cheng), 1962

Synonyms: *Osteochilus hunanensis* Cheng, 1962, p. 336, plate I,1.

Amyzon hunanensis, Chang et al., 2001, p.579, fig. 2a, new combination.

Holotype: IVPP V 1102, a nearly complete fish lacking caudal fin and part of anal fin.

Age/Horizon: early – middle Eocene, Xiawanpu Formation (Hsiawanpu Formation).

Type locality: Xiawanpu (Hsiawanpu), 7.5 km southwest of the city Xiangxiang, Hunan, China (Fig. 5.1 G)

The holotype of *Amyzon hunanense* IVPP V 1102, was described as a cyprinid, *Osteochilus huanensis*, by Cheng (1962). It was the only specimen known at that time and was recovered from

gray marl of the Xiawanpu Formation (spelled Hsiawanpu Formation in the original description). In addition to a brief description of the ichthyofauna of Xiawanpu, Cheng (1962) described the sedimentary sequence in that area with a section map of the Xiawanpu Formation, which is valuable for collecting more specimens from the type locality.

Chang et al. (2011) revised the systematic assignment of this species based on more complete specimens (IVPP V 12571.1–6) that are also preserved in gray marl from the Xiawanpu Formation. Based on upper jaw morphology consisting of both premaxilla and maxilla and the presence of 16 branched caudal fin rays, Chang et al. (2001) suggested that this species belonged to the family Catostomidae rather than Cyprinidae. Based also on meristic and morphometric features, Chang et al. (2001) assigned this fish to the Eocene catostomid genus *Amyzon*, and hypothesized a vicariance-dispersal event during the evolution of catostomids.

Another IVPP expedition followed in Xiangxiang, Hunan in 2010, when additional specimens IVPP V 17906.1–53 were collected (including complete fish and disarticulated bones: Fig. 5.2). Pharyngeal teeth are preserved in situ in specimen IVPP V 17906.3a (Fig. 5.2C) confirming the family level assignment by Chang et al. (2001). The pharyngeal teeth are compressed and tall with a pointed tip. The shapes of the frontal, parietal, premaxilla, dentary, and rib 4 are close to that of other *Amyzon* spp. (Liu et al., 2016; Chapter 3).

Amyzon hunanense is a small to medium sized catostomid with SL ranging from 43.7 mm (IVPP V17906.31a) to 155.2 mm (IVPP V 12571.6). The estimated maximum SL on larger but incomplete specimens is about 200 mm (Liu and Chang, 2009), which is much smaller than the

measured maximum standard length of 272 mm in *A. aggregatum* (UALVP 32266), 242 mm in *A. gosiutense* (Grande et al., 1982), and 370 mm in *A. kishenehnicum* (Liu et al., 2016).

Plesiomyxocyprinus arratiae Liu and Chang, 2009

Synonym: Catostomidae indet. Chang et al., 2001 pp.580–581, fig. 3.

Holotype: IVPP V 12572.1, a nearly complete fish lacking snout and part of caudal fin.

Age/Horizon: Huadian Formation, early Eocene.

Type locality: Huadian, Jilin, China (Fig. 5.1 C).

This species provided the first detailed description of an Eocene catostomid from Asia, and is also the first fossil catostomid closely related to the living Asian endemic, the high fin banded shark *Myxocyprinus* (Liu and Chang, 2009; Liu et al., 2016). *Pleisiomyxocyprinus arratiae* is a large-sized and extremely deep-bodied catostomid fish with an estimated SL ~300 mm, and the BD/SL is about 0.52. It resembles *Myxocyprinus* in many features, such as the high BD/SL ratio, and the high number of dorsal and anal fin rays. It differs from *Myxocyprinus* in having a well-developed coronoid process on the dentary, and a narrower and more elongated opercular arm.

Vasnetzovia artemica Sytchevskaya, 1986

Holotype: PIN N3882/1, a nearly complete fish.

Age/Horizon: late Eocene, Uglov Svita (meaning "coal formation", also translated as "Wuglovaya Formation")

Type locality: Artyom (Artëm), Primorskyi Territory (Premorie), Russia (Fig. 5.1 D).

Sytchevskaya (1986) described this taxon based on two nearly complete specimens, PIN N3882/1 (Fig. 5.3 A) and PIN N3882/2 (Fig. 5.3 B), preserved on the same slab. Both specimens are shallow-bodied and small to medium sized fish compared to the size ranges in *Amyzon* (Liu et al., 2016). The SL of both specimens is around 120 mm with BD/SL ratio 0.29–0.31. Skull bones in these two specimens are crushed, incomplete, and fragmentary, making them difficult to compare with other fishes. The presence of elements associated with the Weberian apparatus indicates it is cypriniform. Traces of a ventrally projected and robust rib 4 on PIN N3881/2 are observed, supporting its family assignment to the Catostomidae. The caudal fin ray count of 18 (i,8,8,i) is also considered apomorphic for Catostomidae, compared to 19 in Cyprinidae and the basal cypriniform *Jianghanichthys*.

The specimens of *Vasnetzovia* were collected from the Artyom (Artëm) brown coal (lignite) mine, where a well described and reviewed mammal fauna had been reported (Russell and Zhai, 1987; Lucas et al., 2004). Russell and Zhai (1987) considered the Uglov Svita as late Eocene to early Oligocene, whereas Lucas et al. (2004) referred it to the mammalian locality as Ergilian, middle to late Eocene age.

Sytchevskaya (1986) also described seven nominal species that were referred to extant catostomid genera, as well as two new species of *Amyzon*, and also identified *A. gosiutense*, based on disarticulated pharyngeal teeth from Eocene and Oligocene deposits of Zaissan Basin of East Kazakhstan, East Siberia, and Mongolia. Unfortunately, the size and shape of catostomid

pharyngeal teeth gradually changes in both extant and fossil catostomids (Liu et al., 2016), so differences among a small sample of disarticulated pharyngeal teeth may not be sufficient to provide accurate specific or even generic determination (Smith, 1992; Chang and Chen, 2008). Sytchevskaya's (1986, pp.71–80) nominal species *Amyzon interruptus*, *Amyzon zaissanicus*, *Carpiodes brevidens*, *Cycleptus robustus*, *Catostomus columnaris*, *Erimyzon luxus*, *Minytrema shevyrevi*, *Xyrauchen rotundus*, and *Moxostoma fungidens* are thus considered nomina dubia here. However, most of the pharyngeal teeth illustrated by Sytchevskaya (1986, plate XII) undoubtedly belong to catostomids, and provide important paleogeographic distribution information for catostomid fish that they were once expanded their distribution to Central Asia and even east end of Europe. .

Catostomidae indet. 1

Material: AMNH FF 8442, four nearly complete opercles and two centra; AMNH FF 10344, an incomplete subopercle.

Age/horizon: Ulan Shireh Formation, middle Eocene.

Locality: Shara Murun region, Inner Mongolia, China (Fig. 5.1 B).

These materials, including opercles and centra (Fig. 5.4 A–F), were collected by the AMNH Central Asian Expedition and assigned to the extant genus *Catostomus* in the family Catostomidae (Hussakof, 1932). Nelson (1949) questioned the generic, and even familial, assignment solely based on the opercle. He also tried to categorize these specimens with his "OP1" and "OP2" types, which mainly differ in the acuteness of the angle at the inferior border of the opercle.

Although an opercular arm and auricular process occurs in some cyprinids and characids in addition to catostomids (Hussakof, 1932), and also occur in the stem cypriniform *Jianghanichthys* (Liu et al., 2015), the catostomid opercle differs from those of other fishes in the shape and sizes of the opercular arm and auricular process, and the general opercle shape. For example, both the opercular arm and auricular process are thick and truncated or rounded at their dorsal tips, whereas both are thin and pointed in *Jianghanichthys*. Moreover, where the opercular arm and auricular process are present in cyprinids and characids, they are very blunt, dorsally positioned and lack a broad dorsal concavity between them. The isolated opercles from Ulan Shireh Formation have a well-developed and thick opercular arm and auricular process, broad dorsal concavity, and a straight anterior border with groove and notch (Fig. 5.4 A & B), like those of other catostomid fishes.

The opercular arm is rectangular and slender, lacking the bilateral constriction. A prominent ridge originates at the anterodorsal corner of the arm and extends to a point below the opercular fossa and toward the center of the opercle. The rectangular shape of the opercular arm resembles that of *Amyzon*, *Myxocyprinus*, *Carpiodes*, and *Ictiobus*. Overall, the shape and ridge of the opercular arm resemble most that of *Plesiomyxocyprinus* (Liu and Chang, 2009).

Regarding the category of the "OP" types of Nelson (1949), one of the Gobi opercles was thought to be the "OP1" type, and the other three were "OP2". OP1 and OP2 mainly differ in the inferior border angle, the former about 30°, and the latter about 20° (Nelson, 1949). None of the catostomid opercles from Ulan Shireh Formation was complete, especially the ventral and posterior margin. While it is difficult to assign these specimens unambiguously to any "OP" types,

they resemble OP2 the most. At the time the Gobi specimens were examined for this study, there were five opercles in total catalogued under the number AMNH FF 8442. One of the opercles had a straight anterior border to similar to the others; however, there was no evidence of an anterior notch, anteroventral corner, or a groove along the anterior border, which can be seen in the other specimens and all catostomids. This specimen should be removed from the Gobi catostomids. Worth mentioning, the inferior border angle is about 30°, visibly larger than that of the rest of the opercles.

Two centra were also collected with the opercles. One is an antero-posteriorly flattened centrum 1 (Fig. 5.4 C, D) morphologically similar to that associated with the Weberian apparatus in catostomids. The other one is a regular trunk centrum, more like one from the caudal region.

Catostomidae indet. 2

Material: AMNH FF 6278, anterodorsal portion of an opercle including opercular arm and opercular socket.

Age/horizon: Ergelin Dzo Svita, late Eocene.

Locality: Ergil Obo (Ardyn Obo), Ergelin Dzo, Dornogobi, Mongolia (Fig. 5.1 A).

The specimen label shows that this material was recovered from the "Ardyn Obo Formation" by the AMNH Central Asia Expedition in 1923. The fish material had not been noticed before, although the abundant mammal fossils have been well studied and are helpful for aging the horizon (Matthew and Granger, 1923; 1925a; 1925b). Berkey et al. (1923) described the Ardyn Obo as "one of the better localities" at "South of Sair Usu, on the main Kalgan-Uliasutai Trail,"

and suggested the locality to be in the Ardyn Obo Formation. The trail is "about 150 miles from Sair Usu and 350 miles from Kalgan" (Mattew and Granger, 1923, p.1), of which Kalgan is nowadays Zhangjiakou, Hebei, China. Russel and Zhai (1987) clarified that the fossil locality of Ardy Obo is known today as Ergelin Dzo, Mongolia. Based on the biostratigraphy of mammal assemblages the age of Ergelin Dzo is early Oligocene (Russell and Zhai, 1987). Wang (2014) compared the Ergil Obo (Ardy Obo) of the Ergelin Dzo fossil locality with the Urtyn Obo Formation in China, and suggested that both date from the middle early Oligocene.

The well-developed opercular arm and large-sized opercular socket both suggest that the specimen belongs to a catostomid. The opercular arm is broad, thick, and nearly not tapered at all in the middle of the arm (Fig. 5.4 G, H), resembling that of *Myxocyprinus*, *Cycleptus*, and *Ictiobus*. The length of the opercular arm is moderate, unlike the elongated ones in *Cycleptus* and *Ictiobus*. The lateral surface of the opercular arm has very fine striations nearly parallel to the arm, whereas much deeper and wider striations radiate from the root of the opercular arm towards the periphery. Overall, the opercular arm is closest to the shape of that in *Myxocyprinus*.

To summarize, Asian fossil catostomids have so far only been found in East and Central Asia and are of Eocene and possibly early Oligocene age. Three Eocene genera with three species have been described based on skeletons (Sytchevskaya, 1986; Chang et al., 2001; Liu and Chang, 2008). Disarticulated bones from the Eocene and Oligocene of southern Mongolia and Eocene of northern China (Inner Mongolia), and disarticulated pharyngeal teeth from Eocene and Oligocene deposits of Zaissan Basin of East Kazakhstan, East Siberia, and Mongolia (Sytchevskaya, 1986) demonstrate the last appearances of Asian fossil catostomids in Central Asia.

"Problematic catostomids": Jianghanichthyidae

Several problematic catostomid-like fishes from the Eocene of China have been classified as nominal species of the genus "*Osteochilus*." Apart from one, which was referred to *Amyzon hunanense*, they are pending revision. This section will revise the systematic paleontology of those taxa, and discuss the morphological features of so far the only fossil-only family of Cypriniformes known so far, Jianghanichthyidae. New species based on new materials will be described. An emended diagnosis of the genus is presented below.

Jianghanichthys (Lei), 1987

Revised Diagnosis: medium sized Paleocene – Eocene cypriniform fish, body deep to very deep with ratio of BD/SL ranges 0.34–0.48 in juveniles and 0.4–0.63 in adults, frontal broad anteriorly and narrow posteriorly, premaxilla triangular, dorsal surface of anterior end of dentary broad, opercle bearing dorsally pointed opercular arm and auricular process with concave dorsal margin in between, cephalic fontanelle absent, cephalic sensory canal ossified and running underneath, enclosed, or superficial to bones, D 10–13, A 6–8, caudal vertebrae 11–13, caudal peduncle short and tapered posteriorly with narrowest point at caudal fin base.

Type Species: *Jianghanichthys hubeiensis* (Lei), 1977

Included Species: *Jianghanichthys linliensis* (Tang, 1959); *Jianghanichthys sanshuiensis* (Wang et al., 1981); *Jianghanichthys huachongensis* sp. nov.

Distribution: late Paleocene – middle Eocene, South China.

Jianghanichthys hubeiensis (Lei), 1977

Synonyms: *Osteochilus hubeiensis* Lei, 1977, p. 134, plate 49, figs. 3–4 (original description).

Jianghanichthys hubeiensis (Lei, 1977): Lei, 1987, p. 191 (new combination).

Lectotype: GMC V1810-1 (V 25404 in Lei, 1977; 1987), a complete fish.

Age/Horizon: Yangxi Formation (early Eocene).

Type locality: Songzi, Hubei, China (Fig. 5.1 E).

The species is the type genus and type species for the extinct family Jianghanichthyidae. Liu et al. (2015; Chapter 2) re-described *Jianghanichthys hubeiensis* and erected the fossil-only family based on morphological comparison and phylogenetic study.

Jianghanichthys linliensis (Tang), 1959

Holotype: 58F-1.1 listed in Tang (1959).

Synonyms: *Osteochilus linliensis* Tang, 1959, p. 212, plate I (original description)

Osteochilus linliensis: Cheng, 1962, p. 337, plate I.2, I.3

Age/Horizon: Xiejiashan oil shale, unknown formation (middle – early Eocene).

Type locality: Xiejiashan, 18 km northwest of Linli, Hunan, China (Fig. 5.1 F).

Two specimens preserved on the same slab (Fig. 5.5) were described and photographed by Tang (1959). The original description including measurements and meristic characters of the species were based on the larger one (Tang, 1959). According to the original description, this species possesses 29 vertebrae and D iii, 11, which are close to those of *Jianghanichthys hubeiensis*.

Based on observation of the photograph (Fig. 5.5), this species resembles *Jianghanichthys hubeiensis* in having an extremely deep body in the adult (BD/SL > 0.5) but shallower in younger individuals, short neural spines, short caudal peduncle (CPD/CPL > 1), number of caudal vertebrae 11, and a rectangular parietal with a posterolateral extension behind the pterotic. All these characters and the numbers of vertebrae and dorsal fin rays are very different from those of *Osteochilus*, but agree with *Jianghanichthys. hubeiensis*

Specimens were collected from the Xiejiashan oil shale of Linli, Hunan, which has been correlated with the Xiawanpu Formation and with Eocene sediments from Hengyang Basin, Hunan (Young, 1944; Tang, 1959; Liu et al., 1962). Cheng (1962) reported the same species from Xiawanpu Formation as well (Cheng, 1962, p. 337, plate I.2, I.3). However, the correlation between the Xiejiashan and Xiawanpu formations requires verification by fieldwork in that region.

Jianghanichthys sanshuiensis (Wang et al., 1981)

Synonyms: *Osteochilus sanshuiensis* Wang et al., 1981, p.4, plates I no.1–3, II no.1–3.

Osteochilus longipinnatus Wang et al., 1981; p.6, plate III no.1–3.

Osteochilus laticorpus Wang et al., 1981, p.8, plate IV 1–3, V no.2.

Age/Horizon: Buxin Formation (Paleocene).

Type locality: Sanshui, Guangdong, China (Fig. 5.1 H).

All referred specimens were collected from Honggang and Langxi, which fall within the Lower and Upper Buxin Formation respectively (Wang et al., 1981). Wang et al. (1981) assigned specimens from Honggang to two nominal species, *Osteochilus sanshuiensis* (Fig. 5.6 A) and *O. longipinnatus* (Fig. 5.6 B), whereas all the Langxi specimens were assigned to *O. laticorpus* (Fig. 5.6 C). Unfortunately, these specimens cannot now be relocated (pers. comm. through Drs. Mee-mann Chang and Gengjiao Chen). The following observations and comparisons are based on the published plates and the original description.

All the photographed specimens of those three nominal species in Wang et al. (1981) belong to the genus *Jianghanichthys* based on the resemblance to the type species *J. hubeiensis* in the following diagnostic characters. First, the neural spines are relatively short, given the deep body of the fish. Compared to the other early cypriniforms from Asia, Eocene cyprinids are shallow bodied (Sytchevskaya, 1986; Zhou, 1990; Su, 2011; Chen et al., 2015a), whereas the Eocene catostomids are deep bodied with long neural spines (Liu et al., 2005, fig. 9). Second, the caudal vertebrae number (11–13) resembles that of *J. hubeiensis*, fewer than in Eocene catostomids (Wilson, 1977a; Grande et al., 1982; Chang et al., 2001; Liu and Chang, 2009) and far fewer than in cyprinids (Zhou, 1990; Su, 2011). Moreover, the caudal peduncle depth of the Sanshui specimens is greater than its length (CPD/CPL >1), whereas this is rarely seen in Eocene

catostomids and cyprinids. The only other Eocene cypriniform with (CPD/CPL >1) is *Plesiomyxocyprinus*, which possesses a much higher number of caudal vertebrae (~20). Furthermore, the dorsal and ventral outlines of the caudal peduncle in *Jianghanichthys* gradually converge posteriorly, becoming narrowest at the base of the caudal fin, whereas the narrowest depth often occurs in the middle of the peduncle in other Eocene cypriniforms. Last but not least, the opercle shape resembles that of *J. hubeiensis* in having a dorsal, concave opercular arm and an auricular process, both of which are pointed dorsally. Therefore, these specimens are here assigned to *Jianghanichthys*.

According to the original description (Wang et al., 1981), the major difference between the Honggang specimens referred to *Osteochilus sanshuiensis* and *O. longipinnatus* is the length of the dorsal fin rays; the anterior fin rays in *O. longipinnatus* are extraordinarily long (Fig. 5.7 B), giving rise to the specific name. However, the corresponding fin rays in specimens assigned to *O. sanshuiensis* are mostly broken, making them seem shorter than in *O. longipinnatus*. Moreover, individuals of *O. longipinnatus* are generally smaller than those of *O. sanshuiensis*; the SL of the measured specimen was 39 mm for the former, and 68 mm for latter (Wang et al., 1981, table 1 and 2). In *J. hubeiensis*, small individuals (presumed to be juveniles) possess relatively longer dorsal fin rays than larger ones. Thus, the supposed difference between *O. sanshuiensis* and *O. longipinnatus* can be accounted for by preservation and/or ontogenetic variation, and are not systematically reliable.

The diagnostic character of *Osteochilus laticorpus* from Langxi is its supposedly deep body. However, the measured specimen (SL 79 mm, Wang et al., 1981, table 3) is larger than other

Langxi specimens. A positive correlation between SL and body depth has been described for *J. hubeiensis* (Liu et al., 2015; Chapter 2). Moreover, Liu et al. (2015) also suggested that the slender bodied young individuals of *J. hubeiensis* were usually less than 70 mm in SL, suggesting that the greater body depth in *O. laticorpus* is not systematically useful.

Another supposedly significant difference between fishes from those two sites is the position of the pelvic fin insertion relative to the dorsal fin origin. In the Langxi specimens, the dorsal fin origin is slightly anterior to the pelvic fin insertion (Wang et al., 1981). However, this feature also occurs in some specimens from Honggang (Wang et al., 1981, plate I.2), whereas others have the dorsal fin origin opposite the pelvic fin insertion.

Geological remarks: The Buxin Formation was first considered to be of Eocene – Oligocene age, with strata about 100 –140 m in thickness (Tang and Liang, 1965). It was subsequently renamed the Buxin Group (Tang et al., 1980) and divided into the Upper, Middle, and Lower Buxin formations (*sensu stricto*). In the discussion of the geological age of the fossil fishes, Wang et al. (1981) used a geological setting similar to that of Tang et al. (1980). In a recent study, both *sensu lato* and *sensu stricto* usage of Buxin Formation have been seen (Wang and Zhang, 1997; Zhao et al., 2015). Another formation, the Xinzhuang Formation, seems to have replaced the Lower Buxin section of the Buxin Group (Wang and Zhang, 1997). Some literature even used both Buxin Formation and Buxin Group without clarification (Zhou et al., 2009). The stratigraphy and geochronology of the Sanshui Basin is in need of a more comprehensive study based on integrative data.

The authors who originally described and collected specimens of *Jianghanichthys sanshuiensis*

suggested that specimens were collected from the Lower and Middle Buxin Formation, of which the Lower Buxin Formation is late Paleocene, and may be of equivalent age to the Xinzhuang Formation. Therefore, in all likelihood, *Jianghanichthys sanshuiensis* is of Paleocene to Eocene age. In addition to fossil fishes, fossil mammals and birds have also been found in the Buxin Formation (Wang and Zhang, 1997; Zhao et al., 2015)

It is concluded that "*Osteochilus*" *sanshuiensis*, "*O.*" *longipinnatus*, and "*O.*" *laticorpus* should all be referred to *Jianghanichthys*. Furthermore, until more compete fossils become available, these species are considered to be junior synonyms of *J. sanshuiensis.* The presence of *Jianghanichthys* in the Buxin Formation extends its stratigraphic range from the Eocene into the Paleocene, making it the oldest cypriniform genus known from complete specimens. The maximum SL of the Paleocene *Jianghanichthys* is generally smaller than that from the Eocene (Liu et al., 2015).

Jianghanichthys huachongensis sp. nov.

Age/Horizon: Huachong Formation (middle Eocene).

Type locality: Zidongxu, Foshan, Guangdong, China (Fig. 5.1 I).

Holotype: IVPP V 23184. 2 (Fig. 5.7)

Materials: IVPP V 23184.1a, 1b, and 3–6.

Etymology: 'huachong-' is the geological formation name, from which this fish was recovered. In southeast China, '-chong' refers to streams or gush. Huachong Formation is sometimes misspelled as "Huayong".

Geology remarks: As stated in the etymology, the Huachong Formation is sometimes misspelled as "Huayong" Formation, because the Chinese character "涌" used in that term has two pronunciations "-yong" and "-chong" in standard Chinese Pinyin. Although "-chong" is less commonly used in general, it means "branch of river" and is usually used in place and location names, and thus more appropriate for a geological name that is after the place name. Few references have been using "huachong" instead of "huayong" (Zhou et al., 2009). The age of the Huachong Formation has been suggested to be early Eocene (Wang et al., 2011) or middle Eocene (Editorial Committee of Stratigraphical Lexicon of China, 1999). As the Huachong Formation is suggested to overlie volcanic rocks with an average age 49.78 Ma dated by K-Ar isotope (Editorial Committee of Stratigraphical Lexicon of China, 1999), a middle Eocene age for the Huachong Formation is used here. Vertebrates (mammals and birds; Wang et al., 2012; Bai et al., 2014; Mao et al., 2015), invertebrates (Zhang et al., 2008), and avian track fossils have been reported from the Huachong Formation.

Diagnosis: small-sized Eocene jianghanichthyid, opercle relatively broad, posterior border of opercle strongly convex, preopercular sensory canal and infraorbital canal connected, temporal sensory canal enclosed in the parietal.

Description

Jianghanichthys huachongensis is a small-sized and deep-bodied fish, with SL 46.1–68.6 mm and BD/SL 0.38–0.48. Articulated specimens are invariably preserved in lateral view. The dorsal and ventral outlines of the body are both slightly convex. The origin of the dorsal fin is almost

opposite the pelvic fin insertion. The fish has a short and deep caudal peduncle, resembling that of other jianghanichthyids.

The skull bones are nearly identical to those of *J. hubeiensis*, apart from the shape of the opercle and subopercle (Fig. 5.8 A, B). The caudal skeleton (Fig. 5.8 C) also resembles that of *J. hubeiensis* in general. Moreover, the infraorbital series is better preserved than that of *J. hubeiensis*. The cephalic sensory canals are ossified and unusually preserved providing more evidence of the sensory canal distribution. The osteological features of *J. hubeiensis* have been descried in detail in Liu et al. (2015; Chapter 2), and the following description will merely emphasize the differences of this new species from *J. hubeiensis*, along with the additional morphology of jianghanichthyids that the new specimens provide.

Opercular series–The opercle resembles that of other jianghanichthyids in having the dorsally directed and pointed opercular arm and auricular process, a slightly curved anterior border, and a rounded anteroventral corner. Unlike the condition in *J. hubeiensis*, the posterior border of the opercle in *J. huachongensis* is strongly convex, resulting in a relatively wider opercle. The greatest opercular width (perpendicular to the anterior border) is nearly equal to the opercular height (measured from the opercular fossa to the anteroventral corner) in *J. huachongensis*, whereas the ratio of opercular width to length in *J. hubeiensis* is about 0.85. Also, the ventral border of the opercle is at an angle from the horizontal in *J. huachongensis*, while it is nearly horizontal in *J. hubeiensis*. In addtion, the subopercle is also wider than that of *J. hubeiensis*.

Sensory canals ─ The sensory canals are extraordinarily preserved in specimens of *J.*

huachongensis. The distribution pattern mostly resembles the reconstructed arrangement in *J. hubeiensis*. From anterior to posterior and dorsal to ventral, there are three main paired branches of cephalic sensory canals in *J. huachongensis*. The supraorbital branch solely contains the supraorbital canal, which may extend anteriorly to the ethmoid region. The infraorbital branch extends at least to the lacrimal (infraorbital 1), and may extend even farther onto the snout region. The preopercular branch consists of the mandibular and preopercular sensory canals. The infraorbital and preopercular canals converge in the post-orbital region and may connect to the otic sensory canal before meeting the supraorbital sensory canal on the skull roof and forming the temporal canal. The supratemporal commissure crosses the skull and connects the left and right temporal canal, which then leads to the posttemporal lateral line canals on each side (Fig. 5.8 A).

The supraorbital sensory canal runs through the frontal and parietal longitudinally. It is superficial at the anterior end of the frontal, but may have been roofed by a dorsal ridge on the frontal as in *J. hubeiensis*. Instead of being enclosed in the bones, this canal passed beneath the bone of the posterior frontal and anterior parietal. The canal is fused to the inner surface of the bones in *J. huachongensis* (Fig. 5.8 B), whereas it is preserved partially in a medially preserved specimen of *J. hubeiensis* (Liu et al., 2015, fig.6A). The junction of the supraorbital sensory canal and the otic sensory canal is enclosed within the parietal. Beyond this junction, the temporal canal is enclosed in the parietal in *J. huachongensis*, whereas it is mostly exposed in *J. hubeiensis*.

The infraorbital sensory canal runs through the infraorbital bones, including the lacrimal. Given the thin nature of the infraorbital bones, the sensory canal has a raised appearance. Infraorbital 4, carrying the infraorbital canal as well, is small and triangular and is preserved sitting over the

hyomandibula.

The mandibular part of the preopercular sensory canal runs through the dentary, anguloarticular, and preopercle, from anterior to posterior. This canal is enclosed by bones within the dentary, and may also be enclosed within the anguloarticular, and it is also partially enclosed in the preopercle. In the middle portion of the preopercle, the canal is most likely enclosed by bone, whereas it is superficial at both ends of the preopercle. This condition has been also observed in *J. hubeiensis*. The preopercle and infraorbital sensory canals converge and meet above infraorbital 4, anterior to the opercular fossa. The canal then continues anteriorly towards the sphenotic, and may or may not connect with the otic sensory canal.

Dorsal and anal fins－The dorsal fin includes 11–12 principal rays, of which the first one is unbranched, as in *J. hubeiensis*. The anal fin originates behind the point opposite the end of the dorsal fin. It is roughly triangular in shape. There are 7–8 principal anal fin rays preceded by two unbranched procurrent rays. The second, and last, unbranched fin ray is about half the length of the first principal ray, i.e. the first principal ray is branched.

Caudal vertebrae, skeleton, and fin－There are 11–13 caudal vertebrae (most specimens have 12); the small number corresponds to the relatively short caudal region. The caudal peduncle is also short, approximately equal to the caudal peduncle depth. The caudal fin is gently forked, with 19 principal fin rays (i,9,8,i).

Discussion

The Huachong specimens share a suite of features with *Jianghanichthys*, suggesting that they should be assigned to the genus. Differences between *J. huachongensis* and the type species *J. hubeiensis* include the shape of the opercle ventrally and the enclosure of the temporal sensory canal in the parietal in *J. huachongensis*. Detailed comparison with the other nominal species of *Jianghanichthys* is unfortunately not possible, but the geological age and geographic distribution of *J. huachongensis* are distinctive among all known occurrences of *Jianghanichthys*. A new species is described here with the aims to better understanding the only fossil-only cypriniform family Jianghanichthyidae and the evolutionary traits of basal cypriniforms.

The difference between *J. huachongensis* and *J. hubeiensis* is evident from the previous description. First, the opercle is wider in *J. huachongensis* and narrower in *J. hubeiensis*, because of a protruding posteroventral margin in *J. huachongensis*. Second, the temporal sensory canal is enclosed in the parietal, whereas it is fused to the parietal medially in that of *J. hubeiensis*. Another difference between them is that the preopercular canal connects to the infraorbital canal in *J. huachongensis* but not in *J. hubeiensis*. Additionally, the opercular canal is not seen in the former, but is present in the latter. An opercular canal and a connection between the infraorbital and preopercular canals are both found in some extant cypriniform fishes. The presence of the opercular canal has been hypothesized to be a synapomorphy of Cyprinidae, whereas the connection between the infraorbital and preopercular canal occurs in many cypriniforms (Conway, 2011). These two connection patterns are not seen in any family of extant cypriniform, but probably both are present in *Jianghanichthys*.

The morphological features shared by *J. huachongensis* and *J. hubeiensis* confirm the unique and basal characters of *Jianghanichthys*. First of all, the first principal ray of the anal fin is branched, a feature that is not seen in any of the comparative taxa. In other words, the last unbranched anal fin ray is not sufficiently developed to be a leading fin ray. In both *J. huachongensis* and *J. hubeiensis*, the last unbranched anal fin ray is about half the length of the leading and first principal ray.

Second, the opercles of *J. huachongensis* and *J. hubeiensis* commonly have a well-developed and dorsally pointed opercular arm and auricular process, with a concave dorsal margin between them. The well-developed opercular arm and auricular process resembles that of crown catostomids, whereas the narrow dorsal concavity is similar to that of gyrinocheilids. Furthermore, the thin and laminated bone texture of the opercular arm and auricularprocess also resemble the gyrinocheilid condition (although there it is less well developed), whereas these processes are more robust and thicker in catostomids. In addition, the opercular fossa that articulates with the hyomandibular is far below the dorsal margin of the opercle, a feature shared by jianghanichthyids and gyrinocheilids. Overall, therefore, the opercle of *Jianghanichthys* is unique in shape but shares a few traits with both catostomids and gyrinocheilids.

Third, there is a consistently low number of caudal vertebrae across the species referred here to *Jianghanichthys*, with a range of 11–13, usually 12. The number is comparatively higher in Eocene catostomids. For example, in the Eocene catostomid genus *Amyzon*, there can be 14–18; e.g., *Amyzon aggregatum* (14–17), *A. gosiutense* (14), *A. commune* (17), *A. hunanense* (14–15), *A. kishehnicum* (15–18); and in the genus *Plesiomyxocyprinus*, the number is 20. The number is also

higher in Asian Eocene cyprinids whose caudal vertebrae can be counted, e.g., *Paleogobio zhongyuanensis* (18; Zhou, 1990) and *Tianshanicus liui* (21–22; Su, 2011). Moreover, the caudal peduncle depth of *Jianghanichthys* is greater than or equal to the length of the caudal peduncle, with the dorsal and ventral outlines of the caudal peduncle converging towards the base of the caudal fin, a feature that has not been observed in other Paleogene cypriniform fossils. The unique combination of caudal vertebrae number, caudal peduncle depth/length ratio, and the caudal peduncle outline is thus considered diagnostic for *Jianghanichthys*.

While the description of *J. huachongensis* confirms certain basal characters of *Jianghanichthys*, it also raises a question regarding the sensory canal patterns. There is a noteworthy difference between cephalic sensory canal patterns in *Jianghanichthys*, and extant cypriniforms, the presence or absence of two sensory canal interconnections within the parietal. This unique sensory canal connection was noted by Liu et al. (2015; Chapter 2) when describing *J. hubeiensis*, where the supraorbital and otic ("temporal" in some literature) sensory canals meet within the parietal and the supratemporal commissure is also continued on the parietal. These two connects are also observed in *J. huachongensis*. There are usually two types of sensory canal arrangements in the posterior skull roof of extant cypriniforms. First, if the supraorbital and otic sensory canals connect to each other, the supraorbital branch commonly meets the otic sensory canal in the otic region, then connect to the supratemporal commissure; e.g., some cyprinids (Illick, 1956; Gosline, 1974), psilorhychids (Conway, 2011), some catostomids (*Cycleptus* and *Hypentelium*), and gyrinochelids. Where the supraorbital and otic sensory canals are separate, the supraorbital sensory canal may enter the parietal, but does not usually connect to the supratemporal commissure; e.g., some cyprinids (Illick, 1956) and catostomids (*Catostomus* and *Moxostoma*). If

sensory canals in the postorbital and posterior cranium area, during evolution from basal to derived cypriniforms, tended to reduce connections and drift away from the parietal, a missing link between *Jianghanichthys* and extant cypriniforms probably would have one sensory canal connection, associated with the parietal.

Brief Comparison with *Osteochilus*

Paleogene *Amyzon* and *Jianghanichthys* from China were all previously assigned to the genus *Osteochilus*. The osteology of *Osteochilus* is briefly described here for comparison. In previous descriptions, the morphological characters of Eocene catostomids and jianghanichthyids had been compared with cyprinids and catostomids in general. To eliminate nominal species from the genus *Osteochilus*, direct comparison is unavoidable. If not denoted, the following osteological description is based on an *Osteochilus* skeleton AMNH I-94472SD (Fig. 5.9), and the comparisons are made between *Osteochilus*, Asian *Amyzon*, and *Jianghanichthys*, of which the later two taxa were once assigned to the former.

Osteochilus (Family: Cyprinidae) are small to medium sized freshwater fishes distributed in small rivers, creeks, and streams in Southeast Asia, such as in southern China, Vietnam, Myanmar, Thailand, Malaysia, and Indonesia. They possess 10–18 branched dorsal fin rays, 5–6 branched anal fin rays, and 3 rows of pharyngeal teeth (Chu, 1935; Yue and Editoral-Committee, 2000). If the last unbranched fin ray is included in the principal fin ray count (common practice for cypriniforms; Hubbs et al., 2004), the principal dorsal fin ray count for *Osteochilus* is 11–19 (Fig.

5.9 A) and 6–7 for the anal fin rays (Fig. 5.9 F). The principal dorsal fin ray number in *Osteochilus* thus falls within the ranges of *Jianghanichthys* (11–13) and *Amyzon* (19–33).

The skull of *Osteochilus*, resembling other cyprinids, consists of the ethmoid complex (median), frontals, and parietals in dorsal view (Fig. 5.2 B & C). The frontal is narrower anteriorly and wider posteriorly, the reverse of *Jianghanichthys* and *Amyzon*. An ethmo-frontal and fronto-parietal fontanelle are both absent, whereas both are present in *Amyzon* (Liu et al., 2016). The supraorbital sensory canal is completely enclosed by the frontal, and probably does not enter the parietal, whereas the canal is semi-enclosed within the parietal in *Jianghanichthys*. In lateral view (Fig. 5.2B), there are four large infraorbital bones (the first being identified as the lacrimal), and one supraorbital. The dermosphenotic sits at the posterodorsal corner of the orbit and is underlain by the autosphenotic, which is located between and largely covered by the frontal and dermosphenotic. The sphenotic is largely exposed and seems to be a composite bone in *Jianghanichthys* and *Amyzon*. The pterotic is located lateral to the parietal and has a lateral ridge, but is without deep depressions or openings like those observed in *Jianghanichthys* and *Amyzon*.

The opercular series (Fig. 5.9 B), as in other cypriniforms, consist of the opercle, preopercle, interopercle, subopercle, and three branchiostegals. The opercular socket for the hyomandibula is large. There is no dorsal concavity in the opercle. An opercular arm and auricular process are not developed; instead, a square-like, large process at the antero-dorsal corner is present. The posterodorsal corner of the opercle is oblique and lacks an auricular process. Although the absence of the opercular arm and auricular process, and the presence of a concave opercular dorsal margin are all typical cyprinid features, they are different from those of *Jianghanichthys*

and *Amyzon*.

As in cyprinids generally, the maxilla of *Osteochilus* is excluded from the margin of the mouth, which is formed only by the premaxilla and dentary. However, in *Jianghanichthys* and Asian *Amyzon* previously assigned to *Osteochilus*, the maxilla is not excluded from the mouth margin.

The pharyngeal teeth in *Osteochilus* are 3-rowed, 2, 4, 5/5, 4, 2 (Fig. 5G). The teeth are slender and conical, with tongue-shaped tips and spoon-like depressions on the dorsal-lateral surface. Recently-discovered pharyngeal teeth of *Amyzon hunanense* (IVPP V 17906.3a) are approximately triangular and extremely compressed, resembling those of most catostomids. The pharyngeal teeth are arguably not well developed and may be rudimentary (Liu et al., 2015). On the basis of pharyngeal tooth morphology, therefore, *Jianghanichthys* and Asian *Amyzon* differ from *Osteochilus*.

The Weberian apparatus (Fig. 5.2 D) typically includes four pairs of Weberian ossicles (claustrum, scaphium, intercarlarium, and tripus), four modified centra, supraneural 2, neural complex, neural arches 3, neural arch and spine 4, rib 4, transverse processes on centrum 1 and 2，and os suspensorium. The sagittal plate neural complex is large, wider distally and narrower proximally. The dorsal margin of the neural complex is nearly parallel to the thoracic vertebral column. The neural spine 4 is long, reaching the dorsal margin of the neural complex. The rib 4 is short, pitted, and projecting anteroventrally with the length about half of that in ordinary ribs. Unlike *Osteochilus*, the rib 4 of *Amyzon* is robust and elongated ventrally, whereas that of *Jianghanichthys* is slightly pointed posteriorly and bifurcated at the distal tip.

The caudal skeleton (Fig. 5.9 E) consists of the caudal complex, pleurostyle, epural, parhypural, and five hypurals with which 19 principal caudal fin rays are associated. Hypural 1 and the parhypural are fused at their proximal ends and together they are attached to the caudal complex (a synapomorphy of cypriniforms that has been confirmed in all the compared specimens of *Osteochilus*, Asian *Amyzon*, and *Jianghanichthys*). Hypural 2 is fused with the caudal complex, whereas the hypurals 3–5 are attached under the pleurostyle and decrease in size dorsally.

The dorsal fin has 16 principal rays (Fig. 5.2A), whereas the anal fin has 6 principal rays (Fig. 5.2F). The first principal ray of the median fins is unbranched, while the rest of the fin rays are branched. The arrangement of fin rays and pterygiophores is similar to that of catostomids. However, the number of principal anal fin rays is fewer in *Osteochilus* and many other cyprinids, whereas the principal anal fin rays are consistently more than 7 in both catostomids and jianghanichthyids.

From this comparison, the Asian *Amyzon*, and *Jianghanichthys* are strikingly different from the extant cyprinid genus *Osteochilus*. This suggests that *Osteochilus* was not in fact present in the Eocene, and raises doubts about the assignment of another putative Eocene occurrences of *Osteochilus*, such as those from Sumatra (Sanders, 1934), which clearly deserve further study in order to clarify their systematic position.

Conclusion

This study comprehensively reviews the fossil record of Asian non-cyprinid and non-loach

cypriniforms, which were previously identified either as catostomids or problematic catostomid-like forms. So far, all the Asian non-cyprinid cypriniform fossils seem to belong either to Catostomidae or Jianghanichthyidae (which are effectively stem catostomids). New materials of Jianghanichthyidae from Huachong Formation and re-discovery of catostomid material from collections of AMNH Central Asia Expedition are also described.

The geological age of Asian fossil catostomids ranges from early Eocene to early Oligocene. Sytchevskaya (1986) suggested that one of her Central Asian localities is Oligocene. The recently re-discovered specimen AMNH FF 6278 from Ergil Obo (Ardyn Obo), Ergelin Dzo, Dornogobi, Mongolia confirms the presence of Oligocene catostomids in Asia. Asian fossil catostomids are now known from East Siberia, Russia to the North, Hunan, China to the south, Pacific coast to the east, and Kazakhstan to the west. Interestingly, the only Oligocene localities are restricted in Central Asian and represented by disarticulated specimens, and the rest of the localities are Eocene.

Most of the Eocene forms from China previously assigned to "*Osteochilus*" (Tang, 1959; Lei, 1977; Wang et al., 1981) are re-assigned here to *Jianghanichthys*, except for one record of the catostomid *Amyzon hunanense* (Cheng, 1962; Chang et al., 2001). Morphological variations of "*Osteochilus sanshuiensis*", "*Osteochilus longipinnatus*", and "*Osteochilus laticorpus*" are considered here to represent mainly ontogenetic/allometric variation within a single species (*Jianghanichthys sanshuiensis*). The occurrence of *J. sanshuiensis* from the Buxin Formation extends the stratigraphic range of jianghanichthyids from the Eocene into the Paleocene. The new species *Jianghanichthys huachongensis* from the Huachong Formation further increases the

known Eocene diversity of the genus.

The Asian catostomid and jianghanichthyid fossils reviewed here are confined to a relatively short time period, from the early Paleocene to Oligocene and have so far not been discovered in post-Oligocene sediments. While catostomids were distributed in Central Asia and Asia from the early Eocene to Oligocene, jianghanichthyids are restricted in south China from the Paleocene to Eocene. These two basal families of cypriniforms partly co-occurred with each other in the Eocene and in south China along the Yangtze River.

Table 5. 1 Revision and summary on the Eocene catostomids and problematic catostomids from East Asia. Arabic numbers in the Locality column corresponding to those in Fig. 1. Meristics and morphometrics of *Amyzon hunanense* are from Chang et al. (2001), those of *Plesiomyxocyprinus arratiae* are from Liu and Chang (2009), of *Jianghanichthys hubeiensis* from Liu et al. (2015; Chapter 2); of *Jianghanichthys linliensis* from Tang (1959), and of *Jianghanichthys sanshuiensis* from Wang et al. (1981). Counts and measurements of *Vasnetzovia artemica* are based on photographs of the type specimen. Abbreviations: D, number of principal dorsal fin rays; A, number of principal anal fin rays; C, number of principal caudal fin rays; Vert, number of vertebrae including the modified centra associated with the Weberian apparatus; VertC, number of caudal vertebrae; BD/SL, the ratio of body depth to standard length. Within the adopted dataset, if principal fin ray number was not provided in the reference, it is calculated as branched fin ray number plus one; if the BD/SL was not provided, the ratio was calculated with the provided reverse ratio or with the raw data. "Fm." is short for Formation.

Assignment	Taxa	Synonyms	Horizon	Locality	D	A	C	Vert	VertC	BD/SL
Catostomidae	*Amyzon hunanense* (Cheng), 1962	*Osteochilus hunanensis* (Cheng, 1962); *Amyzon huananensis* (Chang et al., 2001)	Xiawanpu Fm.	6	19–20	10	18	34–35	14–15	0.35-0.43
	Plesiomyxocyprinus arratiae Liu et Chang, 2009	Catostomidae indet. (Chang et al., 2001)	Huadian Fm.	2	～50	18-19	18	42	20	~0.52
	Vasnetzovia artemica Sychevskaya, 1986	----	Wuglovaya Fm.	3	>11	7–9	18	----	16-18	0.29-0.32
	Catostimidae indet.	*Catostomus* indet. (Hussakof, 1932)	Ulan Shireh Fm.	1	----	----	----	----	----	----
Jianghanichthyidae	*Jianghanichthys hubeiensis* (Lei), 1977	*Osteochilus hubeiensis* (Lei, 1977)	Yangxi Fm.	4	12–13	7	19	32-33	12-13	0.34-0.63
	Jianghanichthys linliensis (Tang), 1959	*Osteochilus linliensis* (Tang, 1959; Cheng, 1962)	----	5	12	6	14(?)	33	----	0.41
	Jianghanichthys sanshuiensis (Li et Wang), 1981	*Osteochilus sanshuiensis* (Wang et al., 1981); *Osteochilus longipinnatus* (Wang et al., 1981); *Osteochilus laticorpus* (Wang et al., 1981)	Buxin Fm.	7	10–12	6–7	19	34	12-14	0.37-0.43
	Jianghanichthys sp.		Huachong Fm	8						

Figure 5. 1 Catostomid and problematic catostomid fossil localities from East Asia. Circles represent the localities of catostomids, and the stars represent the localities of jianghanichthyid and problematic catostomids that are assigned to Jianghanichthyidae in this study. In total, they represent the Paleogene non-cyprinid cypriniforms of Asia. **A**, Ergil Obo (Ardyn Obo), Ergelin Dzo, Dornogobi, Mongolia; **B**, Ulan Shireh, Inner Mongolia, China; **C**, Huadian, Jilin, China; **D**, Artem brown coal (lignite) mine, Premorie, Russia; **E**, Songzi, Hubei, China; **F**, Xiejiashan, Linli, Hunan, China; **G**, Xiawanpu, Xiangxiang, Hunan, China; **H**, Sanshui, Guangdong, China; **I**, Zidongxu, Foshan, Guangdong, China.
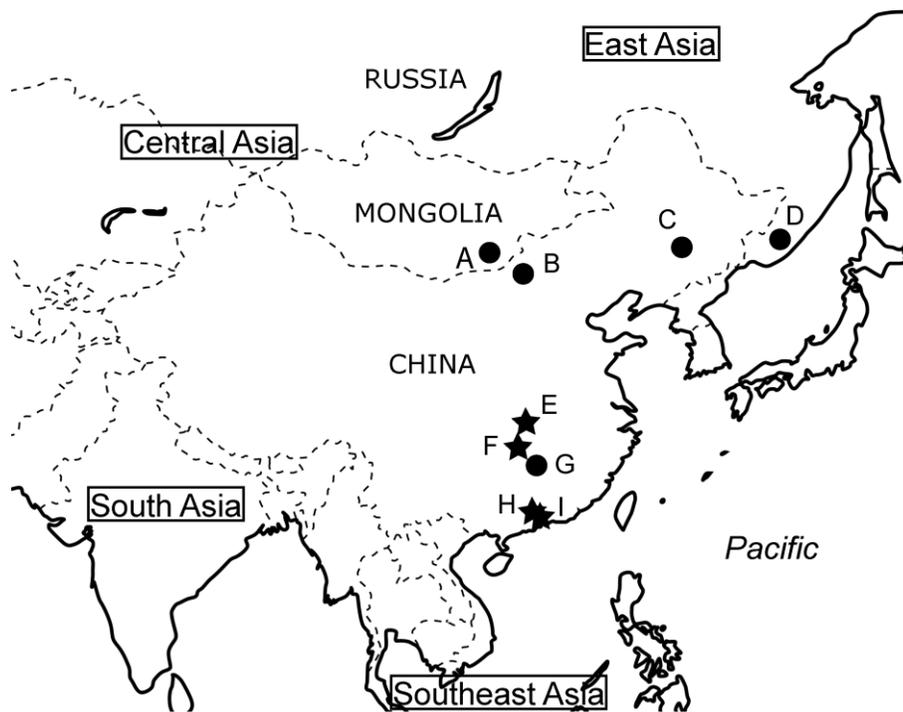
Figure 5. 2 *Amyzon hunanense* (Cheng), 1962 from the Eocene Xiawanpu Formation (Fm.), Hunan, China. A, a complete adult fish, IVPP V 17906.6a; B, a nearly complete juvenile, IVPP V 17906.23; C, two pharyngeal teeth preserved *in sito* on IVPP V 17906.3. Scale bar represents 10 mm.
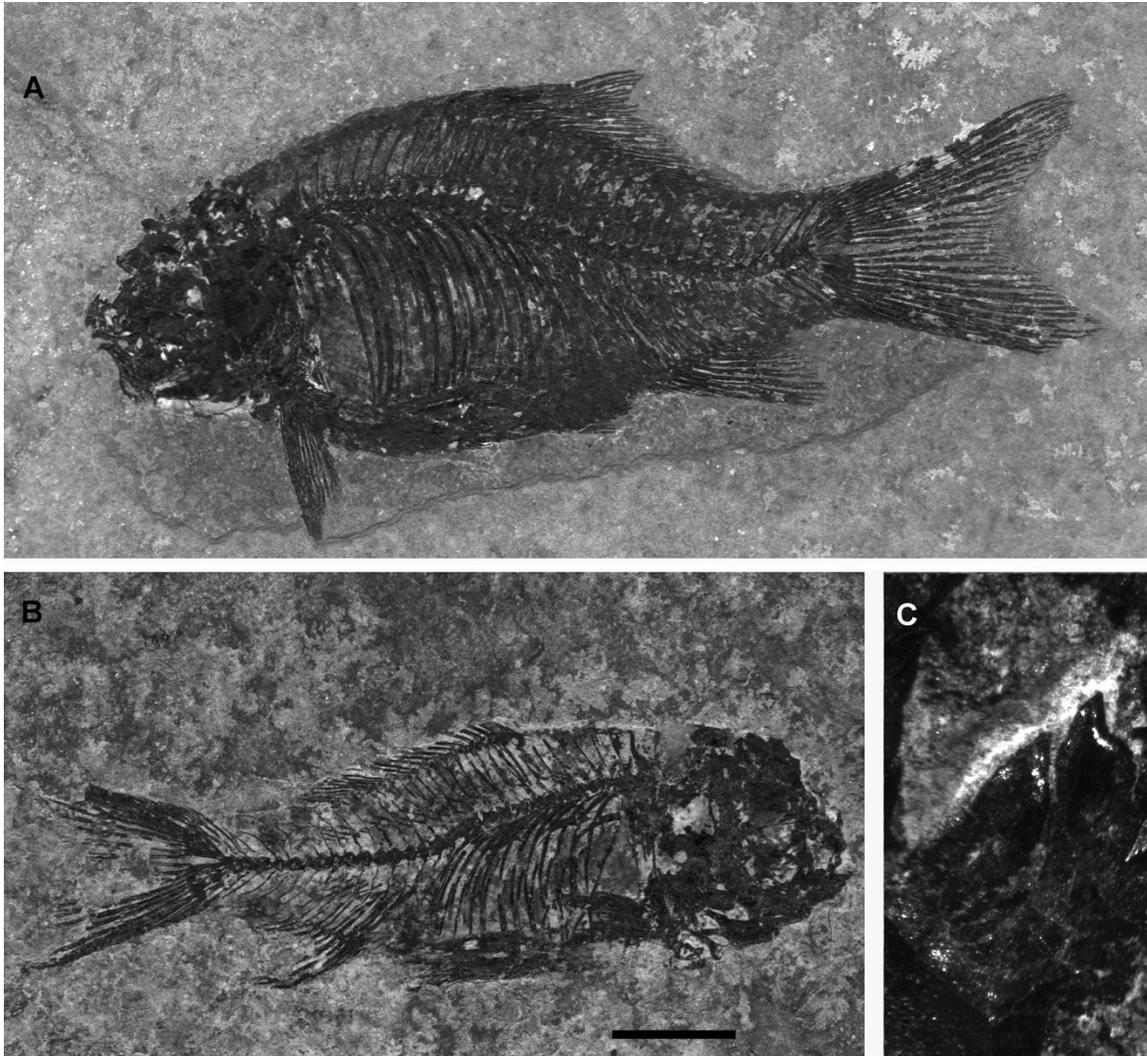
Figure 5. 3 *Vasnetzovia artemica* Sychevskaya, 1986 from the Eocene Wuglovaya Formation Artem brown coal (lignite) mine, Premorie, Russia. A, holotype, nearly complete fish, PIN N3882/1; B, nearly complete fish, PIN N3882/2. Scale bars represent 10 mm.
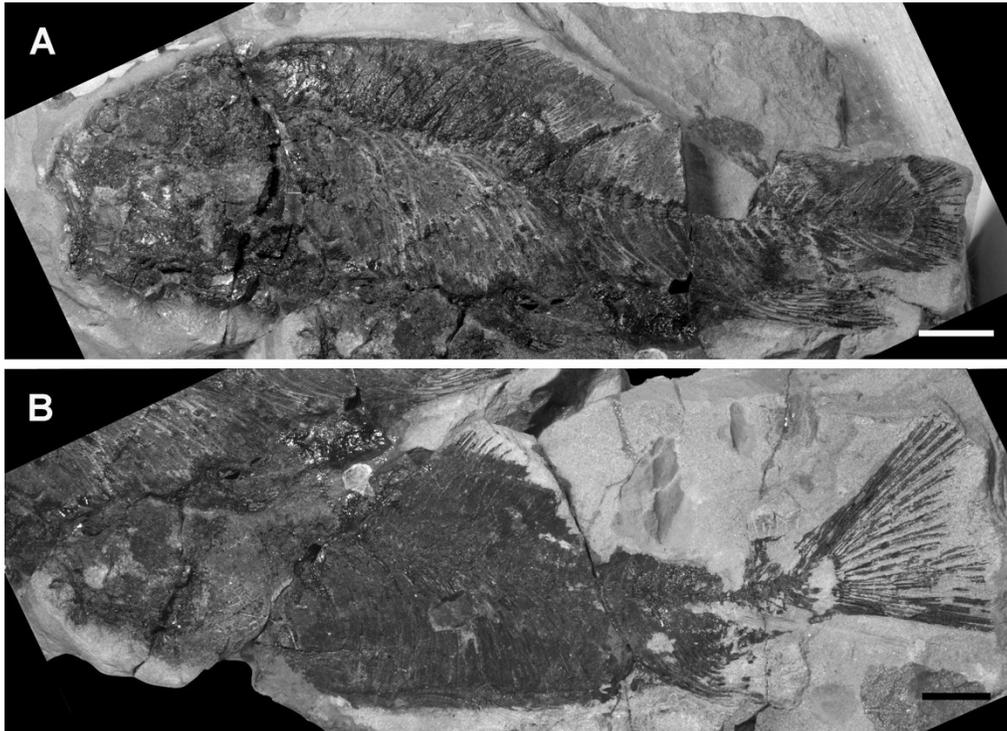
Figure 5. 4 Catostomidae indet. from the Oligocene-Eocene sediments of the Gobi dessert in China and Mongolia. A-F, AMNH FF 8442, catostomid opercle and centra from the middle Eocene Ulan Shireh Formation, Shara Murun region, Inner Mongolia, China; G and H, AMNH FF 6278, lateral and medial view of a partial opercle from the late Eocene Ergelin Dzo Svita, Ergil Obo (Ardyn Obo), Ergelin Dzo, Dornogobi, Mongolia. A and B, lateral and medial view of an opercle, which was also figured in Hussakof (1932, p. 16, fig. 25A); C and D, transverse and lateral view of the centrum 1; E and F, transverse and lateral view of a regular centrum. Abbreviations: **ap**, auricular process; **oa**, opercular arm; **opf**, opercular fossa. Scale bar represents 10 mm.
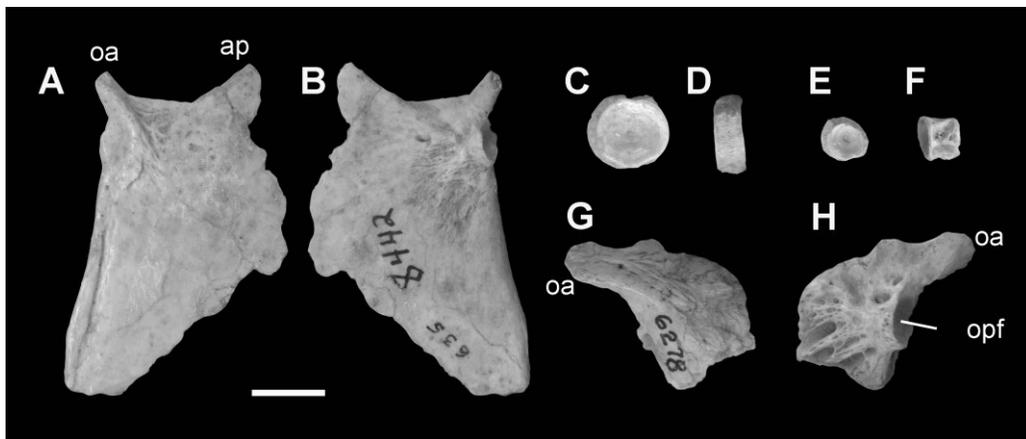
Figure 5. 5 *Jianghanichthys linliensis* (Tang), 1959 from the Eocene Xiajiashan mine, Linli, Hunan, China. Photograph is scanned from Tang (1959). The bigger fish on this specimen slab was designated as the holotype by the original author, with a registration number 58F-1.1, without institutional information.   Standard length (SL) of the holotype is 100 mm, and body depth (BD) is 34 mm.
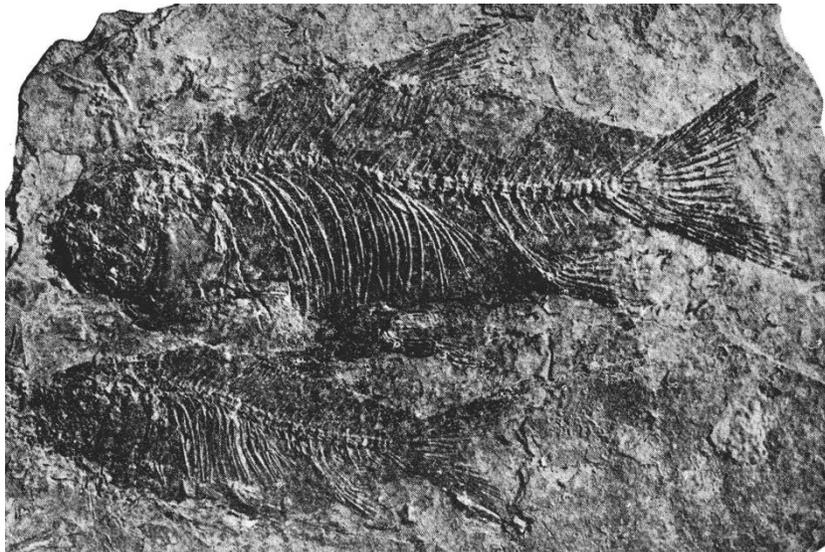
Figure 5. 6 *Jianghanichthys sanshuiensis* (Wang et al.), 1981 from the Paleocene Buxin Formation, Sanshui, Guangdong, China. A, nearly complete fish, designated as the holotype for *Osteochilus sanshuiensis* by Wang et al. (1981), catalogue number R. 741125-1, SL 68 mm, BD 25 mm; B, nearly complete fish, designated as the holotype for *Osteochilus longipinnatus* by Wang et al. (1981), catalogued R. 741177, SL 39 mm; BD 15 mm; C, nearly complete fish, designated as the holotype for *Osteochilus laticorpus* by Wang et al. (1981), catalogued R 74131, SL 79 mm, BD 34 mm. Photos are scanned from Wang et al. (1981).
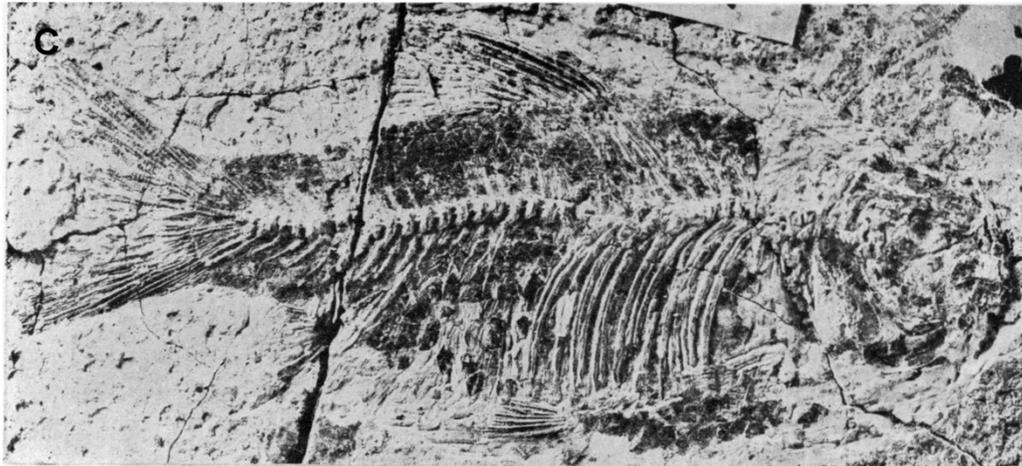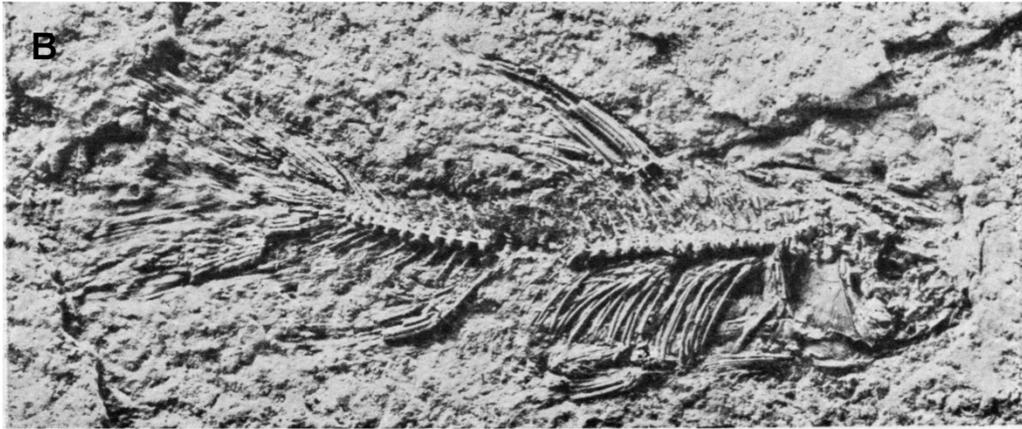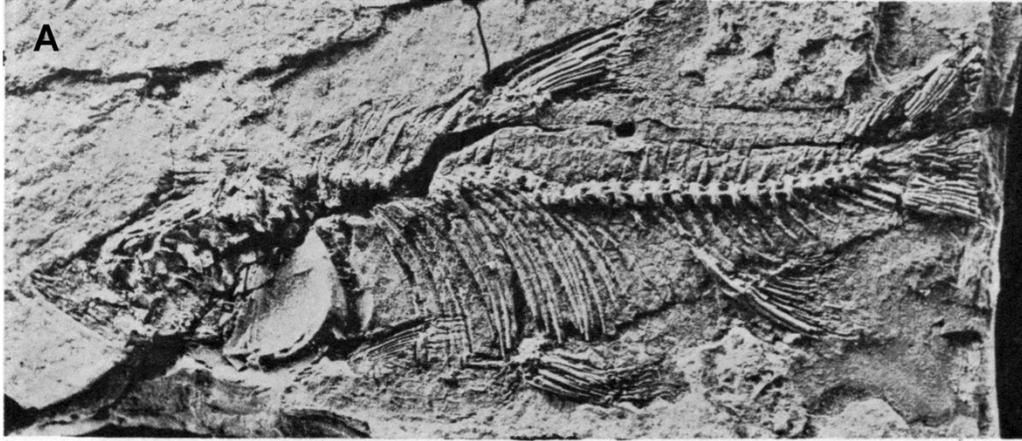
Figure 5. 7 *Jianghanichthys huachongensis* sp. nov. from the early Eocene Huachong Formation, Foshan, Guangdong, China. Holotype, IVPP V 23184.2, a nearly complete fish, scale bar represents 10 mm.

Figure 5. 8 *Jianghanichthys huachongensis* sp. nov. from the early Eocene Huachong Formation, Foshan, Guangdong, China. A, reconstruction showing skull bones and associated sensory canals; the maxilla, ethmoid complex, lateral ethmoid, anguloarticular, retroarticular, the otic sensory canal, and sensory canal openings are not reconstructed because of the lack of good preservation in the specimens; B, skull region of IVPP V 23184.2; C, caudal bones and fin, IVPP V 23184.8; D, complete opercle IVPP V 23184.6; E, convergence of infraorbital and preopercular sensory canals, IVPP V 23184.7. Abbreviations: **ap**, auricular process; **cl**, cleithrum; **den**, dentary; **fr**, frontal; **hyo**, hyomandibular; **iob 1–4**, infraorbital 1–4 (anterior to posterior); **iop**, interopercle; **IOC**, infraorbital sensory canal; **oa**, opercular arm; **op**, opercle; **OTC**, otic sensory canal; **par**, parietal; **pmx**, premaxilla; **POC**, preopercular sensory canal; **pop**, preopercle; **PTC**, posttemporal canal; **ptt**, posttemporal; **ptr**, pterotic; **scl**, supracleithrum; **soc**, supraoccipital; **SOC**, supraorbital sensory canal; **sop**, subopercle; **sph**, sphenotic; **STC**, supratemporal sensory commissure; **TC**, temporal sensory canal. Anterior in A, B, and C faces right; in D and E faces left. Scale bars represent 10 mm.
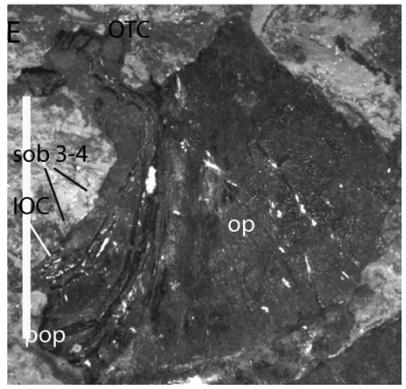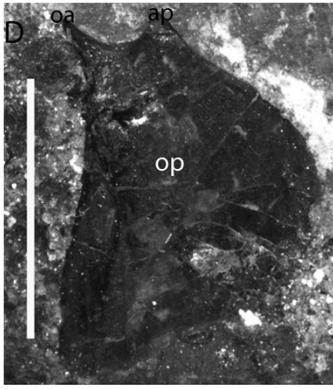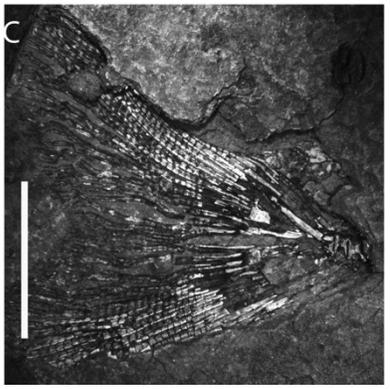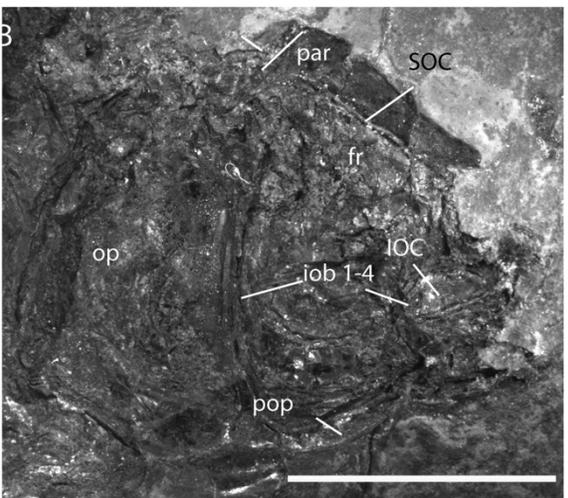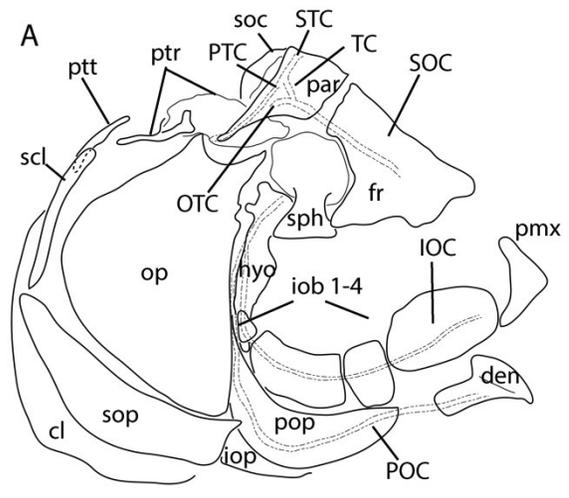
Figure 5. 9 Dry skeleton of *Osteochilus* sp. AMNH I-94472SD (SL 215mm). A, lateral view of dorsal fin; B, lateral view of skull; C, dorsal view of skull; D, lateral view of Weberian apparatus; E, lateral view of caudal skeleton; F, lateral view of anal fin; G, dorsal view of gill arches. All lateral views show the left side of the fish. A through E, anterior of the fish is on the left, and to the top in G. Abbreviations: **1pr**, 1st principal fin ray; **1ptg**, 1st pterygiophore; **afs**, anal fin stay; **asph**, autosphenotic; **cc**, caudal complex; **cls**, claustrum; **dsph**, dermosphenotic; **ep**, epural; **fr**, frontal; **em**, ethmoid complex; **hyp 1–5**, hypural 1 through 5; **iob1**, infraorbital 1 (lacrimal); **iob2–4**, infraorbital 2 to 4; **itc**, intercalarium; **lem**, lateral ethmoid; **na3/4**, neural arch 3/4 (on centrum 3/4); **nc**, neural complex; **ns4**, neural spine 4 (on centrum 4); **op**, opercle; **par**, parietal; **pb**, pharyngeal bone; **phy**, parhypural; **pop**, preopercle; **ps**, pleurostyle; **pt**, pharyngeal teeth; **ptr**, pterotic; **r4**, the fourth rib (on centrum 4);   **scp**, scaphium; **sn2**, supraneural 2; **sob**, supraorbital; **sop**, subopercle; **tp**, the transverse process; **trp**, tripus.
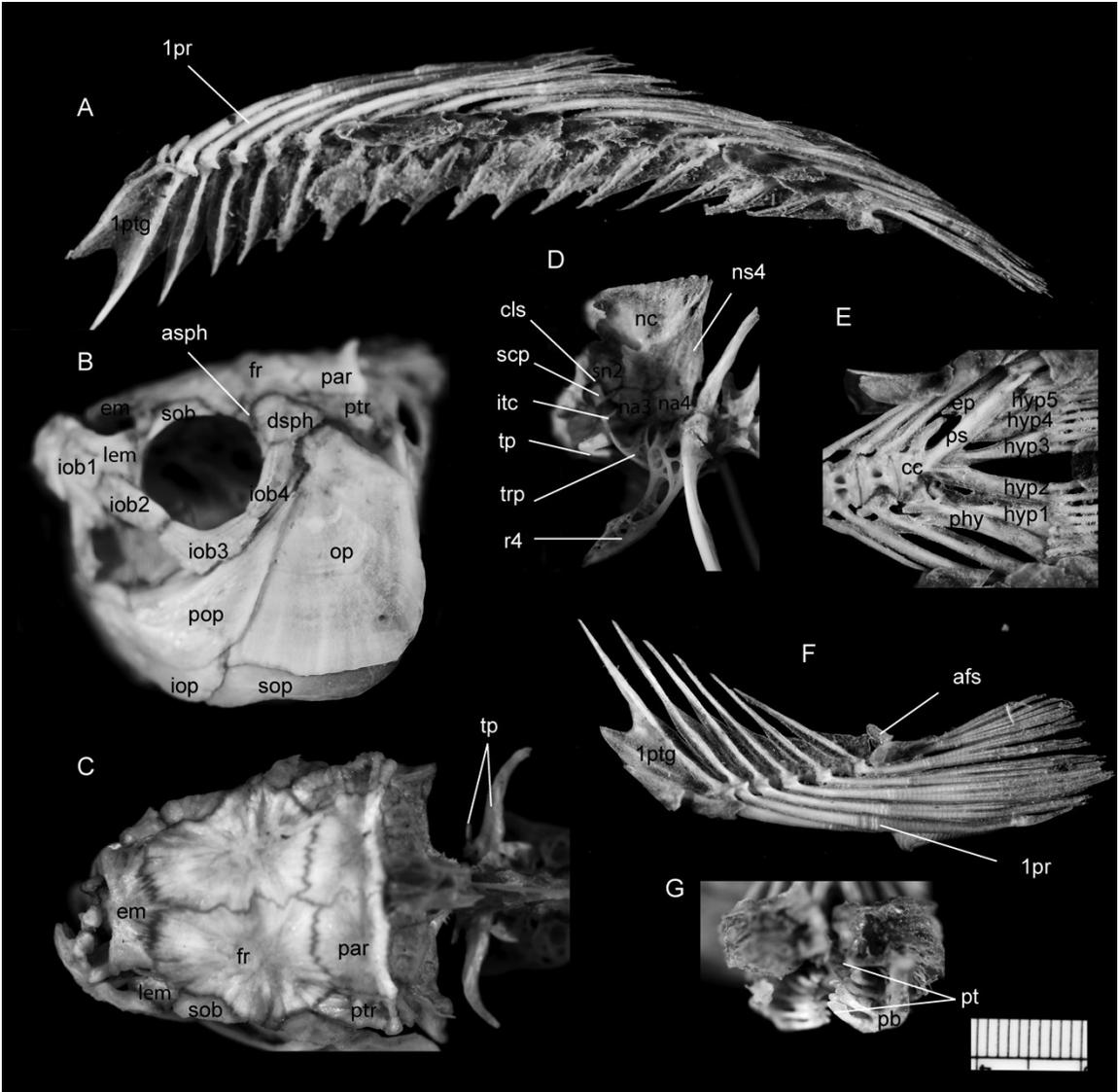
Chapter 6 The Osteological Characters and Phylogeny of Catostomidae

Introduction

The Catostomidae are a family of carp-like fishes (Order Cypriniformes) that are commonly known as suckers (Nelson et al., 2016). The common name "sucker" is derived from their protrusible, fleshy lipped, subterminal mouths used in food suction. Extant catostomids consist of thirteen genera with 78 species in the family Catostomidae (Nelson et al., 2016). While 77 extant species occur in North America, the range of one of them, *Catostomus catostomus*, also extends to northeastern Siberia. Only one extant species, *Myxocyprinus asiaticus*, is found solely outside North America, as an endemic form in the Yangtze River of China (Meng et al., 1995; Nelson et al., 2016). One North American species *Moxostoma lacerum* became extinct during the early 1900s (Simon, 2006). The majority of catostomids are widely distributed in North America and range south to Guatemala. They inhabit a wide range of environments from large lakes and rivers, such as the Mississippi (USA) and Yangtze (China) rivers (Rupprecht and Jahn, 1980; Meng et al., 1995), to small tributaries, such as streams along the Rocky Mountains (Smith, 1966); and from large lakes such the Great Lakes (Hubbs et al., 2004) to small unnamed ponds. Their body shapes range from extremely deep to very shallow, and also change through ontogeny (Nelson and Paetz, 1992; Meng et al., 1995).

The monophyletic family Catostomidae has been recognized by both morphological (Siebert, 1987; Conway, 2011) and molecular (Mayden et al., 2009; Poulsen et al., 2009; Doosey et al., 2010) systematic studies. The members of the family are well defined by synapomorphic osteological characters. Comprehensive osteological descriptions of extant species have been published for several species. Ramaswami (1957) compared the skull and Weberian ossicles of *Catostomus* sp. ("*Catostomus catostomus camersoni*" of the author), *Carpiodes* sp., and *Myxocyprinus asiaticus* based on young individuals. Weisel (1960) studied the osteocranium of *Catostomus macrocheilus* with comparison to *Carpiodes carpio* and a cyprinid fish. Branson (1962) described the osteology of *Cycleptus elongatus*. Lo and Wu (1979) described and discussed the osteology of *Myxocyprinus asiaticus* based on adult Chinese suckers with one of the specimens nearly 1000 mm in standard length. Furthermore, the development of osteological structures has also garnered attention. Some developmental characters have been used even in phylogenetic analyses (Fuiman, 1985). Butler (1960) studied the development of the Weberian apparatus of *Catostomus plebeius*. Weisel (1967) studied the development of pharyngeal teeth in larval and juvenile *Catostomus* and the early ossification pattern of *Catostomus macrocheilus* with comparison to the guppy (Cyprinodontiformes). These detailed descriptions have served as valuable comparative materials as well as study materials for students of catostomids. A short summary of the known osteological synapomorphies of catostomids, are pharyngeal bones and teeth with a comb-like arrangement, in single row (Eastman, 1977); also, a transverse plate and a robust rib 4 fused with the ventral transverse process of centrum 2 are associated with the Weberian apparatus (Nelson, 1948; Bird and Hernandez, 2007).

Among the extinct species, many of them have been thoroughly described and compared with

other catostomids. Fink and Humphries (2010) described the skeleton of the recently extinct *Moxostoma lacerum* using high-resolution X-ray computed tomography scanning. This new and non-destructive technology was used to explore the osteology of this specimen-poor species without any alteration to the specimens, and indicated the direction of future morphological studies on catostomids. Wilson (1974) described fossil catostomids in detail based on a large collection, which has served as a comparison for other recently discovered specimens. In a subsequent study, (Grande et al., 1982; Liu and Chang, 2009; Liu et al., 2016; Chapter 3) explored more osteological features of Paleogene catostomids. Neogene catostomids, which are usually represented by disarticulated bones and were not included in this study, also provided important osteological characters (Smith, 1975; Smith et al., 2000; Alvarado-Ortega et al., 2006).

Comprehensive investigations across members of Catostomidae on particular organs/structures have been conducted extensively. Edwards (1926) studied the protrusible mouth (osteology and musculature of the upper jaw, lower jaw, and palatine region) of the catostomids. Nelson (1948) broadly investigated the Weberian apparatus in species of Catostomidae. Nelson (1949) also studied the opercular series and later Nelson (1961) described and noted the variation of the swim bladder chambers of catostomids. Miller and Evans (1965) studied the external morphology of the brain and lip and their taxonomic usefulness. Lundberg and Marsh (1976) examined the functional anatomy of the pectoral fin of catostomids with comparison to other cypriniforms. Eastman (1977) investigated the pharyngeal bone and teeth, and also Eastman (1980) studied the caudal skeleton. These morphological studies, especially the osteological studies (Nelson, 1948; Nelson, 1949; Eastman, 1977; Eastman, 1980), have shed light on the evolutionary implications and intra-family classification of catostomids.

The classification and phylogeny has been established and hypothesized using a large array of characters along with the development of knowledge, technology, and methodology (Fig. 6.1). When he recognized the family Catostomidae, Gill (1861) established three subfamilies Catostominae, Cycleptinae, and Bubalichthyinae (type genus *Carpiodes*) based on the general appearance of the fishes. Three subfamilies, Ictiobinae (*Ictiobus+Carpiodes*), Cycleptinae (*Cycleptus+Myxocyprinus*), and Catostominae (the rest of the genera), are generally recognized in subsequent studies and are supported by a comprehensive and convincing phylogenetic study (Smith, 1992). Fowler (1958) proposed that *Myxocyprinus* should belong to a monotypic subfamily, Myxocyprininae, and this is also well supported by morphological evidence (Nelson, 1948) and widely recognized in molecular systematic studies (e.g., Harris and Mayden, 2001; Sun et al., 2002; Doosey et al., 2010; Fig. 6.1). This four-subfamily classification that includes Cycleptinae (*Cycleptus*) and Myxocyprininae (*Myxocyprinus*) is used in the following text (Fig. 6.1).

The first hypothesized phylogeny of Catostomidae was depicted based on a review of morphological studies (Miller, 1959). The hypothetical phylogenetic tree of Miller (1959) suggested that *Amyzon* arose from the stem of Ictiobinae, in addition to the three-subfamily hypothesis (Fig. 6.2). Smith (1992) published the most comprehensive phylogeny of catostomids to date that was based on a large number of morphological characters and incorporated duplicated gene expression (Ferris and Whitt, 1978a), larval characters (Fuiman, 1985), and biochemical data (Smith and Koehn, 1971; Fig. 6.2). Among molecular systematic studies, mitochondrial rDNA (Harris and Mayden, 2001), mitochondrial and nuclear DNA (Sun et al., 2007), mitochondrial

protein coding genes (Doosey et al., 2010), duplication growth hormone gene (Bart et al., 2010a), and nuclear DNA (Chen and Mayden, 2012) have been used to hypothesize the phylogeny of Catostomidae (Fig. 6.1). The phylogenetic relationships at the genus and tribe levels (Jenkins, 1970; Smith and Koehn, 1971) have been hypothesized as well.

Among the above phylogenetic studies, Ictiobinae and Catostominae are generally resolved as monophyletic groups, and Cycleptinae and Myxocyprininae are either sister groups or not with variable systematic positions (Fig. 6.1; 6.2). Fossil catostomids, which carry the evolutionary history of this group of fish, have only been coded in a few phylogenetic studies with limited numbers of fossil taxa and characters that can be coded (Smith, 1992; Liu et al 2016), although their systematic position has been inferred from morphological studies (Miller, 1959). Whereas Smith (1992) suggested that *Amyzon* belonged to Ictiobinae, Miller (1959) hypothesized that *Amyzon* was a stem sister to both Ictiobinae and Catostominae (Fig. 6.2). Liu et al. (2016; Chapter 3) coded characters for and added three species of *Amyzon* to the data matrix of Smith (1992) based on a large number of fossil specimens. The additional fossil data altered the position of *Amyzon* from within Ictiobinae to becoming the most basal clade of Catostomidae. However, only certain osteological characters could be coded for the fossil specimens, so that the character list of Smith (1992) was not sufficient to satisfy a growing number of ingroups including more fossil taxa with limited specimens to code.

This study, therefore, aims to better understand the evolution of catostomid fishes. The significance of including fossil taxa in phylogenies is that fossil catostomids can carry evolutionary information that may not preserved with extant species, and thus they play a critical

role (Donoghue et al., 1989; Novacek, 1992), The interrelationships of fossil catostomids and their systematic position within the family directly represent the early evolutionary history of catostomid fishes. This study will present an osteological character list to accommodate fossil taxa and perform phylogenetic analyses including important fossil species and a large number of extant species.

Materials and Methods

Fossil materials studied in this project and specimens of extant fishes used for comparison and character coding are listed by taxon in General Appendix II. For terminology for opercles, pharyngeal bones, and pelvic bones, see Chapter 4.

Ingroup selection: To create as complete an understanding of the phylogeny as our current knowledge allows, this study includes as many fossil taxa as was possible. Fossil catostomids with specimens that can be coded for relevant characters include: *"NewGenus" brevipinne*, *Amyzon aggregatum*, *A. commune*, *A. gosiutense*, *A. kishenehnicum, A. hunanense*, and *Plesiomyxocyprinus arratiae*. A large number of extant catostomids are included to represent the majority of the genera of the family and interspecific variations.

Outgroup selection: Five outgroup taxa were selected to represent the major clades of Cypriniformes: *Cyprinus carpio* of Cyprinidae, *Gyrinocheilus aymonieri* of Gyrinocheilidae, *Cobitis taenia* and *Chromobotia macracanthus* of the loach families, and *Jianghanichthys hubeiensis* of the fossil family Jianghanichthyidae. When the outgroup is limited to being only one taxon, such as analysis in TNT and Mr. Bayes, *Jianghanichthys* is designated to be outgroup.

Catostomidae, Gyrinocheilidae and all the loach families were suggested to form the superfamily Cobitoidea by Siebert (1987), which has been widely accepted (Liu et al., 2002; Šlechtová et al., 2007). Based on morphological characters, Gyrinocheilidae was hypothesized to be sister group of Catostomidae (Wu et al., 1979; Wu et al., 1981; Conway, 2011), and sister group of Catostomidae plus the loach families (Siebert, 1987). In molecular phylogenetic studies, Gyrinocheilidae has been suggested to be the sister group of Catostomidae based on mtDNA data (Saitoh et al., 2006; Tang et al., 2006; Mayden et al., 2009; Poulsen et al., 2009), but is identified as a sister group of the clade formed by the loach families, with the two together forming the sister group to Catostomidae based on ncDNA sequence (Mayden et al., 2009; Chen et al., 2013). Although, the intrarelationships of Cobitoidea are still to be resolved, Catostomidae, Gyrinocheilidae and the loach families have been consistently suggested to be united in the Cobitoidea. Therefore, members of gyrinocheilids and the loach families are selected to represent an outgroup that may be sister to Catostomidae. Meanwhile, *Cyprinus* is chosen to represent the Cyprinoidea that may further relate to Catostomidae, whereas *Jianghanichthys* is the stem fossil clade of Cypriniformes. Also, cyprinids, catostomids, and jianghanichthyids are the oldest cypriniforms that are so far known from the Eocene and possibly prior to the Eocene. That makes cyprinids and jianghanichthyids ideal candidates for outgroups to investigate the phylogeny of the family Catostomidae, and especially in regard to fossil taxa.

Characters selection: Valuable osteological studies of certain species (Ramaswami, 1957; Weisel, 1960; Branson, 1962; Lo and Wu, 1979) and certain structures (Nelson, 1948; Nelson, 1949; Eastman, 1977; Eastman, 1980) of catostomids have been previously published. Smith (1992) presented a comprehensive phylogenetic study using a combined dataset that included a

reasonable proportion of osteological characters. However, a phylogenetic study using only osteological characters has never been done previously.

Four Eocene species were coded by Liu et al. (2016; Chapter 3) with characters from Smith (1992). In addition to some missing osteological characters, soft tissue, gene expression, larval, and biochemical characters used in the analysis of Smith (1992) were not available for the Eocene fossil species. Phylogenetic relationships were resolved with more steps (804 vs. 778 steps) and significantly more numbers of most parsimonious trees (MPCs; 1038 vs. 233) than the MPCs from the original data matrix (Liu et al., 2016). Given the fact that the number of characters was 157, the addition of more taxa with a large number of missing data reduced the accuracy of the parsimony-based phylogeny, compared to what was also found in previous studies (Wiens and Reeder, 1995; Dunn et al., 2003).

A test analysis, coding all code-able Eocene species with characters of Smith (1992) and combining the data matrix, was initiated in PAUP 4b10 and TNT 1.5 with parsimony criterion, but generated high-polytomy, comb-like strict consensus trees of MPCs. Introduction of an inevitably larger number of missing data in the parsimony analysis has failed to resolve the interrelationships of all catostomids and the systematic position of fossil catostomids. Although a larger number of characters, e.g., such as in a supermatrix with over 1000 characters, has been suggested to be less negatively affected by missing data (Driskell et al., 2004; Wiens and Morrill, 2011), in the case of the fossil catostomids and the dataset of Smith (1992), introducing non-osteological characters that may not be preserved in fossils will increase the ratio of missing data, and thus reduce the accuracy of the phylogeny (Wiens, 1998). Therefore, thoroughly exploring and comparing

osteological characters is needed to resolve the phylogeny of Eocene catostomids and their relatives. These are assembled, designed, and described in this study. Along with the additional catostomids and other cypriniform fish fossils already recovered, osteological character recognition is also important to determine the taxonomy and systematic position of future fossil discoveries.

To accommodate fossil taxa and create a less biased dataset for future combined character analysis, osteological and osteology-derived characters are exclusively selected in this study. Sixty-one of the 134 characters described and used in this study are adopted or modified from the analysis of Smith (1992), and a few others are from that of Conway (2011), Wu et al. (1981), Sawada (1982), Fink and Fink (1981; 1996), and Siebert (1987). The rest were discovered during the course of examining specimens for this study.

Character coding: When possible, characters are coded for dry skeletons of large size specimens for extant taxa and relatively large individuals for fossil taxa. For taxa in which only cleared and stained specimens were available, e.g., *Gyrinocheilus aymonieri* and *Cobitis taenia,* characters were verified from the literature: Wu et al. (1979) and Ramaswami (1952) for the former and Ramaswami (1953) and Jalili et al. (2015). This was done because some characters are affected by ontogenetic changes or ossification level, and coding might be different between dry skeletons and cleared and stained specimens.

Phylogenetic analysis: All characters were coded and entered in Microsoft Excel and then transferred to Mesquite version 3.04 (Maddison and Maddison, 2011). The data matrix was first

analyzed in PAUP* 4beta10 for Mac (Swofford, 2002; Swofford, 2003) using parsimony criterion. Heuristic searches with 1000 random replicates were performed using unordered and unweighted characters with "furthest" addition sequence with no topological constraints enforced. Character states were optimized with accelerated transformation (ACCTRAN). Another parsimony analysis was performed in TNT 1.5 (Goloboff et al., 2008) using both traditional and new technology search with 1000 replicates. Exploratory parsimony analyses were also performed with topology constraint on enforcing all species of *Amyzon* or all North American species of *Amyzon* as a monophyletic group. To evaluate the cladogram support, decay indices and bootstrap support value (1000 replicates) were calculated in PAUP, whereas bremer support was calculated in TNT.

A Bayesian analysis of the same data matrix using Bayesian inferences was explored for comparison and to evaluate support for clades. The analysis was performed in MrBayes (Ronquist et al., 2012) on XSEDE (3.2.6) through CIPRES Science Gateway (https://www.phylo.org/, NSF-sponsored Cyberinfrastructure for Phylogenetic Research Project).

Synapomorphies are optimized and mapped onto a strict consensus tree. Character changes of certain clades noted are common changes summarized from all most parsimonious cladograms. This was done in TNT 1.5 (Goloboff et al., 2008).

Osteological character descriptions for catostomid fishes

Osteological characters of catostomids and outgroup fishes are described below. The description is arranged in sections from anterior to posterior and from dorsal to ventral: neurocranium, infraorbital series, opercular series, mandibular and hyopalatine arches, branchial arches

(including pharyngeal), fins (including shoulder and pelvic girdles), vertebral column (including Weberian apparatus and caudal skeleton), and general appearance. Criteria for coding characters are generally given when ambiguity might occur. Character state distribution is provided, when patterns are apparent.

Neurocranium

1. Dermal component of ethmoid shape (modified from Smith, 1992: character 18): [0] narrower anteriorly (Fig. 6.3H); [1] nearly parallel bilaterally (Fig. 6.3G); [2] constricted bilaterally at middle (Fig. 6.3A); [3] narrower posteriorly (Fig. 6.3F); [4] nearly rod shaped, extremely narrow posteriorly, slight broader anteriorly (Fig. 6.3I).

The ethmoid of catostomids is a complex bone formed by the ontogenetic fusion of the dermal supraethmoid and the endochondral mesethmoid, as in other cypriniform fishes. It is also known as the ethmoid complex (Harrington, 1955; Cubbage and Mabee, 1996; Conway, 2011; Liu et al., 2016). The dermal dorsal portion is roughly rectangular with an anterior spine, whereas the endochondral portion is porous and sutured to the vomer. The lateral margins of the dorsal plate are parallel in *Ictiobus*, *Cycleptus*, *Hypentelium*, *Myxocyprinus*, and †*Amyzon*, but are variable in *Catostomus* and *Moxostoma*. This structure in the outgroup *Cyprinus* and *Gyrinocheilus* has state [0], whereas *Cobitis* has state [4]. Within the ingroup, either the lateral margins are slightly narrower anteriorly or posteriorly is coded as [1].

2. Dermal component of ethmoid spine (modified from Smith, 1992: character 136): [0] no distinct division between the spine and the anterior margin of the dorsal component of ethmoid, ethmoid spine long and broad (Fig. 6.3H); [1] short with broader base (Fig. 6.3G); [2] short, roughly rectangular (Fig. 6.3D); [3] long and slender with broad base; [4] long and robust,

227

rod-like (Fig. 6.3B); [5] long and slender (Fig. 6.3E); [6] moderately long, constricted at base.

The ethmoid spine is more or less developed in the examined specimens. In the outgroups *Cyprinus* and *Cobitis*, the anterior margin is strongly convex and thus gives the appearance of lacking a division between the spine and the dermal dorsal component of the ethmoid. Overall, *Amyzon*, *Carpiodes*, *Ictiobus*, *Myxocyprinus*, and some species of *Moxostoma* have a shorter ethmoid spine, whereas the rest of the catostomids have a long spine.

3. Lateral ethmoid (Smith, 1992: character 145): [0] non-porous bone (Fig. 6.3H); [1] triradiate in longitudinal section, more or less porous; [2] spinous (Fig. 6.3I).

The lateral ethmoid of catostomids usually has a porous dorsolateral plate with the bone-enclosed nasal canal in the middle, and a lateral orbital process reaching the orbit, resembling that of *Gyrinocheilus* except it is non-porous. The lateral ethmoid in the basal cypriniform *Jianghanichthys* and the fossil catostomid *Amyzon* overall resembles that of extant catostomids with the plate, but it is much less porous. The lateral ethmoid of *Cobitis* is much thicker and modified as a suborbital spine.

4. Lateral ethmoid and ethmoid contact (modified from Smith, 1992: character 22): [0] anterior corners close or connected (Fig. 6.3H); [1] anterior corner slightly separated from the ethmoid, nasal canal complete (Fig. 6.3F); [2] anterior corner well separated from the ethmoid, nasal canal fused with the porous structure (Fig. 6.3C); [3] anterior corner spine-like (Fig. 6.3I).

The outgroup *Cobitis* has the spine-like anterior corner because of its overall spiny shape without a plate or a bone enclosed nasal canal. Another outgroup, *Gyrinocheilus*, possesses a well-separated anterior corner of the lateral ethmoid, which is also spine shaped. The other two

outgroup taxa, *Cyprinus* and *Jianghanichthys*, and the fossil catostomid *Amyzon* have the anterior corner of the lateral ethmoid close to the ethmoid, resembling that of the catostomids *Carpiodes*, *Cycleptus*, *Myxocyprinus*. The anterior corner of the lateral ethmoid *Catostomus leopoldi* and the species of *Ictiobus* is intermediate in separation from the ethmoid, whereas that of the rest of the catostomids is well separated with a strongly porous plate and fused with the nasal canal. Notably, the separation between anterior corner of the lateral ethmoid and ethmoid, if present, is more apparent in younger individuals of catostomids.

5. Orbital process of lateral ethmoid: [0] absent (Fig. 6.3H); [1] projecting anteriorly (Fig. 6.3C); [2] projecting posteriorly (Fig. 6.3F).

The orbital process of the lateral ethmoid is not well developed in *Cyprinus*, but it projects anteriorly in *Gyrinocheilus* and posteriorly in the rest of the outgroups. This process is known as the laterocaudal process of the suborbital spine in *Cobitis*. The process projects anteriorly in *Carpiodes*, *Cycleptus*, *Erimyzon*, *Ictiobus*, and *Myxocyprinus*, and posteriorly in the rest of the catostomids including *Amyzon*.

6. Frontal shape: [0] extremely narrow anteriorly, posterior portion roughly square; [1] irregular shape, the width of anterior portion narrower or equal to the posterior portion (Fig. 6.3H); [2] overall rectangular, anterior portion moderately broader; [3] anterior portion fan-shape, posterior rectangular and much narrower (Fig. 6.3A–G).

The frontal is usually the largest of the paired bones on the skull roof of cypriniforms. The anterior portion of the frontal is usually above the orbit. Correspondingly, the posterior portion is beyond

the posterior limit of the orbit. These two portions are apparent in catostomids and loaches, as the width of both portions are dramatically different. All the catostomids, except "NewGenus", have a fan-shaped broad anterior portion and narrow posterior portion. The outgroup *Cobitis* has the anterior portion simplified into a rod-shape, whereas *Cyprinus* and *Gyrinocheilus* have frontals of irregular shape with the posterior portion slightly broader. The frontal of "NewGenus" *brevipinne* resembles that of the basal cypriniform *Jianghanichthys* with an overall rectangular shape and the moderately wide anterior portion.

7. Anterior edge of frontal: [0] curved (Fig. 6.3H); [1] truncated (Fig. 6.3F).

The anterior edge of the frontal in the outgroups *Cyprinus* and *Gyrinocheilus* is convex , and the division between the ethmoid and frontal is curved instead of straight. In *Jianghanichthys* and the ingroup except "NewGenus", the anterior profile of frontal is truncate. This character is inapplicable to *Cobitis*, in which the posterior portion of the ethmoid and anterior portion of the frontals are rod-shape.

8. Frontal contact with orbitosphenoid and pterosphenoid (Smith, 1992: character 32): [0] sutured; [1] cartilage.

The suture between the frontal and the endochondral orbitosphenoid and pterosphenoid bones is observed in the genus *Moxostoma*, consistent with the coding of Smith (1992). The suture is not observed in the rest of the taxa, in which cartilage may forms the connection between the bones.

9. Supraorbital process of frontal: [0] absent, but the anterolateral margin of the frontal is largely exposed between the supraorbital and sphenotic; [1] wedge-shaped, between

supraorbital and sphenotic, not reaching orbit (Fig. 6.3G); [2] wedge-shaped, reaches the orbit with its tip (Fig. 6.3A, H); [3] absent, lateral margin of anterior portion of frontal extending laterally being the only component of the dorsal orbital rim (Fig. 6.3C–F).

The frontal of *Gyrinocheilus*, *Jianghanichthys*, *Cyprinus*, and *Cobitis* have character status [0] to [3] consecutively and respectively. Within the ingroup, the frontal of *Carpiodes* possesses a wedge-shaped supraorbital process that reaches the orbit, whereas that of *Amyzon*, *Cycleptus*, *Ictiobus*, and *Myxocyprinus* is of similar shape but is excluded from the orbit. In the rest of the catostomids, i.e.: *Catostomus*, *Erimyzon*, *Hypentelium*, *Moxostoma*, and *Xyrauchen*, the lateral margin of the frontal is the main component of the dorsal orbital rim.

10. Dorsal ridge of frontal: [0] absent, dorsal surface may be slightly domed (Fig. 6.3H, I); [1] present (Fig. 6.3A–G).

The longitudinal dorsal ridge runs in the middle of the anterior portion and near the lateral margin of the posterior portion of the frontal. It is absent in *Gyrinocheilus*, *Cyprinus*, and *Cobitis*, but present in *Jianghanichthys* and all catostomids. The Eocene catostomids, *Amyzon hunanense*, *Plesiomyxocyprinus arratiae*, and "NewGenus" *brevipinne*, have a low frontal ridge.

11. Ornamentation on dorsal ridge of frontal: [0] roof-like or flange forms a dorsolateral extension along ridge; [1] dorsal or lateral projections along ridge.

Cycleptus, *Chasmistes*, and most species of *Catostomus* and *Moxostoma* possess a flange-shaped dorsolateral extension on the frontal dorsal ridge, whereas the rest of the catostomids have projections. The projections are either large, or small, or weak, or robust, or even clustered. The thickness of the projections and flanges usually display ontogenetic change. Specimens of similar

size are comparable. The frontal dorsal ridge of *Jianghanichthys* is roof-like with a lateral extension, with the sensory canal running beneath. This character is inapplicable to the outgroups in which the dorsal ridge is absent, as well as the taxa with a slightly domed ridge, e.g. *Amyzon hunanense*, *Plesiomyxocyprinus arratiae*, and "NewGenus" *brevipinne*.

12. Association of the supraorbital sensory canal and the frontal: [0] enclosed in bone; [1] partially enclosed in bone; [2] superficial, detached from the frontal.

The frontal portion of the supraorbital sensory canal is complete enclosed in bone in *Gyrinocheilus* and cyprinids, whereas it is detached from the bone in catostomids and loaches. The supraorbital sensory canal in the frontal of *Jianghanichthys* is partially enclosed under the roof-like frontal ridge with radiating sensory canal openings.

13. Ethmo-frontal fontanelle: [0] absent (Fig. 6.3C, E, F, H); [1] present (Fig. 6.3B, D, G).

Also known as the anterior cranial fontanelle, the ethmo-frontal fontanelle is a small dorsal opening located between the ethmoid and the frontal. It is absent in all outgroups except *Gyrinocheilus*, whereas it is present in *Amyzon*, *Carpiodes*, *Cycleptus*, *Hypentelium*, *Ictiobus*, and *Myxocyprinus* of the ingroup.

14. The position of the ethmo-frontal fontanelle relative to the surrounding bones: [0] mostly in ethmoid (Fig. 6.3B); [1] in the middle of frontal and ethmoid (Fig. 6.3G); [2] mostly in frontal (Fig. 6.3D).

The ethmo-frontal fontanelle, when present, is often mostly enclosed in the ethmoid, such as in *Amyzon*, *Carpiodes*, *Cycleptus*, and *Ictiobus*, in which the frontal only forms the posteriormost

margin. It is either in the middle of the ethmoid and frontal, such as in *Gyrinocheilus*, *Carpiodes*, and *Myxocyprinus*, or mostly within the frontals, i.e.: *Hypentelium*. In both the latter conditions, the frontal bears an anteromedial notch which forms the lateral and posterior margins of the fontanelle.

15. Fronto-parietal fontanelle (Smith, 1992: character 66): [0] absent (Fig. 6.3B, H); [1] partial (Fig. 6.3F); [2] prominent, narrow or wide (Fig. 6.3A, C–E, G, I).

Also known as the posterior cranial fontanelle, the fronto-parietal fontanelle is absent in all outgroups except the loaches, whereas it is present in all ingroups except *Catostomus plebeius* and species of *Cycleptus*. Among the fontanelle-bearing ingroups, most species possess a wide, elongate, and prominent fontanelle, but a few species have extremely narrow or short fontanelles that can possibly be missed during specimen examination. The partial fontanelle occurs in some small-sized species of *Catostomus*, i.e., *Catostomus cahita*, *C. platyrhynchus*, *Catostomus rimiculus*, *C. santaanae*, and *C. wigginsi*. The partial fontanelle is very limited and very easy to overlook (Fig. 6.3F), so that some of these species are coded as 'fontanelle absent' in Smith (1992), but the partial fontanelle is present in the specimens examined here.

16. Left and right parietals: [0] contact each other or closely abut at posterior end (Fig. 6.3 (Fig. 6.3B); [1] not in contact (Fig. 6.3C–E, F, I).

In those taxa without a fronto-parietal fontanelle, the two parietals are apparently sutured together. Overall, most catostomids that bear a wide fontanelle have no contact between left and right parietals; a few of them have the parietals closely abutting or even contacting each other at the posteromedial ends, such as in *Catostomus leopoldi*. However, in two taxa with a partial fontanelle,

Catostomus cahita and *C. rimiculus*, the two parietals are very close but not connected to one another.

17. Dermosphenotic (modified from Smith, 1992: character 147): [0] present as last infraorbital bone (Fig. 6.3H); [1] fused with autosphenotic into the sphenotic complex (Fig. 6.3A–G); [2] reduced (Fig. 6.3I).

The dermosphenotic of cypriniforms, if present, is or functions as the most posterior bone of the infraorbital series (Dahdul et al., 2010). In cyprinids, when present, the dermosphenotic floats in the orbit over the autosphenotic (Harrington, 1955). In *Gyrinocheilus*, *Jianghanichthys*, and all catostomids, the dermal portion of the sphenotic is prominent and forms the posterior rim of the orbit, possessing the same position and function as the dermosphenotic in other cypriniforms. Therefore, the dermal portion of the sphenotic is very likely to be homologous with the dermosphenotic, and the sphenotic in the family Gyrinocheilidae, Jianghanichthyidae, and Catostomidae is a complex bone formed by the fusion of the dermosphenotic and autosphenotic. In *Cobitis*, the dermosphenotic is completely reduced along with other the infraorbital bones except the lacrimal.

18. Pterotic ridge, lateral surface portion of the pterotic (modified from Smith, 1992: character 58): [0] broad; [1] intermediate; [2] reduced to a sharp vertical ridge, nearly no smooth lateral portion.

To my understanding, "pterotic ridge" in Smith (1992) refers to the portion of the pterotic forming the lateral surface. In catostomids, the pterotic is usually composed of fossa, ridges, and flanges, but lacks a complete, smooth, lateral surface that encloses the sensory canal, as found in cyprinids

(eg, *Cyprinus carpio*). However, in some species, for example *Carpiodes*, the smooth-surfaced portion of the pterotic is large, and it hardly has a ridge or is like a ridge. Also, this smooth-surfaced portion gives rise to ridge-like structures or flanges (see Character 19). To avoid confusion on the character description, the "portion of pterotic forming the lateral surface ' is called pterotic ridge here following Smith (1992), whereas the derived ridge-like or flanges on the ridge are called pterotic flanges as in the next character. This character is inapplicable to those taxa without a pterotic ridge. The criterion for the presence of the pterotic ridge used here is the presence of a pterotic opening following the lateral smooth surface. Under this criterion, the pterotic ridge is present in *Gyrinocheilus* and *Carpiodes*, although the lateral smooth surface is as broad as that of cyprinids. *Jianghanichthys* has two ridges, and the anterior primary ridge is intermediately broad. The pterotic ridge is absent in the rest of the outgroups except *Jianghanichthys*.

19. Vertical flange on pterotic ridge: [0] absent; [1] one flange; [2] two flanges.

The vertical flange on the pterotic ridge is absent in the outgroup taxa except *Jianghanichthys*. The flanges are thin and delicate, and may arise from the middle of a pterotic ridge, at the anterior or posterior margin, or be equivalent to the reduced sharp pterotic ridge. Most catostomids have two pterotic flanges, such as in *Catostomus*, *Chasmistes*, *Erimyzon*, *Ictiobus*, and *Xyrauchen*. Both flanges are vertical, the one near the sphenotic composed by both the sphenotic and pterotic or by the pterotic alone, the other one at the posterior margin of the pterotic and composed of the pterotic only. The two-flange condition often overlaps with the "broad pterotic ridge" condition of Smith (1992), in that the anterior and posterior vertical margins of the "broad pterotic ridge" extend laterally and are flange-like. The sharp pterotic ridge is reduced to be a delicate flange and

considered to be the one flange condition here, which is observed in *Cycleptus*, *Hypentelium*, *Moxostoma*, and *Myxocyprinus*.

20. Pterotic fossa (modified from Smith, 1992: character 149): [0] absent; [1] anterodorsal to epiotic; [2] anterior to epiotic.

The pterotic fossa (pterotic opening) is posterior to the pterotic ridge (surface part of the pterotic, character 18). The opening may be separated into two fossae by a small ridge (e.g., *Jianghanichthys*), in which case the posterior one is used for this character. The outgroups *Cyprinus* and *Cobitis* don't have the pterotic opening. In the specimens of Catostominae examined, the pterotic fossa is more laterally placed and anterior to the epiotic only.

21. Epiotic process (Smith, 1992: character 19): [0] present; [1] absent.

The epiotic process is present in most ingroup taxa except *Moxostoma*, *Hypentelium*, and *Xyrauchen*. *Cyprinus* is the only outgroup taxon showing the presence of an epiotic process.

22. Intercalar (opisthotic; Smith, 1992: character 60): [0] present; [1] absent.

The intercalar is present in almost all extant catostomids, except *Hypentelium* and some *Moxostoma*. It is a medial bone located at the ventral corner of the skull where the pterotic and epiotic meet. *Cyprinus* has an intercalar, but it is exposed on the lateral surface of the skull.

23. Anterior parasphenoid (modified from Smith, 1992: character 33): [0] narrow, rod-like; [1] broad and flat; (2) vertically keeled.

In sampled catostomids, a broad and flat anterior portion of the parasphenoid is present in

Catostomus, *Ictiobus*, and *Xyrauchen*, whereas it is narrow and rod-like in *Chasmistes*, *Cycleptus*, *Erimyzon*, *Hypentelium*, *Moxostoma*, and *Myxocyprinus*. The anterior parasphenoid of *Carpiodes* is, exceptionally, compressed laterally.

24. Vertical extension of anterior basioccipital (basioccipital keel): [0] rod-like, keel absent; [1] keel present.

The basioccipital keel is present in *Carpiodes*, *Chasmistes*, *Erimyzon*, *Ictiobus*, and some species of *Catostomus*. The keel is uniquely bifurcated in the basioccipital of *Catostomus plebeius*.

25. Pharyngeal process of basioccipital (Smith, 1992: character 141): [0] absent; [1] present and solid; [2] fenestrated.

The solid basioccipital process in cyprinids is attached to the ovoid keratinized chewing pad that serve as an occlusion surface for the pharyngeal teeth. Whereas it is solid in all cyprinids, all catostomids have a fenestrated basioccipital process. The chewing pad of catostomids is lunate and located posteriorly on the surface of the palate organ (Doosey and Bart, 2011). The chewing pad is absent from species of loaches and gyrinocheilids (Doosey and Bart, 2011).

26. Posterior process of supraoccipital: [0] absent or slightly developed; [1] long and strongly keeled.

The supraoccipital is the posteriormost bone on the skull roof. Its posterior process, if present, is usually superior to the Weberian apparatus. In catostomids, the posterior process is strongly keeled and elongated near the neural complex in most genera. It is under-developed in species of *Catostomus*, *Moxostoma*, *Hypentelium*, and most Eocene species.

27. Otic foramina (Smith, 1992: character 1): [0] enlarged; [1] restricted; [2] absent.

The otic foramina (Smith, 1992, fig. 1d, 1e) is enlarged in *Carpiodes*, *Ictiobus*, *Xyrauchen*, and one species of *Moxostoma*, whereas it is restricted in the rest of the extant catostomids. Some of the enlarged otic foramina are caused by the fusion of the exit for the ninth cranial nerve with the otic foramina (Character 28). The foramina are absent in *Chromobotia macracanthus*.

28. IX cranial nerve exit (modified from Smith, 1992: character 131): [0] through prootic; [1] between exoccipital and prootic; [2] through exoccipital; [3] fused with otic foramina.

The fusion of the IX cranial nerve exit and the otic foramina is seen in *Carpiodes*, *Cycleptus*, *Ictiobus*, and *Xyrauchen*, whereas the IX cranial nerve exit is surrounded by the exoccipital and the prootic in *Catostomus*, *Chasmistes*, *Erimyzon*, *Moxostoma*, and *Myxocyprinus*. The intermediate condition, in which the IX nerve is enclosed by the exoccipital but not fused with the otic foramina is only observed in *Hypentelium*. In the examined cyprinid specimens, the IX cranial nerve exit merely through the prootic.

29. Subtemporal fossa (Smith; 1992: character 23): [0] deep, [1] shallow with exoccipital corner present in the fossa; [2] shallow with exoccipital excluded from the fossa; [3] absent.

 The outgroup *Cyprinus* has an extremely deep and large subtemporal fossa, whereas *Cobitis* has no subtemporal fossa observed. Extant catostomids and gyrinocheilids generally have a shallow subtemporal fossa, of which *Catostomus* has a relatively deep subtemporal fossa.

30. Posttemporal fossa (Smith, 1992: character 28): [0] absent; [1] restricted; [2] large.

The posttemporal fossa is located postero-laterally on the skull. It is present in catostomids and gyrinocheilids, but is not observed in cyprinids. It was suggested to be a symplesiomorphy of catostomids and gyrinocheilids (Wu et al., 1979). The posttemporal fossa is mainly composed of the pterotic opening and is surrounded by the pterotic, parietal, and epiotic. The size of the posttemporal fossa is positively correlated with the pterotic opening. The criterion to determine between the character states "restricted" and "large" is the comparison of the size of the posttemporal fossa to the pterotic ridge and parietal.

31. Supraorbital sensory canal and parietal: the supraorbital sensory canal [0] enclosed in the parietal and connect to the supratemporal sensory commissure through the parietal; [1] enclosed in the parietal, terminated before the supratemporal sensory commissure; [2] not associated with the parietal, supraorbital sensory canal joins the infraorbital sensory canal line in the otic region, enclosed in bones; [3] not associated with the parietal, supraorbital sensory canal joins the infraorbital sensory canal line in the otic region, detached.

The supraorbital sensory canal is enclosed in *Jianghanichthys* and some cyprinids (eg., *Cyprinus*). While it is uniquely joined to the supratemporal sensory commissure in *Jianghanichthys*, it generally terminates before the supratemporal sensory commissure in those cyprinids in which the supraorbital sensory canal is enclosed in the parietal. The supraorbital sensory canal is not associated with the parietal in gyrinocheilids and catostomids, where it is enclosed in bones in the former and detached in the latter.

32. Supratemporal sensory commissure: [0] enclosed in parietal, or parietal and supraoccipital; [1] enclosed by the posterior ridge of parietal; [2] not enclosed in bone, along the posterior ridge

of parietal.

In examined cyprinids, the supratemporal commissure is enclosed in the left and right parietal and crosses the skull posteriorly (Fig. 6.3H), whereas it is enclosed in both the parietal and supraoccipital in gyrinocheilids. The sensory canal may cause a little bump on the surface, but not develope into a distinctive ridge. In jianghanichthyids and catostomids, a posterior ridge crosses the parietal medio-laterally. The supratemporal sensory commissure is enclosed in the ridge in jianghanichthyids, whereas it runs along the ridge posteriorly in catostomids.

Infraorbital Series

33. Supraorbital (modified from Smith, 1992: character 10): [0] semi-circular or roughly triangular (Fig. 6.3 A, B, G); [1] crescent shape (Fig. 6.3H); [2] absent (Fig. 6.3 C–F, I).

The supraorbital is semi-circular or roughly triangular in *Carpiodes*, *Cycleptus*, *Ictiobus*, *Myxocyprinus*, and Eocene species (Fig. 6.4D), whereas it is absent in the rest of the catostomids. The outgroup *Cyprinus* has a slender and shallow supraorbital, resembling a new moon.

34. Number of infraorbitals (modified from Smith, 1992: character 64): [0] more than 4; [1] 4; [2] only lacrimal present.

The infraorbital bones of cypriniforms vary in number and shape. In catostomids, the lacrimal (infraorbital 1) is large, infraorbital 2 and sometimes infraorbital 3 are large and border the orbit ventrally, and the rest of the infraorbital(s) tends to be reduced. Because of significant reduction, four infraorbitals are observed in the majority of catostomids. Among the sampled taxa, IOB 4 in *Cycleptus*, *Ictiobus*, and *Myxocyprinus* appears segmented with a mild division; so more than 4 infraorbitals are counted for these taxa. In young individuals (cleared and stained specimens), the

reduced infraorbitals beyond infraorbital 3 are in general fused with the associated ossified sensory canal tube.

35. Shape of infraorbital 2–3 (modified from Smith, 1992: character 65): [0] heavy and deep; [1] thin and deep; [2] thin and slender; [3] string-like.

Catostomids, in general, have deep infraorbitals 2 and 3 (Fig. 6.4A, C, D). However, infraorbital 2 and 3 are reduced to a string-like appearance in *Cycleptus* (Fig. 6.4B). This character and Character 36 are inapplicable to *Cobitis* which doesn't possess infraorbital 2–3.

36. Shape of infraorbital 4 and beyond in adult fish: [0] deep or relatively deep; [1] string like.

This character is inapplicable to taxa in which the infraorbitals number less than four and juvenile specimens. Unlike the outgroup taxa, the infraorbitals posterior to the orbit are generally string like in catostomids (Fig. 6.4B). However, deep infraorbitals 4+ are observed in *Ictiobus* (Fig. 6.4A, C), *Myxocyprinus*, and *Moxostoma*.

37. Infraorbital sensory canal and infraorbitals 1–3: [0] enclosed in bone; [1] attached to the bone surface.

In catostomids, the infraorbital sensory canal is enclosed/fused in IOB 4 and beyond. In some others, the infraorbital sensory canal is attached superficially on infraorbital 1 through 3. It is enclosed in bones in the outgroups which have them, as well as in *Amyzon*.

Opercular Series

38. Preopercle (Smith, 1992: character 81): [0] slender, obtuse (Fig. 6.5A, B, and C); [1] intermediate (Fig. 6.5D, F, and G); [2] wide, triangular (Fig. 6.5E).

This character displays high intrageneric variation. All three states can be observed in one genus, for instance in that of *Catostomus*. It is relatively conserved in the genus *Moxostoma*.

39. Lower limb of preopercle (Smith, 1992: character 94): [0] long (Fig. 6.5E); [1] short (Fig. 6.5A, C, D, F, and G); [2] abbreviated (Fig. 6.5B).

In general, the preopercle of cypriniforms is curved at about the middle, which results in a vertical limb and lower (horizontal) limb. In some catostomids, such as *Myxocyprinus* and *Moxostoma*, the lower limb is significantly reduced and thus is considered abbreviated (Fig. 6.5B). When the lower limb of the preopercle is longer or equal to the vertical limb, the taxon is coded with long lower limb. Otherwise, it is coded is short. This character is conservative at the genus level except in *Catostomus*.

40. Preopercular sensory canal (modified from Smith, 1992: character 133): [0] enclosed in bone; [1] partially enclosed in the middle of the bone (Fig. 6.5C, F, and G); [2] attached tightly behind the preopercle ridge, may be partly bone-enclosed (Fig. 6.5D); [3] detached (Fig. 6.5A and E).

The preopercular sensory canal is well enclosed in cyprinids and "NewGenus", but varies in catostomids. It is partially enclosed in *Chasmistes*, *Cycleptus*, *Amyzon*, and *Jianghanichthys* where is is enclosed in the middle of the bone and exposed at both ends. In some catostomids, such as *Carpiodes*, *Ictiobus*, *Myxocyprinus*, and *Plesiomyxocyprinus*, the preopercle has a ridge at the midline creating a thicker antero-dorsal half and thinner postero-ventral half on the vertical and lower limb of the preopercle. In these fish, the sensory canal is attached tightly to the ridge. Species of *Amyzon* have the same ridge to accommodate the sensory canal; however, the sensory

canal is also more or less enclosed in bone and thus coded with state "1". In *Catostomus* and *Moxostoma*, the sensory canal floats above the bone.

41. Preopercular sensory canal and infraorbital sensory canal: [0] disjunct; [1] meet at orbital region; [2] meet at otic region.

The infraorbital sensory canal (*sensu lato*) consists of the infraorbital, otic, and maybe the temporal branches. The preopercular sensory canal connects to the infraorbital sensory canal at the orbit in catostomids and gyrinocheilids. In the rest of the sampled cypriniforms, these two sensory canals are either disjunct or connect in the otic region. An opercular sensory canal, extending across the anterodorsal corner of the opercle and connecting the preopercular sensory canal and the otic sensory canal, is not observed in and cyprinid, but is seen in the loach *Chromobotia macracanthus* (AMNH 56394-2)

42. Dorsal concavity of the opercle (modified from Smith, 1992: character 8): [0] no broad concavity behind opercular arm; [1] broad concavity at dorsal edge (Fig. 6.6A, B, D–I); [2] relatively short, strongly concave dorsal edge (Fig. 6.6C; Liu et al., 2015, fig 6A).

Catostomid opercles are characterized by a dorsal concavity created by the opercular arm and auricular process. A similar concavity may be seen in other fish, such as in *Jianghanichthys*, a few cyprinids, and a few characids; however, the combination of a sturdy opercular arm, a broad dorsal concavity, and unpointed auricular process has not been observed in any non-catostomid.

43. Opercular arm ("anterodorsal head of opercle" of Conway (2011)): [0] not well developed; [1] pointed and thin   (Liu et al., 2015, fig. 6A; Chapter 3 fig. 3-6A); [2] sturdy, flat and thick,

with strong striations (Fig. 6.6B, C, E–I); [3] rod-like, overall narrower than that of [2] and narrower in the middle (Fig. 6.6A, D).

The opercular arm of catostomids is the anterodorsal process of the opercle that is extraordinarily developed in length and robustness. In general it is not well developed in cyprinids, loaches, and gyrinocheilids. Within catostomids, the opercular arm is sturdy, flat, and thick with strong striations in that of *Carpiodes*, *Cycleptus*, *Ictiobus*, *Hypentelium*, *Myxocyprinus*, *Xyrauchen*, some *Moxostoma*, and a few *Catostomus*. The other type of opercular arm is slender, smoother on the surface, and constricted in the middle, which is seen in *Erimyzon*, *Chasmistes*, most *Catostomus*, and some *Moxostoma*. The opercular arm of "NewGenus" *brevipinne* is flat and thus coded as state [1]. However, it is shorter and thinner than the rest of the taxa that have the same character state.

44. Auricular process of opercle: [0] not developed; [1] simple rounded or angled corner (Fig. 6.6A, B, F–H); [2] extending dorsally, exceptionally developed (Fig. 6.6C–E, I).

Catostomids tend to have the auricular process of the opercle more or less developed. The developmental level of the auricular process varies within the genus, eg. *Catostomus*, *Ictiobus*, and *Moxostoma*.

45. External striation (peripheral) of the opercle (modified from Smith, 1992: character 9): [0] absent; [1] shallow and few (Fig. 6.6A, C–E, G–I); [2] deep and numerous (Fig. 6.6B, F).

Catostomids have few to numerous striations on the opercle. In some taxa, the striations are deep and strong, such as in *Carpiodes* and *Ictiobus*. In the rest of the catostomids, the striations are shallow, and may not appear all over the opercle, which results in a smooth surface of the opercle.

244

The striations may be increased in number or depth in older individuals.

46. Ventral corner of opercle angle formed by the anterior vertical margin and the ventral margin of opercle: [0] broad and shallow, angle > 60° (Fig. 6.6B, C, E, G); [1] intermediate, angle about 60° (Fig. 6.6A, D, F, H, I); [2] deep and narrow, angle < 60°.

Most catostomids have the ventral corner of the opercle forming an angle of about 60° except *Erimyzon*, *Ictiobus*, *Xyrauchen*, a few *Catostomus*, and a few *Moxostoma*. In cases where the anterior margin of the opercle is not straight, a line drawn through the opercular fossa and the anteroventral corner of the opercle was used as a proxy for measuring the angle. This character is equivalent to the complementary angle of the "angle of the inferior border" of Nelson (1949).

47. Outline of the anterior border of the opercle: [0] straight, not anteriorly concave; [1] anteriorly concave (Fig. 6.6F).

The anterior border of the opercle, excluding the flange contacting the hyomandibula, is usually straight and vertical. Only *Cycleptus*, *Hypentelium*, and *Ictiobus bubalus* are observed to have a strongly anteriorly concave margin. That of *Carpiodes cyprinus* and *Catostomus snyderi* is mildly concave and coded with "0" here.

48. The opercle height and width: [0] height ≤ width (Fig. 6.6E); [1] height > width (Fig. 6.6A); [2] height >> width (Fig. 6.6B).

The opercle height is measured as the vertical distance from the opercular fossa to the anteroventral corner of the opercle. The opercle width is the widest measurement of the opercle perpendicular to the opercle height. The general form of the opercle in catostomids is tall with the

opercle height moderately larger than the width. In extreme conditions, the opercle height is far larger than width, for example in *Catostomus wigginsi*, *Hypentelium nigricans*, *Moxostoma carinatum*, and *Moxostoma erythrurum*. In a few catostomids, e.g., *Deltistes luxatus*, *Catostomus tahoensis*, *Xyrauchen texanus*, and "NewGenus" *brevipinne*, the opercle is broad with the width sub-equal to or larger than the height.

49. Interopercle (modified Smith, 1992: character 17): [0] semi-lunate, anteroventral process longer and pointed; [1] semi-lunate, anteroventral and anterodorsal processes about equally developed; [2] slender semi-lunate; [3] slender angular.

This character changes states across the family members and is only conservative in the genus *Moxostoma* which has a slender angular shaped interopercle. The main difference between state [2] and the first two states is that the slender semi-lunate shape is much more elongated.

50. Subopercle: [0] broad; [1] slender.

The subopercle of catostomids is generally broad, resembling a shallow semi-circle with an anterodorsal process. It is slender, resembling an elongated rectangle, in *Moxostoma* and *Hypentelium*, and a few species of *Catostomus*.

Mandibular and Hyopalatine Arches

51. Kinethmoid: [0] absent or unossified; [1] overall rod shape, slightly compressed, elongate, longer than ascending process of premaxilla, one end rounded, the other end tapered (Fig. 6.7M); [2] laterally compressed, nearly straight, length about equal to half the height of maxilla or length of ascending process of premaxilla (Fig. 6.7A, B, K, L); [3] strongly

compressed, nearly straight, shorter than half the height of maxilla and length of ascending process of premaxilla (Fig. 6.7C, D); [4], strongly compressed, curved, shorter than half the height of maxilla and length of ascending process of premaxilla (Fig. 6.7E–J); [5] extremely compressed, curved, short, strong projection at middle; [6] complicated shapy, may present multiple projections.

The presence of the kinethmoid is the unique synapomorphy of Cypriniformes (Fink and Fink, 1981; Fink and Fink, 1996), yet the shape varies considerably across the members of the order (Staab et al., 2012a). In general, the kinethmoid of catostomids is roughly cylindrical or rod-like with the variations ranging as noted in character states [1] through [5]. The long, thin, high aspect ratio kinethmoid is also commonly found across cyprinids and some cobitids. Meanwhile, a more complicated shaped kinethmoid, for example complicated-shaped, thick, and/or laterally expanded, occurs in gyrinocheilids, some cyprinids, and the majority of loaches (Staab et al., 2012a). In catostomids, the relatively thin and slender kinethmoid is more or less laterally compressed in extant catostomids, whereas it is overall rod-shape in Eocene catostomids, such as *Amyzon aggregatum* (UALVP 31125) and *A. gosiutense* (FMNH PF 10574) although they display some intrageneric variations (Liu et al., 2016; Chapter 3). A projection at the middle of the kinethmoid is more or less developed, and separates the kinethmoid into two halves. The dorsal half is usually more compressed, whereas the ventral half is more rod-like.

52. Maxilla excluded from mouth gape: [0] no; [1] yes.
In catostomids, gyrinocheilids, and jianghanichthyids, the mouth gape is composed by the premaxilla, dentary, and maxilla. In cyprinids, the labial process of the premaxilla is elongated and curved, and the maxilla is excluded from the mouth gape.

53. Premaxilla (modified from Smith, 1992: character 138): [0]"L" shaped, labial process much longer than ascending process; [1] "L" shaped, labial process sub-equal to the ascending process (Fig. 6.8B, D, and F); [2] "L" shaped, labial process shorter than dorsal process (Fig. 6.8C, E, F); [3] triangular shape (Fig. 6.8A).

For those cypriniforms of which the maxilla is excluded from the mouth gape, the labial process of the premaxilla is much longer than the ascending process. Otherwise, the labial process is sub-equal to, or shorter than, the ascending process, e.g., in the catostomids (Fig. 6.8).

54. Dorsal end of ascending process of premaxilla: [0] slender, rod-shaped, may be slightly twisted (Fig. 6.8B and C); [1] flat (Fig. 6.8A and F); [2] rounded and robust with ridge (Fig. 6.8D and E).

The dorsal end of the ascending process of the premaxilla is used for attachment of the premaxilla-kinethmoid ligament which is directly involved in the kinematics of the kinethmoid for the protrusible jaw (Staab et al., 2012a). Because it is affected by the function, the shape and the size of the ascending process may vary among members of the same genus.

55. Corner of ascending process and labial process of premaxilla: [0] sharp right angle (Fig. 6.8A and B); [1] rounded (Fig. 6.8C through F).

This difference was noticed between the species of *Amyzon* (Liu et al., 2016; Chapter 3). The same type of premaxilla corner is repeatedly observed in the same species, and thus is a reliable trait. However, this character displays high intrageneric variations.

56. Premaxillary process of maxilla (Smith, 1992: character 62): [0] arises posteriorly on neck; [1] shifted to below head of bone; [2] directed anteriorly.

There are two processes at the dorsal end of the maxilla in catostomids and many other cypriniforms. The process projecting antero-medially reaches the premaxilla, and is thus called the premaxillary process. However, this process connects to the kinethmoid through a ligament (observed in *Catostomus catostomus* AMNH FF 55944). When an ambiguous condition is apparent, it is assigned state "0" when the end of the premaxillary process is at a point dorsal to its origination, otherwise it is coded "1". Since the coding criterion is consistent for this character, the large difference from the original coding by Smith (1992) is accepted.

57. Dorsal-posterior process of maxilla (Smith, 1992: character 26): [0] elongate posterior arm; [1] short posterior arm.

The posterior process at the dorsal end of the maxilla is usually larger and more robust than the premaxillary process. It is also in general larger and more robust in catostomids than that of the outgroup fishes. This process connects to the autopalatine through a ligament and the prepalatine(s).

58. Number of dorsal processes of maxilla: [0] two processes angled; [1] three processes angled.

In cypriniforms, the maxilla in general possesses two dorsal processes that are more or less developed. The only exception occurred in *Jianghanichthys*. Three dorsal processes were observed, of which only the posterior one (equivalent to the posterior process in Character 57) is enlarged and robust.

59. Maxilla neck: [0] absent; [1] present.

The maxilla neck is the shrink between maxilla dorsal end and the maxilla body the maxilla (neck of maxilla; Miller and Smith, 1967). All catostomids possess such a narrow neck except *Cycleptus*. The maxilla neck is attached with the *maxillaris dorsalis*, a large muscle, in *Catostomus* (Weisel, 1960).

60. Lateral ridge on the maxilla neck: [0] slightly projecting; [1] strong ridge with projection pointing posteriorly or laterally.

The lateral ridge on the maxilla neck is more or less present in catostomids. In the exceptionally well-developed condition, the ridge is flange like. This character is inapplicable to taxa in which the maxilla neck is not present. Most *Catostomus* have a low ridge on the maxilla neck, whereas it is larger and sturdier in the rest of the species.

61. Ventral process of maxilla (modified from Smith, 1992: character 82): [0] directed ventrally, rod-shaped or knob-like; [1] low curve; [2] intermediate, moderately curved; [3] strong anteroventral ridge for muscle attachment.

The ventral process of maxilla is either directed ventrally or curved forward. The surface is usually striated for muscle/ligament attachment. In *Carpiodes*, the ventral process is exceptionally enlarged and curved. The ventral process in that of gyrinocheilids is rod-like without enlargement at the ventral end.

62. Medial projection on ventral process of maxilla: [0] absent; [1] present.

A prominent projection on the medial side of the ventral process of the maxilla is present in the

majority of catostomids. In *Carpiodes*, *Ictiobus*, and *Myxocyprinus*, and outgroup *Cyprinus*, it is absent. In these taxa, instead of a medial projection, the ventral process is slightly thickened.

63. Protrusion on posterior margin of maxilla: [0] Margin straight; [1] margin rounded, no extra protrusion; [2] protruding ventrally; [3] protruding dorsally.

The main body of the maxilla is rounded posteriorly in *Carpiodes* and *Ictiobus*. In most of the rest of the catostomids the maxilla protrudes dorsally or ventrally at the posterior margin.

64. Dorsal end (head) of maxilla (modified from Smith, 1992: character 63): [0] rounded; [1] knob-like with slight projection/ridge; [2] expanded postero-dorsally with flange; [3] radiated three dorsal processes triradiated directly from the dorsal head.

The dorsal end, or head of maxilla (Miller and Smith, 1981), is rounded or knob-like right above the maxilla neck (Character 59), and may or may not be slightly ridged in catostomids except *Cycleptus*. The outgroup taxa that don't possess a maxilla neck, have a larger maxilla head with a flange-like expansion dorsally and posteriorly.

65. Gnathic ramus of dentary (modified from Smith, 1992: character 24): [0] long (Fig. 6.9 B, C); [1] moderate long (Fig. 6.9A, F); [2] short (Fig. 6.9D, E).

Catostomids are known to have shorter jaw when compared with cyprinids (Liu et al., 2015). A generally short gnathic ramus of the dentary in catostomids that composes the mouth gape mainly contributes to the so-called shorter mouth, as well to the sub-terminal or slightly inferior jaw. Within the catostomid family, the gnathic ramus length varies. The character states "long", "moderately long", and "short" are made by comparing to the width of the base of the coronoid

process (Character 70) that is located postero-dorsally on the dentary. When the length of the gnathic ramus is about equal to the width of the base of the coronoid process, it is coded as "moderately long". When the gnathic ramus is longer than the width of the base of the coronoid process, it is coded "long"; and when the gnathic ramus is shorter than the width of the base of the coronoid process, it is coded as "short". If the coronoid process is not developed, the gnathic ramus is determined to be long when it is more than half the width of the dentary.

66. Dentary mental foramen position (modified from Smith, 1992: character 137): [0] absent; [1] near to or on dorsal margin (Fig. 6.9D); [2] near Meckel's cartilage (Fig. 6.9C).

The dentary metal foramen in catostomids, when present, is usually displaced from the dorsal margin and is located near Meckel's cartilage in medial view. It is occasionally absent.

67. Dentary mental foramen direction of opening: [0] medio-lateral (Fig. 6.9B, C); [1] oblique, in between medio-lateral and anterior-posteriorly; [2] antero-posteriorly (Fig. 6.9D); [3] dorsal-ventrally.

When both medial and lateral/dorsal openings are present, the foramen may direct medio-laterally (most catostomids), dorso-ventrally (*Ictiobus*), obliquely (*Carpiodes*), or antero-posteriorly that results in a canal (*Chasmistes*, *Cycleptus* and some species of *Catostomus*). This character is inapplicable to taxa in which the mental foramen is absent.

68. Posteroventral process of dentary: [0] short (Fig. 6.9A, B, E); [1] moderate, longer than coronoid process if developed (Fig. 6.9D, F); [2] elongated (Fig. 6.9C).

The posteroventral process of the dentary in catostomids is generally larger than that of cyprinids.

Within catostomids, species of *Catostomus*, *Moxostoma*, and *Cycleptus* possess an exceptionally long posteroventral process. When the posteroventral process is about the same size or slightly larger than the gnathic ramus of the same dentary, the process is considered short.

69. Lateral ridge of dentary originating from anterior tip of gnathic ramus: [0] absent; [1] along gnathic ramus only (Fig. 6.9D, F); [2] extending to the middle of dentary (Fig. 6.9C, E); [3] extending far back nearly to the posterior end of dentary (Fig. 6.9A, B).

A lateral ridge of the dentary is present in most catostomids. It is close to the dorsal edge and probably directly contributes to the thick lip attachment of catostomids. In some species, for example *Catostomus platyrhynchus*, the ridge is flange-like and largely extended anteriorly and laterally. Another special example is that of *Cycleptus elongatus* in which the lateral ridge extends onto the elongated posteroventral process of the dentary (Character 68).

70. Coronoid process of dentary: [0] not developed (Fig. 6.9A, D); [1] moderately developed, crescent shaped (Fig. 6.9B); [2] well developed, semi-circlular shape (Fig. 6.9C, E, F).

The coronoid process, if developed, is the process located at the posterodorsal corner of the dentary. The base, aligning with the gnathic ramus, is considered to be the division of the process and the main body of the dentary when discussing the size of the process. It can be totally absent in catostomids, such as *Cycleptus*, *Hypentelium*, and *Myxocyprinus*.

71. Dorsal view of dentary symphysis: [0] extremely long, longer than the length of the gnathic ramus; [1] moderately long, sub-equal to the length of the gnathic ramus; [2] short; [3] very short.

The dentary symphysis is the symphyseal joint between left and right dentary at the anterior end of the gnathic ramus. The length of the symphysis in dorsal view indicates the size of the fish's bony mouth floor. Catostomids, in general, possess a long dentary symphysis and thus a mouth floor. There is thus more space for attaching thick lips that are correlated to the suction feeding of catostomids.

72. Dorsomedial process of the autopalatine (modified from Fink and Fink, 1981: character 21; Conway, 2011: character 36): [0] absent; [1] short, rudimentary; [2] long, well developed.

The dorsomedial process of the autopalatine extends from the body of the autopalatine and reaches towards the ethmoid complex, which gives the autopalatine a triradiate shape. It is well developed in catostomids and cyprinids, rudimentary in *Jianghanichthys*, and absent in the gyrinocheilids and sampled loaches.

73. Ethmoid process of autopalatine (Smith, 1992: character 157): [0] short; [1] long.

This is a medio-ventral process with a cup-like end hugging the preethmoid and anterolateral corner of the vomer from the ventrolateral side. It is generally long and broad in catostomids and cyprinids as compared to that of gyrinocheilids and loaches.

74. Mandibular sensory canals (modified from Smith, 1992: character 144): [0] enclosed in bones; [1] absent or detached from bones.

All catostomids have the mandibular sensory canal detached from the bone. It is enclosed in the dentary and may also be enclosed in the anguloarticular of cyprinids and jianghanichthyids, whereas it is not enclosed in bones in the examined gyrinocheilids and loaches.

75. Metapterygoid (Smith, 1992: character 6): [0] simple posterior lamina near hyomandibula; [1] lamina braces hyomandibula (Fig. 6.6F, G); [2] prominent lateral lamina and mesial struts brace hyomandibula; [3] as in state 2 with mesial ventral process bracing quadrate; [4] lateral strut braces hyomandibula.

The metapterygoid is a large laminate bone in catostomids and cyprinids tightly abutting the hyomandibula, whereas it is reduced in size and has less contact with the hyomandibula in loaches. Within catostomids, the contact between the metapterygoid and hyomandibula varies with modification of the metapterygoid to brace the hyomandibula.

76. Flat dorsal portion of quadrate: [0] simple diamond shape, anterior corner slightly projected (Fig. 6.6G); [1] diamond shape, anterior corner strongly projected extending past the articulation of quadrate and anguloarticular (Fig. 6.6F); [2] diamond shape with edges strongly curved; [3] rectangular; [4] fused with endopterygoid.

The quadrate is axe shaped with a roughly diamond to rectangle shaped flat dorsal portion and a horizontal strut ventrally (Fig. 6.6G). The edges of the diamond dorsal portion vary from straight to strongly curved. A projection at the anterior corner is usually present and enlarged in some species of catostomids.

77. Horizontal strut of quadrate: [0] rod shape, long and slender (Fig. 6.6G); [1] short and broad (Fig. 6.6F).

The horizontal strut is the ventral portion of the quadrate. It is short and broad in most catostomids. The criterion used here to determine between long and short horizontal struts is whether it extends

beyond the posterior corner of the dorsal portion of the quadrate. The posterior end of the strut is often overlapped by the preopercle.

78. Symplectic (Smith, 1992: character 7): [0] wedge-shape with simple contact to metapterygoid (Fig. 6.6F); [1] sutured into metapterygoid notch (Fig. 6.6G); [2] complex tripartite and sutured into metapterygoid.

The symplectic anteriorly fits in the slot between the dorsal portion and ventral strut of the quadrate. Posteriorly, it connects to the metapterygoid. This connection is simple in catostomids, such as in *Carpiodes*, *Ictiobus*, *Myxocyprinus*, and *Xyrauchen*. The outgroup show a simple contact and it may be merely below the metapterygoid, e.g., *Cyprinus*. In the rest of the catostomids, the symplectic is commonly sutured in a notch of the metapterygoid. In some species of *Catostomus* and *Hypentelium*, the symplectic has a complex tripartite shape and fits into the metapterygoid notch. The criterion for a notch-suture connection used here is that at least two edges of the symplectic are surrounded by the metapterygoid.

79. Hyomandibula, overall shape (modified from Smith, 1992: character 80): [0] broad, truncated; [1] intermediate; [2] slender (Fig. 6.6G, F).

The hyomandibula of catostomids is slender and curved resembling a slender "S" in overall shape. In the large sized cyprinids it is broader, less curved, and roughly triangular in shape. That of *Jianghanichthys* is slender resembling that of catostomids, but truncated and less curved which resembles that of cyprinids (Liu et al. 2015, Chapter 2).

80. Pterygoid notch of hyomandibula: [0] absent (Fig. 6.6F); [2] present (Fig. 6.6G).

Along the hyomandibular strut and below the dorsal condyle, a thin, flat laminar flange is present. A notch is present on the anterior flange of the hyomandibula opening towards the pterygoid series in species of *Erimyzon*, *Hypentelium*, and *Moxostoma*. This notch is absent in most catostomids, and cyprinids.

81. Dorsal condyles of hyomandibula (Smith, 1992: character 142): [0] anterior condyle elongate, articulates with sphenotic and pterosphenoid; [1] anterior condyle small, articulates only with sphenotic.

Two dorsal articulating condyles connect the hyomandibular to the neurocranium. The anterior condyle is smaller and articulates with only the sphenotic in all catostomids. In cyprinids, it articulates with both sphenotic and pterosphenoid.

82. Vertical strut of hyomandibula: [0] straight; [1] slightly convex posteriorly (Fig. 6.6F, G).

The vertical strut of the hyomandibula serves as a backbone of the hyomandibula extending from the bottom of the dorsal condyles to the ventral end. In catostomids, it is slightly convex posteriorly, which increases the curvature of the overall shape of the hyomandibula. It is straight in cyprinids and jianghanichthyids.

83. Hyomandibular and preopercular contact (modified from Smith, 1992: character 31): [0] slot on the posterior edge of hyomandibula (Fig. 6.6F); [1] slot and flange (Fig. 6.6G); [2] flange only.

The first type of contact between the hyomandibula and preopercle is that in which the the anterior edge of the preopercle dorsal limb simply fits into a slot on the posterior edge of the hyomandibula.

Cyprinids, jianghanichthyids, and some catostomids (e.g. *Carpiodes*, *Hypentelium*, and *Ictiobus*) have this type of contact. Most species of catostomids (*Catostomus*, *Cycleptus*, *Erimyzon*, *Moxostoma*, *Myxocyprinus*, and *Xyrauchen*) have both the hyomandibular slot as well as a flange-like extension covering the contact area. The slot is reduced in a few species of catostomid (*Chasmistes*).

84. Ceratohyal (Smith, 1992: character 21): [0] long with posteroventral process well developed; [1] medium, process well developed (Smith, 1992: fig. 2p, q and s); [2] short, process reduced or absent (Smith, 1992: fig. 2r and t).

The ceratohyal is generally well developed with a posteroventral process in most catostomids. It is elongate in *Catostomus*, *Chasmistes*, *Erimyzon*, *Ictiobus*, and *Xyrauchen*, and it is relatively shorter in *Hypentelium*, *Moxostoma*, and *Myxocyprinus*. The process is reduced or absent in *Cycleptus elongatus* and *Moxostoma poecilurum*, in which the ceratohyal itself is short.

85. Urohyal process for hypohyal ligaments and median lamina (Smith, 1992: character 4): [0] hypohyal processes adjacent at anterior end of robust median lamina (Smith, 1992: fig. 2c and d); [1] adjacent hypohyal processes at anterior end of a neck that tapers posteriorly into median and horizontal lamina (Smith, 1992: fig. 2a and b); [2] widely separated and robust hypohyal processes (Smith, 1992: fig. 2e, f, i, l, and m); [3] weak and widely separated hypohyal processes on transverse shield with long median lamina (Smith, 1992: fig. 2g, j and k); [4] processes separated and median lamina short (Smith, 1992: fig. 2h and n); [5] median lamina nearly abscent.

The urohyal is a median bone anterior and ventral to the rest of the hyoid bones. The shape of the

urohyal is complicated and highly varied across the species of catostomids (Smith, 1992: fig. 2). It consists of two perpendicular laminas, a median one and a horizontal one (Character 86), that vary in shape and size. Two anterior processes for the hypohyal ligament may be distinct or reduced, and may be adjacent or widely separated. The junction of the median and horizontal lamina forms a broad slot on each side for insertion of the powerful sternohyoideus muscles (Weisel, 1960).

86. Urohyal horizontal lamina (Smith, 1992: character 5): [0] slender anterior constriction; [1] moderate anterior constriction; [2] moderately long, broad, and tapered; [3] about as short as broad; [4] extremely broad, robust wings anteriorly placed; [5] horizontal lamina reduced to posterior flanges on corners of a vertical triangle; [6] horizontal lamina absent.

The shape of the urohyal horizontal lamina varies from slender to broad, from long to short, and from roughly triangular to oval, wing, and bar-shaped, and reduced in some taxa. Although the differences of the lamina ranges broadly within the family, it is relatively conservative for the members of the same species. The similarity between species and disparity among genera is also observed in Character 85, and thus the urohyal may play a critical role in species identification.

Branchial Arches

87. Hypobranchial 3 (Siebert, 1987: character 15; Conway, 2011: character 76): [0] present; [1] cartilage only.

Hypobranchial 3 is generally present in cypriniforms, except members of Catostomidae and Gyrinochelidae and a few species of Psilorhynchidae (Ramaswami, 1952; Siebert, 1987; Conway and Mayden, 2007). Cartilages positioned between the basibranchial and ceratobranchial of the third gill arch are observed in skeletons of catostomid fishes.

88. Gill rakers (Smith, 1992: character 25): [0] simple ridges with spines; [1] spines in clusters; [2] rakers forming secondary branches; [3] secondary branches dominate; [4] three-dimensional net of raker branches.

The specialized gill raker in certain catostomids was noticed and photographed by Smith (1992: fig. 5). Willink (2002) studied the variation of gill raker shape and size and its correlation with prey size. Characters regarding gill rakes (Character 88, 89, and 90) are adopted and coded following Smith (1992) that were also used in Willink (2002). Gill raker of most catostomids have simple ridges with spines. The spines are in clusters in *Hypentelium*, and some species of *Catostomus* and *Moxostoma*. Secondary branches of the gill rakers are developed in *Deltistes*, whereas the branches of gill rakers form net-like structures in *Chasmistes*.

89. Median branchial ridges on gill rakers (Smith, 1992: character 61): [0] broad; [1] narrow; [2] with accessory knobs; [3] bridged over by conjoint rakers.

The median branchial ridges on the gill rakers are generally narrow in catostomids (except *Myxocyprinus* and *Cycleptus*) in comparison to those of cyprinids and loaches. Specialized ridges that bridge over conjoint rakers are seen in *Ictiobus*, *Carpiodes*, and *Chasmistes*. Fossil taxa are coded with "?" for this and the next character.

90. Gill raker number (Smith, 1992: character 77): [0] 15–22; [1] 22–25; [1] 26–31; [3] 32–39; [4] 40–50.

Gill raker number is affected by the pharynx size, gill raker width, and gill raker interval. The gill raker width and interval are correlated with prey size (Willink, 2002), and seem more

constrained by the fishes' feeding habit and therefore should be less constrained by phylogeny. High variety of gill raker number is observed in the genus *Catostomus*. However, it is conservative in some genera, e.g. *Ictiobus*, *Carpiodes*, *Chasmistes*, *Erimyzon*, *Hypentelium*, and *Thoburnia*.

91. Pharyngeal teeth: [0] absent; [1] present in one row (Fig. 6.10); [2] present in more than one row.

In cypriniform fishes, although the gill raker teeth are absent, the pharyngeal teeth are ankylosed to the pharyngeal bone (greatly enlarged 5th ceratobranchial) and are extraordinarily well-developed (Fink and Fink, 1981). The only exception is that pharyngeal teeth are absent in gyrinocheilids. They are arguably absent in jianghanichthyids which have only rudimentary teeth-like structures in the pharyngeal area. Catostomids and loaches have the pharyngeal teeth in one row, whereas the teeth are aligned in one to three rows in cyprinids.

92. Number of pharyngeal teeth: [0] under 35 (Fig. 6.10A, B); [1] 36–100 (Fig. 6.10C, D, G); [2] over 100.

Pharyngeal teeth of catostomids become gradually smaller and tend to be more numerous from the anteroventral limb of the pharyngeal bone to the posterodorsal end. The intraspecific variation was assessed by (Eastman, 1977), but has never been fully documented. The counts for pharyngeal tooth number have also been grouped across species without a distinctive division between groups. The most distinctive group is that of the species of *Ictiobus* which have far more than 100 teeth and create quite a gap between them and the rest of the catostomids (which usually have fewer than 100 teeth), which was also observed by Eastman (1977). Another group consists of cyprinids and

261

few catostomids which have fewer than 35 teeth that are relatively large at least on the anteroventral limb of the pharyngeal bone. The rest of the catostomids have tooth counts within the range of 36‑100 which may vary in shape but cannot be put into smaller groups with a smaller tooth range without using arbitrary ranges. This character is inapplicable to taxa in which pharyngeal teeth are absent.

93. Shape of pharyngeal tooth crown: [0] height > width (Fig. 10 H); [1] about equal; [2] height < width .

Pharyngeal teeth of catostomids are laterally compressed. Their overall shape changes along the pharyngeal bone. In general, the first 1 to 4 teeth, counting from the anteroventral position, are large, robust, and relatively thick with grinding facets. Teeth on the posterodorsal third of the pharyngeal bone are tiny and lack the curved and pointed tip. Teeth in the middle portion of the pharyngeal bone are usually consistent in shape with the size gradually diminishing towards the dorsal end. This character applies to the teeth in the middle portion of the bone in which the crowns lack an enamel-like material on the surface.

94. Posterodorsal edentulous process (modified from Smith, 1992: character 98): [0] gradually narrowing to dorsal point (Fig. 6.10A–D); [1] dorsal knob (Eastman, 1977, fig. 12, 13) present; [2] no enlarged pharyngeal bone.

The pharyngeal dorsal knob is an extension and projection on the dorsal edentulous process (Fig. 6.10). In the sampled taxa, only the specimen of *Erimyzon* has a knobbed dorsal end of the pharyngeal bone. This is also described and illustrated in Eastman, （1977). Smith (1992) suggested that *Minytrema* had the dorsal knob as well.

95. Pharyngeal bone (modified from Smith, 1992: character 151): [0] low triangular cross-section, few teeth; [1] low triangular cross-section, many teeth (Fig. 6.10A, B); [2] high triangular cross-section, many teeth (Fig. 6.10C, D); [3] high, flat cross-section, extremely numerous teeth; [4] 5th ceratobranchial not significantly enlarged into pharyngeal bone.

The pharyngeal bone is modified from the fifth ceratobranchial in Cypriniformes except Gyrinochelidae and Jianghanichthyidae. The cross-section of the pharyngeal bone ranges from narrow and flat to broad and high. In general, the pharyngeal bone of catostomids is narrow and compressed in comparison to the complicated shape in that of cyprinids.

96. Anteroventral edentulous process of pharyngeal bone: [0] short (Fig. 6.10A, B); [1] long (Fig. 6.10C, D).

The left and right anteroventral processes of the pharyngeal bone are joined to each other. They connect to the basibranchial at the anterior end. They are generally short in catostomids except *Carpiodes*, *Xyrauchen*, and some species of *Catostomus* and *Moxostoma*.

97. Posterolateral surface of pharyngeal bone: [0] very narrow, ribbon-like (Fig. 6.10C, D); [1] broad ventrally, tapered toward the dorsal end (Fig. 6.10A, B); [2] nearly triangular.

The posterolateral side of the pharyngeal bone is opposite the dentigerous side. The width of the posterolateral side represents the thickness of the pharyngeal bone. The band-shape pharyngeal bone, observed in *Carpiodes*, *Ictiobus*, *Hypentelium*, and *Myxocyprinus*, resembles a regular ceratobranchial. The rest of the catostomids have a thicker pharyngeal bone than the above taxa. The posterolateral side of the pharyngeal bone in cyprinids is generally broad and roughly

triangular.

98. Fenestration on the posterolateral side of the pharyngeal bone: [0] porous (Fig. 6.10C and D);

   [1] pores moderately enlarged (Fig. 6.10A and B); [2] large pit for muscle attachment.

The posterolateral side of the pharyngeal bone is generally porous in catostomid fishes, while the

pores are moderately enlarged in *Catostomus*, *Cycleptus*, *Moxostoma*, *Chasmistes*, and *Xyrauchen*.

It is full of large pits in cyprinids and is thus called pitted side (Chu, 1935).

Shoulder and Pelvic Girdles, and Median and Paired fins

The number of principal dorsal fin rays in catostomids ranges from 10 to 57, whereas the number

of anal fin rays ranges from 7 to 11 except for *Myxocyprinus* with 11–13 and *Plesiomyxocyprinus*

with 18–19. The first principal dorsal and anal fin rays are preceeded by 2–5 procurrent rays,

which are unbranched and unsegmented. The first principal ray is segmented and unbranched. The

rest of the principal rays are branched. The last principal ray is usually doubled with two rays

supported by one pterygiophore.

The dorsal fin and anal fin are supported by pterygiophores. Whereas the first pterygiophore

supports all the procurrent rays, the second one supports only the first principal ray and this one to

one relationship continue for the remainder of the rays. The first pterygiophore is large, thick, and

medially broad, consisting of a broad median sheet of bone anteriorly and a spine-like posterior

part. The last pterygiophore is significantly smaller than the second to last, and has a trianguler or

quadrangular shape. The rest are spine-like and become gradually smaller anteroposteriorly. This

observation is consistent in Catostomidae.

99. Posttemporal (modified from Smith, 1992: character 148): [0] prominent; [1] reduced; [2] absent.

The posttemporal, positioned dorsal to and partly lying under the supracleithrum, connects the pectoral girdle to the neurocranium. It is a vertically slender and flat bone. In some catostomids, e.g., *Carpiodes*, *Cycleptus*, *Ictiobus*, *Myxocyprinus*, and few species of *Moxostoma*, the posttemporal is prominent, resembling that of cyprinids in size. This bone is reduced in the rest of the catostomids and absent in *Cobitis*.

100.   Anteromedial symphysis of cleithrum (Smith, 1992: character 152): [0] anterior to anterolateral margin; [1] sub-equal; [2] posterior.

This character is adopted from Smith (1992); however, it is coded quite differently from that of Smith (1992) except for the character status of *Ictiobus* and *Moxostoma*. Consistent with Smith (1992), the character state is identical among species of the same genus.

101.   Cleithrum-coracoid fenestra (Smith, 1992: character 153): [0] much larger than scapular fenestra; [1] reduced to size of scapular fenestra; [2] minute or absent.

The scapular fenestra in the middle of the scapular is of similar size across cypriniforms. The cleithrum-coracoid fenestra is relatively large, sub-equal, or small in catostomid fish in comparison to the scapular fenestra. The cleithrum-coracoid fenestra is large in *Carpiodes*, *Ictiobus*, *Cycleptus*, *Erimyzon*, *Myxocyprinus*, and *Xyrauchen*.

102.   Postcleithrum: [0] ventral ramus short, less than double length of dorsal ramus; [1]

ventral ramus long, nearly equal or more than double length of dorsal ramus; [2] ventral ramus long, dorsal ramus reduced.

The postcleithrum is attached posteriorly on the vertical ramus of the cleithrum. The dorsal ramus of the postcleithrum is sutured to the cleithrum, while the curved ventral ramus is free-floating in the muscle. The dorsal ramus is reduced in *Gyrinocheilus* and *Cobitis*.

103. Posterodorsal projection at ventral ramus of postcleithrum: [0] absent; [1] present.

The ventral ramus of the postcleithrum usually has a smoothly curved rod shape. In some species of *Catostomus* and *Chasmistes*, it develops projections at the convex part of the ventral ramus.

104. Number of pectoral radials (Sawada, 1982; character 36; Conway 2011, character 113): [0] four; [1] three.

Cypriniforms commonly possess four pectoral radials, which are small bones supporting the pectoral fin rays on the pectoral girdle. In fishes of the loach family Cobitidae and one species of Nemacheilidae (*Barbatula barbatula*), the fourth pectoral radial is reduced (Sawada, 1982).

105. Pelvic splint: [0] flat, laminated; [1] split into multiple forks

The pelvic bone of cypriniforms is generally bifurcated anteriorly into a rod-like lateral strut and a flat medial splint. The splint may be split into multiple secondary forks in some catostomids; these are all shallower than the main fork and become gradually shallower medially if more than one secondary fork is present. The pelvic bone of *Jianghanichthys* is frequently preserved; however, it is small and thin, and the specimens do not allow a good view of the pelvic splint and fork.

106.   The pelvic fork of pelvic bone: [0] fork shallow, PFL ≤ 1/3 PL [1] fork medium, around half the length of the pelvic bone; [2] fork deep, PFL ≥ PL.

The pelvic bone length (PL) is represented by the pelvic strut length, which is measured from the anterior tip of the strut to the posterior end of the pelvic bone excluding the ischial process. The pelvic fork length (PFL) is measured from the anterior point of the strut to the posteriormost point of the fork (Liu et al., 2016；Chapter 3). In catostomids, *Carpiodes* and *Myxocyprinus* posses a shallow pelvic fork, whereas *Moxostoma* has a deep pelvic fork. The rest of the species have either medium or deep forks. The variation of pelvic fork length is also observed in cyprinids.

107.   Pelvic splint and pelvic strut: [0] pelvic splint length (PSL) sub-equal to pelvic strut length (PL); [1] PSL < PL.

The pelvic splint length (PSL) is measured from the anterior-most point of the splint to the posterior end of the pelvic bone excluding the ischial process. The PSL is sub-equal to PL in *Carpiodes* and *Cycleptus*, whereas it is much shorter in the rest catostomids. Similar variation is also observed in cyprinids.

108.   Posterior projection of pelvic bone (ischial process): [0] posterior projection rod-like, and posteriorly pointed; [1] large, posterior projection triradiate or branched; [2] roughly rectangular or triangular, short and truncated, and barely any posterior pointed projection.

The ischial process of the pelvic bone is highly diversified in size and shape in catostomids. It is in simple rod-like shape in *Cyprinus* and *Myxocyprinus*, whereas it is usually small, truncated, and laminate in *Catostomus* and *Moxostoma*. The rest of the catostomids have a robust, triradiate, and pointed ischial process. In gyrinocheilid it is roughly triangular.

109.   Origin of anal fin: [0] behind dorsal fin; [1] before the end of dorsal fin.

The insertion of the anal fin is anterior to the point where the dorsal fin ends in *Carpiodes*, *Cycleptus*, *Ictiobus*, and *Myxocyprinus*. The rest of the extant catostomids have the anal fin completely posterior to the dorsal fin. The origin of the anal fin in *Amyzon aggregatum*, *A. gosiutense*, and *A. hunanense*, is nearly opposite the point where the dorsal fin ends. As a subtle difference, the anal fin is usually slightly anterior to the insertion of the dorsal fin in *Amyzon aggregatum* and *A. hunanense*; however, it is usually behind the dorsal fin insertion in *A. gosiutense*. This character is somewhat affected, but not completely determined by the number of dorsal fin rays..

110.   Number of principal dorsal fin rays (modified from Smith, 1992: character 99): [0] = ≤18;

   [1] 19–37; [2] 52–57.

The dorsal fin ray number in catostomids ranges from 10 (*Catostomus cahita*) to 57 (*Myxocyprinus asiaticus*). Most catostomid species have dorsal fin rays numbering fewer than 18, e.g., members of *Catostomus*, *Moxostoma*, *Erimyzon*, *Hypentelium*, *Chasmistes*, and *Deltistes*. Deeper bodied species belonging to *Ictiobus*, *Cycleptus*, and the fossil *Amyzon* possess 19 to 37 principal dorsal fin rays. The dorsal fin ray number is distinctively high in *Myxocyprinus* (52‑57).

111.   Number of principal anal fin rays: [0] ≤7; [1] 7; [2] 8–11; [3] ≥11.

Anal fin ray number of catostomids is more conservative than that of the dorsal fin. Most species have 7 principal anal fin rays, whereas *Ictiobus*, *Amyzon*, and a few species of *Moxostoma* have 8–

11 principal anal fin rays. Similar to the condition of the dorsal fin, the anal fin ray number is distinctively high in *Myxocyprinus* (12–14). Six principal anal fin rays are found in gyrincheilid specimens.

112.   Number of caudal fin rays (Smith, 1992: character 150): [0] 19; [1] 18.

In general, catostomids have 18 principal caudal fin rays, whereas cyprinids have 19. The basal cypriniform Jianghanichthyidae have 19.

Weberian Apparatus, Vertebral Column, and Caudal Skeleton

113.   Transverse process on centrum 1 (modified from Smith, 1992: character 12): [0] long; [1] small; [2] minute/absent.

The transverse process on the anteroposteriorly-compressed centrum 1 is usually minute it is as long as the 2nd transverse process in *Ictiobus*. In the condition of *Ictiobus*, together with the commonly seen transverse process 2, the Weberian apparatus has the appearance of "a pair of transverse processes" (Nelson, 1948). The intermediate length of the first transverse process is observed in *Myxocyprinus* and *Carpiodes*. This character is equivalent to character 104 of Conway (2011) with further investigation in that of catostomids.

114.   2nd pleural rib of Weberian apparatus (Smith, 1992: character 143): [0] descending process absent; [1] descending process present but unsutured to 4th rib; [2] descending process of 2nd and 4th rib broadly sutured together.

The 2nd pleural rib (descending process) of centrum 2 is sutured with pleural rib 4 and contributes to a robust and large rib 4 in catostomids. In cyprinids, the descending process is absent, and it is

present but not sutured with rib 4 in loaches (Bird and Hernandez, 2007). In contrast to the observation of Bird and Hernandez (2007), the descending process of centrum 2 is broadly sutured to rib 4 in grinocheilids. Also, rib 4 is not bifurcated at the ventral end in the examined material.

115.   Ridge on neural complex (Smith, 1992: character 14): [0] present (Fig. 6.11A, B); [1] absent (Fig. 6.11E, F).

The neural complex is developed from the cartilaginous supradorsals 3 and 4 fused with supraneurals 2 and 3 in Cypriniformes (Hoffmann and Britz, 2006). A vertical ridge, in the middle of the neural complex, is present in catostomid species of the genera *Carpiodes* and *Ictiobus*. Lateral ridges on the neural spine of gyrinocheilids are wing-shaped, large and massive. The neural complex in the Weberian apparatus of *Chromobotia macracanthus* is small and tightly sutured anteriorly to the cranium and posteriorly to neural spine 4.

116.   Anterodorsal profile of neural complex (modified from Smith, 1992: character 132): [0] round, or margin delicate, not well defined; [1] protruding anteriorly (Fig. 6.11D); [2] steep, or right angled with round corner (Fig. 6.11A, B, E); [3] slanting posteriorly (Fig. 6.11F).

The size and shape of the neural complex varies across genera of catostomids, and across species of *Catostomus*. It protrudes anteriorly in *Carpiodes*, *Ictiobus*, *Xyrauchen*, and some species of *Catostomus*. The dorsal margin and anterior margin are nearly perpendicular with a rounded corner in *Chasmistes*, *Cycleptus*, *Erimyzon*, *Hypentelium*, *Myxocyprinus*, and some species of *Catostomus* among extant catostomids. In "NewGenus", *Plesiomyxocyprinus*, and *Amyzon*, the

dorsal margin is oval shaped. The reclining anterodorsal profile is only observed in *Moxostoma*. A zigzag shaped anterodorsal profile in *Catostomus macrocheilus* is coded with state [1].

In some catostomids, adjacent structures are modified to resemble the neural complex and probably contribute to the function of the neural complex. The fifth neural spine of *Erimyzon* is laterally compressed and enlarged (Fig. 6.11E). In *Xyrauchen*, the four supraneurals positioned between each pair of neural arches of centrum 5 through 8 are heavily ossified and enlarged into plates and connected to the neural complex (Fig. 6.11D).

117.   Posterodorsal profile of neural complex: [0] round, or margin delicate, not well defined; [1] steep, or rounded (Fig. 6.11D); [2] moderately angled at about 45° (Fig. 6.11A, B, G); [3] acute angled (Fig. 6.11E).

The neural complex of *Erimyzon*, *Chasmistes*, and most species of *Catostomus* is extending far back with the posterodorsal corner forming an acute angle. It is moderately angled in *Cycleptus*, *Moxostoma*, *Hypentelium*, and *Myxocyprinus*, whereas it is steep in *Carpiodes Xyrauchen*, and the majority of species of *Ictiobus*. Species of "NewGenus" and *Amyzon* possess a rounded posterodorsal profile, whereas that of *Plesiomyxocyprinus* is moderately angled.

118.   Transverse plate of Weberian apparatus: [0] absent; [1] partial; [2] present (Fig. 6.11C).

The ventral transverse plate, positioned between the left and right rib 4 and anterior to the os suspensorium, is a unique synapomorphy of catostomid fish (Bird and Hernandez, 2007). This feature was described and considered to be a difference that separates cyprinids and catostomids (Nelson, 1948), but has received little attention since then. Gyrinocheilids possess a similar

structure formed by expanding rib 4 laterally.

119.   Os suspensorium: [0] arises from the ventral surface of the 4th centrum; [1] projects

medially from 4th pleural rib (Nelson 1948).

The Os suspensorium is known as a "miniature transverse plate" in catostomids that have the

massive transverse plate (Nelson, 1948). It is generally derived from rib 4 in catostomids, whereas

in other species it usually arises separately from rib 4, coming from the ventral surface of centrum

4 (Nelson, 1948). Cyprinidae has character state 0, whereas Catostomidae has state 1.

120.   Intervertebral space of centrum 2 and 3: [0] prominent; [1] obliterated.

The prominent 2nd–3rd intervertebral space was suggested to be one of the critical characters of

the Weberian apparatus (Nelson, 1948). In fact, the fusion of centrum 2 and 3 (intervertebral

space obliterated) is observed in certain species of cyprinids and catostomids (Nelson, 1948; Chen,

1993). However, it is not always possible to observe because of the modification of the

zygapophysis and neural arch around centrum 2 and 3. To avoid damage to the specimen, the use

of X-ray ct-scanning (Nelson, 1948) or other new technologies are required. In catostomids, the

intervertebral space of centrum 2 and 3 is clearly present in *Myxocyprinus*, *Cycleptus*, *Thoburnia*,

Hypentelium, and *Moxostoma*; whereas it is obliterated in *Minytrema*, *Erimyzon*, *Chasmistes*,

Xyrauchen, *Ictiobus*, and *Carpiodes* (Nelson, 1948; Chen, 1993). The presence is varied among

species of *Catostomus* and yet to be systematically studied.

121.   Length of neural spine 4: [0] long, as high as the neural complex (Fig. 6.11A, B, E); [1]

short, around half height of the neural complex; [2] reduced, minute (Fig. 6.11D, F).

The fourth neural spine in *Carpiodes*, *Cycleptus*, *Ictiobus*, and *Myxocyprinus* is long with the dorsal tip reaching or nearly reaching the dorsal margin of the neural complex. In species of *Catostomus* and *Erimyzon*, and some species of *Moxostoma*, neural spine 4 is significantly reduced. The length of neural spine 4 in *Catostomus* corresponds to the shape of the neural complex that is strongly slanted posteriorly. The fourth neural spine in gyrinocheilids is not as tall as the neural complex, but is also laterally compressed and antero-posteriorly expanded. The fourth neural spine is about the same height as the neural complex in *Jianghanichthys*. However, the neural complex of *Jianghanichthys* is small, so that neural spine 4 is only half the length of the regular neural spine that articulates to a non-Weberian vertebra.

122.   Neural arches and spines 4 and 5 (modified from Smith, 1992: character 11): [0] only neural arches and spine 4 form part of Weberian apparatus; [1] neural arches 5 with zygapophysis to neural arch 4 and maybe neural complex; [2] neural arches and spine 5 significantly articulated to neural arch 4 and maybe to neural complex.

In most catostomids, neural arch and spine 5 contributes to the Weberian apparatus by a supportive zygapophysis. In several genera of catostomids, e.g., *Erimyzon*, *Hypentelium*, and *Xyrauchen*, neural spine 5 is antero-posteriorly expanded and contacts the neural complex. In sampled cyprinids, neural arch 5 is clearly separate from the Weberian apparatus.

123.   Length and thickness of 4th pleural rib: [0] short and thin; [1] short, thick, slightly less or sub-equal to half the length of rib 5 (Fig. 6.11B); [2] long and robust, more than half the length of rib 5 (Fig. 6.11A, C, D, E, F).

The thick, sturdy, and robust rib 4 formed from the fusion of the vertebral processes of vertebrate

2 and 4 is a unique feature of catostomids. It is extraordinarily long in that of *Carpiodes*, *Ictiobus*, and *Myxocyprinus*. In the rest of the catostomids, including the Eocene species, it is slightly shorter at about half the length of rib 5 (the first regular rib behind the Weberian apparatus).

124.   Direction of rib 4 in lateral view: [0] slanting anteriorly; [1] extends straight downward (Fig. 6.11B, E); [2] slanting posteriorly (Fig. 6.11A, D, F).

In cypriniform fishes, rib 4 that is modified for the Weberian apparatus generally extends anteroventrally, whereas the regular ribs extend posteroventrally (Bird and Hernandez, 2007). This condition has been seen in *Catostomus* and *Chasmistes* among catostomids. In the rest of the catostomids, rib 4 either extends straight downward (*Carpiodes*, *Ictiobus*, *Myxocyprinus*, *Erimyzon*, "NewGenus", and most *Amyzon*), or slants posteroventrally (*Cycleptus*, *Hypentelium*, *Moxostoma*, and *Xyrauchen*).The fourth rib of *Amyzon gosiutense* slants posteriorly (Fig. 6.11G).

125.   The left and right fourth rib: [0] more or less parallel to each other; [1] diverge laterally forming an angle with the 4th centrum as its apex.

The left and right rib 4 are nearly parallel to each other in *Carpiodes*, *Erimyzon*, and *Ictiobus*, whereas in the the rest they diverge.

126.   Lateral surface of rib 4: [0] nearly smooth, may be pitted, no deep groove (Fig. 6.11A, F, G); [1] a deep vertical groove in the middle (Fig. 6.11B, D, E).

A deep vertical groove extends nearly from the dorsal root to the ventral end of the rib in *Carpiodes*, *Erimyzon*, *Ictiobus*, *Myxocyprinus*, *Xyrauchen*, and some species of *Moxostoma*. Most

species of Eocene catostomids except *A. gosiutense* have the deep groove as well. The fourth rib of *Amyzon gosiutense* is exceptionally short and thick without the lateral deep groove (Fig. 6.11G).

127.   Anterior surface of the transverse plate: [0] undulating; [1] nearly even, but porous.

An undulating and a porous surface are probably two different strategies for muscle or tissue attachment. The former condition has been seen in *Carpiodes*, *Erimyzon*, *Ictiobus*, *Myxocyprinus*, *Xyrauchen*, and the majority of species of *Moxostoma*, whereas the latter condition is observed in *Catostomus*, *Chasmistes*, and *Cycleptus*. This character is inapplicable to non-catostomids in which the transverse plate is absent.

128.   Hypural 3: [0] tightly attached to compound centrum (Fig. 6.12B, C); [1] fused to compound centrum (Fig. 6.12A, D, E).

In addition to the general fusion of hypural 2 (hyp2) with the compound centrum in cypriniforms, hypural 3 (hyp3) is also fused to the compound centrum in catostomids. Among extant catostomids, hyp3 is extensively fused to the compound centrum in *Minytrema* and *Erimyzon* (Liu et al., 2016; Chapter 3), and sampled specimens of *Myxocyprinus*, *Ictiobus*, *Carpiodes*, *Cycleptus* (occasionally not fused), and *Xyrauchen*. Among fossil species, *Amyzon kishenehnicum* and *Plesiomyxocyprinus arratiae* have hyp3 fused to the compound centrum. The hyp3 of *Amyzon aggregatum* is occasionally fused to the compound centrum. Since the majority of specimens have hyp3 fused to the compound centrum, this character is coded with "0" for *Amyzon aggregatum*.

129.   Hypural 6 (Smith, 1992: character 16): [0] present (Fig. 6.12A, C–E); [1] absent (Fig. 6.12B).

Catostomid fish commonly have 6 hypurals, although hypural 6 may be tiny in some taxa. It is only found to be absent in *Erimyzon*, which is inconsistent with the observation of Eastman (1980). Hypural 6 is present in Eocene catostomids. It is occasionally missing in *Amyzon aggregatum* and that is treated as intraspecific variation.

130.   Number of post-Weberian vertebrae (modified from Smith, 1992: character 97): [0] 28–37; [1] 37–44.

Similar to the condition of pharyngeal teeth number, the variation of vertebral number across species of the family Catostomidae is continuous and lacking distinctive divisions at the generic or even tribe level. However, within this large range, some species possess fewer vertebrae, whereas some others possess more. To minimize the artificial effects but still take the difference of vertebral number into account for the phylogenetic signal, two vertebral number ranges are used here to represent more and fewer vertebrae. In cases where more specimens were available and showed intraspecific variation across the boundary of the two states, the average vertebral number for the species is used, for example for that of *Amyzon aggregatum*.

Body form and scales.

131.   Scales: [0] large; [1] small; [2] tiny, embedded in skin.

The size of scales is evaluated based on scales from the mid-body below the dorsal fin and around the lateral line. Ambiguous samples were coded in reference to the number of lateral line scales, of which fewer than 60 lateral lines scales are conventionally treated as "larger scale". Species of *Ictiobus*, *Carpiodes*, *Cycleptus*, *Hypentelium*, *Minytrema* (not sampled for the phylogenetic analysis), *Myxocyprinus*, and Eocene genera *Amyzon* and *Plesiomyxocyprinus* possess larger

scales, whereas the rest of the catostomid species generally have relatively small scales. The outgroups *Jianghanichthys* and *Cyprinus* have larger scales, whereas scales of *Gyrinocheilus* are relatively small. Sampled loaches have tiny scales that are usually embedded in the skin.

132.　　Maximum body size: [0] total length (TL) < 300 mm; [1] 300 < TL < 800 mm; [2] TL over 1000 mm

Most catostomids are fast growing, large-sized, and long-lived. The maximum total length has been recorded as over 1000 mm in *Deltistes* (Moyle, 2002) and *Myxocyprinus* (Wu et al., 1990). On the other hand, miniature catostomids, species of *Thoburnia* (Raney and Lachner, 1946), are also important members of Catostomidae. Western species of *Catostomus* with limited geographic ranges are also small-sized with short lifespans, e.g., *C. platyrhynchus*, *C. plebeius*, *C. microps*, *C. santaanae*, and *C. wigginsi* (Harris et al., 2014). The majority of those small sized *Catostomus* species have been suggested to belong to a subgenus *Pantosteus* (Smith, 1966). This character is coded according to Harris et al. (2014) and Jacquemin and Doll (2015).

133.　　Body form (modified from Smith, 1992: character 127): [0] deep; [1] moderate; [2] slender.

The body form of catostomids usually changes through ontogeny. For example, *Myxocyprinus* are deep-bodied and roughly triangular as juveniles, and then deep and elongate in adults. Species of *Amyzon* are fusiform as juveniles, and deep-bodied as adults. This character refers to the adult body form, which is conservative within species of the same genus or even subfamily. In extant catostomids, species of *Carpiodes*, *Ictiobus*, and *Myxocyprinus* are deep-bodied, whereas those of

Catostomus, *Hypentelium*, and *Moxostoma* are slender. The body form of the rest of the sampled extant catostomids is moderately deep. Paleogene fossil catostomids are all deep-bodied except "NewGenus" *brevipinne*.

134.   Ratio of head length to standard length (modified from Smith, 1992: character 71): [0] equal or over 0.24; [1] lower than 0.24.

The ratio of head length to standard length represents the size of fish's head relative to its body size. This is another continuous trait with considerable intraspecific variation. The range divided at any number cannot be perfect. The ratio 0.24 works in the current sample pool, as well as being consistent with one of the divisions in Smith (1992). According to the criterion of this character, species of *Erimyzon*, *Hypentelium*, *Ictiobus*, *Myxocyprinus*, *Xyrauchen*, and the Eocene *Amyzon* have relatively large heads.

Results

All parsimony phylogenetic analyses using 43 taxa and 134 osteological characters resulted in four equally most parsimonious cladograms. Each of them has 834 steps with a consistency index (CI) of 0.32 and retention index (RI) of 0.58. The strict consensus cladogram (Fig. 6.13) supports the four-subfamily classification of extant catostomids, of which Myxocyprininae is sister to the clade of Cycleptinae plus Catostominae, and together they are sister to Ictiobinae. The tribes Catostomini and Moxostomini are also recognized, but with the position of *Hypentelium* being sister to these two tribes. For Eocene taxa, it shows that species of *Amyzon* and "NewGenus" are

stem taxa of the catostomid family, whereas *Plesiomyxocyprinus* falls into the crown group and is sister to the clade of Myxocyprininae (Cycleptinae + Catostominae). While *A. aggregatum*, *A. gosiutense*, and *A. kishenehnicum* comprise a monophyletic group, *A. hunanense*, *A. commune*, and "NewGenus" *brevipinne* form basal lineages each by itself with considerable support from decay indices and bremer support value (Fig. 6.13).

The explorative phylogenetic analysis using Bayesian inferences of the same data matrix does not support the topology of Eocene taxa found in the parsimony cladogram. However, relationships among higher ranks of extant catostomids are supported, of which Ictiobinae, Cycleptinae, and Catostominae are distinctive groups. Noteworthy is that *Hypentelium* is grouped within Moxostomini, which is also supported by bootstrap resampling (Fig. 6.14).

Discussion: Phylogeny of Catostomidae

Systematic Position and Intrarelationships of *Amyzon*, and Plesiomorphic Characters of Eocene Catostomids

Amyzon was depicted to be a stem catostomid close to Ictiobinae (Miller, 1959), then hypothesized to be extinct members of the subfamily Ictiobinae in the phylogenetic study of Smith (1992). Drawing on the character list of Smith (1992), Liu et al. (2016; Chapter 3) replaced the ingroup taxon "*Amyzon*" of Smith (1992) with individual coding of the species *Amyzon aggregatum*, *A. gosiutense*, and *A. kishenehnicum* and added the stem cypriniform *Jianghanichthys* to the outgroup, and added the Asian catostomid *Plesiomyxocyprinus*. Parsimony analysis of Liu et al. (2016) suggested that *Amyzon* is the most basal clade of Catostomidae, and *A.*

aggregatum, *A. gosiutense*, and *A. kishenehnicum* comprised a monophyletic group.

The phylogenetic analysis of this study uses extant taxa that represent the major clades of Cypriniformes and the stem cypriniform *Jianghanichthys* as an outgroup. For the ingroup, in addition to a large number of extant catostomids, Eocene catostomids with specimens that could be coded for the characters are exhaustively sampled including "NewGenus" *brevipinne*, *A. commune*, and the Asian *A. hunanense* plus those Eocene species analyzed in (Liu et al., 2016; Chapter 3). Drawing on a larger collection and more Eocene species with a large osteological character list, this study finds that *A. aggregatum*, *A. gosiutense*, and *A. kishenehnicum* comprised a monophyletic group resembling the results of Liu et al. (2016; Chapter 3). "NewGenus", which was separated from *Amyzon* in Chapter 4, undoubtedly belongs as a separate lineage by itself with high support (Fig. 6.13). However, another two species of *Amyzon*, *A. commune* and the Asian *A. hunanense*, are also not grouped with the other three species.

Appendix 6.2 shows a summary of synapomorphies of the major clades from all four most parsimonious trees that are mapped onto the strict consensus tree; characters that contribute to the current topology of *Amyzon* and related species are displayed. The following discussion is based on the character list with most emphasis on the comparison of species of *Amyzon* (*sensu lato*, all species of *Amyzon*). The monophyletic clade of *A. aggregatum*, *A. gosiutense*, and *A. kishenehnicum* hereafter is used as *Amyzon* (*sensu stricto*). Osteological characters that also appear in the Character Description are denoted in brackets (Ch. = character, followed by the character description number).

A. commune has been believed to be a valid species of *Amyzon* since it was described (Cope, 1875; Bruner, 1991; Liu et al., 2016). New and better-preserved specimens (FMNH PF 116, 117) reveal more osteological features that account for its new systematic position in this study. Noticeably, *A. commune* differs from *Amyzon* (*sensu stricto*) and *A. hunanense* in several osteological characters. First, *A. commune* possess more dorsal fin rays (31–33) than all species of *Amyzon* (18–27; including Asian species). Second, the pterotic region of *A. commune* is different from that of *Amyzon* (*sensu stricto*). The pterotic ridge is intermediately broad without any flanges observed in the former, rather than broad and possessing two flanges in that of *Amyzon* (*sensu stricto*; Ch. 18, 19). Also, the pterotic fossa is more dorsally placed relative to the position of the epiotic in *A. commune* (Ch. 20). Third, in the opercular region of *A. commune*, the outer surface of the opercle is smooth, barely carrying any peripheral sriations and the subopercle is slender (Ch. 45, 50) compared to that of *Amyzon* (*sensu stricto*). Fourth, in the jaw bones, the gnathic ramus and posteroventral process of the dentary are relatively short in *A. commune*, but the dentary symphysis in dorsal view is relatively broader compared to that of *Amyzon* (*sensu stricto*).

A. hunanense was originally described as a cyprinid (Cheng, 1962; Chang et al., 2001). Similar to the situation of *A. commune*, it is an *Amyzon*-like catostomid in general appearance; however, it may not be a species of *Amyzon* in a strict sense. First, the frontal differs from that of *Amyzon* (*sensu stricto*) in the supraorbital process of the frontal reaching the orbit, and the ethmo-frontal fontanelle located in the middle of the ethmoid and frontal (Ch. 9, 14). Second, the anterior parasphenoid is vertically keeled, unlike any Eocene catostomid from North America (Ch. 23). Third, in the opercular region of *A. hunanense*, the preopercle is wide rather than intermediate in depth, the opercular arm is rod like rather than flat and thick, and the ventral corner of the opercle

is broad and shallow in comparison with that of *Amyzon* (*sensu stricto*; Ch, 38, 45, 46). The fourth region that differs from that of *Amyzon* (*sensu stricto*) is the jaw region. The ventral process of the maxilla is directed ventrally, the posterior margin of the maxilla is rounded without a protrusion, and the gnathic ramus of the dentary is relatively long.

If comparing both *A. hunanense* and *A. commune* with the rest of the species of *Amyzon*, certain characters of these two species bracket morphological variation in the rest of *Amyzon*. For instance, there are 18 to 21 principal dorsal fin rays in *A. hunanense*, 31 to 33 in *A. commune*, and 21 to 27 (Liu et al., 2016, table 1; Chapter 3, table 3-1) in the rest of the *Amyzon* species. As evident from the summarized phylogenetic support and morphological difference, *A. commune* and *A. hunanense* may or may not belong to the genus *Amyzon*.

Whether *A. commune* and *A. hunanense* are *Amyzon* or not, together with all the rest of the Eocene catostomids they have revealed plesiomorphies of stem catostomids that shorten the branch length of the phylogeny. Three key anatomical features can be used to reconstruct ancestral states of catostomids. First, the kinethmoid of Eocene catostomids is generally slender, with a high aspect ratio, and rod-like, as is represented by *Amyzon aggregatum* (UALVP 31125) and *A. gosiutense* (FMNH PF 10574). Second, pharyngeal teeth number about 20 in "NewGenus" and 35 to 60 (Liu et al., 2016; Chapter 3) in *Amyzon* and *Plesiomyxocyprinus,* which are all on the low side of extant catostomid pharyngeal tooth numbers. Third, the Weberian apparatus differs from that of extant catostomids in the combination of a neural complex with an oval shape, rib 4 moderately long and about half the length of the first regular ribs, lateral groove present on rib 4 (except that of *A. gosiutense*), neural spine 4 long and sub-equal to the length of regular neural spine. These

features would all likely represent the ancestral state for Catostomidae.

Subfamilies of Catostomidae

Recent phylogenetic studies either support the three-subfamily (Smith, 1992; Chen and Mayden, 2012) or four-subfamily classification (Harris and Mayden, 2001; Doosey et al., 2010; Liu et al., 2016; Chapter 3) for extant catostomids. The major difference between these two classifications depends on whether *Myxocyprinus* and *Cycleptus* are sister groups or not.   Based on osteological characters, none of the phylogenetic analyses in this study recovered the sister-group relationship of *Cycleptus* and *Myxocyprinus* (Fig. 6.13).

Among extant catostomids, both inter- and intra- relationships of the four subfamilies are well resolved in this study (Fig. 6.13). Two major tribes, Catostomini and Moxostomini in Catostominae are relatively well-resolved with the systematic position of *Hypentelium* uncertain across different analyses (Fig. 6.14). The separation of *Hypentelium* from the other members of Catostominae is not strongly supported by bremer values and decay indices (Fig. 6.13). Also, *Hypentelium* is usually resolved as a member of basal clade of Moxostomini (Harris and Mayden, 2001; Harris et al., 2002; Doosey et al., 2010; Chen and Mayden, 2012), as suggested in the bootstrap consensus tree of this study (Fig. 6.14). Instead of being removed from Moxostomini, this study suggests that *Hypentelium* may preserve more plesiomorphic characters than previously thought and needs further morphological attention.

Of the Eocene catostomids, *Amyzon* was hypothesized to be a member of Ictiobinae (Smith, 1992),

and later suggested to be a basal clade of Catostomidae (Liu et al., 2016; Chapter 3). This study found the species of *Amyzon* that were sampled by Liu et al. (2016; Chapter 3) to be monophyletic as well. However, the systematic positions of additional Eocene species in this study disrupt the monophyly of *Amyzon* by having some species excluded from the clade. Also, *Plesiomyxocyprinus* is consistently resolved as the sister to all extant catostomids except Ictiobinae. These results suggest that Eocene catostomids may not belong to any extant catostomid subfamily.

Paleogeography of Catostomids: Evolution and Elimination

Catostomid fossil records from North America and Asia, which are reviewed in Chapter 4 and 5, clearly show that these were abundant freshwater fishes on both continents during the early Eocene. The taxonomic clarification, description of new materials, and the phylogenetic analysis presented here suggest that the diversification of catostomids was greater than previously thought. The paraphyletic *Amyzon* indicates that taxonomic diversity above the species level was probably even higher than previously known. This period of time of unprecedented diversity coincides with the Early Eocene Climate Optimum (EECO) and Mid-Eocene Climate Optimum (MECO; Zachos et al., 2001; Zachos et al., 2008).

After the Eocene, catostomids declined in Asia with only a few known occurrences of disarticulated bones (Chapter 5). Meanwhile, catostomids became common freshwater fishes in the late Cenozoic of North America. However, catostomids lose their dominant position in the freshwater ecosystems of North America, as cyprinids that had not been present in the Eocene are more diversified and abundant in later Cenozoic sediments (Smith, 1981) and currently (Warren

and Burr, 2014). This dramatic paleogeographic change coincided with the early Oligocene cooling event (Zachos et al., 2001; Zachos et al., 2008) and a regional extinction and faunal turnover (Meng and McKenna, 1998; Woodburne et al., 2009; Costa et al., 2011).

When Eocene cypriniforms were still sparsely reported, Darlington (1957) had hypothesized that catostomids dispersed from Asia to North America through the Bering Land Bridge (Beringia) at "about the beginning of the Tertiary" (Darlington, 1957; p.101). Later, Chang et al. (2001) suggested an Eocene vicariant event contributed to the paleogeographic and current disjunct distribution pattern of catostomids. The vicariance model was based on the first skeleton-based fossil catostomid record in Asia and the phylogenetic hypothesis of Smith (1992). While these hypotheses were accurate from a certain perspective, our understanding of catostomid fossils and phylogeny have moved forwards and with new information and this may impact paleogeographic hypotheses.

More taxonomic diversity of catostomids from both continents has been brought to light recently (Liu and Chang, 2009; Liu et al., 2016; Chapter 4 and 5). Unlike the scheme of relationships that was the basis of the vicariant model above, the phylogenetic analysis of this study suggests that, Eocene species (except *Plesiomyxocyprinus*) are stem lineages, and *Amyzon* is paraphyletic. *Plesiomyxocyprinus* was hypothesized to be a basal clade of non-ictiobinine catostomids. If this hypothesis is true, major clades of extant catostomids, i.e., at the subfamily level, must have diverged before the middle Eocene. This also indicates that a dispersal event for Eocene catostomids should have happened at least twice, which supports multiple continental connections through Beringia during the middle to early Eocene. To further understand the taxonomic

communication through Beringia during the Paleogene, sediments of Central to Northeast Asia (i.e., North to Northeast China, Mongolia, and the far east region of Russia), a historical gateway leading to Beringia, need more attention for not only catostomids but also other freshwater fishes.

Figure 6. 1 Simplified recent molecular systematic hypothesis on the phylogeny of Catostomidae from previous studies: A, Harris and Mayden (2001) based on parsimony analyses of the Mitochondrial SSU rDNA Sequences, and Chen and Mayden (2012) depicted from partitioned maximum-likelihood analysis of nucleotides from IRBP2 exon 1 region; B, Sun et al. (2007) based on mitochondrial cytochrome b and nuclear 18S-ITS1-5.8S DNA sequences; C, Harris and Mayden (2001) based on parsimony analyses of the Mitochondrial LSU rDNA Sequences and combined LSU and SSU dataset; D, Doosey et al. (2010) using nucleotides of mitochondrial ND4 and ND5 protein coding genes and intervening tRNAs; E, Chen and Mayden (2012) based on nearly the complete gene of the nuclear IRBP2.
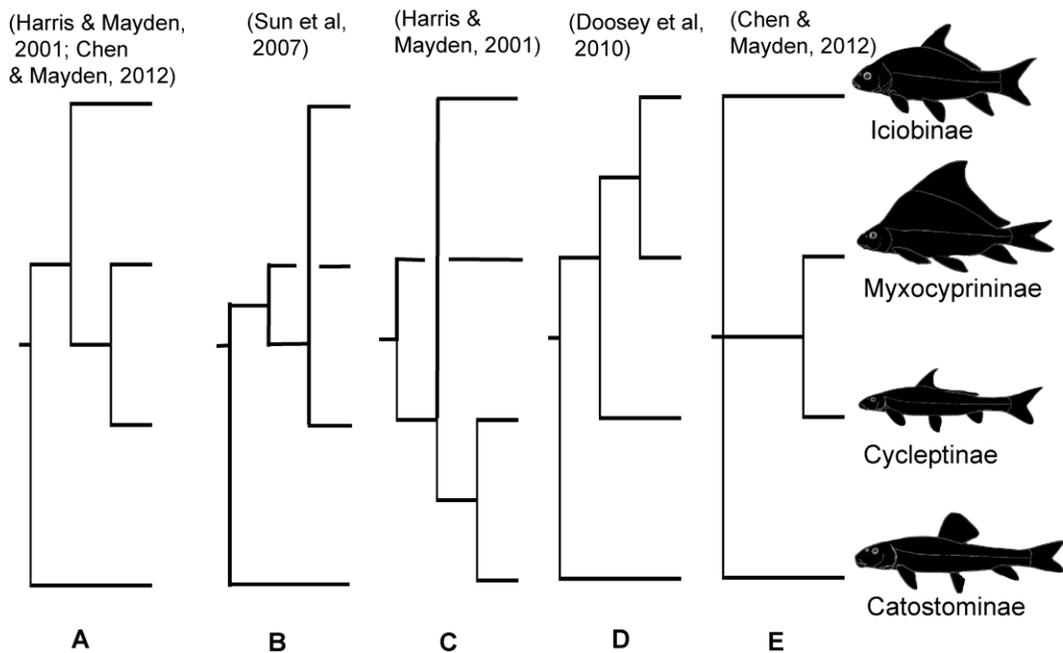
Figure 6. 2 Simplified phylogenetic hypothesis of Catostomidae including fossil genus *Amyzon*: Left, from Miller (1959) based on morphology; right, from Smith (1992) based on combined characters including morphology, biochemistry, gene expression, and development. The illustration of *Amyzon* skeleton is from Grande et al. (1982).

Miller (1959)   Smith (1992)

Myxocyprininae

Cycleptinae

Catostominae

Iciobinae
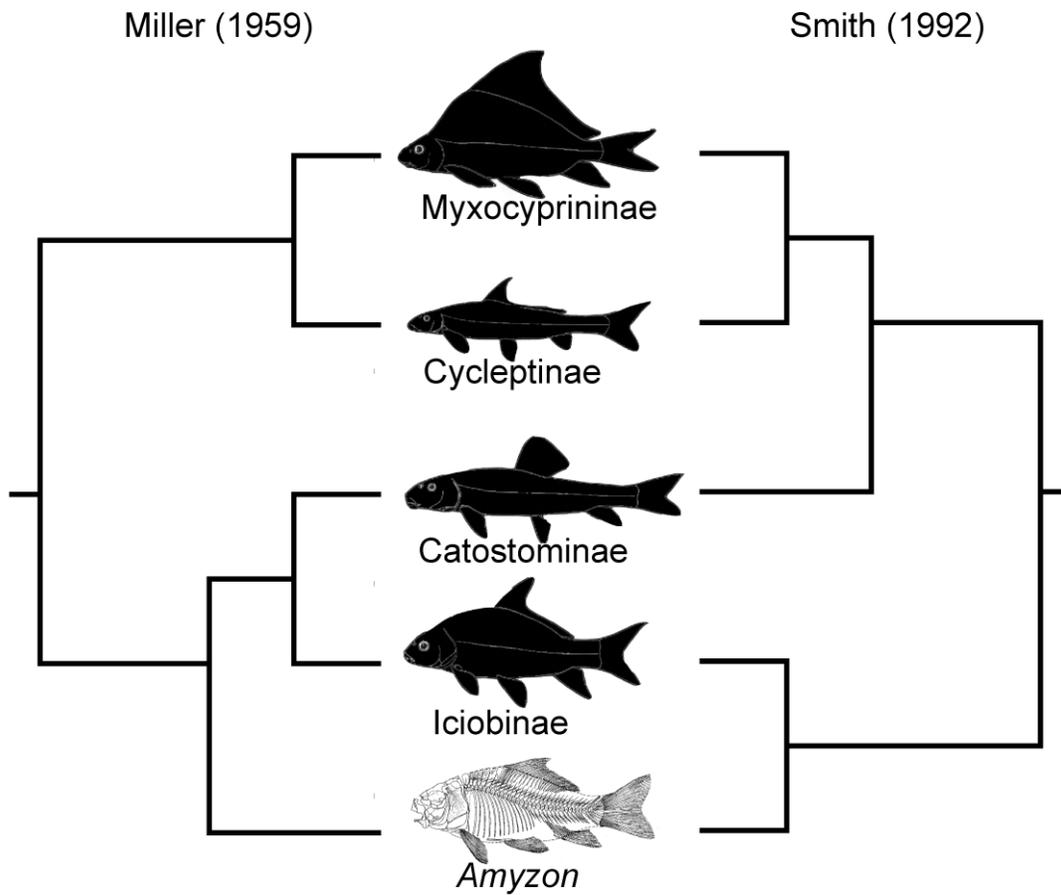
Amyzon

Figure 6. 3 Illustration of skull roof of catostomid fish and outgroups. A, *Carpiodes cyprinus*; B, *Cycleptus elongatus*; C, *Erimyzon oblongus*; D, *Hypentelium nigricans*, E, *Xyrauchen texanus*; F, *Catostomus wigginsi*; G, *Myxocyprinus asiaticus*; H, *Cyprinus carpio* (Cyprinidae); I, *Chromobotia macracanthus* (Botiidae). Abbreviations: **af**, anterior fontanelle; **dsp**, dermosphenotic; **em**, ethmoid complex; **ems**, ethmoid spine; **fr**, frontal; **frr**, frontal ridge; **lem**, lateral ethmoid; **nsc**, nasal canal; **ole**, orbit process of lateral ethmoid; **par**, parietal; **pf**, posterior fontanelle; **ptr**, autopterotic; **spf**, supraorbital process of frontal; **spn**, sphenotic; **ssc**, sensory canal; **stc**, supratemporal sensory commissure.
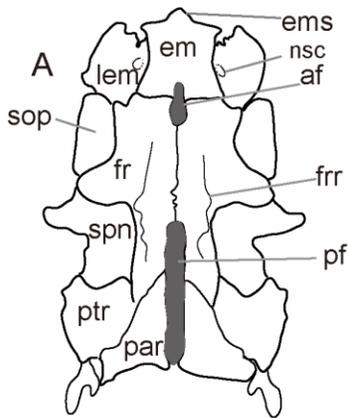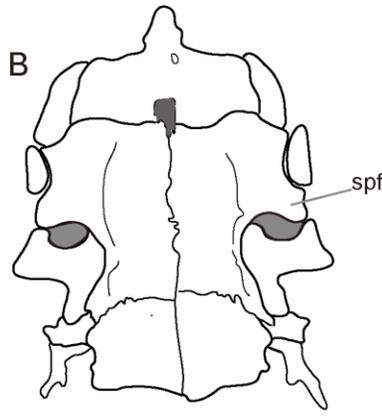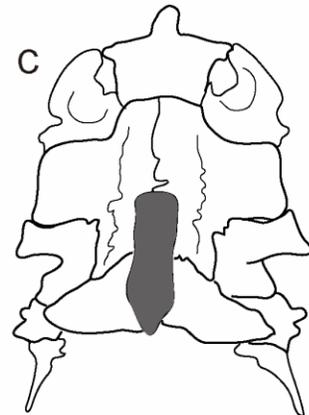
A *Carpiodes cyprinus*

B *Cycleptus elongatus*

C *Erimyzon oblongus*
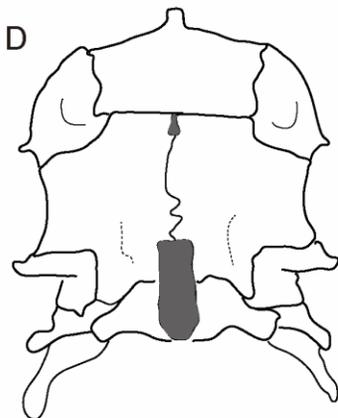
D *Hypentelium nigricans*
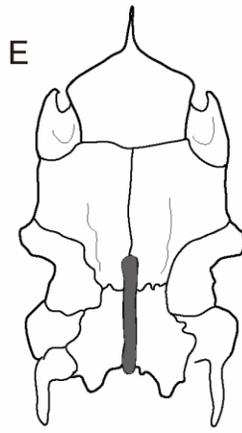
E *Xyrauchen texanus*
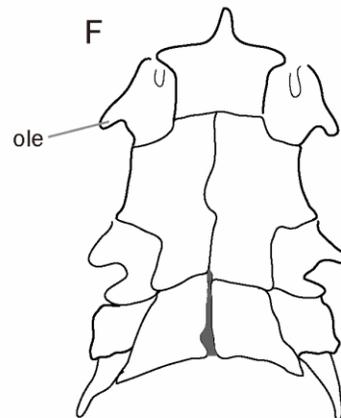
F *Catostomus wigginsi*
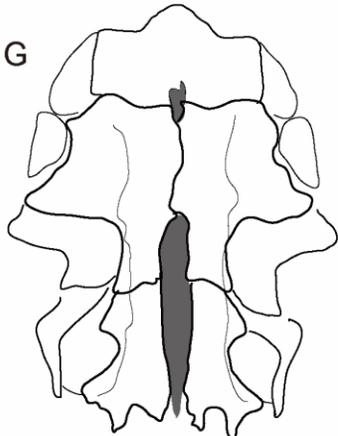
G *Myxocyprinus asiatics*
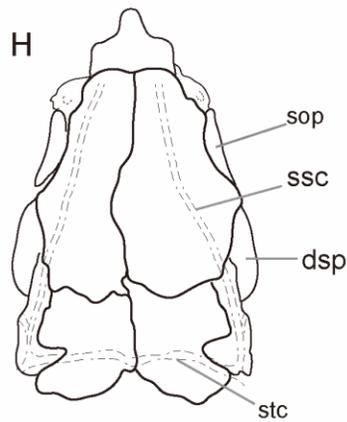
H *Cyprinus carpio*
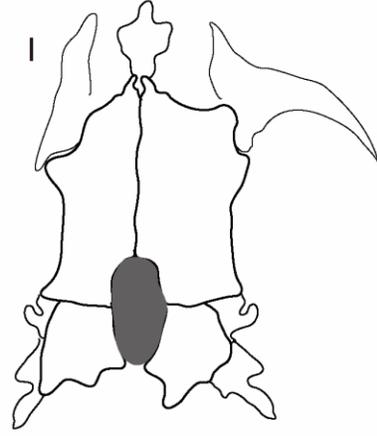
I *Chromobotia macracanthus*

Figure 6. 4 Infraorbital series of catostomid fishes. A. *Ictiobus cyprinellus*; B, *Cycleptus elongatus*; C, *Ictiobus bubals*; D, *Amyzon gosiutense* (FMNH PF 10575). Abbreviations: **iob1**, infraorbital 1 (lacrimal); **iob2** through **4**, infraorbital 2 through 4; **isc**, infraorbital sensory canal; **max**, maxilla; **op**, opercle; **sob**, supraorbital. Anterior to the left. Scale bar represents 10 mm for A, B, and D, and 5 mm for C.
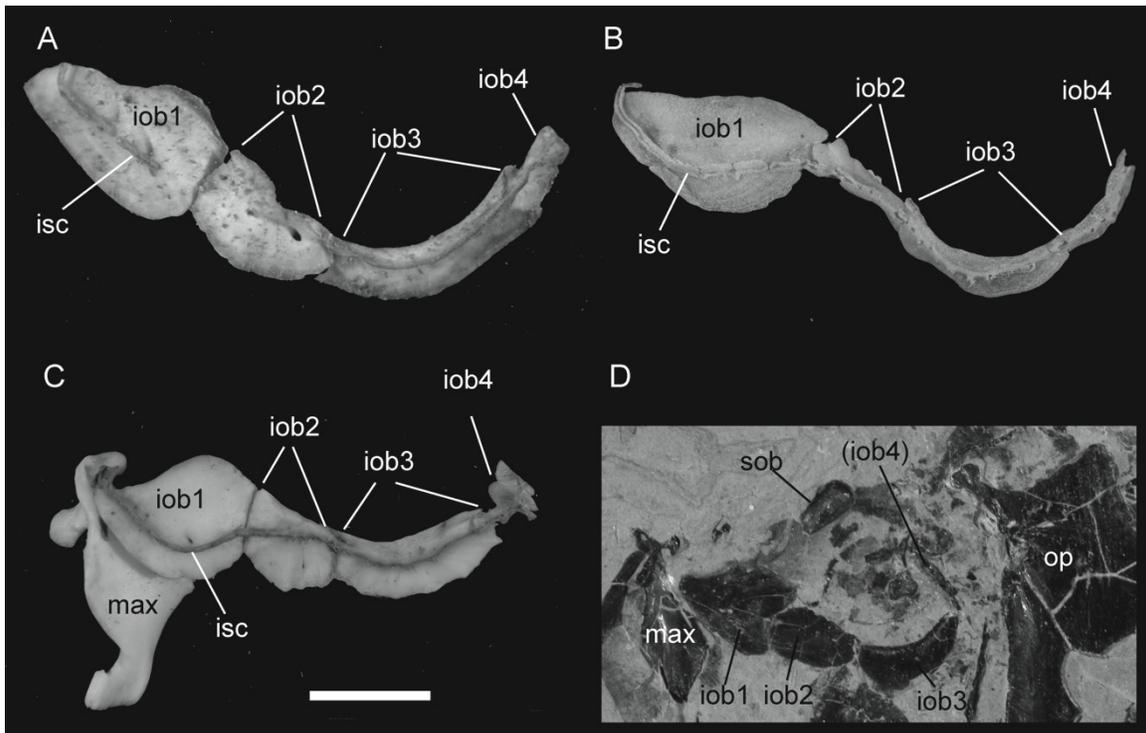
Figure 6. 5 Preopercles of catostomid fishes. A. *Catostomus catostomus*; B, *Myxocyprinus asiaticus*; C, *Chasmistes brevirostris*; D, *Carpiodes cyprinus*; E, *Pantosteus plebeius*; F and G, *Amyzon aggregatum* (UALVP 19540). Abbreviations: **hlm**, horizontal limb of preopercle; **hyo**, hyomandibula; **qua**, quadrate; **sym**, symplectic; **vlm**, vertical limb of preopercle. Anterior is to the left for A through E, and right for F and G. Arrows indicate the preopercle ridge that accommodates the preopercular sensory canal. Scale bar represents 10 mm for A through D, F, and G, whereas it represents 2.5 mm for E.
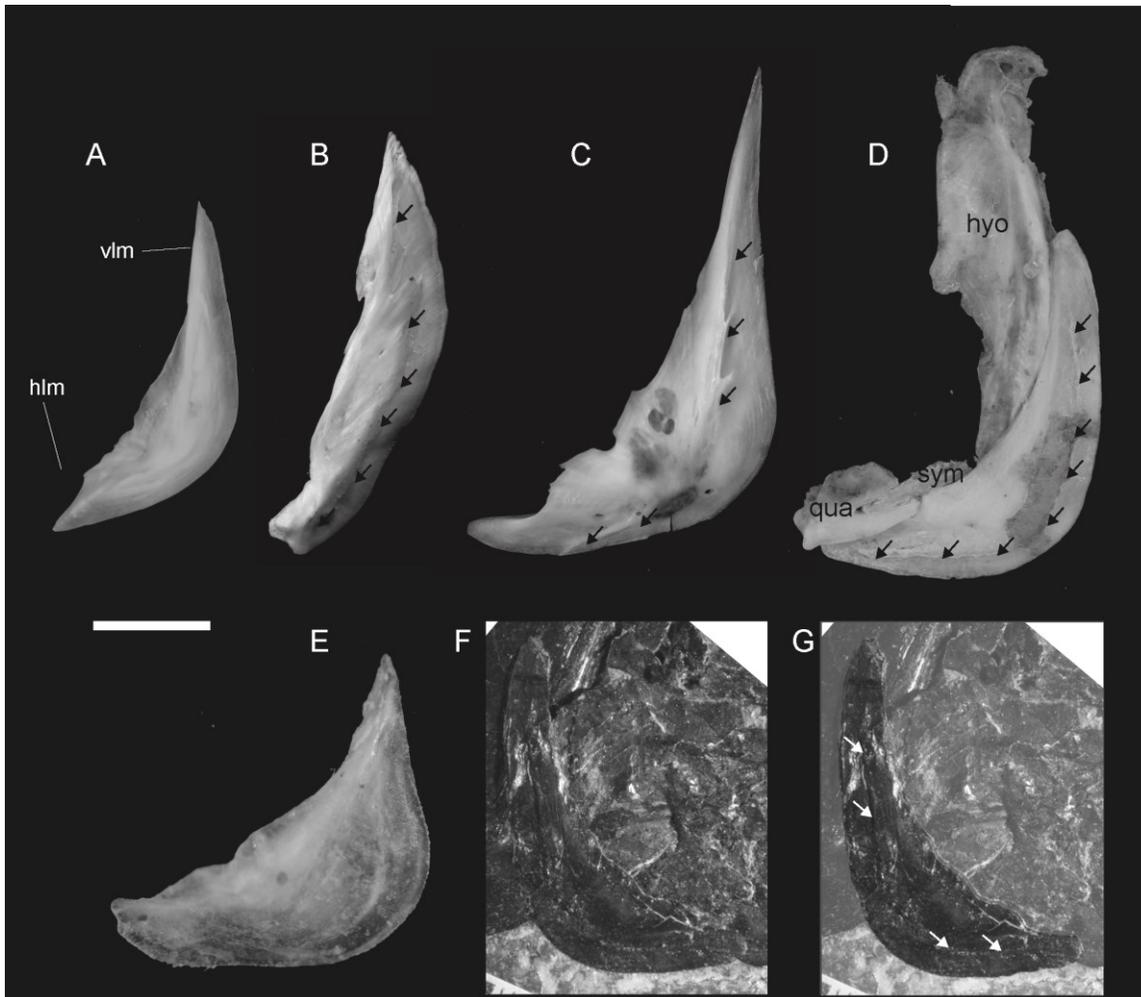
Figure 6. 6 Opercles of catostomid fishes. A. *Chasmistes brevirostris*; B, *Carpiodes cyprinus*; C, *Myxocyprinus asiaticus*; D, *Catostomus catostomus*; E, *Xyrauchen texanus*; F, *Ictiobus bubals*; G, *Erimyzon oblongus*; H, *Amyzon aggregatum*; I, *Plesiomyxocyprinus arratiae*. Abbreviations: **acq**, anterior corner of quadrate; **aup**, auricular process; **ecp**, ectopterygoid; **edp**, endopterygoid; **hym**, hyomandibular; **iop**, interopercle; **mpt**, metapterygoid; **odc**, dorsal concave of opercular; **op**, opercle; **opa**, opercular arm; **opf**, opercular fossa; **oph**, opercle height; **opn**, opercular notch; **opw**, opercle width; **pnh**, pterygoid notch of hyomandibular; **pop**, preopercular; **qua**, quadrate; **sup**, subopercle; **sym**, symplectic; **vsq**, ventral strut of quadrate. Scale bar represents 10 mm for all except 5 mm for F (*Ictiobus bubalus*).
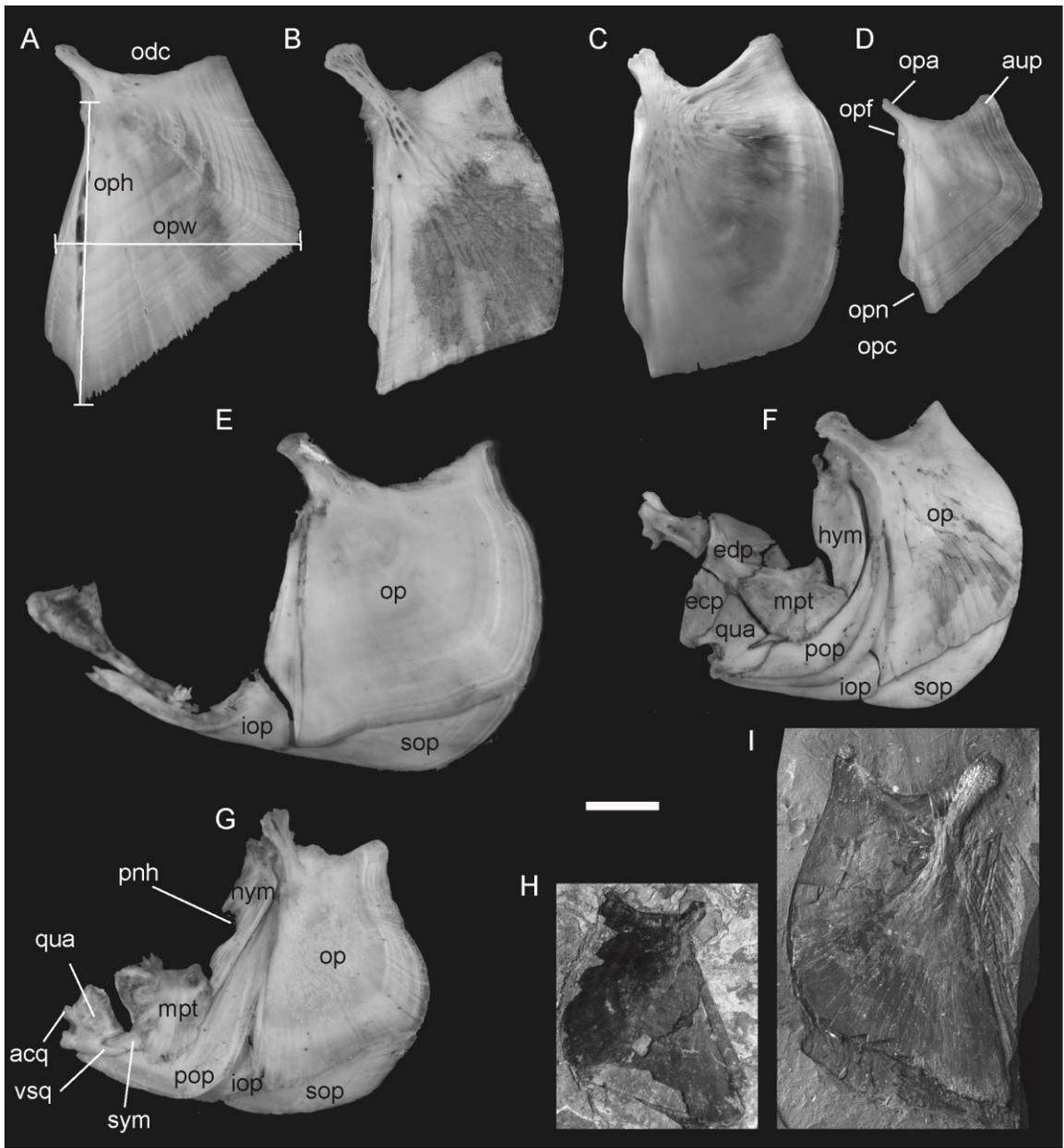
Figure 6. 7 Kinethmoid of catostomid fish. A, lateral and B, ventral view of kinethmoid in *Chasmistes brevirostris*; C, lateral and dorsal and D, posteriorview of kinethmoid in *Erimyzon oblongus*; E, lateral and dorsal and F, posterior view of kinethmoid in *Catostomus tahoensis*; G, lateral and H, ventral/anterior view of kinethmoid in *Hypentelium nigricans*; I, lateral view of kinethmoid in *Catostomus catostomus*; J, lateral view of kinethmoid in *Cycleptus elongatus*; K, lateral and dorsal and L, posterior view of kinethmoid in *Ictiobus bubalus*; M, lateral view of kinethmoid in *Amyzon aggregatum*. Anterior is to the left in A, C, E, G, I through K, and M. Jaw is protruded in M of which the dorsal end of kinethmoid flipped forward and ventral end rotated caudally. Scale bar represents 5 mm. Abbreviations: **apa**, autopalatine; **kem**, kinethmoid; **em**, ethmoid; **max**, maxilla; **pmx**, premaxilla.
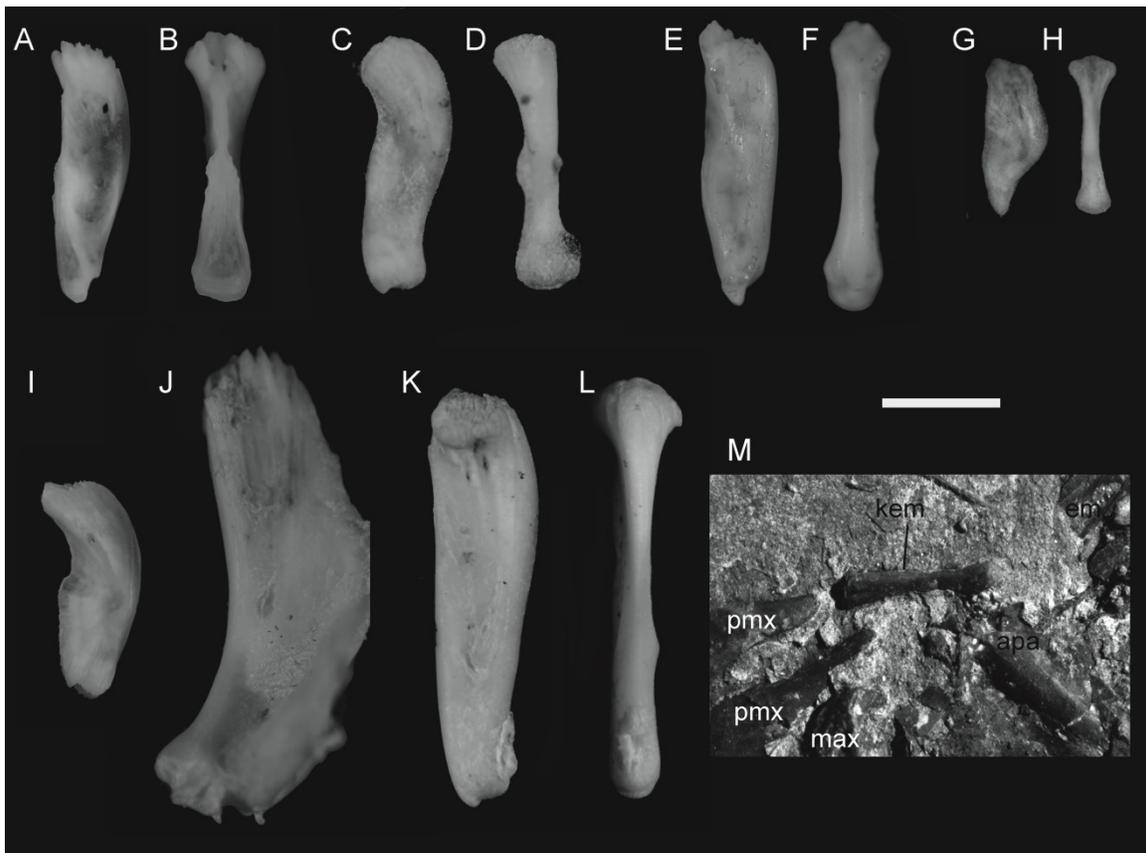
Figure 6. 8 Premaxilla of catostomid fish. A. *Erimyzon oblongus*; B, *Xyrauchen texanus*; C, *Hypentelium nigricans*; D, *Ictiobus cyprinellus*; E, *Pantosteus plebeius*; F, *Amyzon aggregatum*. Abbreviations: **ap**, ascending process of premaxilla; **lp**, labial process of premaxilla. Scale bars represent 5 mm. A through E are at the same scale. Anterior facing out, medial on the left, lateral on the right for each premaxilla.
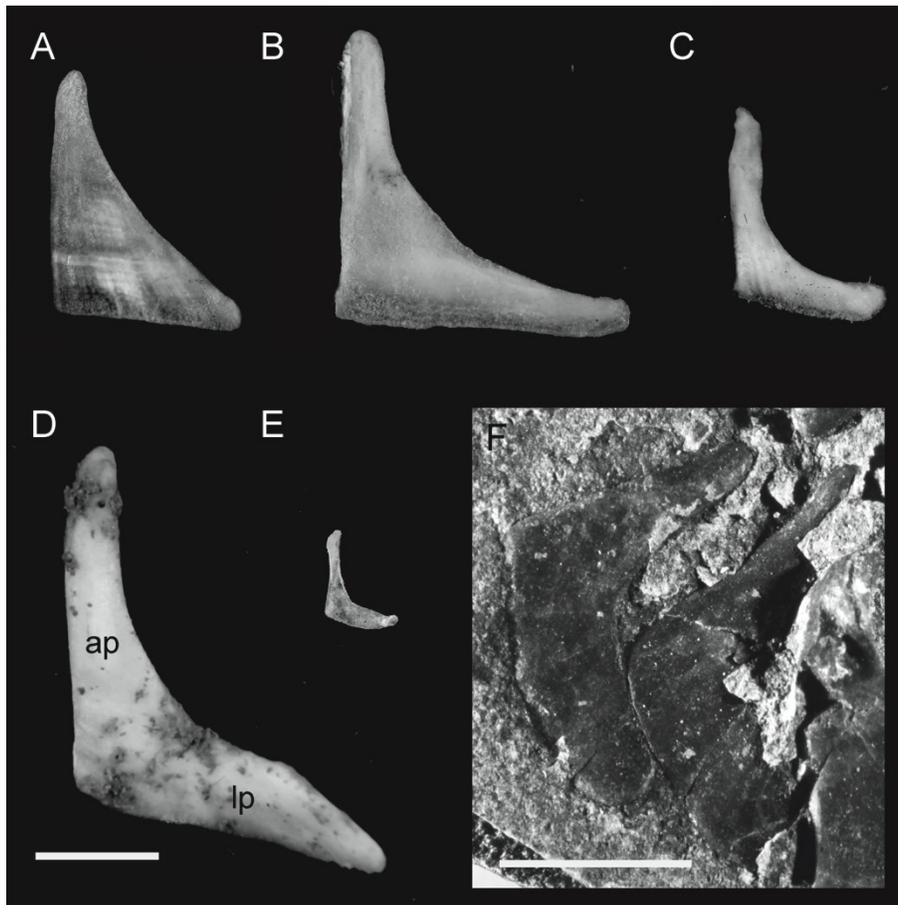
Figure 6. 9 Dentary of catostomid fishes. A, *Myxocyprinus asiaticus*; B, *Chasmistes brevirostris*; C, *Catostomus catostomus*; D, *Hypentelium nigricans*; E, *Ictiobus cyprinellus*; F, *Amyzon gosiutense* (AMNH FF 10460). Abbreviations: **aa**, anguloarticular; **df**, dentary ridge; **gr**, gnathic ramus; **cnp**, coronoid process; **mf**, mental foramen; **pvp**, posteroventral process; **ra**, retroarticular. Anterior is to the left in A through E, and to the right in F. Dentaries are aligned by the gnathic ramus and may not reflect the natural position of the bone. Scale bars represent 5 mm.
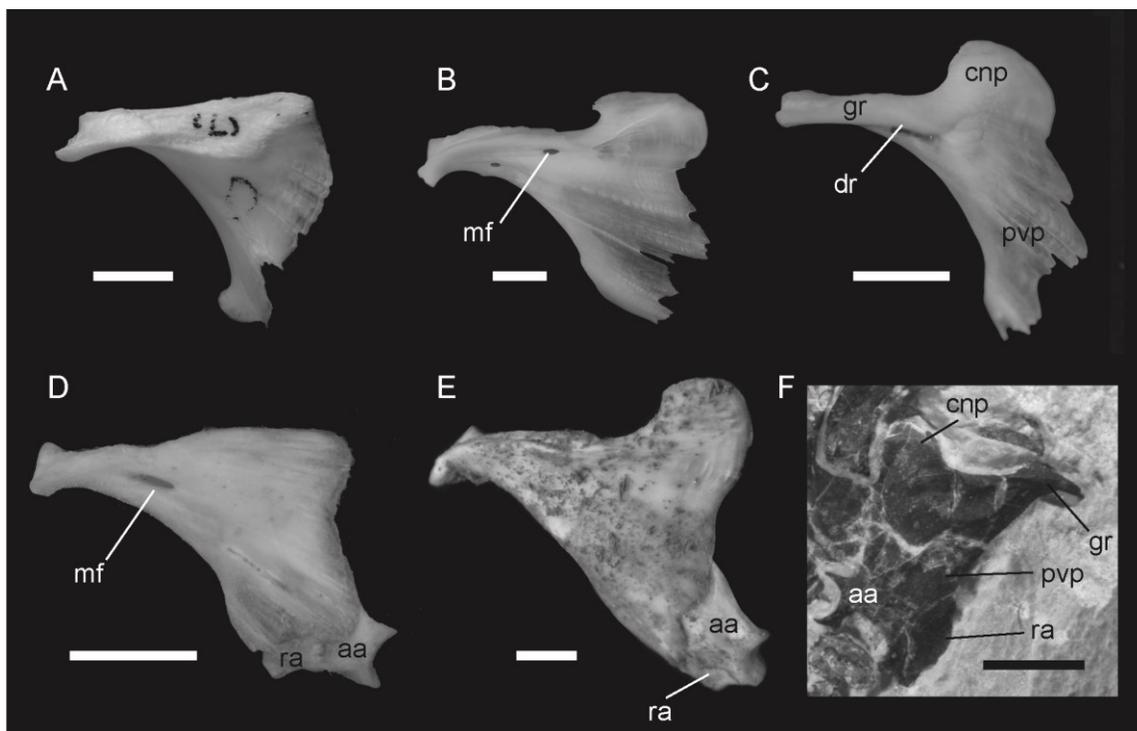
Figure 6. 10 Pharyngeal bones and teeth of catostomid fishes. Anterodorsal (A) and posteroventral (B) view of the right pharyngeal bone of *Catostomus catostomus*; anterodorsal (C) and posteroventral (D) view of articulated right and left pharyngeal bones; E and F, disarticulated pharyngeal teeth of *Amyzon aggregatum* (UALVP 33286); G, pharyngeal teeth *in situ* of *Amyzon gosiutense* (FMNH PF 10425); H, pharyngeal teeth *in situ* of *Amyzon hunanense* (IVPP V 17906.3a). Abbreviations: **aep**, anteroventral edentulous processes; **pep**, posterodorsal edentulous processes; **pls**, posterolateral surface (usually pitted surface); **R.**, right pharyngeal bone. Scale bars in A through D represent 10 mm, and in E through I represent 1 mm.
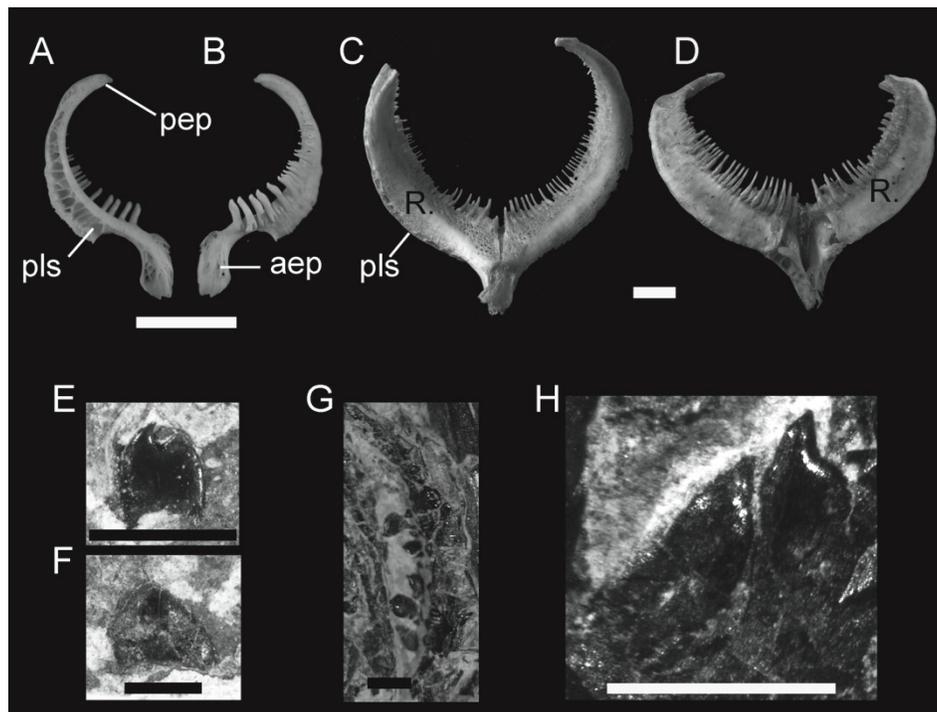
Figure 6. 11 Weberian apparatus of catostomid fishes. A, *Cycleptus elongatus*; B, *Ictiobus bubals*; C, *Amyzon aggregatum*; D, *Xyrauchen texanus*; E, *Erimyzon oblongus*; F, *Moxostoma carinatum*; G, *Amyzon gosiutense*. Abbreviations: **nc**, neural complex; **ncr**, neural complex ridge; **ns4/5**, neural spine 4/5; **os**, Os suspensorium; **r4**, rib 4; **sn**, supraneural; **tp2**, transverse process of centrum 2; **tpl**, transverse plate. Scale bars represent 5 mm.
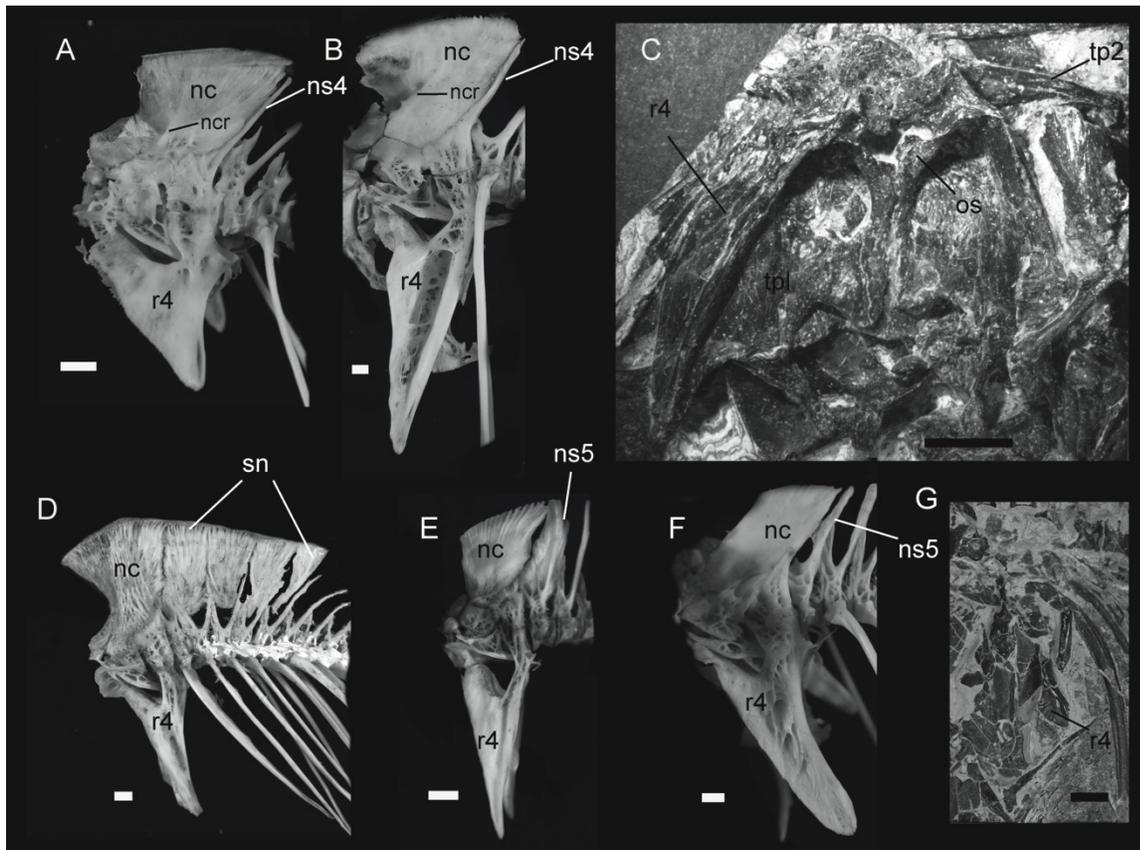
Figure 6. 12 Caudal skeleton of catostomid fishes. A, *Ictiobus cyprinellus*; B, *Erimyzon oblongus*; C, *Hypentelium nigricans*; D, *Cycleptus elongatus*; E, *Xyrauchen texanus*. Abbreviations: **cc**, compound centrum; **ep**, epural; **hyp 1–5**, hypural 1 through 5; **pap**, parhypural. Scale bar represents 10 mm.
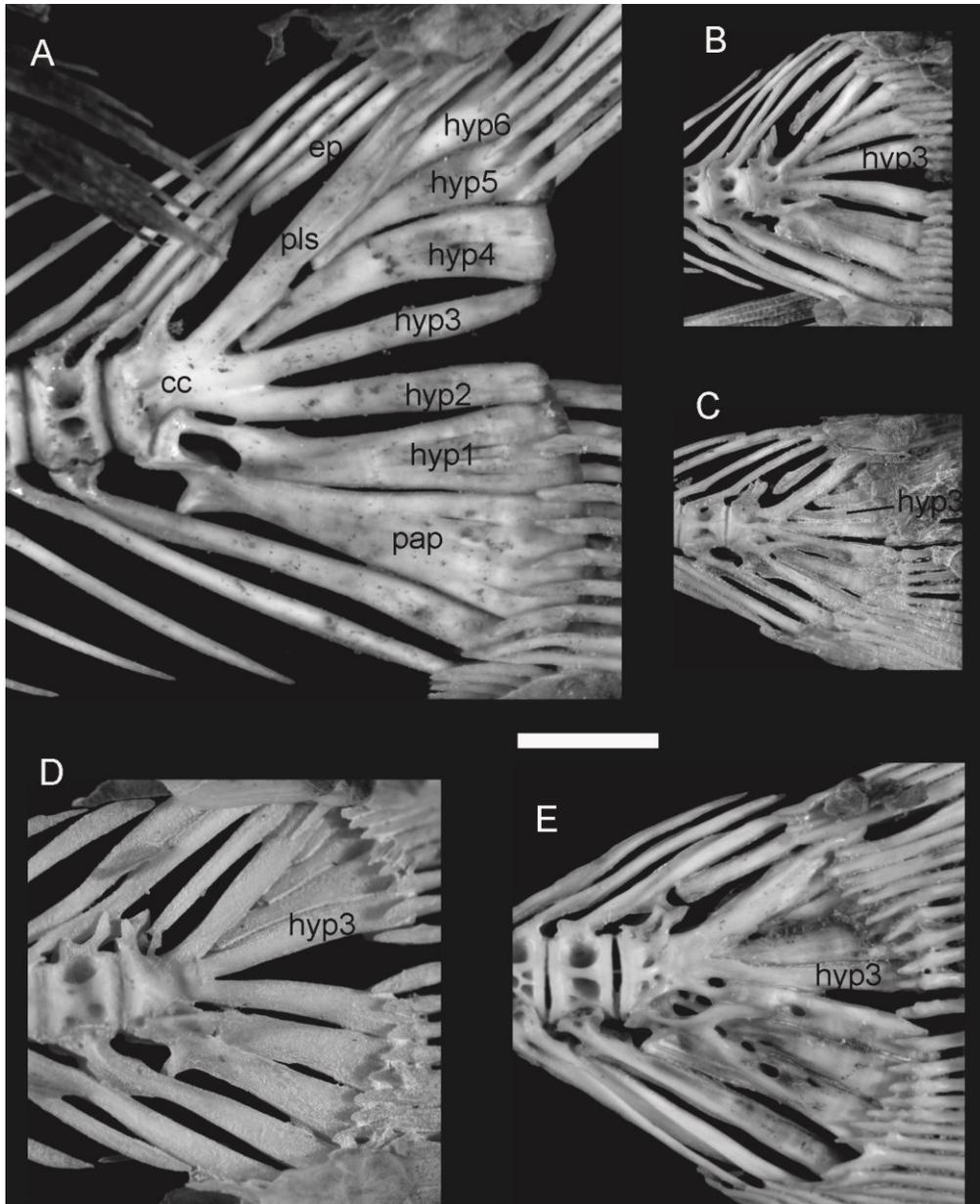
Figure 6. 13 Catostomidae phylogenetic hypothesis: Strict consensus of 4 equally most parsimonious cladograms resulting from parsimony analyses. Heuristic search in PAUP 4b10, traditional and new technology search of TNT 1.5 were performed respectively on the 43 taxa and 134 osteological characters. Each cladogram has 834 steps with CI 0.32 and RI 0.58. Numbers above branches indicate decay indices (PAUP) and bremer support (TNT), and are separated by a slash if not identical. Numbers below branches indicate node number that summarized with synapomorphies in Appendix 6.2. Heuristic search and traditional search was performed with 1000 random replicate respectively. Both searches resulted in the same topology for the ingroup, with the outgroup arranged differently as TNT only allow one taxon to be assigned to the outgroup and all five taxa labeled were used as outgroups in PAUP 4b10. Five outgroup taxa representing major clades of Cypriniformes were designated in PAUP: *Cyprinus carpio*, *Gyrinocheilus aymonieri*, *Cobitis taenia*, *Chromobotia macracanthus*, and *Jianghanichthys hubeiensis*. Eocene species are bolded. "NA *Amyzon*" stands for North American species of *Amyzon*, whereas the only known Asian *Amyzon* is labeled. Four subfamilies of extant catostomids (Ictiobinae, Myxocyprininae, Cycleptinae, and Catostominae) and two tribes of Catostominae (Catostomini and Moxostomini) are well resolved as monophyletic groups with the exception of *Hypentelium* being a basal clade of the subfamily.
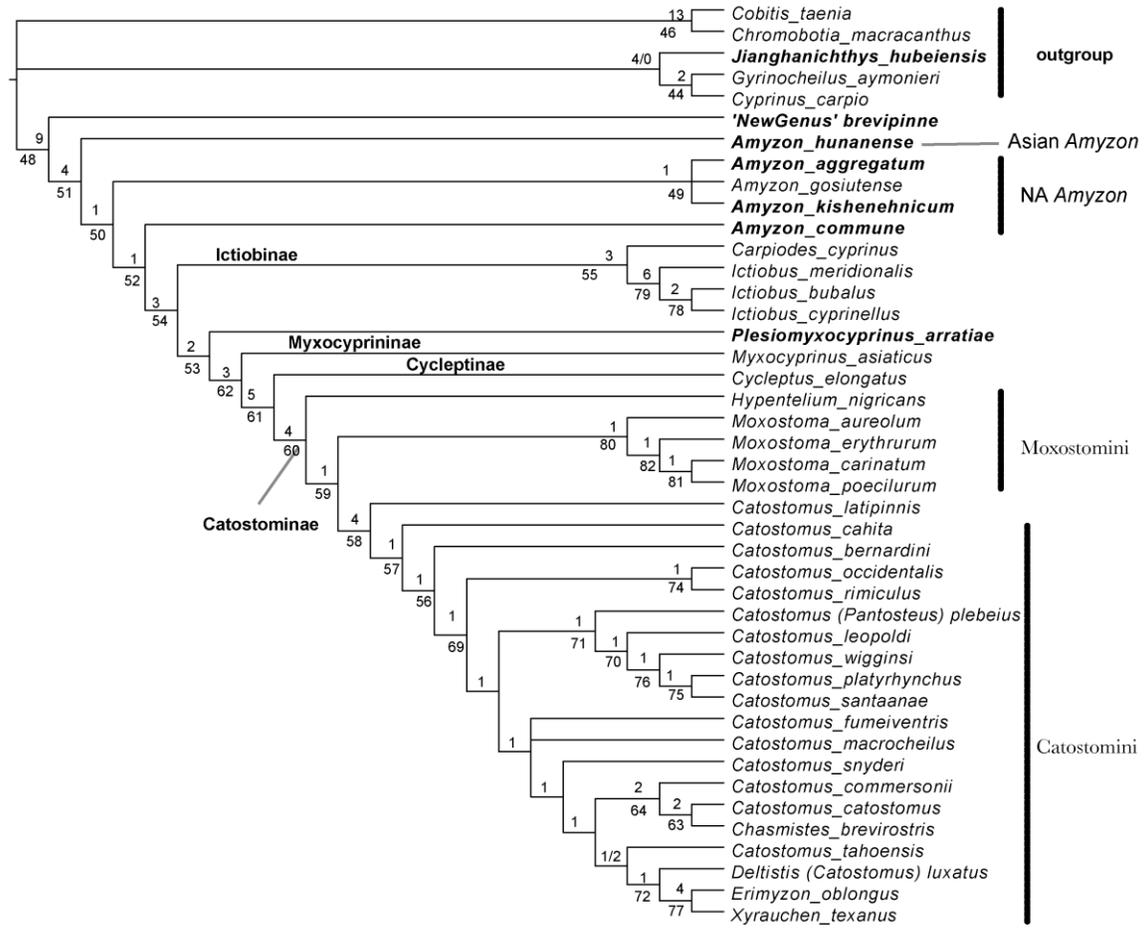
Figure 6. 14 Catostomidae phylogeny from Bayesian and Bootstrap 50% majority-rule consensus cladograms. Both analyses are based on the 43 taxa and 134 osteological characters. The former analysis was performed in MrBayes 3.2.6 using Markov chain Monte Carlo (MCMC) analysis with 10000000 generations. The latter analysis was performed in PAUP 4b10 with 1000 bootstrap replicates. Both analyses generate similar topologies of the ingroup except the relationships of *Moxostoma* and *Hypentelium*. The gray and thicker lines indicate the cladogram generated from bootstrap analysis where it differs from the Bayesian analysis. Numbers beside nodes indicate the Bayesian probability/bootstrap support value. Eocene species are bolded.
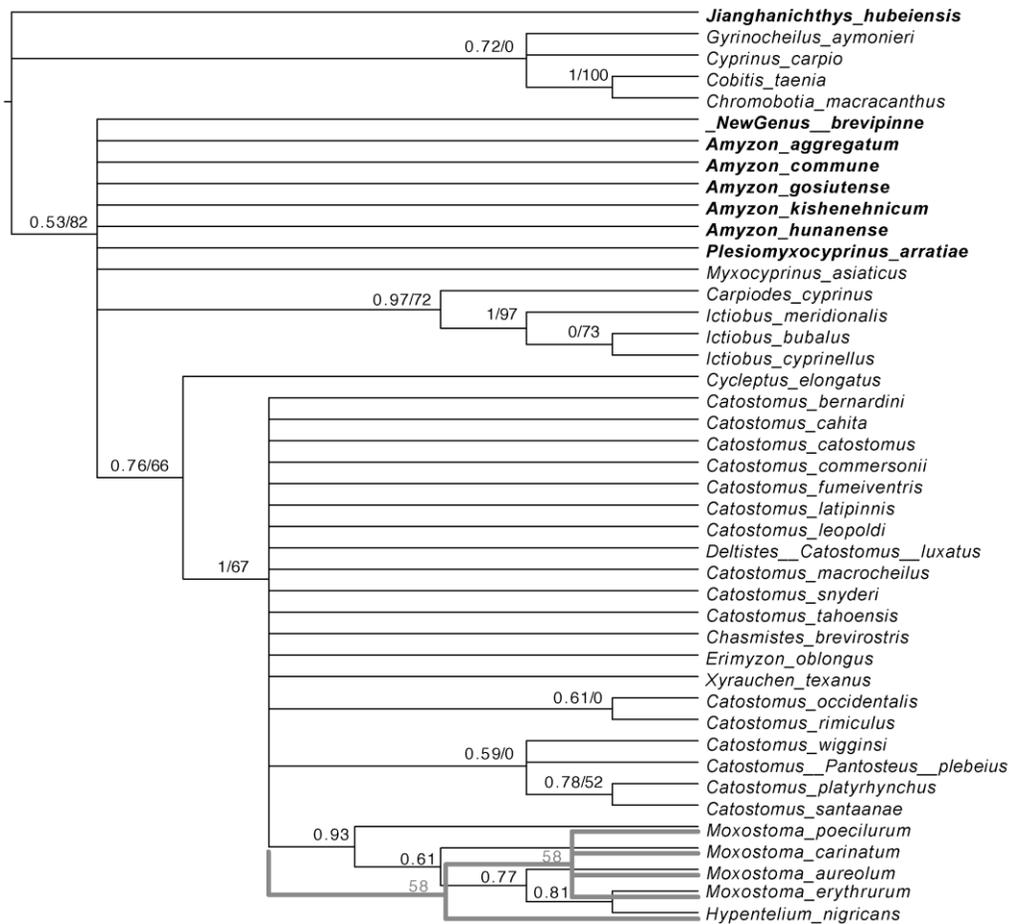
Appendix 6. 1 Data matrix of 44 taxa including 5 outgroup and 39 catostomid species and 134 osteological characters used for phylogenetic analysis of Catostomidae.

species/characters	1	2	3	4	5	6	7	8	9	10	11	12	13	14	15	16	17	18	19	20	21	22	23	24	25	26	27	28	29	30
Gyrinocheilus aymonieri	0	0	0	3	0	1	0	1	0	0	-	0	1	1	0	0	1	0	0	1	1	0	0	0	0	0	1	1	1	1
Cyprinus carpio	0	0	0	0	0	1	0	1	1	0	-	0	0	-	0	0	0	-	0	0	0	0	0	0	1	1	0	0	0	0
†*Jianghanichthys hubeiensis*	0	2	1	0	1	2	1	?	2	1	0	1	0	-	0	0	1	1	2	2	1	?	1	?	0	0	?	?	?	2
Cobitis taenia	4	2	2	3	2	0	-	1	3	0	-	2	0	-	2	1	2	-	0	0	1	?	0	1	0	0	0	0	3	1
Chromobotia macracanthus	5	5	2	3	2	2	0	0	3	0	-	2	0	0	2	1	2	2	0	0	1	0	2	0	0	0	2	0	1	1
†"NewGenus" *brevipinne*	?	1	?	?	?	2	0	?	2	1	-	2	1	?	2	?	1	?	1	?	0	?	2	?	?	0	?	?	?	1
†*Amyzon aggregatum*	1	1	1	0	2	3	1	?	2	1	0	2	1	0	2	?	1	0	2	1	0	0	0	?	2	1	?	?	?	2
†*Amyzon commune*	?	?	1	0	2	3	0	?	2	1	0	2	?	?	2	1	1	1	0	2	0	?	1	?	?	0	?	?	?	2
†*Amyzon gosiutense*	1	1	1	0	?	3	1	?	2	1	1	2	1	?	2	?	1	0	2	1	0	0	0	?	2	0	?	?	?	2
†*Amyzon kishenehnicum*	1	1	1	0	2	3	1	?	2	1	1	2	1	0	2	?	1	0	2	1	0	?	0	?	2	0	?	?	?	2
†*Amyzon hunanense*	1	1	1	0	2	3	1	?	1	1	-	2	1	1	2	1	1	1	?	1	0	?	2	?	2	0	?	?	?	2
†*Plesiomyxocyprinus arratiae*	?	?	?	?	?	3	1	?	1	1	-	2	1	3	2	?	?	1	?	1	0	?	?	?	2	1	?	?	?	2
Carpiodes cyprinus	2	2	1	0	1	3	1	1	1	1	1	2	1	1	2	0	1	0	0	1	0	0	2	1	2	1	0	3	2	1
Catostomus bernardini	3	5	1	2	2	3	1	1	3	1	1	2	0	-	2	1	1	0	2	2	0	0	1	0	2	0	1	1	0	1
Catostomus cahita	3	5	1	2	2	3	1	1	3	1	1	2	0	-	1	1	1	0	2	2	0	0	1	0	2	0	1	1	0	1
Catostomus catostomus	3	5	1	?	2	3	1	1	3	1	0	2	0	-	2	?	1	0	2	2	0	0	1	0	2	0	1	1	0	1
Catostomus commersonii	1	5	1	2	2	3	1	1	3	1	1	2	0	-	2	1	1	0	2	2	0	0	1	1	2	0	1	1	0	1
Catostomus fumeiventris	1	?	1	?	2	3	1	1	3	1	0	2	0	-	2	?	1	0	2	2	0	0	1	0	2	0	1	1	0	1
Catostomus latipinnis	3	5	1	2	2	3	1	1	3	1	1	2	0	-	2	1	1	0	2	2	0	0	1	0	2	0	1	1	0	1
Catostomus leopoldi	3	?	1	1	2	3	1	1	3	1	0	2	0	-	2	0	1	0	2	2	0	0	1	0	2	0	1	1	0	1
Deltistes (Catostomus) luxatus	1	4	1	?	2	3	1	1	3	1	0	2	0	-	2	?	1	0	2	2	0	0	1	0	2	0	1	1	0	1
Catostomus macrocheilus	1	5	1	2	2	3	1	1	3	1	?	2	0	-	2	?	1	0	2	2	0	0	1	0	2	0	1	1	0	1
Catostomus occidentalis	2	5	1	2	2	3	1	1	3	1	1	2	0	-	2	1	1	0	2	2	0	0	1	0	2	0	1	1	0	1

Species	1	2	3	4	5	6	7	8	9	10	11	12	13	14	15	16	17	18	19	20	21	22	23	24	25	26	27	28	29	30
Catostomus platyrhynchus	?	?	1	?	2	3	1	1	3	1	?	2	0	-	1	?	1	2	2	2	0	0	1	0	2	0	1	1	0	1
Catostomus rimiculus	1	5	1	2	2	3	1	1	3	1	1	2	0	-	1	0	1	0	2	2	0	0	1	0	2	0	1	1	0	1
Catostomus santaanae	?	?	1	?	2	3	1	1	3	1	?	2	0	-	1	?	1	2	2	2	0	0	1	0	2	0	1	1	0	1
Catostomus snyderi	3	?	1	?	2	3	1	1	3	1	0	2	0	-	2	1	1	0	2	2	0	0	1	1	2	0	1	1	0	1
Catostomus tahoensis	2	4	1	2	2	3	1	1	3	1	0	2	0	-	2	1	1	0	2	2	0	0	1	0	2	0	1	1	0	1
Catostomus wigginsi	3	5	1	1	2	3	1	1	3	1	0	2	0	-	1	?	1	0	2	2	0	0	1	0	2	0	1	1	0	1
Chasmistes brevirostris	3	5	1	?	2	3	1	1	?	1	0	2	0	-	2	?	1	0	2	?	?	0	1	1	2	0	1	1	?	?
Cycleptus elongatus	1	4	1	0	1	3	1	1	2	1	0	2	1	0	0	0	1	0	1	2	0	0	0	0	2	1	1	3	1	2
Erimyzon oblongus	2	2	1	2	1	3	1	1	3	1	1	2	0	-	2	1	1	1	2	2	?	0	0	1	2	1	1	1	2	1
Hypentelium nigricans	1	6	1	2	2	3	1	1	3	1	1	2	1	2	2	1	1	2	1	?	1	1	0	0	2	0	1	2	2	1
Ictiobus bubalus	1	3	1	1	1	3	1	1	2	1	1	2	?	?	2	?	1	0	2	1	0		1	1	2	1	0	3	1	2
Ictiobus cyprinellus	1	2	1	1	1	3	1	1	2	1	1	2	?	?	2	1	1	0	2	1	0	0	1	1	2	1	0	3	1	2
Ictiobus meridionalis	1	2	1	1	1	3	1	1	2	1	1	2	1	0	2	1	1	0	2	1	0	0	1	1	2	1	0	3	1	2
Moxostoma aureolum	1	1	1	2	2	3	1	0	3	1	0	2	0	-	2	1	1	1	1	2	1	1	0	0	2	0	1	1	2	1
Moxostoma carinatum	2	3	1	2	2	3	1	0	3	1	0	2	0	-	2	1	1	2	1	2	1	0	0	0	2	0	1	1	2	1
Moxostoma erythrurum	2	1	1	?	2	3	1	0	3	1	0	2	0	-	2	1	1	2	1	2	1	?	0	0	2	0	0	1	2	1
Moxostoma poecilurum	2	3	1	2	2	3	1	0	3	1	1	2	0	-	2	1	1	1	1	2	1	0	0	0	2	0	1	1	2	1
Myxocyprinus asiaticus	1	1	1	0	1	3	1	1	2	1	1	2	1	2	2	1	1	2	1	1	0	0	0	0	2	1	1	1	2	2
Catostomus (Pantosteus) plebeius	3	6	1	2	2	3	1	1	3	1	?	2	?	?	0	0	1	1	2	2	0	?	0	1	2	0	1	1	2	1
Xyrauchen texanus	2	5	1	2	2	3	1	1	3	1	1	2	0	-	2	1	1	0	2	2	1	0	1	0	2	1	0	3	2	1

species/characters	31	32	33	34	35	36	37	38	39	40	41	42	43	44	45	46	47	48	49	50	51	52	53	54	55	56	57	58	59	60
Gyrinocheilus aymonieri	3	0	0	0	2	1	0	2	0	0	1	2	0	2	0	0	0	0	3	0	6	0	3	1	0	2	0	0	0	-
Cyprinus carpio	1	0	1	0	0	0	0	1	1	0	2	0	0	0	2	1	0	1	0	1	1	1	0	1	0	1	0	0	0	
†*Jianghanichthys hubeiensis*	0	1	0	1	1	0	0	0	0	1	2	2	1	2	1	0	0	1	?	0	0	0	3	1	0	2	1	1	0	0
Cobitis taenia	?	?	2	2	-	-	-	0	0	?	?	0	0	0	0	0	0	0	3	1	5	0	2	0	0	2	1	1	1	0
Chromobotia macracanthus	3	?	2	0	3	1	0	0	1	3	1	1	3	1	0	2	0	1	3	0	5	0	2	0	1	2	1	1	1	0
†"NewGenus" *brevipinne*	?	2	0	0	2	0	?	1	0	1	?	1	2	2	1	0	0	0	0	0	?	0	1	0	1	1	0	0	1	0
†*Amyzon aggregatum*	?	2	0	1	1	?	0	1	1	1	1	1	2	1	1	1	0	1	0	0	1	0	1	0	1	1	1	0	1	0
†*Amyzon commune*	?	2	0	1	0	?	0	1	0	1	?	1	2	1	0	1	0	1	0	1	?	0	2	0	1	?	0	0	1	1
†*Amyzon gosiutense*	?	2	0	1	1	1	0	1	0	1	1	1	2	2	1	1	0	1	0	0	1	0	2	0	0	0	0	0	1	1
†*Amyzon kishenehnicum*	?	2	0	1	1	?	0	1	0	1	1	1	2	2	1	1	0	1	0	0	1	0	1	0	0	1	0	0	1	1
†*Amyzon hunanense*	?	2	0	1	0	?	0	2	0	1	?	1	3	2	1	0	0	1	0	0	2	0	2	0	1	0	0	0	1	0
†*Plesiomyxocyprinus arratiae*	?	?	0	?	?	?	?	2	1	2	?	1	2	2	1	1	0	1	0	0	?	0	2	1	1	?	?	?	?	?
Carpiodes cyprinus	2	2	0	?	1	1	?	1	1	2	1	1	2	0	2	1	0	1	0	0	?	0	2	0	1	1	1	0	1	1
Catostomus bernardini	2	2	2	1	1	1	1	1	1	3	1	2	3	1	1	1	0	1	2	0	5	0	3	0	0	0	0	0	1	0
Catostomus cahita	2	2	2	1	1	1	1	2	1	3	1	2	3	1	1	1	0	1	2	0	3	0	?	?	?	0	0	0	1	0
Catostomus catostomus	2	2	2	1	1	1	1	0	2	3	1	1	3	2	1	1	0	1	0	1	4	0	1	1	0	0	0	0	1	0
Catostomus commersonii	2	2	2	1	1	1	1	1	1	3	1	1	3	?	1	1	0	1	2	0	5	0	3	0	0	0	0	0	1	1
Catostomus fumeiventris	2	2	2	1	1	1	1	1	1	3	1	1	3	2	1	1	0	1	2	0	3	0	2	1	1	0	0	0	1	?
Catostomus latipinnis	2	2	2	1	1	1	1	0	2	3	1	2	2	2	1	1	0	1	1	0	5	0	?	2	0	0	0	0	1	1
Catostomus leopoldi	2	2	2	1	1	1	1	2	1	3	1	2	3	1	1	1	0	1	2	0	4	0	3	?	0	0	0	0	1	0
Deltistes (Catostomus) luxatus	2	2	2	1	1	1	1	1	0	3	1	1	3	1	1	0	0	0	1	0	4	0	2	2	0	?	0	0	1	0
Catostomus macrocheilus	2	2	2	1	1	1	1	1	1	3	1	1	3	1	1	1	0	1	1	0	1	0	3	0	0	?	0	0	1	?
Catostomus occidentalis	2	2	2	1	1	1	0	1	1	3	1	1	3	1	1	1	0	1	2	0	2	0	3	2	0	0	0	0	1	0
Catostomus platyrhynchus	2	2	2	1	1	1	1	2	1	3	1	1	3	2	1	1	0	1	2	0	4	0	3	?	?	1	0	0	1	0
Catostomus rimiculus	2	2	2	1	1	1	1	2	1	3	1	1	3	1	1	1	0	1	2	0	4	0	2	2	1	0	0	0	1	0
Catostomus santaanae	2	2	2	1	1	1	1	2	0	3	1	1	3	1	1	1	0	1	2	0	4	0	?	?	?	1	0	0	1	1
Catostomus snyderi	2	2	2	1	1	1	1	1	1	3	1	1	3	1	1	1	0	1	2	0	3	0	2	0	0	0	0	0	1	0
Catostomus tahoensis	2	2	2	1	1	1	1	1	1	3	1	1	3	1	1	0	0	0	2	0	2	0	1	0	0	0	0	0	1	0

Catostomus wigginsi	2	2	2	1	1	1	1	1	0	3	1	1	3	2	1	1	0	2	2	0	4	0	?	0	0	0	0	0	1	0
Chasmistes brevirostris	2	2	?	?	1	1	?	0	1	1	1	1	3	1	1	1	0	1	2	0	2	0	1	1	0	2	1	0	1	0
Cycleptus elongatus	2	2	0	0	2	1	0	0	1	1	1	2	3	1	1	1	1	1	2	0	4	0	2	1	1	1	1	0	0	1
Erimyzon oblongus	2	2	2	?	1	?	?	1	1	?	1	1	3	1	1	0	0	1	1	0	3	0	3	1	0	0	0	0	1	1
Hypentelium nigricans	2	2	2	?	1	?	?	0	0	3	1	2	2	2	1	1	1	2	3	1	4	0	2	0	1	1	0	0	1	1
Ictiobus bubalus	2	2	0	0	1	1	0	1	0	2	1	1	2	1	2	0	1	1	2	0	2	0	2	2	1	?	0	0	1	1
Ictiobus cyprinellus	2	2	0	0	1	1	0	1	0	2	1	1	2	2	2	0	0	1	1	0	2	0	2	2	1	1	0	0	1	1
Ictiobus meridionalis	2	2	0	0	1	1	0	2	0	2	1	1	2	2	2	0	0	1	1	0	3	0	1	0	0	0	0	0	1	1
Moxostoma aureolum	2	2	2	1	1	0	1	0	2	3	1	2	3	2	1	1	0	1	3	1	?	0	3	?	?	1	1	0	1	1
Moxostoma carinatum	2	2	2	1	1	0	1	0	2	3	1	2	2	2	1	0	0	2	3	1	?	0	?	?	0	1	0	0	1	1
Moxostoma erythrurum	2	2	2	1	1	0	1	0	2	3	1	2	2	1	1	1	1	2	3	1	3	0	3	1	1	1	0	0	1	1
Moxostoma poecilurum	2	2	2	1	1	0	1	0	2	3	1	2	2	2	1	1	0	1	3	1	?	0	3	0	1	1	1	0	1	1
Myxocyprinus asiaticus	2	2	0	0	1	0	0	0	2	2	1	2	2	1	1	1	0	1	1	0	1	0	1	0	1	1	1	0	1	0
Catostomus (Pantosteus) plebeius	2	2	2	?	?	?	?	2	0	3	1	1	3	0	1	1	0	1	1	0	3	0	1	2	1	0	0	0	1	0
Xyrauchen texanus	2	2	2	?	?	?	?	2	0	3	1	1	2	2	1	0	0	0	2	0	?	0	3	0	0	0	0	0	1	1

species/characters	61	62	63	64	65	66	67	68	69	70	71	72	73	74	75	76	77	78	79	80	81	82	83	84	85	86	87	88	89	90
Gyrinocheilus aymonieri	0	?	1	0	1	?	?	2	?	0	1	0	0	1	0	0	0	0	0	0	1	1	0	0	?	?	1	?	?	?
Cyprinus carpio	2	0	3	2	0	1	1	0	3	2	3	2	1	0	0	0	0	0	0	0	0	0	0	0	0	0	0	0	0	0
†*Jianghanichthys hubeiensis*	0	?	3	0	2	1	1	1	3	0	0	1	?	0	1	0	0	0	1	0	1	1	0	0	1	2	?	?	?	?
Cobitis taenia	3	0	0	3	0	2	?	1	1	2	3	0	1	1	0	2	0	0	1	1	1	1	0	?	?	?	0	0	0	0
Chromobotia macracanthus	3	0	0	3	0	2	?	0	0	0	3	1	0	1	4	4	1	0	1	0	1	1	0	1	5	6	0	?	?	?
†"NewGenus" *brevipinne*	1	?	3	0	1	?	?	0	1	2	2	2	?	1	?	1	0	0	2	0	1	1	0	?	1		?	?	?	?
†*Amyzon aggregatum*	2	?	3	1	1	1	?	1	2	2	2	2	?	1	0	1	0	0	2	0	1	1	0	0	1	0	?	0	2	3
†*Amyzon commune*	1	?	3	1	2	?	?	0	1	2	1	?	?	1	1	0	1	0	1	?	?	1	0	0	?	4	?	?	?	?
†*Amyzon gosiutense*	1	0	3	0	1	1	?	1	1	2	2	2	?	1	0	0	0	0	2	0	1	1	0	0	1	0	?	?	?	?
†*Amyzon kishenehnicum*	2	?	3	0	1	1	?	2	1	2	2	2	?	1	0	0	0	0	2	0	1	1	0	?	?	?	?	?	?	?
†*Amyzon hunanense*	0	?	1	0	0	?	?	1	1	2	2	?	?	1	0	0	0	0	2	0	1	1	0	?	?	?	?	?	?	?
†*Plesiomyxocyprinus arratiae*	?	?	?	?	0	1	?	0	1	2	2	?	?	1	?	0	0	?	?	?	?	?	?	?	?	?	?	?	?	?
Carpiodes cyprinus	3	0	1	1	1	0	1	1	2	2	1	2	1	1	0	1	1	0	2	0	1	1	0	0	?	?	1	0	3	3
Catostomus bernardini	0	1	3	1	1	2	2	1	2	1	2	2	1	1	1	1	1	?	2	0	1	1	1	0	2	3	1	0	1	2
Catostomus cahita	1	1	1	1	2	2	2	2	1	1	2	2	1	1	1	1	1	1	2	0	1	1	1	0	2	3	1	?	?	?
Catostomus catostomus	2	1	2	1	0	1	0	2	2	2	2	2	1	1	1	1	0	2	2	0	1	1	1	0	2	3	1	0	1	2
Catostomus commersonii	2	1	3	1	0	1	0	1	3	1	2	2	1	1	1	1	1	2	2	0	1	1	1	0	2	3	1	0	1	2
Catostomus fumeiventris	1	1	3	1	1	2	1	1	1	2	2	2	1	1	?	1	1	?	2	0	1	1	1	0	2	3	1	0	1	3
Catostomus latipinnis	1	1	2	1	2	2	2	2	2	0	2	2	1	1	?	2	1	?	2	0	1	1	1	0	2	3	1	1	1	3
Catostomus leopoldi	0	1	2	1	1	0	1	2	1	2	2	2	1	1	?	3	1	?	2	0	1	1	1	0	2	3	1	0	1	2
Deltistes (Catostomus) luxatus	1	?	1	0	0	1	0	1	3	1	2	2	1	1	1	0	0	?	2	0	1	1	1	0	2	3	1	3	1	4
Catostomus macrocheilus	1	1	3	1	0	2	1	2	2	2	2	2	1	1	?	0	1	?	2	0	1	1	1	0	2	3	1	1	1	3
Catostomus occidentalis	1	1	2	1	1	2	2	1	2	2	1	2	1	1	?	3	1	?	2	0	1	1	1	0	2	3	1	0	1	2
Catostomus platyrhynchus	0	1	3	1	1	2	2	2	1	2	3	2	1	1	?	?	?	?	2	0	1	1	1	0	2	3	1	0	1	3
Catostomus rimiculus	1	1	?	1	1	2	2	1	3	2	1	2	1	1	?	3	1	?	2	0	1	1	1	0	2	3	1	0	1	2
Catostomus santaanae	0	1	3	1	1	2	2	2	3	2	2	2	1	1	?	1	0	?	2	0	1	1	1	0	2	3	1	0	1	3
Catostomus snyderi	1	1	3	1	1	2	1	1	3	2	2	2	1	1	?	0	1	?	2	0	1	1	1	0	2	3	1	0	1	3
Catostomus tahoensis	1	1	2	1	0	1	0	1	3	1	2	2	1	1	?	0	1	?	2	0	1	1	1	0	2	3	1	0	1	3

Catostomus wigginsi	2	1	3	1	1	2	2	2	2	?	2	2	1	1	?	1	1	0	2	0	1	1	1	0	2	3	1	0	1	1
Chasmistes brevirostris	2	1	3	0	0	1	0	0	3	1	2	2	1	1	1	1	0	?	2	0	1	1	2	0	2	3	1	4	3	4
Cycleptus elongatus	0	1	1	2	2	2	2	2	3	0	0	2	1	1	2	1	1	1	2	0	1	1	1	2	0	4	1	0	0	3
Erimyzon oblongus	1	1	2	?	1	1	2	0	3	2	2	2	1	1	1	0	0	1	2	0	1	1	1	0	1	5	1	0	1	3
Hypentelium nigricans	2	1	3	0	2	2	3	1	1	0	0	2	1	1	2	1	0	2	2	0	1	1	0	1	?	?	1	1	1	2
Ictiobus bubalus	?	0	?	?	2	0	-	0	1	1	1	2	1	1	1	1	1	0	2	0	1	1	0	0	2	2	1	0	3	4
Ictiobus cyprinellus	2	0	1	0	2	0	-	0	2	1	1	2	1	1	1	1	1	0	2	0	1	1	0	0	2	1	1	0	1	4
Ictiobus meridionalis	2	0	1	0	1	2	3	0	2	2	1	2	1	1	1	0	0	0	2	0	1	1	0	0	2	2	1	?	?	?
Moxostoma aureolum	0	1	2	1	1	?	?	2	2	1	2	2	1	1	2	1	1	0	2	0	1	1	1	1	?	?	1	?	?	?
Moxostoma carinatum	0	1	2	1	?	?	?	2	?	1	?	2	1	1	2	1	1	1	2	0	1	1	1	1	5	5	1	0	1	2
Moxostoma erythrurum	1	1	2	0	2	1	0	2	1	1	2	2	1	1	2	1	1	1	2	0	1	1	1	1	5	5	1	0	1	2
Moxostoma poecilurum	1	1	2	1	1	2	2	2	3	1	1	2	1	1	3	1	1	1	2	0	1	1	1	2	5	5	1	0	1	2
Myxocyprinus asiaticus	1	0	2	1	1	-	-	0	3	0	1	2	1	1	1	0	1	0	2	0	1	1	1	1	3	4	1	0	0	3
Catostomus (Pantosteus) plebeius	1	1	3	1	1	2	0	2	2	2	2	2	1	1	?	?	?	?	?	0	1	1	1	0	?	?	1	0	1	3
Xyrauchen texanus	1	1	2	0	0	1	0	1	3	2	0	2	1	1	1	1	1	0	2	0	1	1	1	0	?	?	1	2	1	4

species/characters	91	92	93	94	95	96	97	98	99	100	101	102	103	104	105	106	107	108	109	110	111	112	113	114	115
Gyrinocheilus aymonieri	0	-	-	-	4	-	-	-	0	0	0	2	0	0	0	1	0	2	0	0	0	0	0	2	0
Cyprinus carpio	2	0	2	0	0	1	2	2	0	0	0	0	0	0	0	0	0	0	1	1	0	0	2	0	0
†*Jianghanichthys hubeiensis*	0	-	-	?	?	?	?	?	0	?	?	0	0	0	0	?	?	2	0	0	1	0	?	0	1
Cobitis taenia	1	?	?	?	?	?	?	?	2	1	0	2	0	1	0	0	1	2	0	0	0	0	?	2	0
Chromobotia macracanthus	1	0	0	0	0	1	0	0	2	1	0	2	0	?	?	?	?	?	0	0	0	0	1	2	0
†*"NewGenus" brevipinne*	1	0	0	0	2	0	0	?	0	0	0	1	0	0	0	1	0	0	0	0	2	1	?	2	0
†*Amyzon aggregatum*	1	1	0	0	2	1	0	0	0	0	0	1	0	0	0	1	0	0	1	1	2	1	0	2	0
†*Amyzon commune*	1	?	0	?	1	?	?	?	0	0	?	?	0	0	0	0	?	?	1	1	2	1	0	2	1
†*Amyzon gosiutense*	1	1	0	?	?	?	?	?	0	0	0	1	0	0	0	2	1	0	0	1	2	1	?	2	0
†*Amyzon kishenehnicum*	1	?	?	?	?	?	?	?	0	0	?	1	0	0	0	1	0	0	1	1	2	1	?	2	0
†*Amyzon hunanense*	1	?	0	?	?	?	?	?	0	0	0	1	0	0	0	1	0	0	0	1	2	1	?	2	0
†*Plesiomyxocyprinus arratiae*	1	1	0	0	2	1	0	0	0	0	0	0	0	?	0	0	0	0	1	2	3	1	?	?	0
Carpiodes cyprinus	1	1	0	0	2	1	0	0	0	0	0		0	0	0	0	0	1	1	0	1	1	1	2	0
Catostomus bernardini	1	1	0	0	1	0	1	1	1	0		1	1	0	1	1	1	2	0	0	1	1	2	2	1
Catostomus cahita	1	0	0	0	1	0	1	1	1	0		1	1	0	0	1	1	2	0	0	1	1	2	2	1
Catostomus catostomus	1	0	1	0	1	1	1	1	1	0		1	1	0	1	2	1	2	0	0	1	1	2	2	1
Catostomus commersonii	1	1	1	0	1	1	1	1	1	0	1	1	1	0	1	2	1	2	0	0	1	1	2	2	1
Catostomus fumeiventris	1	1	0	0	1	1	1	1	1	0		1	1	0	1	2	1	2	0	0	1	1	2	2	1
Catostomus latipinnis	1	1	0	0	1	1	1	1	1	0		1	1	0	1	1	1	2	0	0	1	1	2	2	1
Catostomus leopoldi	1	0	0	0	1	1	1	1	1	0		1	0	0	1	2	1	2	0	0	1	1	2	2	1
Deltistes (Catostomus) luxatus	1	1	1	0	2	1	1	1	1	0		1	1	0	1	?	1	2	0	0	1	1	2	2	1
Catostomus macrocheilus	1	1	0	0	1	1	1	1	1	0		1	1	0	1	2	1	2	0	0	1	1	2	2	1
Catostomus occidentalis	1	1	1	0	1	0	1	1	1	0		1	1	0	?	1	1	2	0	0	1	1	2	2	1
Catostomus platyrhynchus	1	0	1	0	1	0	1	1	1	0		1	?	0	?	?	?	2	0	0	1	1	2	2	?
Catostomus rimiculus	1	1	1	0	1	0	1	1	1	0		1	0	0	1	2	1	2	0	0	1	1	2	2	1
Catostomus santaanae	1	?	?	0	1	?	?	?	1	0		1	?	0	?	?	1	?	0	0	1	1	?	2	?
Catostomus snyderi	1	1	1	0	1	1	1	1	1	0		1	1	0	1	1	?	2	0	0	1	1	2	2	1
Catostomus tahoensis	1	1	0	0	1	1	1	1	1	0		1	0	0	1	2	1	2	0	0	1	1	2	2	1

Taxon	1	2	3	4	5	6	7	8	9	10	11	12	13	14	15	16	17	18	19	20	21	22	23	24	25
Catostomus wigginsi	1	0	1	0	1	0	1	1	1	0		1	0	0	?	?	?	?	0	0	1	1	2	2	1
Chasmistes brevirostris	1	1	1	0	2	0	1	1	1	1		1	1	0	1	1	1	2	0	0	1	1	2	2	1
Cycleptus elongatus	1	0	1	0	1	0	1	1	0	1	0	1	0	0	0	1	0	1	1	1	1	1	2	2	1
Erimyzon oblongus	1	1	0	1	2	0	1	0	1	1	0	1	0	0	1	2	1	2	0	0	1	1	2	2	1
Hypentelium nigricans	1	1	0	0	1	?	0	0	1	0		?	?	0	?	?	?	?	0	0	1	1	2	2	1
Ictiobus bubalus	1	2	1	0	3	0	0	1	0	0	0	0	0	0	0	1	1	1	1	1	2	1	0	2	0
Ictiobus cyprinellus	1	2	1	0	3	0	0	0	0	0	0	1	0	0	1	0	1	1	1	1	2	1	0	2	0
Ictiobus meridionalis	1	?	?	0	3	0	0	0	0	0	0	0	0	0	1	1	1	1	1	1	2	1	0	2	0
Moxostoma aureolum	1	0	1	0	1	0	1	1	1	2	2	1	0	0	1	2	1	2	0	0	1	1	2	2	1
Moxostoma carinatum	1	0	2	0	1	0	1	1	0	2		1	0	0	1	2	1	2	0	0	1	1	2	2	1
Moxostoma erythrurum	1	1	2	0	1	0	1	1	1	2		1	0	0	1	2	1	2	0	0	1	1	2	2	1
Moxostoma poecilurum	1	1	2	0	1	0	1	1	1	2		1	0	0	1	2	1	2	0	0	2	1	2	2	1
Myxocyprinus asiaticus	1	1	0	0	2	0	0	0	0	2	0	0	0	0	0	0	1	0	1	0	3	1	1	2	0
Catostomus (Pantosteus) plebeius	1	0	0	0	1	0	1	1	1	0		1	?	0	?	?	1	?	0	0	1	1	2	2	1
Xyrauchen texanus	1	1	1	0	2	1	1	1	1	0	0	1	0	0	1	1	?	?	0	0	1	1	2	2	1

311

species/characters	116	117	118	119	120	121	122	123	124	125	126	127	128	129	130	131	132	133	134
Gyrinocheilus aymonieri	2	2	1	?	1	0	0	1	1	0	1	-	0	1	0	1	0	2	0
Cyprinus carpio	2	2	0	0	1	2	0	0	0	1	0	-	0	0	0	0	2	0	0
†Jianghanichthys hubeiensis	0	0	0	?	0	0	0	0	2	?	0	-	0	0	0	0	0	0	0
Cobitis taenia	1	1	0	?	?	0	1	1	2	0	0	-	0	1	0	2	0	2	1
Chromobotia macracanthus	1	3	1	0	?	0	2	1	2	0	0	-	0	0	0	2	0	1	1
†"NewGenus" brevipinne	0	0	2	1	?	0	1	1	1	?	0	?	0	0	0	1	0	1	0
†Amyzon aggregatum	0	0	2	1	?	0	1	1	1	0	1	0	0	0	0	0	1	0	0
†Amyzon commune	0	0	?	?	0	0	1	1	1	0	1	?	0	0	0	0	1	0	0
†Amyzon gosiutense	0	0	2	1	?	0	1	1	2	1	0	?	0	0	0	0	1	0	0
†Amyzon kishenehnicum	0	0	2	1	?	0	1	1	1	0	1	?	1	0	0	0	1	0	0
†Amyzon hunanense	0	0	?	?	0	0	1	1	1	0	1	?	0	0	0	0	1	0	0
†Plesiomyxocyprinus arratiae	0	2	?	?	?	0	1	1	1	?	1	?	1	0	1	0	?	0	?
Carpiodes cyprinus	1	1	2	1	1	0	1	2	1	0	1	0	1	0	0	0	1	0	1
Catostomus bernardini	2	2	2	1	?	2	1	1	0	1	0	1	0	0	0	1	1	2	?
Catostomus cahita	2	3	2	1	?	2	1	1	0	1	0	1	0	0	?	1	1	2	?
Catostomus catostomus	2	3	2	1	?	2	1	1	2	1	0	1	0	0	?	1	1	2	1
Catostomus commersonii	2	3	2	1	1	2	1	1	0	1	0	1	0	0	1	1	1	2	1
Catostomus fumeiventris	2	3	2	1	?	2	1	1	0	1	0	1	0	0	?	1	1	2	?
Catostomus latipinnis	1	3	2	1	?	2	1	1	0	1	0	1	0	0	?	1	1	2	?
Catostomus leopoldi	1	3	2	1	?	2	1	1	0	1	0	1	0	0	0	1	1	2	?
Deltistes (Catostomus) luxatus	2	3	2	1	?	2	1	2	1	1	0	1	0	0	?	1	2	1	1
Catostomus macrocheilus	2	3	2	1	?	2	1	1	0	1	0	1	0	0	?	1	1	2	1
Catostomus occidentalis	1	3	2	1	?	2	1	1	0	1	0	1	0	0	1	1	1	2	1
Catostomus platyrhynchus	?	?	2	1	?	2	1	1	?	1	?	?	?	0	?	1	0	2	?
Catostomus rimiculus	2	3	2	1	?	2	1	1	0	1	0	1	0	0	?	1	1	2	?
Catostomus santaanae	?	?	2	1	?	2	1	1	?	1	?	?	?	0	?	1	0	2	?
Catostomus snyderi	2	3	2	1	?	2	1	1	0	1	0	1	0	0	?	1	1	2	?
Catostomus tahoensis	2	3	2	1	?	2	1	1	0	1	0	1	0	0	?	1	1	2	?

Species																			
Catostomus wigginsi	2	2	2	1	?	2	1	1	0	1	0	1	0	0	1	1	0	2	?
Chasmistes brevirostris	2	3	2	1	1	?	?	1	0	1	0	1	0	0	?	1	1	1	?
Cycleptus elongatus	2	2	2	1	0	0	1	1	2	1	0	1	0	0	1	0	2	1	1
Erimyzon oblongus	2	3	2	1	1	2	2	1	1	0	1	0	0	1	1	0	1	1	0
Hypentelium nigricans	2	2	2	1	0	1	2	1	2	1	0	1	0	0	0	0	1	2	0
Ictiobus bubalus	1	1	2	1	1	0	0	2	1	0	1	0	1	0	0	0	1	0	0
Ictiobus cyprinellus	1	2	2	1	1	0	0	2	1	0	1	0	1	0	0	0	2	0	0
Ictiobus meridionalis	1	1	2	1	1	0	0	2	1	0	1	0	1	0	0	0	1	0	?
Moxostoma aureolum	3	2	2	1	0	1	1	1	2	1	0	0	0	0	0	1	1	2	?
Moxostoma carinatum	3	2	2	1	0	2	1	1	2	1	?	0	0	0	1	1	1	2	1
Moxostoma erythrurum	3	2	2	1	0	1	1	1	2	1	1	0	0	0	0	1	1	2	1
Moxostoma poecilurum	3	2	2	1	0	2	1	1	2	1	1	1	0	0	1	1	1	2	?
Myxocyprinus asiaticus	2	2	2	1	0	0	1	2	1	0	1	0	1	0	1	0	2	0	0
Catostomus (Pantosteus) plebeius	?	?	2	1	1	?	?	1	?	?	?	?	1	0	?	1	0	2	?
Xyrauchen texanus	1	1	2	1	1	1	2	1	2	1	1	0	1	0	1	1	2	1	0

Appendix 6. 2 Synapomorphies common to four equally most parsimonious trees generated by TNT. Node numbers refer to nodes in strict consensus tree (Fig. 6.13). "Char." is short for Character.

Gyrinocheilus aymonieri: All trees: No autapomorphies;

Cyprinus carpio: All trees: Char. 16: 1 --> 0, Char. 20: 1 --> 0, Char. 24: 0 --> 1, Char. 25: 0 --> 1, Char. 28: 1 --> 0, Char. 29: 1 --> 0, Char. 30: 3 --> 1, Char. 32: 0 --> 1, Char. 38: 0 --> 1, Char. 41: 2 --> 0, Char. 43: 2 --> 0, Char. 45: 0 --> 1, Char. 49: 0 --> 1, Char. 51: 0 --> 1, Char. 52: 3 --> 0, Char. 55: 2 --> 1, Char. 60: 0 --> 2, Char. 63: 0 --> 2, Char. 76: 0 --> 1, Char. 80: 1 --> 0, Char. 81: 1 --> 0, Char. 90: 0 --> 2, Char. 107: 2 --> 0, Char. 108: 0 --> 1, Char. 109: 0 --> 1, Char. 112: 0 --> 2, Char. 120: 0 --> 2, Char. 124: 0 --> 1, Char. 131: 0 --> 2;

Jianghanichthys hubeiensis: All trees: Char. 6: 0 --> 1, Char. 18: 0 --> 2, Char. 19: 01 --> 2, Char. 29: 1 --> 2, Char. 30: 3 --> 0, Char. 33: 0 --> 1, Char. 42: 0 --> 1, Char. 50: 1 --> 0, Char. 64: 01 --> 2, Char. 70: 3 --> 0, Char. 74: 0 --> 1, Char. 85: 0 --> 2, Char. 110: 0 --> 1, Char. 114: 0 --> 1

Cobitis taenia: All trees: Char. 5: 2 --> 0, Char. 23: 0 --> 1, Char. 28: 1 --> 3, Char. 33: 0 --> 2, Char. 41: 1 --> 0, Char. 47: 1 --> 0, Char. 49: 0 --> 1, Char. 79: 0 --> 1, Char. 128: 0 --> 1;

Chromobotia macracanthus: All trees: Char. 1: 2 --> 5, Char. 7: 1 --> 0, Char. 26: 0 --> 2, Char. 38: 0 --> 1, Char. 42: 0 --> 3, Char. 45: 0 --> 2, Char. 68: 1 --> 0, Char. 72: 1 --> 0, Char. 74: 0 --> 4, Char. 76: 0 --> 1, Char. 117: 0 --> 1, Char. 121: 1 --> 2;

"NewGenus" *brevipinne*: All trees: Char. 18: 0 --> 1, Char. 47: 1 --> 0, Char. 52: 2 --> 1, Char. 75: 0 --> 1, Char. 95: 1 --> 0, Char. 130: 0 --> 1;

Amyzon aggregatum: All trees: Char. 25: 0 --> 1, Char. 38: 0 --> 1, Char. 43: 2 --> 1, Char. 56: 0 --> 1, Char. 68: 1 --> 2, Char. 75: 0 --> 1; Some trees: Char. 59: 1 --> 0, Char. 63: 0 --> 1;

Amyzon commune: All trees: Char. 6: 1 --> 0, Char. 19: 1 --> 2, Char. 43: 2 --> 1, Char. 44: 1 --> 0, Char. 49: 0 --> 1, Char. 64: 1 --> 2, Char. 78: 2 --> 1, Char. 94: 2 --> 1, Char. 114: 0 --> 1;

Amyzon gosiutense: All trees: Char. 55: 1 --> 0, Char. 105: 1 --> 2, Char. 106: 0 --> 1, Char. 123: 1 --> 2, Char. 124: 0 --> 1, Char. 125: 1 --> 0; Some trees: Char. 108: 1 --> 0, *Amyzon kishenehnicum*: All trees: Char. 67: 1 --> 2, Char. 127: 0 --> 1;

Amyzon hunanense: All trees: Char. 8: 2 --> 1, Char. 37: 1 --> 2, Char. 42: 2 --> 3, Char. 50: 1 --> 2, Char. 55: 1 --> 0, Char. 62: 3 --> 1;

Plesiomyxocyprinus arratiae: All trees: Char. 8: 2 --> 1, Char. 53: 0 --> 1, Char. 64: 1 --> 0, Char. 70: 1 --> 2, Char. 76: 1 --> 0;

Carpiodes cyprinus: All trees: Char. 8: 2 --> 1, Char. 15: 1 --> 0, Char. 29: 2 --> 1, Char. 43: 2 --> 0, Char. 67: 0 --> 1, Char. 74: 1 --> 0, Char. 110: 2 --> 1, Char. 133: 0 --> 1;

Catostomus bernardini: All trees: Char. 37: 2 --> 1, Char. 50: 3 --> 5, Char. 60: 1 --> 0, Char. 116: 3 --> 2;

Catostomus cahita: All trees: Char. 14: 2 --> 1, Char. 91: 1 --> 0, Char. 104: 1 --> 0;

Catostomus catostomus: All trees: Char. 38: 1 --> 2, Char. 43: 1 --> 2, Char. 48: 2 --> 0, Char. 49: 0 --> 1, Char. 62: 3 --> 2, Char. 68: 3 --> 2, Char. 69: 1 --> 2, Char. 91: 1 --> 0, Char. 123: 0 --> 2;

Catostomus commersonii: All trees: Char. 10: 0 --> 1, Char. 59: 0 --> 1; Some trees: Char. 0: 3 --> 1;

Catostomus fumeiventris: All trees: Char. 43: 1 --> 2, Char. 52: 3 --> 2, Char. 53: 0 --> 1, Char. 54: 0 --> 1, Char. 68: 2 --> 1;

315

Catostomus latipinnis: All trees: Char. 50: 3 --> 5, Char. 53: 0 --> 2, Char. 75: 1 --> 2, Char. 87: 0 --> 1, Char. 89: 2 --> 3, Char. 95: 0 --> 1, Char. 115: 2 --> 1;

Catostomus leopoldi: All trees: Char. 41: 1 --> 2, Char. 62: 3 --> 2, Char. 65: 2 --> 0, Char. 89: 3 --> 2, Char. 95: 0 --> 1, Char. 115: 2 --> 1, Char. 129: 1 --> 0; Some trees: Char. 75: 1 --> 3;

Deltistes (*Catostomus*) *luxatus*: All trees: Char. 52: 3 --> 2, Char. 53: 0 --> 2, Char. 62: 2 --> 1, Char. 87: 0 --> 3, Char. 122: 1 --> 2; Some trees: Char. 0: 2 --> 1;

Catostomus macrocheilus: All trees: Char. 48: 2 --> 1, Char. 50: 3 --> 1, Char. 67: 1 --> 2, Char. 87: 0 --> 1; Some trees: Char. 64: 1 --> 0;

Catostomus occidentalis: All trees: Char. 37: 2 --> 0, Char. 115: 2 --> 1;

Catostomus platyrhynchus: All trees: Char. 70: 2 --> 3;

Catostomus rimiculus: All trees: Char. 14: 2 --> 1, Char. 15: 1 --> 0, Char. 52: 3 --> 2, Char. 54: 0 --> 1, Char. 68: 2 --> 3, Char. 102: 1 --> 0;

Catostomus santaanae: All trees: Char. 59: 0 --> 1;

Catostomus snyderi: All trees: Char. 52: 3 --> 2, Char. 105: 2 --> 1;

Catostomus tahoensis: All trees: Char. 52: 3 --> 1, Char. 92: 1 --> 0;

Catostomus wigginsi: All trees: Char. 37: 2 --> 1, Char. 47: 1 --> 2, Char. 60: 0 --> 2, Char. 89: 3 --> 1;

Chasmistes brevirostris: All trees: Char. 39: 3 --> 1, Char. 55: 0 --> 2, Char. 56: 0 --> 1, Char. 63: 1 --> 0, Char. 82: 1 --> 2, Char. 87: 0 --> 4, Char. 88: 1 --> 3, Char. 89: 2 --> 4, Char. 94: 1 --> 2, Char. 95: 1 --> 0, Char. 99: 0 --> 1, Char. 105: 2 --> 1, Char. 132: 2 --> 1;

Cycleptus elongatus: All trees: Char. 1: 1 --> 4, Char. 10: 1 --> 0, Char. 14: 2 --> 0, Char. 15: 1 --> 0, Char. 17: 2 --> 0, Char. 34: 1 --> 2, Char. 42: 2 --> 3, Char. 53: 0 --> 1, Char. 58: 1 --> 0, Char. 60: 12 --> 0, Char. 63: 1 --> 2, Char. 83: 1 --> 2, Char. 84: 2 --> 0, Char. 91: 1 --> 0, Char. 92: 0 --> 1, Char. 99: 0 --> 1;

Erimyzon oblongus: All trees: Char. 4: 2 --> 1, Char. 17: 0 --> 1, Char. 22: 1 --> 0, Char. 23: 0 --> 1, Char. 47: 0 --> 1, Char. 53: 0 --> 1, Char. 64: 0 --> 1, Char. 66: 0 --> 2, Char. 67: 1 --> 0, Char. 92: 1 --> 0, Char. 93: 0 --> 1, Char. 95: 1 --> 0, Char. 97: 1 --> 0, Char. 99: 0 --> 1, Char. 124: 1 --> 0, Char. 128: 0 --> 1, Char. 130: 1 --> 0;

Hypentelium nigricans: All trees: Char. 1: 1 --> 6, Char. 21: 0 --> 1, Char. 47: 1 --> 2, Char. 63: 1 --> 0, Char. 66: 2 --> 3, Char. 67: 2 --> 1, Char. 76: 1 --> 0, Char. 77: 01 --> 2, Char. 82: 1 --> 0, Char. 87: 0 --> 1, Char. 121: 1 --> 2; Some trees: Char. 60: 1 --> 2;

Ictiobus bubalus: All trees: Char. 1: 2 --> 3, Char. 43: 2 --> 1, Char. 46: 0 --> 1, Char. 48: 1 --> 2, Char. 68: 2 --> 1, Char. 97: 0 --> 1;

Ictiobus cyprinellus: All trees: Char. 85: 2 --> 1, Char. 88: 3 --> 1, Char. 101: 0 --> 1, Char. 116: 1 --> 2, Char. 131: 1 --> 2;

Ictiobus meridionalis: All trees: Char. 37: 1 --> 2, Char. 52: 2 --> 1, Char. 54: 1 --> 0, Char. 55: 1 --> 0, Char. 65: 0 --> 2, Char. 76: 1 --> 0;

Moxostoma aureolum: All trees: Char. 17: 2 --> 1, Char. 21: 0 --> 1, Char. 42: 2 --> 3, Char. 56: 0 --> 1, Char. 60: 1 --> 0, Char. 91: 1 --> 0;

Moxostoma carinatum: All trees: Char. 45: 1 --> 0, Char. 54: 1 --> 0, Char. 60: 1 --> 0, Char. 91: 1 --> 0, Char. 98: 1 --> 0;

Moxostoma erythrurum: All trees: Char. 26: 1 --> 0, Char. 43: 2 --> 1, Char. 46: 0 --> 1, Char. 53: 0 --> 1, Char. 63: 1 --> 0, Char. 65: 2 --> 1, Char. 66: 2 --> 0;

Moxostoma poecilurum: All trees: Char. 10: 0 --> 1, Char. 17: 2 --> 1, Char. 56: 0 --> 1, Char. 74: 2 --> 3, Char. 83: 1 --> 2, Char. 110: 1 --> 2, Char. 126: 0 --> 1;

Myxocyprinus asiaticus: All trees: Char. 35: 1 --> 0, Char. 52: 2 --> 1, Char. 59: 1 --> 0, Char. 84: 2 --> 3, Char. 99: 0 --> 2, Char. 122: 1 --> 2;

Catostomus (*Pantosteus*) *plebeius*: All trees: Char. 1: 5 --> 6, Char. 14: 2 --> 0, Char. 17: 0 --> 1, Char. 22: 1 --> 0, Char. 23: 0 --> 1, Char. 28: 0 --> 2, Char. 43: 1 --> 0, Char. 48: 2 --> 1, Char. 52: 3 --> 1, Char. 53: 0 --> 2, Char. 54: 0 --> 1, Char. 66: 12 --> 0, Char. 127: 0 --> 1;

Xyrauchen texanus: All trees: Char. 26: 1 --> 0, Char. 27: 1 --> 3, Char. 37: 1 --> 2, Char. 42: 3 --> 2, Char. 43: 1 --> 2, Char. 70: 2 --> 0, Char. 75: 0 --> 1, Char. 87: 0 --> 2, Char. 105: 2 --> 1, Char. 115: 2 --> 1, Char. 116: 3 --> 1, Char. 120: 2 --> 1, Char. 123: 1 --> 2, Char. 127: 0 --> 1;

Node 44: All trees: No synapomorphies;

Node 45: All trees: Char. 1: 0 --> 2, Char. 2: 0 --> 1, Char. 5: 1 --> 2, Char. 39: 0 --> 1, Char. 78: 0 --> 1, Char. 115: 2 --> 0, Char. 116: 2 --> 0, Char. 119: 1 --> 0;

Node 46: All trees: Char. 2: 1 --> 2, Char. 3: 0 --> 3, Char. 8: 2 --> 3, Char. 16: 1 --> 2, Char. 32: 0 --> 2, Char. 50: 1 --> 5, Char. 62: 3 --> 0, Char. 63: 0 --> 3, Char. 65: 1 --> 2, Char. 98: 0 --> 2, Char. 99: 0 --> 1, Char. 115: 0 --> 1, Char. 130: 0 --> 2, Char. 133: 0 --> 1;

Node 47: All trees: Char. 14: 0 --> 2, Char. 15: 0 --> 1, Char. 41: 2 --> 1, Char. 52: 3 --> 2, Char. 53: 1 --> 0, Char. 58: 0 --> 1, Char. 68: 3 --> 1, Char. 90: 0 --> 1, Char. 121: 0 --> 1;

Node 48: All trees: Char. 1: 2 --> 1, Char. 12: 0 --> 1, Char. 20: 1 --> 0, Char. 42: 0 --> 2, Char. 55: 2 --> 1, Char. 70: 3 --> 2, Char. 78: 1 --> 2, Char. 94: 0 --> 2, Char. 107: 2 --> 0, Char. 110: 0 --> 2, Char. 111: 0 --> 1, Char. 117: 0 --> 2, Char. 118: 0 --> 1;

Node 49: All trees: Char. 17: 1 --> 0, Char. 18: 0 --> 2;

Node 50: All trees: Char. 45: 0 --> 1; Some trees: Char. 59: 0 --> 1, Char. 108: 0 --> 1;

Node 51: All trees: Char. 5: 2 --> 3, Char. 6: 0 --> 1, Char. 29: 1 --> 2, Char. 33: 0 --> 1, Char. 109: 0 --> 1, Char. 125: 0 --> 1, Char. 131: 0 --> 1;

Node 52: All trees: Char. 70: 2 --> 1, Char. 74: 0 --> 1, Char. 76: 0 --> 1, Char. 85: 0 --> 4, Char. 105: 1 --> 0; Some trees: Char. 63: 0 --> 1;

Node 53: All trees: Char. 110: 2 --> 3, Char. 129: 0 --> 1;

Node 54: All trees: Char. 4: 2 --> 1, Char. 25: 0 --> 1, Char. 33: 1 --> 0, Char. 39: 1 --> 2, Char. 127: 0 --> 1; Some trees: Char. 10: 0 --> 1;

Node 55: All trees: Char. 1: 1 --> 2, Char. 17: 1 --> 0, Char. 23: 0 --> 1, Char. 44: 1 --> 2, Char. 65: 1 --> 0, Char. 68: 1 --> 2, Char. 88: 0 --> 3, Char. 107: 0 --> 1, Char. 115: 0 --> 1, Char. 119: 0 --> 1, Char. 122: 1 --> 2;

Node 56: All trees: Char. 64: 2 --> 1, Char. 67: 2 --> 1;

Node 57: All trees: Char. 37: 0 --> 2, Char. 42: 2 --> 3, Char. 43: 2 --> 1, Char. 59: 1 --> 0;

Node 58: All trees: Char. 0: 1 --> 3, Char. 1: 1 --> 5, Char. 17: 2 --> 0, Char. 18: 1 --> 2, Char. 22: 0 --> 1, Char. 28: 2 --> 0, Char. 54: 1 --> 0, Char. 55: 1 --> 0, Char. 83: 1 --> 0, Char. 102: 0 --> 1, Char. 116: 2 --> 3, Char. 120: 1 --> 2, Char. 123: 2 --> 0;

Node 59: All trees: Char. 12: 1 --> 0, Char. 50: 4 --> 3, Char. 52: 2 --> 3, Char. 70: 0 --> 2, Char. 130: 0 --> 1;

Node 60: All trees: Char. 3: 0 --> 2, Char. 4: 1 --> 2, Char. 8: 2 --> 3, Char. 25: 1 --> 0, Char. 29: 2 --> 1, Char. 32: 0 --> 2, Char. 88: 0 --> 1, Char. 89: 3 --> 2, Char. 98: 0 --> 1, Char. 108: 1 --> 0, Char. 120: 0 --> 1, Char. 129: 1 --> 0;

Node 61: All trees: Char. 19: 1 --> 2, Char. 50: 1 --> 4, Char. 61: 0 --> 1, Char. 64: 1 --> 2, Char. 67: 0 --> 2, Char. 70: 1 --> 0, Char. 74: 1 --> 2, Char. 75: 0 --> 1, Char. 94: 2 --> 1, Char. 101: 0 --> 1, Char. 105: 0 --> 1, Char. 110: 3 --> 1, Char. 114: 0 --> 1, Char. 123: 1 --> 2, Char. 124: 0 --> 1, Char. 125: 1 --> 0, Char. 126: 0 --> 1, Char. 127: 1 --> 0;

Node 62: All trees: Char. 17: 1 --> 2, Char. 41: 1 --> 2, Char. 69: 2 --> 0, Char. 95: 1 --> 0, Char. 115: 0 --> 2;

Node 63: All trees: Char. 37: 1 --> 0, Char. 52: 3 --> 1, Char. 53: 0 --> 1, Char. 76: 1 --> 0;

Node 64: All trees: Char. 60: 1 --> 2, Char. 77: 01 --> 2, Char. 89: 3 --> 2; Some trees: Char. 75: 0 --> 1;

Node 65: All trees: Char. 65: 2 --> 1, Char. 66: 1 --> 0, Char. 69: 2 --> 1; Some trees: Char. 64: 1 --> 0;

Node 66: All trees: Char. 68: 2 --> 3, Char. 92: 0 --> 1;

Node 67: All trees: Char. 37: 2 --> 1, Char. 95: 0 --> 1;

Node 68: All trees: Char. 10: 1 --> 0, Char. 89: 2 --> 3;

Node 69: All trees: Char. 41: 2 --> 1, Char. 69: 1 --> 2, Char. 129: 0 --> 1;

Node 70: All trees: Char. 3: 2 --> 1, Char. 50: 3 --> 4, Char. 60: 1 --> 0;

Node 71: All trees: Char. 15: 1 --> 0, Char. 67: 1 --> 2, Char. 91: 1 --> 0;

Node 72: All trees: Char. 63: 1 --> 0, Char. 94: 1 --> 2, Char. 123: 0 --> 1, Char. 132: 2 --> 1;

Node 73: All trees: Char. 45: 1 --> 0, Char. 47: 1 --> 0, Char. 62: 3 --> 2; Some trees: Char. 0: 3 --> 2;

Node 74: All trees: Char. 53: 0 --> 2, Char. 70: 2 --> 1, Char. 92: 0 --> 1; Some trees: Char. 75: 1 --> 3;

Node 75: All trees: Char. 17: 0 --> 2, Char. 55: 0 --> 1;

Node 76: All trees: Char. 14: 2 --> 1, Char. 92: 0 --> 1;

Node 77: All trees: Char. 10: 0 --> 1, Char. 25: 0 --> 1, Char. 28: 0 --> 2, Char. 59: 0 --> 1, Char. 69: 1 --> 2, Char. 121: 1 --> 2, Char. 125: 0 --> 1, Char. 126: 1 --> 0, Char. 133: 1 --> 0;

Node 78: All trees: Char. 53: 0 --> 2, Char. 64: 1 --> 2, Char. 69: 2 --> 1;

Node 79: All trees: Char. 3: 0 --> 1, Char. 18: 0 --> 2, Char. 45: 1 --> 0, Char. 48: 0 --> 1, Char. 63: 1 --> 0, Char. 94: 2 --> 3, Char. 95: 1 --> 0, Char. 106: 0 --> 1, Char. 121: 1 --> 0;

Node 80: All trees: Char. 7: 1 --> 0, Char. 10: 1 --> 0, Char. 35: 1 --> 0, Char. 99: 0 --> 2, Char. 105: 1 --> 2, Char.

115: 2 --> 3, Char. 126: 1 --> 0;

Node 81: All trees: Char. 1: 1 --> 3, Char. 120: 1 --> 2, Char. 129: 0 --> 1;

Node 82: All trees: Char. 0: 1 --> 2, Char. 125: 0 --> 1, ;

Chapter 7 Analysis of body shape variation, allometry, and evolutionary transformations of Eocene catostomids and jianghanichthyids using geometric morphometrics

Introduction

Species of *Amyzon* and "NewGenus" (Order: Cypriniformes, Family: Catostomidae) are extinct catostomid fishes known from Eocene deposits of North America and East Asia (Cope, 1872; Cope, 1874; Cope, 1875; Cope, 1893; Wilson, 1977a; Grande et al., 1982; Chang et al., 2001; Liu et al., 2016). They are laterally compressed fishes with a terminal mouth, comparing to the usually sub-terminal mouth for suction feeding in extant catostomids. They are also usually the dominant fish in numbers of individuals within a fauna(Grande, 1980; Chang et al., 2001; Barton and Wilson, 2005). Their relative, *Jianghanichthys* (Cypriniformes, Jianghanichthyidae) displays a similar body shape and also tends to be the dominant fish in faunas where they are known (Liu et al., 2015).

The availability of a large number of specimens of several species has revealed considerable

intraspecific variation, eg: *Amyzon aggregatum* (Wilson, 1974), *A. gosiutense* (Grande et al., 1982), *A. hunanense* (Chang et al., 2001), and *A. kishenehnicum* (Liu et al., 2016). Together with the other Eocene catostomids, they possess highly overlapping meristic and metric characters, and this is especially true of the species of *Amyzon* (Bruner, 1991). Brunner (1991) thus designated *Amyzon gosiutense* as a junior synonym of *A. aggregatum*. "NewGenus" was also assigned to *Amyzon* when first described (Cope, 1893) and re-studied (Wilson, 1977a). Even *Jianghanichthys* was once considered to be an Eocene catostomid because of similarity in general appearance (Chang and Chen, 2008).

Maximum body size of Eocene catostomids species ranges from 80 mm (Chapter 4) to about 450 mm (Liu et al., 2016) in standard length. The body depth of Eocene catostomids and jianghanichthyids ranges from extremely deep (Liu and Chang, 2009)to relatively shallow body in "NewGenus" (Chapter 4). Ontogenetic allometry has also contributed to body shape changes. It has been often described as shallow in juvenile and deeper in the adults of Eocene catostomids and jianghanichthyids (Liu et al., 2015; Liu et al., 2016). However, how allometry and interspecific size difference interact with the external morphology of these species is not known.

Large numbers of specimens, subtle difference in meristics and measurements, and usually lateral preservation on a slab make Eocene catostomids and jianghanichthyids ideal candidates for geometric morphometric study, which is potentially able to answer the taxonomic discrimination questions among those species. Geometric morphometrics quantifies body shape variation and allows multivariate analyses and statistical tests that can be powerfully used in biology (Zelditch et al., 2004). It has been widely applied into various fields of study in biology.

This study aims to quantify body shape in Eocene catostomids and problematic catostomids (jianghanichthyids) for interspecific comparison and allometric changes, and mapping of phylogeny onto morphospace to detect possible evolutionary trajectory on body shape.

Materials and Methods

Specimen selection: All available specimens of Eocene catostomids and problematic catostomids were considered. They consist of laterally compressed individuals preserved on slabs in the two-dimensional lateral view. Complete and undeformed specimens are preferentially selected for analysis. Furthermore, specimens are qualified for inclusion in the analysis if all 14 landmarks (see below) were detectable. The ratio of qualified/captured specimens for each taxon are: *Amyzon aggregatum* (Wilson, 1977a), 19/33; "NewGenus" *brevipinne* (Chapter 4; Cope, 1893; Wilson, 1977a), 2/5; *A. commune* (Cope, 1875), 2/5; *A. gosiutense* (Grande et al., 1982), 8/19; *A. hunanense* (Chang et al., 2001) 9/23; *A. kishenehnicum* (Liu et al., 2016), 14/41; *Jianghanichthys hubeiensis* (Liu et al., 2015), 29/73. The total sample size is 83. The complete list of specimen used for this study can be found in the Appendix 7.1.

None of the type specimens of the species described by Cope (1893; 1872; 1874; 1875) was preserved well enough for GM; all were either incomplete or deformed. No specimens of *A. mentale*, *A. fusiforme*, or *A. pandatum*, qualified for the completeness and non-deformation requirements for geometric morphometric analysis, and thus were excluded.

The phylogeny that mapped in morphospace was from Chapter 6.

Image capturing: Eocene catostomids and the basal cypriniform *Jianghanichthys* were laterally compressed fishes, and each is nearly preserved laterally on a single plane of a slab within a shallow depth. This kind of preservation was ideal for surface scanning through imaging to capture body shape and minimizing the deformation from imaging. The scanners Epson Perfection 3590 in UALVP and Uniscan M800U in the IVPP were used. A few specimens were photographed using a Canon 70D with camera stand and manually adjusting the specimen's surface to be horizontal, when a scanner is not available.

Landmarks chosen and recorded: To define body shape, 14 homologous and detectable anatomical loci were recorded in the following order (Fig. 7.1): 1, posterior border of parietal; 2, anteromedial corner of premaxilla; 3, anterior tip of preopercle; 4, center of first centrum excluding Weberian apparatus; 5, origin of pectoral fin; 6, origin of pelvic fin; 7, origin of anal fin; 8, posterior insertion of anal fin; 9, ventral insertion of caudal fin; 10, posterodorsal tip of hypural 3; 11, dorsal insertion of caudal fin; 12, posterior insertion of dorsal fin; 13, origin of dorsal fin; 14, center of first caudal centrum.

The origins of dorsal and anal fins, loci 7 and 13, were recorded at the root of the first rudimentary fin ray. The insertion of paired fins, loci 5 and 7, are recognized on the left fin if the fish is left-side preserved, and vice versa.

Landmark digitization was done in the TPS software programs. The TPS file for each taxon represented by image stacks was created using TPS utility v. 1.68 (Rohlf, 2016). Landmarks were digitized based on selected images using tpsDig2 (Rohlf, 2010). The 14 landmarks were recorded in numerical order on right-side preserved specimens and horizontally flipped left-side preserved specimens. Scales for each image were digitized at the same time.

Geometric morphometric analyses: The following analysis series was performed in MorphoJ v. 1.06c (Klingenberg, 2011). MorphoJ is a graphical user interface analysis software including a range of multivariate statistical tools and exploratory functions for geometric morphometric analyses.

After the dataset has been transferred from TPS dig2 and combined in MorphoJ, Procrustes fit was performed to align the data. Procrustes superimposition was used to remove the position and orientation effect. Subsequent analyses were based on Procrustes coordinates only.

Principal component analysis (PCA), canonical variates analysis (CVA), and discriminant function analysis (DFA) were performed to describe body shape variations and disparity among species. Whereas PCA helps to identify the major axes of variation in the shape data, CVA identifies those shape variables that contribute most significantly to the separation of groups (in this case, species). Both methods plotted data with PCA and CVA scores visually that provided insights into patterns in the data. DFA in the context of geometric mrophometrics examines the effectiveness of the shape variables in predicting *a priori* groupings (in this case, species); *T*-square test and permutation test using Procrustes distance and the *T*-square statistic were run to

assess discrimination between species in terms of body shape.

To test whether size allometry significantly explains body shape variation among species, I conducted regression analysis on Procrusted coordinates and log-transformed centroid size. The null hypothesis tested was that size allometry is not a significant predictor of body shape difference between species. To further examine body shape variation after accounting for size, regression residuals was extracted from the regression analysis between central size and shape. A PCA was then conducted on the regression residuals.

Phylogeny including sampled taxa was mapped into the morphospace defined by the first two PCA and CVA axes, respectively.

Results

Body Shape Variations

PCA on species of Eocene catostomid and jianghanichthyid from North America and East Asia was performed (Fig. 7.2). The first two PC axes together account for 64.3% of the total variance, of which the first axis 40.4% and second axis 23.9%. Specimens located on the positive end of PC1 axis exhibit deeper body, larger head, more ventrally placed snout, and more posteriorly placed anal fin, whereas specimens with more positive PC2 values show shallower body, larger head, and more terminally placed snout. Species of catostomids are clustered, whereas jianghanichthyid is nearly separated from catostomids with a combination of high PC1 values and slightly positive PC2 values. 95% confidence ellipses of *Amyzon aggregatum*, *A. kishenehnicum*, *A. gosiutense*, *A. hunanense*, and *Jianghanichthys hubeiensis* are drawn on the

PC plot assuming equal frequency. The confidence ellipse of *Jianghanichthys* is well separated from all catostomids. The confidence ellipse of *A. kishenehnicum*, and *A. hunanense*, are somewhat overlapped with each other, whereas those of *A. aggregatum*, and *A. gosiutense*, are highly overlapped with each other. Notably, the Asian species, *A. hunanense* and *Jianghanichthys* are both located at the right end of the morphospace, whereas the North American species are on the left.

The CVA, as expected, reveals higher disparity between groups (Fig. 7.3). The first axis of the CVA (CV1 75.5%) and CV2 (12.1%) accounts for 87.7% variation among groups, scaled by the inverse of the within-group variation. CV1 shows longer dorsal fin, shallow caudal peduncle, and more anteriorly placed anal fin towards more positive values, whereas CV2 suggests much shallower body, shorter dorsal and anal fin base, longer caudal peduncle, more terminal mouth, and larger head towards more positive values. In the CV1-CV2 morphospace, jianghanichthyids are well separated from catostomids, whereas the 95% confidence ellipses of catostomid species overlap to each other. *A. gosiutense* is in the middle of catostomid cluster. in the Asian catostomid *A. hunanense*, the 95% confidence ellipse slightly overlaps with that of *A. gosiutense*. Permutation tests (10000 permutation rounds) performed on differences in Procrustes distances among groups reveal significant differences between paired species that both have larger sample sizes (Table 7.1).

The DFA comparing each pair of the species by parametric *T*-square test for the difference between group means found significant differences between *Amyzon aggregatum* and *Amyzon gosiutense*, and between *Amyzon aggregatum* and *Amyzon kishenehnicum*, and Jianghanichthys

hubeiensis versus each species that has considerate sample size (Table 7.1). A permutation test using Procrustes distances and the *T*-square parameters suggest there are significant differences between all species pairs except those with low sample sizes.

Allometry and Body Shape

Procrustes coordinates are regressed on log-transformed centroid size to characterize body shape variation with allometric changes (Fig. 7.4). A pooled within-species regression analysis was conducted. A permutation test (10000 rounds) for the correlation between size and shape returned a *p*-value of 0.524. If significance level is set at 0.05, the permutation test result does not reject the null hypothesis; therefore, the Procrustes coordinates are independent of centroid size. In the other words, the size resulting from growth does not significant affects the disparity in body shape among tested species.

Regression residuals are extracted from the regression analysis to remove the allometric effect, and then plotted in PCA (Fig. 7.5). The first two PCs account for 66.08% of the variance. The interspecific pattern in the morphospace of PC1 and PC2 resemble that of PCA scores with allometric effects (Fig. 7.2). However, the intraspecific variations are different from that of the previous PCA (Fig. 7.2). Similarly, CVA on regression residuals (Fig.7.6) display an equivalent interspecific distribution pattern as the PCA on Procrustes coordinates, but intraspecific positions vary. All of the *p*-values from permutation tests (10000 rounds) are much smaller than 0.05 (Table 7.1) except the pair of taxa with very small sample size.

Evolutionary Trajectories Through Morphospace and Phylogenetic Trees

The phylogeny from Chapter 6, a strict consensus tree including all the sampled species, is mapped onto both PC and CV morphospaces (Fig. 7.7). Hypothetical ancestral nodes of Catostomidae, *Amyzon*, and North American species of *Amyzon* were reconstructed with body shapes relative to the root of the phylogenetic tree (Fig. 7A). Except for the polytomy of *A. aggregatum*, *A. gosiutense*, and *A. kishenehnicum*, both PC and CV morphospaces show strong phylogenetic patterning in the morphospace, with only a single branch, that of *A. gosiutense*, crossing over the branch between the *Amyzon* node and the North American *Amyzon* node.

Discussion

Body Shape of Eocene Catostomids

To examine the body shape differences among species of Eocene catostomids and jianghanichthyids, geometric morphometric analyses were performed on body shape comparison with additional tests for effects of allometry and phylogeny. The PCA and DFA indicate that body shapes are significantly different between jianghanichthyids and catostomids, and between North American catostomids and Asian catostomids. CVA provides additional resolution for body shape differences that most significantly separate the nominal taxa. The interspecific disparity among North American species of *Amyzon* is recognized by additional analyses in CVA and DFA (Table 7.1).

Although the meristic and metric characters of *Amyzon* species are extensively overlapping with

a large count or measurement range (Bruner, 1991), comparisons using quantitative analyses of body shape indicate significant differences among species. *Amyzon aggregatum* and *A. gosiutense*, which were suggested to be senior and junior synonyms because of highly overlapping meristics and metrics (Bruner, 1991), occupy adjacent and moderately overlaping morphospaces in PCA and CVA. However, discriminant analysis (Table 7.1) suggests they are significantly different in body shape, in accordance with the osteological study of Liu et al. (2016).

Allometric Effect in Body Shape Comparison

Preservation of fossil fishes is affected by the ancient lake environment (Wilson, 1980a), seasonal change (Wilson, 1984), and geological events etc. The size of collected fossil fishes is not only a result of growth, but also often biased through preservation and collecting. Collections of a particular taxon do not usually include a complete range of different sizes.

The sampled specimens in this study have been seen to have interspecific size variations. To examine the size effect on the body shape variations, regression analysis and use of regression residuals in PCA were performed. The regression analysis pooled with intraspecies variations indicates that size and allometry does not significantly affect body shapes differences with sampled specimens. Also, after removing the size effect, the observations of species are distributed in a similar pattern with size in the both PCA and CVA. Permutation tests of CVA values using regression residuals (Table 7.1) suggest significant body shape differences between all species except the species with limited number of specimens, *Amyzon commune* and

"NewGenus" *brevipinne*.

To sum up, the regression analysis and PCA and CVA on regression residuals suggest that fish size and allometry do affect the interspecific body shape differences. For direct comparisons of body shape among catostomid species, when possible, one should compare individuals in similar size. After removing allometric effect, the sampled species except *Amyzon commune* and "NewGenus" *brevipinne* are significantly different from each other in body shape.

Evolutionary Trends in Body Shape

To examine the evolutionary trend in body shape of Eocene catostomids, strict consensus phylogenetic tree including all sampled catostomids was mapped onto the PCA and CVA morphospace (Fig. 7.7). In both analyses, the evolutionary trajectory of body shapes expands through the morphospaces and is congruent with the phylogeny. The jianghanichthyids and catostomids, *Amyzon* and "NewGenus", and North American *Amyzon* and Asian *Amyzon* are distributed close to each other. The reconstructed evolutionary trends along the trajectory through the nodes of Catostomidae, *Amyzon*, and North American *Amyzon* are roughly parallel to the PC2 and CV2 axis respectively (Fig. 7.7).

Interrelationships of *Amyzon aggregatum*, *A. gosiutense*, and *A. kishenehnicum* have not been resolved in the strict consensus cladogram from Chapter 6. The 50% majority consensus cladogram from the phylogeny study of Chapter 6 suggests that *A. aggregatum* is sister to the clade consisting of *A. gosiutense* and *A. kishenehnicum*. The only other phylogeny study including species of *Amyzon* hypothesized that *A. aggregatum* is sister to *A. kishenehnicum*, and

then together they are sister to *A. gosiutense* (Liu et al 2016, chapter 3). Neither of the hypothesized interrelationships of these three species corresponds with the relative position and distance between species. Moreover, the Procrustes distance between *A. aggregatum* and *A. gosiutense* is far less than that of either to *A. kishenehnicum*. According to body shape variation, *A. aggregatum* is closer to *A. gosiutense* than to *A. kishenehnicum*. Whether this similarity represents functional convergence or shared ancestral features remains to be studied.

Conclusions

Using a fixed landmark-based geometric morphometric method, this study compares the body shape difference of Eocene catostomids and jianghanichthyids using PCA, CVA, and DFA, evaluates allometric effects on their body shape variations, and considers body shape variations in the context of phylogeny. The catostomids and jianghanichthyids occupy non-overlapping regions of morphospace defined by the axis of PC1 versus PC2 and CV1 versus CV2. Permutation tests in CVA and DFA indicate that body shape of all sampled species except those with small sample size (*Amyzon commune* and "NewGenus" *brevipinne*), e.g. *A. aggregatum*, *A. gosiutense*, *A. hunanense*, *A. kishenehnicum*, and *Jianghanichthys hubeiensis*, are significantly different from each other. DFA finds significant body shape difference between jianghanichthyids and all well-sampled catostomid species, and between *A. aggregatum* versus *A. gosiutense*, as well as *A. aggregatum* versus *A. kishenehnicum*. Regression analysis on Procrustes coordinates and centroid sizes with pooled intraspecific variations shows that allometry does not significantly affect body shapes in catostomids and jianghanichthyids. When performing PCA and CVA on regression residuals to remove allometric effect; the interspecific disparities and distributions among sample species in morphospace are similar to those of PCA

and CVA with allometric effects. The phylomorphospace shows evolutionary trajectories and trends through the main lineages of Eocene catostomids and jianghanichthyids. Except for the relationships of *A. aggregatum*, *A. gosiutense*, and *A. kishenehnicum*, the interspecific variation and distribution in morphospace of PCA and CVA complement the phylogeny. The Procrustes distance of *A. aggregatum* and *A. gosiutense* is smaller than either is to *A. kishenehnicum* and may represent either functional convergence or shared ancestral condition worthy of further investigation. All statistic analyses from body shape data finds significant difference between *A. aggregatum* and *A. gosiutense*, which supports their separation as different species. The body shape disparity and distribution in morphospace suggest *A. aggregatum* and *A. gosiutense* are closer to each other than either is to *A. kishenehnicum*.

Table 7. 1 *P*-value generated from Canonical Variate Analysis (CVA) and Discriminant Function Analysis (DFA) on Eocene catostomids and Jianghanichthyids. The data in each cell is generated from CVA and DFA for the comparison of each paired taxa. Each cell contains four parameters: *p*-value from CVA permutation tests on Procrustes coordinates / *p*-value from DFA (parametric) / *p*-values from DFA permutation tests /*p*-value from permutation tests from CVA of regression residuals. The *p*-values from CVA permutation tests (10000 permutation rounds), both CVAs on Procrustes coordinates and regression residual, are for Procrustes distances among groups, whereas the DFA permutaion tests (1000 permutation runs) use Procrustes distance and the *T*-square statistic from DFA. The significance level is set at 0.05. Significant differences between species in all four analyses are bolded. The gray numbers indicate the total sample size of paired taxa is small relative to the number of landmarks, that the separation between groups is not reliable. The gray cells indicate that the sample size for the two compared species are too different that may not represent the true difference. The sample sizes for each species indicated in a bracket following the species name.

	A. commune (2)	A. gosiutense (8)	A. hunanense (9)	A. kishenehnicum (14)	J. hubeiensis (29)	"NewGenus" brevipinne (2)
A. aggregatum (19)	0.08/0.88/0.08/0.05	**0.0002/0.01/<.0001/0.0001**	<.0001/0.08/<.0001/0.0001	**<.0001/0.001/<.0001/0.0001**	**<.0001/<.0001/ <.0001/0.0001**	0.003/0.53/0.004/0.005
A. commune		0.02/0.77/0.002/0.02	0.01/0.82/0.01/0.01	0.02/0.72/0.03/0.02	0.0001/0.0001/0.002/0.001	0.33/0.87/0.32/0.33
A. gosiutense			<.0001/0.80/<.0001/<.0001	0001/0.21/<.0001/<.0001	**<.0001/<.0001/<.0001/<.0001**	0.02/0.51/0.02/0.01
A. hunanense				<.0001/0.54/<.0001/<.0001	**<.0001/<.0001/<.0001/<.0001**	0.02/0.86/0.01/0.02
A. kishenehnicum					**<.0001/<.0001/<.0001/<.0001**	0.13/0.90/0.14/0.11
J. hubeiensis						0.002/0.0005/<.0001/0.002

Figure 7. 1 1 Anatomical landmarks used in geometric morphometrics analysis using example of left-side preserved specimen of *Amyzon aggregatum* (UALVP 17489a). See Material and Methods for explanation of the landmarks.
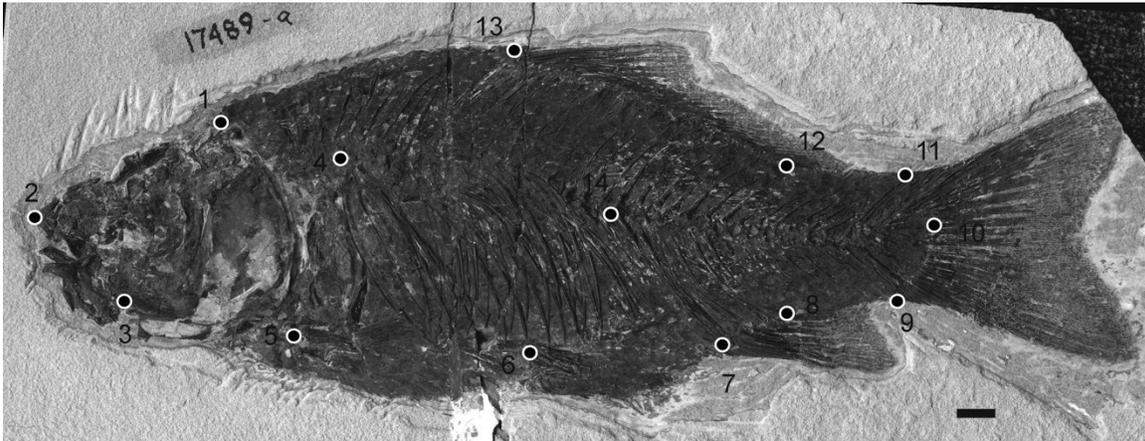
Figure 7. 2 Scatter plot of PC scores from principal component analysis (PCA) of landmark based body shape changes on species of Eocene catostomids and jianghanichthyids. First two principal components (PC1 and PC2) are displayed. Body shape deformation along axis of PC1 and PC2 are mapped. 95% equal frequency confidence ellipse is drawn by species.
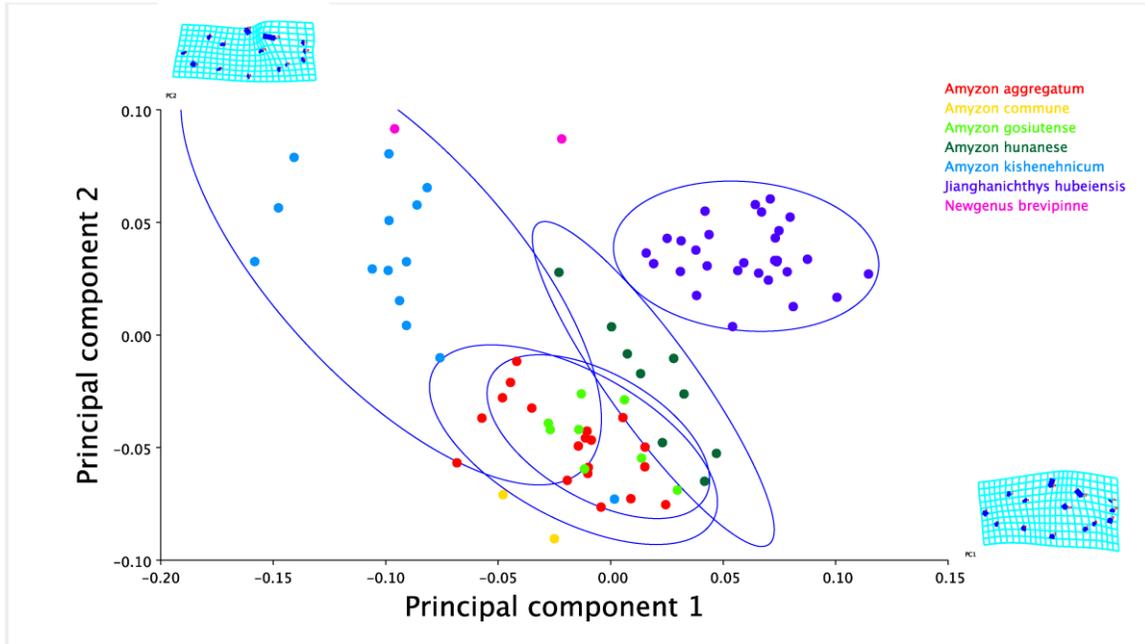
Figure 7. 3 Scatter plot of the CV scores from canonical variate analysis (CVA) of landmark based body shape changes on species of Eocene catostomids and jianghanichthyids. First two canonical variates (CV1 and CV2) are displayed. Body shape deformation along axis of CV1 and CV2 are mapped. 95% equal frequency confidence ellipse is drawn by species.
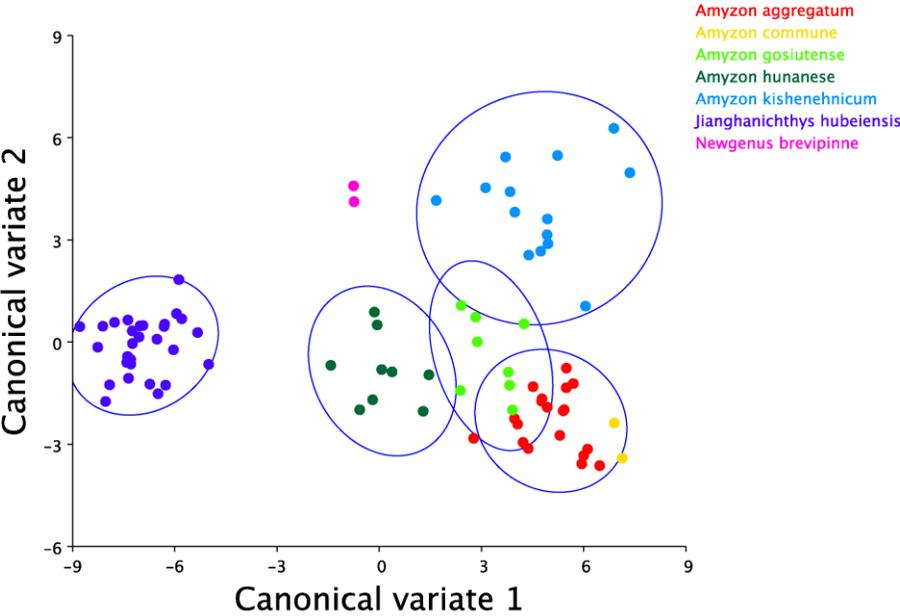
Figure 7. 4 Group-centered scatter plot of regression scores from regression of Procrustes coordinates on log-transformed centroid size of Eocene catostomids and jianghanichthyids. The analysis is a pooled within-group regression for each sampled species.
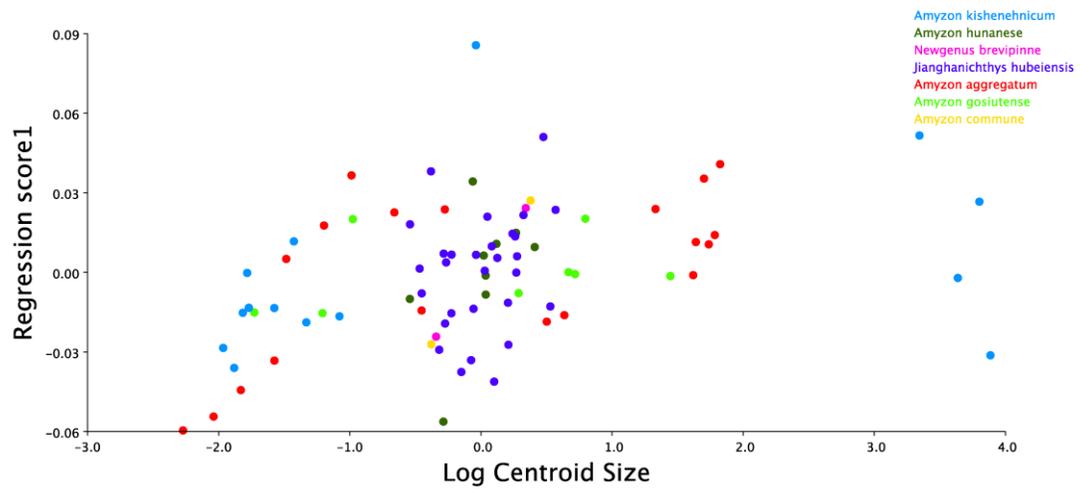
Figure 7. 5 Scatter plot of PC scores from PCA of regression residuals on species of Eocene catostomids and jianghanichthyids. The regression residuals are from the regression analysis of Figure 4. PC1 and PC2 are displayed. Body shape deformation along axis of PC1 and PC2 are mapped. 95% equal frequency confidence ellipse is drawn by species.
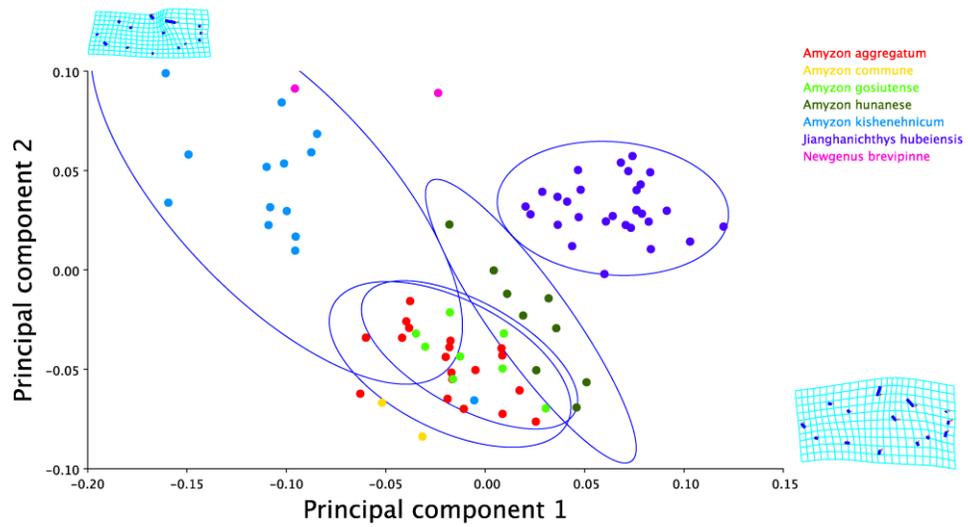
Figure 7. 6 Scatter plot of CV scores from CVA of regression residuals on species of Eocene catostomids and jianghanichthyids. The regression residuals are from the regression analysis of Figure 4. CV1 and CV2 are displayed. Body shape deformation along axis of CV1 and CV2 are mapped. 95% equal frequency confidence ellipse is drawn by species.
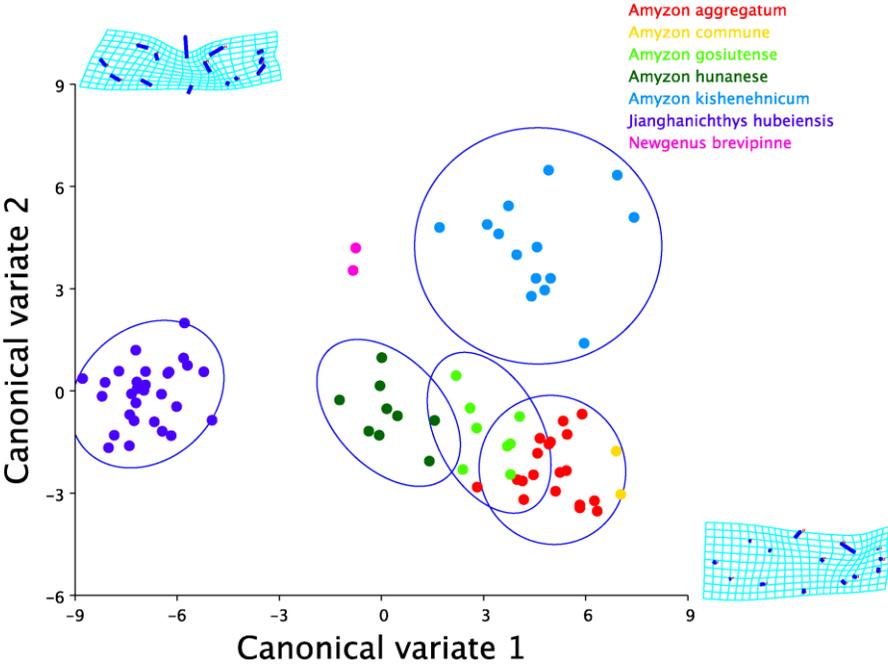
Figure 7. 7 Phylogeny mapped over PC1 versus PC2 scores (A) and CV1 versus CV2 scores (B). Phylogeny is from Chapter 6. PC and CV scores are a consensus from each species and equivalent to that of the previous PCA (Fig. 7.2) and CVA analyses (Fig. 7.3).
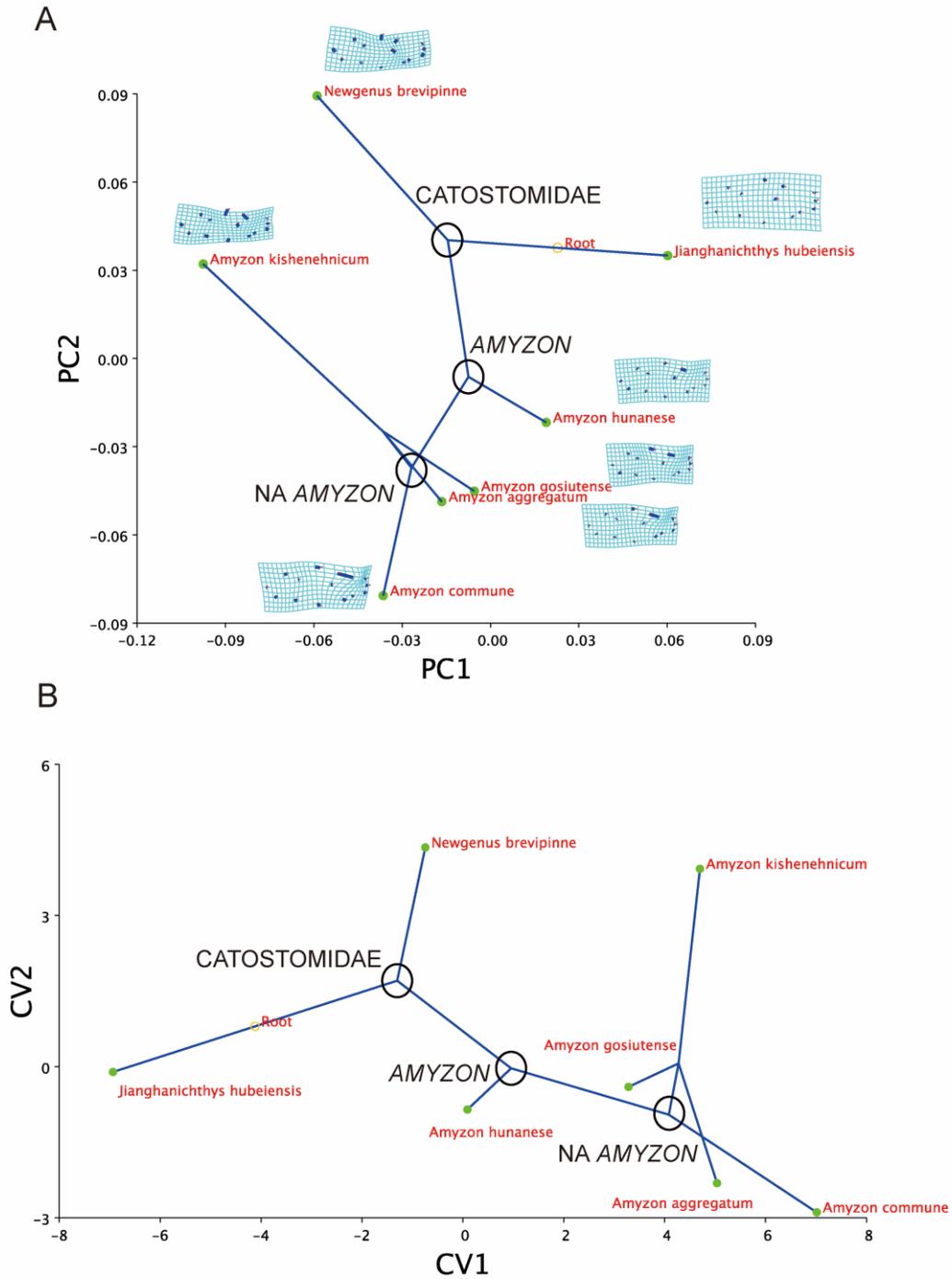
Appendix 7. 1 Specimens used in geometric morphometric analysis.

Amyzon aggregatum:

UALVP 15825, UALVP 15833, UALVP 15835, UALVP 17456a, UALVP 17462, UALVP 17465, UALVP 17466, UALVP 17489a, UALVP 22875a, UALVP 32265, UALVP 33114, CMN 6190, ROM 11034b, ROM 11042a, ROM 11041a, ROM 11051a, ROM 11094b, ROM 11067a, ROM 11070a, and ROM 11019a.

Amyzon commune

AMNH FF 2579 and FMNH PF 116.

Amyzon gosiutense

UALVP 14723, UALVP 14725, AMNH FF 10460, FMNH PF 10425, FMNH PF 10427, FMNH PF 10577, FMNH PF 10579, and FMNH PF 10580.

Amyzon hunanense

IVPP V 12571.1–6, IVPP V 17906.6a, IVPP V 17906.7a, IVPP V 17906.9, IVPP V 17906.15b, IVPP V 17906.23, IVPP V 17906.31a, IVPP V 17906.35a, IVPP V 17906.38, IVPP V 17906.47a, IVPP V 17906.48, IVPP V 17906.49, IVPP V 17908.1a, and IVPP V 17908.2a.

Amyzon kishenehnicum

UALVP 55260，UALVP 23947, UALVP 24137, UALVP 24139, UALVP 24140, UALVP 24142, UALVP 24144, UALVP 24145, UALVP 24149, UALVP 24150, UALVP 24151,

UALVP 24157, UALVP 38967, and UALVP 39031.

"NewGenus" *brevipinne*

CMN 2042 and ROM 11163a.

Jianghanichthys hubeiensis

IVPP V 12163.1a, IVPP V 12163.4–7, IVPP V 12163.9–12, IVPP V 12163.14a, IVPP V

12163.15,   IVPP V 12163.17–23, IVPP V 12163.25, IVPP V 12163.26, IVPP V 12163.28–31,

IVPP V 12163.33, IVPP V 12163.334, IVPP V 12163.36b, IVPP V 12163.38–40, IVPP V

12163.49, IVPP V 12163.52, IVPP V 12163.53, IVPP V 12163.56, IVPP V 12163.57, IVPP V

12163.62, IVPP V 15712.2a, IVPP V 15712.3, GMC V1810-1 (V 2504 in Lei, 1977; 1987).

Chapter 8 Conclusion

This thesis integratively studied morphology, taxonomy, phylogeny, and quantitate morphology (geometric morphometrics) of Eocene catostomids and problematic catostomids. Drawing on a larger collection and exhaustive taxa sampling of Eocene catostomids, a clearer picture of the evolutionary history of Catostomidae near the stem is depicted. The understanding to the evolution of Cypriniformes is also improved by implications from catostomids and problematic fossils.

Morphology of Catostomids and Problematic Catostomids (*Jianghanichthys*)

Morphology is the basis of taxonomy, systematics, and many other subjects. Morphological description and comparison is especially important for fossil taxon recognition and clarification. In this thesis, I studied the entire sampled fossil and extant taxa's morphology. New fossil taxa, i.e., *Jianghanichthys hubeiensis*, *Amyzon kishnehnicum*, and "NewGenus" *brevipinne* are described in detail, whereas comparisons are made comprehensively with related materials. 134 osteological characters used in phylogenetic analysis are described based on both Eocene and extant catostomids.   Key characters that may be used for diagnosis are summed as below:

General osteology of extant catostomids: small to larger sized freshwater fish, single row pharyngeal teeth (20 to 200) ankylosed on the pharyngeal bone that modified from fifth ceratobranchial; kinethmoid slender with length range from about 1/3 length to more than the full length of ascending process of premaxilla in the same individual; correlation to suction feeding, gnathic ramus of dentary moderately short to short, and posteroventral process of dentary moderately long to elongated; frontal broad anterior and very narrow posterior with large sphenotic sutured laterally; fronto-parietal fontanelle often wide and elongated; Weberian apparatus characterized in the large plate-like neural complex, robust rib 4 fused by ventral directing process from centrum 2 and 4, a transverse plate in between left and rite rib 4 and anterior to the os suspensorium, neural spine 4 reduced to full length; both hypural 2 and 3 fused to compound centrum in a large array of genera; caudal fin rays 18; cephalic sensory canals are superficial that not enclosed in bones.

General morphology of Eocene catostomids: single row pharyngeal teeth 18 to 60; kinethmoid slender and elongated, with the length sub-equal to the ascending process of premaxilla; gnathic ramus of dentary long to moderately short, posteroventral process of dentary short to moderately long; supraorbital present; frontoparietal fontanelle wide; sphenotic largely exposed; neural complex oval shape, rib 4 relatively robust about half length of rib 4; transverse plate present, neural spine 4 at full length; hypural 3 of a few species fused to compound centrum; cephalic sensory canal partially enclosed in preopercle and infraorbitals.

General morphology of Jianghanichthyids: pharyngeal teeth rudimentary and spine like, or

absent; kinethmoid probably unossified; premaxilla and maxilla compose the mouth gape; sphenotic largely exposed; frontoparietal fontanelle absent; opercular arm and auricular process flat and pointed; Weberian apparatus with small and thin neural complex, slender, rod-like rib 4 with ventral end hooked derived from centrum 4 only; neural spine 4 at full length; caudal fin rays 19; cephalic sensory canals enclosed in bones.

Additional osteological characters that may not be conservative for a fish group can display high interspecific variations. These can be quite useful for species recognition and clarification given the genus status is confirmed. For instance, the antero-mesial corner of premaxilla is consistently either round-off or sharp-angled in the species of *Amyzon*. This variation is also seen in other genera, but won't restrain the capability of such characters' effect on specific comparisons.

Taxonomic Clarification Of Eocene Catostomids And Problematic Catostomids

Taxonomy of Eocene catostomids has long been questioned and confusing. Eocene catostomid and problematic catostomid records from Asia and North America are reviewed and revised in this study (Table 8.1, Fig. 8.1). Major changes are highlighted as below.

First of all, the Asian problematic catostomid *Jianghanichthys hubeiensis* has long been a puzzle. It was assigned to an extant genus *Osteochilus* of Cyprinidae (Lei, 1977), and then given its own genus (Lei, 1987). It was suggested to be a catostomid fish in a later study (Chang and Chen, 2008; Liu et al., 2010). However, osteological comparison and phylogeny analysis

349

suggested it to be a stem cypriniform with its own family status (Liu et al., 2015; Chapter 2). Further reviews on the rest *Osteochilus* reported from China (Tang, 1959; Wang et al., 1981) indicated they all belong to *Jianghanichthys* (Chapter 5). Also of paleogeographic interests, several species of *Jianghanichthys* were only found in south China including Xijiashan, Linli, Hunan and Sanshui Basin, Sanshui, Guangdong with geological age ranges from Paleocene to middle Eocene.

A less puzzling but not ubimportant taxonomic confusion in North America happened between *Amyzon aggregatum* (Wilson, 1974) and *A. gosiutense* (Grande et al., 1982). Both are among the well described and thus best known species of *Amyzon*, while previously described species were briefly described and discussed (Cope, 1872; 1874; 1875; 1893). *A. gosiutense* was suggested to be junior synonym of *A. aggregatum* based on highly overlapped morphometric and meristic characters (Bruner, 1991). However, this study found a suite of osteological characters that are able to distinguish these two species (Liu et al., 2016).

Another long-known species from North America, "NewGenus" *brevipinne* from Allenby Fm., is so far the only relatively shallow bodied, small sized catostomid species recovered from fluvial sediments (Chapter 4). It was assigned to *Amyzon* when firstly described (Cope, 1893). A re-description of "NewGenus" *brevipinne* well established the taxon at species level (Wilson, 1974). However, a few critical characters only became available recently on new materials. The new characters, such as the nearly complete pharyngeal bone with much fewer teeth than *Amyzon* and the distinctive frontal unlike any known catostomids, suggest it should be removed from *Amyzon*.

In addition to clarification of known catostomids, new materials representing a new taxon is described. *Amyzon kishenehnicum* from Kishenehn Formation is established and compared with other *Amyzon* species (Chapter 3). The description of new, well-preserved species is not only adding to taxonomic diversification, but also contributing to the osteological variations that help taxonomic clarification.

Phylogeny of Catostomids

Phylogeny is the foundation to understanding evolution and fundamental for many biological studies, such as functional morphology, ecomorphology, growth characteristics, divergence time, diversity rates, and paleogeography, etc. To understand the evolution of catostomids and related problematic fossils, multiple sets of phylogenetic analyses based on different character list have been performed in this study.

First, the character list and data matrix of Conway (2011) was adopted to help understand the systematic position of *Jianghanichthys* (Chapter 2). The characters list of Conway (2011) included a large array of synapomorphic characters for the major clades of Cypriniformes, and thus it is suitable for coding the taxonomically long-puzzled *Jianghanichthys*. The addition of *Jianghanichthys* breaks down the previously well-resolved inter-family relationships of Cypriniformes. In subsequent analysis, backbone constraint using the nuclear DNA based molecular systematic study (Chen et al., 2013) was performed with the parsimonious analyses. Although none of the analyses well resolved the systematic position of *Jianghanichthys*, they

clearly demonstrated *Jianghanichthys* represent a basal clade of Cypriniformes and cannot be assigned to any known family.

The second set of phylogenetic analyses was performed to resolve systematic position and interrelationships of *Amyzon* species, which had not been studied at species level before (Liu et al., 2016; Chapter 3). The characters to code *Amyzon* species were adopted from that of Smith (1992). Smith (1992) had long been the most comprehensive phylogeny study of Catostomidae using combined characters of osteology, soft tissue, gene expression, lava, and biochemical. Three best-preserved species, *A. aggregatum*, *A. gosiutense*, and *A. kishenehnicum*, were analized with the data matrix of Smith (1992). They were well resolved to be a monophyletic basal clade of Catostomidae in a strict consensus tree of 1,238/73 (PAUP/TNT) most parsimonious tree. The hypothesized phylogeny also suggested that *Myxocyprinus* and *Cycleptus* were not a sister group, and *Plesiomyxocyprinus* is the sister group of all extant catostomids except ictiobinines.

To optimize the utilization of important fossil taxa to the phylogeny, a character list consisting 134 osteological characters was created and described for a third set of phyletic study. About half of the character list was original, and 61 out 134 osteological characters are adopted and modified from that of Smith (1992). Several characters are from those of Conway (2011), Wu et al. (1981), Sawada (1982), Fink and Fink (1981; 1996), and Siebert (1987). Data matrix was exhaustively collected and assembled on all code-able Eocene catostomids, most genera of extant catostomids, and outgroup selection to represent all major clade of cypriniforms. Strict consensus tree form four most parsimonious tree suggested that most Eocene catostomids

(except *Plesiomyxocyprinus*) were stem taxa of Catostomidae, and "NewGenus" *brevipinne* represented the most basal clade. Consistent with the second phylogenetic analysis set, *A. aggregatum*, *A. gosiutense*, and *A. kishenehnicum* composed a monophyletic clade, *Myxocyprinus* and *Cycleptus* were not a sister group, and *Plesiomyxocyprinus* sistered to all extant catostomids except ictiobinines. This study also found that known species of *Amyzon* were not monophyletic, with *A. hunanense* and *A. commune* being a distinctive basal clade.

Body Shape Changes of Eocene Catostomids

General appearances are quite similar among Eocene catostomids. Especially three species of them, *A. aggregatum*, *A. gosiutense*, and *A. kishenehnicum*, have largest and best-preserved collection. The well-documented intraspecific variations of these species result in enlarged and overlapping ranges. Highly overlapped morphometric and meristic characters make them hard to be distinguished based on counting and measurement. Using landmark based geometric morphometric method to quantify morphology on body shape, this study compared the body shape difference of Eocene catostomids and jianghanichthyids. Principle components analysis (PCA), Canonical variate analysis (CVA), and discriminant function analysis (DFA) were performed to describe body shape variations and disparity among species in digitized morphospace. All analyses found significant body shape differences between jianghanichthyids and all well-sampled catostomid species, *A. aggregatum* versus *A. gosiutense*, and *A. aggregatum* versus *A. kishenehnicum*. Regression analysis on Procrustes coordinates and centroid sizes with pooled intraspecific variations showed that allometry significantly does not affect body shapes in catostomids and jianghanichthyids. By removing allometric effect, the

interspecific disparities and distributions among sample species in morphospace had no difference to that of PCA and CVA with allometric effect. Phylogenetics mapped onto morphospace showed evolutionary trajectories and trends through main branches of Eocene catostomids and jianghanichthyids. All statistic analyses from body shape data found significant differences between *A. aggregatum* and *A. gosiutense*, which support that these two were different species. Their body shape disparity and distribution in morphospace suggested *A. aggregatum* and *A. gosiutense* were closer to each other than either were to *A. kishenehnicum*,

Early Evolution of Catostomidae, with Implications for Cypriniformes

From taxonomic clarification of Eocene catostomids, it is confirmed that three genera with three species occurred in Asia, whereas two genera with six species were distributed in North America (Table 8.1). The Asian "*Amyzon" hunanense* and North American "*Amyzon" commune* may be different genera of themselves respectively according to my phylogeny hypothesis. If these species represent new genera, Asia and North America reached equivalent diversity, but did not share known species or genera during the Eocene.

The phylogeny of Catostomidae shows that "*Amyzon" hunanense* inserts in the middle of North American stem catostomids, whereas the other Asian taxon, *Plesiomyxocyprinus*, is sister to the majority of extant catostomids (Myxocyprininae, Cycleptinae, and Catostominae). The mosaic distribution of the few Asian taxa across the phylogeny reveals that there were multiple taxonomic communication during the early evolution of catostomids and probably through

Beringian connection before the middle Eocene (the age of *Plesiomyxocyprinus*).

The problematic catostomids *Jianghanichthys* are clarified to be stem cypriniforms and are so far the only extinct family of Cypriniformes. The rest of problematic catostomids, Eocene "*Osteochilus*" from Xiejiashan, Hunan and Sanshui Basin, Guangdong, are determined to be *Jianghanichthys* as well. The occurrences of jianghanichthyids spanned from Paleocene to middle Eocene in south China with a range from the Yangtze River to the south coast. The recognition of Jianghanichthyidae indicates major clades, including extinct stems, probably diverging during the Paleocene and early Eocene in South Asia (represented by south China fossil locality).

Whereas jianghanichthyids are known as early as in the Paleocene, Asian catostomids are only recovered from Eocene sediments. Unlike jianghanichthyids restricted in south China, catostomids are so far only seen from the north edge of south China to northeast China and Fareast Russia (Fig. 8.1). Combining paleogeographic distribution of cyprinids, which are the only known Eocene cypriniforms other than catostomids and jianghanichthyids, cyprinids were widely distributed in East Asia during the middle to late Eocene (Sytchevskaya, 1986; Zhou, 1990; Su, 2011; Böhme et al., 2013; Chen et al., 2015a). From the distribution of Eocene cypriniforms (Fig. 8.1), it is clear to see that the only overlapping region that all early cypriniforms occurred in is South Asia (including south China). Adding on the oldest known skeleton based loach from South Asia (Nanning Basin, south China; Chen et al., 2015b), South Asia is undoubtedly the hotspot of Cypriniformes' origin and major clades' divergence. Central Asia, including north, northwest, and north east China, Mongolia, Kazakhstan, and Fareast

Russia, preserved the last remains of catostomids fossil in Asia (Chapter 5) and recorded cyprinids' dispersal route, is a gateway leading the dispersal events west to the Europe and east to North America through Beringia.

Summary and Future Study

Taxonomy, morphology, phylogeny, quantified morphology (geometric morphometrics) are influenced by one another. This study integratively studied these aspects of catostomids to understand a clearer picture of the evolution of Catostomidae, even the Cypriniformes.

Osteological characters are described and compared among extinct and extant catostomids. A character list containing 134 osteological and related characters are described and coded for phylogenetic analysis. Critical characters, such as pharyngeal teeth, kinethmoid, and Weberian apparatus are compared and summarized in Eocene catostomids.

Taxonomy of Paleogene catostomids and problematic catostomids are clarified. Problematic Asian catostomids, *Jianghanichthys* and Eocene "*Osteochilus*", are determined to be members of an extinct family Jianghanichthyidae. Oligocene occurrence of Asian catostomids with only disarticulated bones from north China and Mongolia are reviewed and confirmed with their Catostomidae assignment. On the North America side, *Amyzon gosiutense* remains its own species status according to osteological difference from *A. aggregatum*. "*Amyzon*" *brevipinne* is revised to be "NewGenus" brevipinne. New materials on *Amyzon kishenehnicum* sp. nov. and *Jianghanichthys huachongensis* sp. nov. are described as well.

A series of phylogenetic analyses have been performed. *Jianghanichthys* is found to be a stem clade with interrelations with other cypriniform families uncertain. "NewGenus" and *Amyzon* are resolved to be stem catostomids, whereas *Plesiomyxocyprinus*, is sister to the clade of Myxocyprininae (Cycleptinae + Catostominae). The Asian *Amyzon hunanense* and North American *Amyzon commune* fell out of the clade of "true *Amyzon*". They potentially represent distinctive stems of Catostomidae. Mosaic distribution of Asian catostomids across the phylogeny of Catostomidae indicates that multiple dispersal events probably happened before middle Eocene. The geological age and geographical distribution of catostomids and jianghanichthyids, combining with record of other early cypriniform (Table 8.1), suggest that south Asia is a hotspot of Cypriniformes evolution, whereas central Asia is the gateway of various dispersal events of Cypriniformes.

Future study in the evolution of catostomids even cypriniforms should pay more attention to the fossil localities of south and central Asia. The larger array of osteological characters list created in this study prepared catostomids to be incorporated into total evidence studies that combines with molecular characters to calculate divergence time of the main and important branches of Catostomidae, even Cypriniformes

Table 8. 1 Summary of Eocene cypriniform fossil records. Materials not examined in this study are referred to the cited literature in the brackets following materials. Abbreviations: Co., Continent; F., Family; Fm., Formation.

Co.	F.	Taxon	Age	Horizon	Fig. 8.1	Locality	Materials (Reference)
Asia	Catostomidae	*Amyzon hunanense*	middle–early Eocene	Xiawanpu Fm.	Q	Xiangxiang, Hunan, China	skeletons, pharyngeal teeth
		Plesiomyxocyprinus arratiae	early Eocene	Huadian Fm.	M	Gonglangtou, Huadian, Jilin, China	skeleton, disarticulated bones, pharyngeal teeth
		Vasnetzovia artemica	late Eocene	Uglov Svita	L	Artyom (Artëm), Primorskyi Territory (Premorie), Russia	skeletons (Sytchevskaya, 1986)
		Catostomidae indet 1	middle Eocene	Ulan Shireh Fm.	N	Shara Murun region, Inner Mongolia, China	disarticulated bones
		Catostomidae indet 2	late Eocene	Ergelin Dzo Svita	V	Ergil Obo (Ardyn Obo), Ergelin Dzo, Dornogobi, Mongolia	disarticulated bones
	Jianghanichthyi dae	*Jianghanichthys hubeiensis*	early Eocene	Yangxi Fm.	P	Songzi, Hubei Province, China	skeletons
		Jianghanichthys linliensis	middle–early Eocene	Xiejiashan oil shale	T	Xiejiashan, 18 Km northwest of Linli, Hunan, China	skeletons
		Jianghanichthys sanshuiensis	Paleocene–Eocene	Buxin Fm.	S	Sanshui, Guangdong, China	skeletons

		Jianghanichthys huachongensis	middle Eocene	Huachong Fm.	U	Zidongxu, Foshan, Guangdong, China	skeletons, disarticulated bones
	Cyprinidae	*Eoprocypris maomingensis*	late Eocene	Youganwo Formation	Z	Jintang, Maoming County, Guangdong, China	skeleton, disarticulated bones, pharyngeal teeth (Chen et al 2015)
		Tianshanicus liui	late Eocene	Anjihaihe Fm.	X	Junggar Basin, Manas County, Xinjiang	skeleton, disarticulated bones, pharyngeal teeth (Su, 2011)
		Palaeogobio zhongyuanensis	early middle Eocene	Shahejie Fm. Level 4	Y	Fanxian, China	skeletons, pharyngeal teeth (Zhou, 1990)
		Rostrogobio maritima	late Eocene to early Oligocene		AC	Primorye, Russia	skeletons (Sytchevskaya, 1986)
		Parabarbus mynsajensis	middle Eocene	——	W	Zaissan Basin, Kazakhstan	pharyngeal teeth (Sytchevskaya, 1986)
		Planktophaga minuta	late Middle–Late Eocene	Rhin Chua Fm.	AA	Na Duong Basin, Vietnam	pharyngeal teeth (Böhme et al 2013)
		cyprinid	Eocene		AB	Sumatra, Indonesia	Skeletons of multiple species (Sanders, 1934)
North America	Catostomidae	*Amyzon aggregatum*	middle Eocene	——	A	Horsefly mine, British Columbia, Canada	skeleton, disarticulated bones, pharyngeal teeth
		Amyzon commune	late Eocene	Florissant Formation	K	South Park, Colorado, USA	skeletons
		Amyzon gosiutense	middle Eocene	Green River Fm.	J	Lake Gosiute locality, Wyoming, U.S.A	skeleton, disarticulated bones, pharyngeal teeth
		Amyzon mentale	Eocene	——	I	Osino, Nevada, USA	skeletons (Cope, 1872)

359

		Amyzon kishenehnicum	middle Eocene	Kishenehn Fm.	E	Flathead River (Middle Fork), Montana, USA	skeleton, disarticulated bones, pharyngeal teeth
		"NewGenus" *brevipinne*	middle Eocene	Allenby Fm.	B, C	Princeton, British Columbia, Canada	skeleton, disarticulated bones, pharyngeal teeth
		Amyzon sp 1	early Eocene	Klondike Mountain Fm.	D	Tom Thumb Mine, Republic, Washington, USA	skeletons
		Amyzon sp 2	Eocene	Clarno Fm.	H	Ochoco Pass, Mitchell, Oregon. USA	disarticulated bones
		Catostomidae indet 3	Eocene	Renova Fm.	F	Grant, Montana, USA	skeletons

Figure 8. 1 Distribution of unambiguous Eocene cypriniforms. Taxa, locality, age and horizon, and materials see Table 8.1 with associated labels.

Literature Cited

Adams, L. A. 1940. Some characteristic otoliths of American Ostariophysi. Journal of Morphology, 66(3):497–527.

Agassiz, L. 1850. Lake Superior: its physical characters, vegetation, and animals, compared with those of other and similar regions. Gould, Kendall, and Lincoln's Publications, Boston, 137–428pp, pl. i-viii.

Allis, E. P. 1889. The anatomy and development of the lateral line system in *Amia calva*. Journal of Morphology, 2(3):463–566.

Alvarado-Ortega, J., O. Carranza-Castaneda, AND G. Alvarez-Reyes. 2006. A new fossil species of *Ictiobus* (Teleostei : Catostomidae) from Pliocene lacustrine sediments near Tula de Allende, Hidalgo, Mexico. Journal of Paleontology, 80(5):993–1008.

Arratia, G. 2008. Actinopterygian postcranial skeleton with special reference to the diversity of fin ray elements, and the problem of identifying homologies, p. 49–101. *In* G. Arratia, H.-P. Schultze, and M. V. H. Wilson (eds.), Mesozoic Fishes 4. Verlag Dr. Friedrich Pfeil, München.

Arratia, G., AND A. Cione. 1996. The record of fossil fishes of southern South America. Muenchner Geowissenschaftliche Abhandlungen Reihe A Geologie und Palaeontologie, 30:9–72.

Arratia, G., AND H. P. Schultze. 1991. Palatoquadrate and its ossifications: development and homology within osteichthyans. Journal of Morphology, 208(1):1–81.

Bai, B., Y. Wang, J. Meng, Q. Li, AND X. Jin. 2014. New Early Eocene basal tapiromorph from southern China and its phylogenetic implications. Plos One, 9(10):e110806.

Bart, H. L., Jr., M. D. Clements, R. E. Blanton, K. R. Piller, AND D. L. Hurley. 2010a. Discordant molecular and morphological evolution (Actinopterygii: Catostomidae). Molecular Phylogenetics and Evolution, 56(2):808–820.

Bart, H. L., P. C. Reneau, M. H. Doosey, AND C. D. Bell. 2010b. Evolutionary divergence of duplicate copies of the growth hormone gene in Suckers (Actinopterygii: Catostomidae). International Journal of Molecular Sciences, 11(3):1090–1102.

Barton, D. G., AND M. V. H. Wilson. 1999. Microstratigraphic study of meristic variation in an Eocene fish from a 10 000-year varved interval at Horsefly, British Columbia. Canadian Journal of Earth Sciences, 36(12):2059–2072.

Barton, D. G., AND M. V. H. Wilson. 2005. Taphonomic variations in Eocene fish-bearing varves at Horsefly, British Columbia, reveal 10,000 years of environmental change. Canadian Journal of Earth Sciences, 42(2):137–149.

Becker, G. C. 1983. Fishes of Wisconsin. University of Wisconsin Press, Madison, WI, 1052 p.

Bird, N. C., AND L. P. Hernandez. 2007. Morphological variation in the Weberian apparatus of Cypriniformes. Journal of Morphology, 268(9):739–757.

Bleeker, P. 1860. Conspectus systematis Cyprinorum. Natuurkundig tijdschrift voor Nederlandsch Indië / uitgegeven door de Natuurkundige Vereeniging in Nederlandsch Indië, 20:421–441.

Bleeker, P. 1865. Notices sur quelques genres et espèces de Cyprinoïdes de Chine. Nederlandsch Tijdschrift voor de Dierkunde, 2:18–29.

Böhme, M. 2008. Ectothermic vertebrates (Teleostei, Allocaudata, Urodela, Anura, Testudines, Choristodera, Crocodylia, Squamata) from the Upper Oligocene of Oberleichtersbach (northern Bavaria, Germany). Courier Forschungsinstitut Senckenberg, 260:161–183.

Böhme, M., M. Aiglstorfer, P.-O. Antoine, E. Appel, P. Havlik, G. Métais, L. The Phuc, S. Schneider, F. Setzer, R. Tappert, D. Ngoc Tran, D. Uhl, AND J. Prieto. 2013. Na Duong (northern Vietnam) – an exceptional window into Eocene ecosystems from Southeast Asia. Zitteliana, A 53:121–167.

Bower, L. M., AND K. R. Piller. 2015. Shaping up: a geometric morphometric approach to assemblage ecomorphology. Journal of Fish Biology, 87(3):691–714.

Branley, A. B. 1962. Comparative cephalic and appendicular osteology of te fish family Catostomidae. part 1, *Cycleptus elongatus* (Lesueur). The Southwestern Naturalist, 7(2):81–153.

Branson, B. A. 1962. Comparative cephalic and appendicular osteology of the fish family Catostomidae. Part I, *Cycleptus elongatus* (Lesueur). The Southwestern Naturalist, 7(2):81–153.

Britz, R., K. W. Conway, AND L. Rüber. 2014. Miniatures, morphology and molecules: Paedocypris and its phylogenetic position (Teleostei, Cypriniformes). Zoological Journal of the Linnean Society, 172(3):556–615.

Bruner, J. C. 1991. Comments on the genus *Amyzon* family Catostomidae. Journal of Paleontology, 65(4):678–686.

Butler, J. L. 1960. Development of the Weberian apparatus of a catostomid fish. The Proceedings of the Iowa Academy of Science, 67:532–543.

Cavender, T. M. 1968. Freshwater fish remains from the Clarno Formation Ochoco Mountains of north-central Oregon. Ore Bin, 30:125–141.

Cavender, T. M. 1991. The fossil record of the Cyprinidae, p. 34–54. *In* I. J. Winfield and J. S. Nelson (eds.), Cyprinid Fishes Systematics, Biology and Exploitation. St. Edmundsbury,

Great Britain.

Cavender, T. M., AND M. M. Coburn. 1992. Phylogenetic relationships of North American Cyprinidae, p. 293–327. *In* R. L. Mayden (ed.), Systematics, historical ecology, & North American freshwater fishes. Stanford University Press, Stanford.

Chang, M.-M., AND G. Chen. 2008. Fossil Cypriniformes from China and its adjacent areas and their palaeobiogeographical implications. Geological Society Special Publication, 295:337–350.

Chang, M.-M., D. S. Miao, Y. Y. Chen, J. J. Zhou, AND P. F. Chen. 2001. Suckers (fish, Catostomidae) from the Eocene of China account for the family's current disjunct distributions. Science in China Series D-Earth Sciences, 44(7):577–586.

Chen, G., M.-M. Chang, AND H. Liu. 2015a. Revision of *Cyprinus maomingensis* Liu 1957 and the first discovery of *Procypris*-like cyprinid (Teleostei, Pisces) from the late Eocene of South China. Science China-Earth Sciences, 58(7):1123–1132.

Chen, G.-J., W. Liao, AND L. Xue-Qiang. 2015b. First fossil cobitid (Teleostei: Cypriniformes) from Early-Middle Oligocene deposits of South China. Vertebrata PalAsiatica, 53(4):153‑163.

Chen, G. J., F. Fang, AND M. M. Chang. 2005. A new cyprinid closely related to cultrins plus xenocyprinins from the mid-Tertiary of South China. Journal of Vertebrate Paleontology, 25(3):492–501.

Chen, Q., AND Q. Gao. 1992. The discovery of *Asiocoryphodon conicus* in Yangxi Formation on the northwest margin of Jianghan Basin and its stratigraphic significance Acta Petrolei Sinica, 13(2):3.

Chen, W.-J., S. Lavoué, AND R. L. Mayden. 2013. Evolutionary origin and early

biogeography of Otophysan fishes (Ostariophysi: Teleostei). Evolution, 67(8):2218–2239.

Chen, W.-J., AND R. L. Mayden. 2012. Phylogeny of suckers (Teleostei: Cypriniformes: Catostomidae): further evidence of relationships provided by the single-copy nuclear gene IRBP2. Zootaxa(3586):195–210.

Chen, X. 1993. Development of the anterior vertebrae in the Cyprinidae and their significance in the phylogensis. Acta Hydrobiologica Sinica, 17(1):13‑21.

Chen, Y. 1981. Investigation on the systematic position of *Psilorhynchus* (Cyprinoidei, Pisces). Acta Hydrobiologica Sinica, 7(3):371–376.

Cheng, C.-C. 1962. Fossil fishes from the Early Teriary of Hsianghsiang, Hunan, with discussion of age of the Hsiawanpu formation. Vertebrata PalAsiatica, 6(4):333–348

Chu, Y. T. 1935. Comparative studies on the scales and on the pharyngeals and their teeth in Chinese Cyprinids, with particular reference to taxonomy and evolution. Biological Bulletin of St. John's University, 2:1–225.

Constenius, K. N., M. R. Dawson, H. G. Pierce, R. C. Walter, AND M. V. H. Wilson. 1989. Reconnaissance paleontologic study of the Kishenehn Formation, northwestern Montana and southeastern British Columbia. Montana Geological Society Field Conference Guidebook, 1:189–203.

Constenius, K. N. 1996. Late Paleogene extensional collapse of the Cordilleran foreland fold and thrust belt. Geological Society of America Bulletin 108:20–39.

Conway, K. W. 2011. Osteology of the South Asian Genus *Psilorhynchus* McClelland, 1839 (Teleostei: Ostariophysi: Psilorhynchidae), with investigation of its phylogenetic relationships within the order Cypriniformes. Zoological Journal of the Linnean

Society:1–105.

Conway, K. W., M. V. Hirt, L. Yang, R. L. Mayden, AND A. M. Simons. 2010. Cypriniformes: systematics and paleontology, p. 295–316. *In* J. S. Nelson, H.-P. Schultze, and M. V. H. Wilson (eds.), Origin and Phylogenetic Interrelationships of Teleosts. Verlag Dr. Friedrich Pfeil, München.

Conway, K. W., AND R. L. Mayden. 2007. The gill arches of *Psilorhynchus* (Ostariophysi : Psilorhynchidae). Copeia(2):267–280.

Cooke, S. J., C. M. Bunt, S. J. Hamilton, C. A. Jennings, M. P. Pearson, M. S. Cooperman, AND D. F. Markle. 2005. Threats, conservation strategies, and prognosis for suckers (Catostomidae) in North America: insights from regional case studies of a diverse family of non-game fishes. Biological Conservation, 121(3):317–331.

Cope, E. D. 1872. On the Tertiary coal and fossils of Osino, Nevada. Proceedings of the American Philosophical Society, 12(86):478–481.

Cope, E. D. 1874. Supplementary notices of fishes from the fresh-water Tertiaries of the Rocky Mountain. Bulletin of the U. S. Geological and Geographic Survey of the Territories, 1(2):50.

Cope, E. D. 1875. On the fishes of the Tertiary shales of the South Park. Bulletin of the U. S. Geological and Geographical Survey of the Territories, 2(1):4–5.

Cope, E. D. 1893. Fossil fishes from British Columbia. Natural Sciences of Philadelphia, 1893:2.

Costa, E., M. Garces, A. Saez, L. Cabrera, AND M. Lopez-Blanco. 2011. The age of the "Grande Coupure" mammal turnover: new constraints from the Eocene-Oligocene record of the Eastern Ebro Basin (NE Spain). Palaeogeography Palaeoclimatology

Palaeoecology, 301(1-4):97–107.

Cubbage, C. C., AND P. M. Mabee. 1996. Development of the cranium and paired fins in the zebrafish *Danio rerio* (Ostariophysi, cyprinidae). Journal of Morphology, 229(2):121–160.

Darlington, P. J. 1957. Zoogeography: The geographical distribution of animals, 675 p.

Dombrosky, J., S. Wolverton, AND L. Nagaoka. 2016. Archaeological data suggest broader early historic distribution for blue sucker (Cycleptus elongatus, Actinopterygii, Catostomidae) in New Mexico. Hydrobiologia, 771(1):255–263.

Donoghue, M. J., J. A. Doyle, J. Gauthier, A. G. Kluge, AND T. Rowe. 1989. The importance of fossils in phylogeny reconstruction. Annual Review of Ecology and Systematics, 20:431–460.

Doosey, M. H., AND H. L. Bart, Jr. 2011. Morphological variation of the palatal organ and chewing pad of Catostomidae (Teleostei: Cypriniformes). Journal of Morphology, 272(9):1092–1108.

Doosey, M. H., H. L. Bart Jr, K. Saitoh, AND M. Miya. 2010. Phylogenetic relationships of catostomid fishes (Actinopterygii: Cypriniformes) based on mitochondrial ND4/ND5 gene sequences. Molecular Phylogenetics and Evolution, 54(3):1028–1034.

Driskell, A. C., C. Ane, J. G. Burleigh, M. M. Mcmahon, B. C. O'meara, AND M. J. Sanderson. 2004. Prospects for building the tree of life from large sequence databases. Science, 306(5699):1172–1174.

Dunn, K. A., J. D. Mceachran, AND R. L. Honeycutt. 2003. Molecular phylogenetics of myliobatiform fishes (Chondrichthyes : Myliobatiformes), with comments on the effects of missing data on parsimony and likelihood. Molecular Phylogenetics and

Evolution, 27(2):259–270.

Eastman, C. R. 1917. Fossil fishes in the collection of the United States National Museum. Washington DC Proceedings U S National Museum, 52:235–304.

Eastman, J. T. 1977. The pharyngeal bones and teeth of catostomid fishes. American Midland Naturalist, 97(1):68–88.

Eastman, J. T. 1980. Caudal skeletons of catostomid fishes. American Midland Naturalist, 103(1):133–148.

Editorial Committee of Stratigraphical Lexicon of China. 1999. Stratigraphical lexicon of China 2: The Tertiary. Geological Publishing House., Beijing, 163 p.

Edwards, L. F. 1926. The protractile apparatus of the mouth of the Catostomid fishes. The Anatomical Record, 33:257–270.

Eschmeyer, W., T. Grande, AND L. Grande. 2010. A nomenclatural analysis of gonorynchiform taxa, p. 567–587, Gonorynchiformes and Ostariophysan Relationships. Science Publishers, Enfield.

Farris, J. S. 1989. Hennig86: a PC-DOS program for phylogenetic analysis. Cladistics, 5(2):163.

Ferris, S. D., AND G. S. Whitt. 1978a. Phylogeny of tetraploid catostomid fishes based on the loss of duplicate gene expression. Systematic Zoology, 27(2):189–206.

Ferris, S. D., AND G. S. Whitt. 1978b. Phylogeny of tetraploid catostomid fishes based on the loss of duplicate gene expression Systematic Zoology, 27(2):189~206.

Fink, S. V., AND W. L. Fink. 1981. Interrelationships of the ostariophysan fishes (Teleostei). Zoological Journal of the Linnean Society, 72(4):297–353.

Fink, S. V., AND W. L. Fink. 1996. Interrelationships of ostariophysan fishes (Teleostei), p.

209–249. *In* M. L. J. Stiassny, L. R. Parenti, and G. D. Johnson (eds.), Interrelationships of fishes. Academic Press, New York.

Fink, S. V., P. H. Greenwood, AND W. L. Fink. 1984. A critique of recent work on fossil ostariophysan fishes. Copeia, 1984(4):1033–1041.

Fink, W. L., AND J. H. Humphries. 2010. Morphological description of the extinct North American sucker *Moxostoma lacerum* (Ostariophysi, Catostomidae), based on high-resolution X-Ray Computed Tomography, 5–13.

Forster, J. R. 1773. An account of some curious fishes, sent from Hudson's Bay; in a letter to Thomas Pennant, Esq. Philosophical Transactions of the Royal Society of London, B Biological Sciences, 63:149–160.

Fowler, H. W. 1958. Some new taxonomic names of fishlike vertebrates. Notulae Naturae [Philadelphia], 310:1–16.

Fuiman, L. A. 1985. Contributions of developmental characters to a phylogeny of catostomid fishes, with comments on heterochrony. Copeia, 1985(4):833–846.

Gaudant, J. 1993. Paléoichthyogéographie, paléobiologie et migration intercontinentale: remarques critiques. Bulletin de la Société géologique de France, 164:861–864.

Gayet, M. 1982. Cretaceous cypriniforms in South-America (In French with English abstract). Comptes Rendus De L Academie Des Sciences Serie Iii-Sciences De La Vie-Life Sciences, 295(12):405–407.

Gayet M. 1986. †*Ramallichthys* Gayet du Cénomanien inférieu marin de Ramallah (monts de Judée). Une introduction aux relations phylogénétiques de Ostariophysi. Memoires du Museum National d'Histoire naturelle de Paris, Série C:51: 1–81.

Gayet, M., AND J. F. Meunier. 1998. Maastrichtian to Early Late Paleocene freshwater

Osteichthyes of Bolivia: additions and comments, p. 85–110. *In* L. R. Malabarba, R. E. Reis, R. P. Vari, Z. M. Lucena, and C. A. S. Lucena (eds.), Phylogeny and Classification of Neotropical Fishes. Porto Alegre, Edipurcs.

Gill, T. 1861. On the classification of the Eventognathi or Cyprini, a suborder of Teleocephali. Proceedings of the American Philosophical Society, 13:6–9.

Goloboff, P., S. Farris, AND K. Nixon. 2003. TNT (Tree analysis using New Technology) Tucumán, Argentina.

Goloboff, P. A., J. S. Farris, AND K. C. Nixon. 2008. TNT, a free program for phylogenetic analysis. Cladistics, 24(5):774–786.

Gosline, W. A. 1974. Certain lateral line canals ff the head In cyprinid fishes with particular reference to the derivation of North American forms. Japanese Journal of Ichthyology, 21(1):9–15.

Grande, L. 1980. Paleontology of the Green River Formation, with a review of the fish fauna, Bulletin 63, 1–334 p.

Grande, L., J. T. Eastman, AND T. M. Cavender. 1982. *Amyzon gosiutensis*, a new catostomid fish from the Green River Formation Copeia, 1982(3):523–532.

Grande T. 1996. The interrelationships of fossil and Recent gonorynchid fishes with comments on two Cretaceous taxa from Israel, p. 299–318. *In*: Arratia G, Viohl G, eds. Mesozoic Fishes – Systematic and Paleonecology. Verlag Dr. Friedrich Pfeil, München.

Grande, T., AND F. J. Poyato-Ariza. 1999. Phylogenetic relationships of fossil and Recent gonorynchiform fishes (Teleostei : Ostariophysi). Zoological Journal of the Linnean Society, 125(2):197–238.

Grande, T., AND G. Arratia. 2010. Morphological analysis of the gonorynchiform postcranial

skeleton, p. 39–71. *In* T. Grande, F. J. Poyato-Ariza, and R. Diogo (eds.), Gonorynchiformes and Ostariophysan Relationships. Science Publishers, Enfield.

Greene, C. W., AND C. H. Greene. 1914. The skeletal musculature of the king salmon. Bulletin of the Bureau of Fisheries, 33(1913):21–59.

Greenwalt, D. E., Y. S. Goreva, S. M. Siljestroem, T. Rose, AND R. E. Harbach. 2013. Hemoglobin-derived porphyrins preserved in a middle Eocene blood-engorged mosquito. Proceedings of the National Academy of Sciences of the United States of America, 110(46):18496–18500.

Greenwalt, D. E., AND C. Labandeira. 2014. The amazing fossil insects of the Eocene Kishenehn Formation in northwestern Montana. , 88(5): . Rocks & Minerals, 88(5):434‑441.

Greenwalt, D. E., T. R. Rose, S. M. Siljestrom, Y. S. Goreva, K. N. Constenius, AND J. G. Wingerath. 2015. Taphonomic studies of the fossil insects of the Middle Eocene Kishenehn Formation. Acta Palaeontologica Polonica, 60(4):931–947.

Greenwalt, D. E., AND J. Rust. 2014. A new species of *Pseudotettigonia* Zeuner (Orthoptera: Tettigoniidae) with an intact stridulatory field and reexamination of the subfamily Pseudotettigoniinae. Systematic Entomology, 39(2):256–263.

Grünbaum, T., R. Cloutiet, AND P. Dumont. 2003. Congruence between chondrification and ossification sequences during caudal skeleton development: a Moxostomatini case study, p. 161–176. *In* H. I. Browman and A. B. Skiftesvik (eds.), Big Fish Bang.

Günther, A. C. L. G. 1868. Catalogue of the Physostomi, containing the families Heteropygii, Cyprinidae, Gonorhynchidae, Hyodontidae, Osteoglossidae, Clupeidae, Chirocentridae, Alepocephalidae, Notopteridae, Halosauridae in the collection of the British Museum.

Taylor & Francis, London, 7.

Harbach, R. E., AND D. Greenwalt. 2012. Two Eocene species of *Culiseta* (Diptera: Culicidae) from the Kishenehn Formation in Montana. Zootaxa, 3530:25–34.

Harrington, R. W. 1955. The osteocranium of the American cyprinid fish *Notropis bifrenatus* with an annotated synonymy of teleost skull bones. Copeia, 1955(4):267–290.

Harris, P. M., G. Hubbard, AND M. Sandel. 2014. Catostomidae: Suckers, p. 451–501. *In* J. Melvin L. Warren and B. M. Burr (eds.), Freshwater Fishes of North America: Petromyzontidae to Catostomidae.Volume 1. Johns Hopkins University Press, Baltimore.

Harris, P. M., AND R. L. Mayden. 2001. Phylogenetic relationships of major clades of Catostomidae (Teleostei: Cypriniformes) as inferred from mitochondrial SSU and LSU rDNA sequences. Molecular Phylogenetics and Evolution, 20(2):225–237.

Harris, P. M., R. L. Mayden, H. S. Espinosa Perez, AND F. Garcia De Leon. 2002. Phylogenetic relationships of Moxostoma and Scartomyzon (Catostomidae) based on mitochondrial cytochrome b sequence data. Journal of Fish Biology, 61(6):1433–1452.

He, S., X. Gu, R. L. Mayden, W.-J. Chen, K. W. Conway, AND Y. Chen. 2008. Phylogenetic position of the enigmatic genus *Psilorhynchus* (Ostariophysi : Cypriniformes): evidence from the mitochondrial genome. Molecular Phylogenetics and Evolution, 47(1):419–425.

Hernandez, L. P., N. C. Bird, AND K. L. Staab. 2007. Using zebrafish to investigate cypriniform evolutionary novelties: functional development and evolutionary diversification of the kinethmoid. Journal of Experimental Zoology Part B-Molecular and Developmental Evolution, 308B(5):625–641.

373

Hernandez, L. P., AND K. L. Staab. 2015. Bottom feeding and beyond: how the premaxillary protrusion of cypriniforms allowed for a novel kind of suction feeding. Integrative and Comparative Biology:1–11.

Hilton, E. J. 2002. Osteology of the extant North American fishes of the genus *Hiodon* Lesueur, 1818 (Teleostei: Osteoglossomorpha: Hiodontiformes). Fieldiana Zoology, 100:1–142.

Hilton, E. J., AND L. Grande. 2008. Fossil Mooneyes (Teleostei: Hiodontiformes, Hiodontidae) from the Eocene of western North America, with a reassessment of their taxonomy, p. 221–251. *In* L. Cavin, A. Longbottom, and M. Richter (eds.), Fishes and the Break-up of Pangaea.Volume 295. The Giological Society Publishing House, Bath.

Hoffmann, M., AND R. Britz. 2006. Ontogeny and homology of the neural complex of otophysan Ostariophysi. Zoological Journal of the Linnean Society, 147(3):301–330.

Hora, S. L. 1920. Revision of the Indian Homalopteridae and of the genus *Psilorhynchus* (Cyprinidae). Records of the Indian Museum, Calcutta, 19:195–215.

Hou, L. 1990. An Eocene bird from Songzi, Hubei province. Vertebrata PalAsiatica, 28(1):13.

Hubbs, C. L. 1930. Materials for a revision of the catostomid fishes of Eastern North America. Miscellaneous Publications of the Museum of Zoology University of Michigan, 20:47.

Hubbs, C. L., AND K. F. Lagler. 1947. Fishes of the Great Lakes region. Bulletin of the Cranbrook Institute of Science, 26:1–186.

Hubbs, C. L., K. F. Lagler, C. L. Hubbs, AND K. F. Lagler. 2004. Fishes of the Great Lakes region. Revised edition, 276 p.

Huber, J. T., AND D. Greenwalt. 2011. Compression fossil Mymaridae (Hymenoptera) from Kishenehn oil shales, with description of two new genera and review of Tertiary amber genera. Zookeys(130):4731–4494.

Hussakof, L. 1932. The fossil fishes collected by the Central Asiatic expedition. American Museum Novitates, 553:1–9.

Illick, H. J. 1956. A comparative study of the cephalic lateral-line system of North American Cyprinidae. American Midland Naturalist, 56(1):204–223.

Jacquemin, S. J., AND J. C. Doll. 2015. Macroecology of North American suckers (Catostomidae): tests of Bergmann's and Rapoport's rules. Ecology and Evolution:1–10.

Jalili, P., S. Eagderi, AND H. Mousavi-Sabet. 2015. Descriptive osteology of a spined loach, *Cobitis avicennae* from Iranian part of the Tigris basin. Iranian Journal of Ichthyology, 2(1):53–60.

Jenkins, R. E., AND N. M. Burkhead. 1994. The Freshwater Fishes of Virginia. American Fisheries Society, Bethesda.

Jenkins, R. O. 1970. Systematic studies of the catostomid fish tribe Moxostomatini. PhD, Cornell University, Ithaca, 1–799 p.

Johnson, G. D., AND C. Patterson. 1997. The gill-arches of gonorynchiform fishes. South African Journal of Science, 93:594–600.

Jordan, D. S. 1877. Contributions to North American ichthyology based primarily on the collections of the United States National Museum. No. 2: A. Notes on Cottidae, Cyprinidae, with revisions of the genera and descriptions of new or little known species. . Bulletin of the United States National Museum, 10:5-68.

Klingenberg, C. P. 2011. MorphoJ: an integrated software package for geometric morphometrics. Molecular Ecology Resources, 11:353–357.

Kottelat, M. 2004. *Botia kubotai*, a new species of loach (Teleostei : Cobitidae) from the Ataran River Basin (Myanmar), with comments on botiine nomenclature and diagnosis

of a new genus. Zootaxa(401):1–18.

Kottelat, M. 2012. Conspectus cobitidum: an inventory of the loaches of the world (Teleostei: Cypriniformes: Cobitoidei). Raffles Bulletin of Zoology, Supplement 26:1–199.

Kottelat, M., R. Britz, T. H. Hui, AND K. E. Witte. 2006. *Paedocypris*, a new genus of Southeast Asian cyprinid fish with a remarkable sexual dimorphism, comprises the world's smallest vertebrate. Proceedings of the Royal Society B-Biological Sciences, 273(1589):895–899.

Lacépède, B. G. É. D. 1803. Histoire naturelle des poissons. Plasson, Paris, 5, 803 p.

Lambe, L. M. On *Amyzon brevipinne*, Cope, from the *Amyzon* beds of the Southern Interior of British Columbia. Royal Society of Canda, Twenty-Fifth General Meeting, Section IV Geological And Biological Sciences, Ottawa, 12:151–157.

Lavoué, S., M. Miya, J. G. Inoue, K. Saitoh, N. B. Ishiguro, AND M. Nishida. 2005. Molecular systematics of the gonorynchiform fishes (Teleostei) based on whole mitogenome sequences: Implications for higher-level relationships within the Otocephala. Molecular Phylogenetics and Evolution, 37(1):165–177.

Lei, Y. 1977. Vertebrates, p. 133–136. *In* B. o. g. o. H. P. Hubei Institute of Geological Science (ed.), Atlas of Fossils from Central-Southern China. Geological Publishing House, Beijing

Lei, Y. 1987. Fish, p. 191–194. *In* M. R. Yichang Institute of Geology, Ministry of Geology, Mineral Resources (ed.), Biostratigraphy of the Yangtze Gorges Area (5): Cretaceaous and Tertiary. Geological Publishing House, Beijing

Lesueur, C. A. 1817. A new genus of fishes of the order Abdominales proposed under the name of *Catostomus* and the characters of this genus with those of its species indicated.

Journal of the Academy of Natural Sciences of Philadelphia, 1:88–102.

Li, G. Q., AND M. V. H. Wilson. 1994. An Eocene species of *Hiodon* from Montana, its phylogenetic relationships, and the evolution of the postcranial skeleton in the Hiodontidae (Teleostei). Journal of Vertebrate Paleontology, 14(2):153–167.

Liu, H.-T. 1957. A new fossil cyprinid fish from Maoming, Kwangtung. Vertebrata PalAsiatica, 1(2):151–153.

Liu, H.-Z., C.-S. Tzeng, AND H.-Y. Teng. 2004. Phylogenetic relationships of the cypriniforms tested by mtRNA 12S rRNA sequence variation. Acta Genetica Sinica, 31(2):137–142.

Liu, H. Z., C. S. Tzeng, AND H. Y. Teng. 2002. Sequence variations in the mitochondrial DNA control region and their implications for the phylogeny of the Cypriniformes. Canadian Journal of Zoology, 80(3):569–581.

Liu, J., AND M.-M. Chang. 2009. A new Eocene catostomid (Teleostei: Cypriniformes) from Northeastern China and early divergence of Catostomidae. Science in China Series D Earth Sciences, 52(2):189–202.

Liu, J., M.-M. Chang, AND M. V. H. Wilson. 2010. The fossil catostomid *Jianghanichthys* from China and implications for the evolution of basal catostomids (Cypriniformes, Actinopterygii). Journal of Vertebrate Paleontology, 30(Supplement 2, Society of Vertebrate Paleontology Seventieth Anniversary Meeting, David L. Lawrence Convention Center, East Lobby & Westin Convention Center Pittsburgh Pittsburgh, Pennsylvania USA October 10–13, 2010):123A.

Liu, J., M.-M. Chang, M. V. H. Wilson, AND A. M. Murray. 2015. A new family of Cypriniformes (Teleostei, Ostariophysi) based on a redescription of †*Jianghanichthys*

hubeiensis (Lei, 1977) from the Eocene Yangxi Formation of China. Journal of Vertebrate Paleontology, e1004073:1–23.

Liu, J., AND M. M. Chang. 2008. A New Catostomid from Northeastern China. Journal of Vertebrate Paleontology, 28(3):106A–107A.

Liu, J., M. V. H. Wilson, AND A. M. Murray. 2016. A new Catostomid fish (Ostariophysi, Cypriniformes) from the Eocene Kishenehn Formation and remarks on the North American species of †*Amyzon* Cope. Journal of Paleontology, FirstView:1–17.

Liu, T.-S., H.-T. Liu, AND X. Tang. 1962. A new Percoid fish from south China. Vertebrata PalAsiatica, 6(2):8.

Lo, Y.-L., AND H.-W. Wu. 1979. Anatomical features of *Myxocyprinus asiaticus* and its systematic position. Acta Zootaxonomica Sinica, 4(3):195–203.

Lucas, S. G., S. E. Foss, AND M. C. Mihlbachler. 2004. Achaenodon (Mammalia, Artiodactyla) from the Eocene Clarno Formation, Oregon, and the age of the Hancock Quarry local fauna, p. 89–96. *In* S. G. Lucas, K. E. Zeigler, and P. E. Kondrashov (eds.), Paleogene Mammals,.Volume New Mexico Museum of Natural History and Science Bulletin. Authority of the State of New Mexico, Albuquerque.

Lundberg, J. G., AND E. Marsh. 1976. Evolution and functional anatomy of the pectoral fin rays in cyprinoid fishes, with emphasis on the Suckers (Family Catostomidae). American Midland Naturalist, 96(2):332–349.

Maddison, W. P., AND D. R. Maddison. 2011. Mesquite: a modular system for evolutionary analysis.

Mao, F.-Y., Y.-Q. Wang, Q. Li, AND X. Jin. 2015. New records of archaic ungulates from the Lower Eocene of Sanshui Basin, Guangdong, China. Historical Biology:1–16.

Mayden, R. L., AND W.-J. Chen. 2010. The world's smallest vertebrate species of the genus *Paedocypris*: a new family of freshwater fishes and the sister group to the world's most diverse clade of freshwater fishes (Teleostei: Cypriniformes). Molecular Phylogenetics and Evolution, 57(1):152–175.

Mayden, R. L., W.-J. Chen, H. L. Bart, M. H. Doosey, A. M. Simons, K. L. Tang, R. M. Wood, M. K. Agnew, L. Yang, M. V. Hirt, M. D. Clements, K. Saitoh, T. Sado, M. Miya, AND M. Nishida. 2009. Reconstructing the phylogenetic relationships of the earth's most diverse clade of freshwater fishes--order Cypriniformes (Actinopterygii: Ostariophysi): A case study using multiple nuclear loci and the mitochondrial genome. Molecular Phylogenetics and Evolution, 51(3):500–514.

Melvin L. Warren, J., AND B. M. Burr. 2014. Frewater Fishes of North America: Petromyzontidae to Catostomidae. Johns Hopkins University Press, Baltimore, 644 p.

Meng, J., AND M. C. Mckenna. 1998. Faunal turnovers of Palaeogene mammals from the Mongolian Plateau. Nature, 394(6691):364–367.

Meng, Q., J. Su, AND X. Miao. 1995. Systematics of fishes. China Agriculture Press, Beijing, 1158 p.

Miller, R. J., AND H. E. Evans. 1965. External morphology of the brain and lips in catostomid fishes. Copeia, 1965(4):467–487.

Miller, R. R. 1959. Origin and affinities of the freshwater fish fauna of western North America, p. pp. 187–222. *In* C. L. Hubbs (ed.), Zoogeography. American Association for the Advancement of Science, Washington D.C.

Miller, R. R., AND G. R. Smith. 1967. New fossil fishes from Plio-Pleistocene Lake Idaho. Occasional Papers of University of Michigan Museum of Zoology, 654:1–24.

Miller, R. R., AND G. R. Smith. 1981. Distribution and evolution of *Chasmistes* (Pisces: Catostomidae) in western North America. Occasional Papers of University of Michigan Museum of Zoology, 696:1–46.

Mitchill, S. L. 1814. Report, in part of Samuel L. Mitchill, M.D., on the fishes of New York. D. Carlisle, New York, 28 p.

Moyle, P. B. 2002. Inland fishes of California. Revised and expanded edition, 1–502 p.

MüLler, J. 1845. Über den Bau und die Grenzen der Ganoiden, und über das natürliche System der Fische. Abhandlungen Akademie der Wissenschaften, Berlin 1845 (for 1844):117–216.

Nalbant, T. T. 2002. Sixty million years of evolution. Part one: Family Botiidae (Pisces: Ostariophysi: Cobitoidea). Travaux du Museum National d'Histoire Naturelle "Grigore Antipa", 44:309–333.

Nalbant, T. T., AND P. G. Bianco. 1998. The loaches of Iran and adjacent regions with description of six new species (Cobitoidea). Italian Journal of Zoology, 65(sup1):109–123.

Nelson, E. M. 1948. The comparative morphology of the Weberian apparatus of the Catostomidae and its significance in systematics. Journal of Morphology, 83:225–251.

Nelson, E. M. 1949. The opercular series of the Catostomidae. International Bibliography, Information, Documentation 85:559–567.

Nelson, E. M. 1961. The comparative morphology of the definitive swim bladder in the Catostomidae. American Midland Naturalist, 65(1):101–110.

Nelson, J. S. 2006. Fishes of the World. John. Wiley & Sons, Inc., New Jersey, 601 p.

Nelson, J. S., T. C. Grande, AND M. V. H. Wilson. 2016. Fishes of the World. John Wiley &

Sons, Hoboken, 707 p.

Nelson, J. S., AND M. J. Paetz. 1992. The Fishes of Alberta. The University of Alberta Press, Edmonton, 464 p.

Novacek, M. J. 1992. Fossils as critical data for phylogeny, p. 46–88. *In* M. J. Novacek   and Q. D. Wheeler (eds.), Extinction and Phylogeny Columbia University Press, New York.

Nursall, J. R. 1963. The hypurapophysis, an important element of the caudal skeleton. Copeia, 1963:458–459.

Patterson, C. 1984. *Chanoides*, a marine Eocene otophysan fish (Teleostei: Ostariophysi). Journal of Vertebrate Paleontology, 4(3):430–456.

Patterson, C., AND G. D. Johnson. 1995. The intermuscular bones and ligaments of teleostean fishes. Smithsonian Contributions to Zoology, 559:1–76.

Pierce, H. G., and K. N. Constenius. 2014. Terrestrial and aquatic mollusks of the Eocene Kishenehn Formation, Middle Fork Flathead River, Montana. Annals of Carnegie Museum 82:305–329.

Poulsen, J. Y., P. R. Møller, S. Lavoué, S. W. Knudsen, M. Nishida, AND M. Miya. 2009. Higher and lower-level relationships of the deep-sea fish order Alepocephaliformes (Teleostei: Otocephala) inferred from whole mitogenome sequences. Biological Journal of the Linnean Society, 98(4):923–936.

Rafinesque, C. S. 1818. Discoveries in natural history, made during a journey through the western region of the United States. American Monthly Magazine and Critical Review, 3(5):354–356.

Ramaswami, L. S. 1952. Skeleton of cyprinoid fishes in relation to phylogenetic studies. I. The systematic position of the genus *Gyrinocheilus* Vailliant. Proc. nat. Inst. Sci. India,

18:125–140.

Ramaswami, L. S. 1953. Skeleton of cyprinoid fishes in relation to phylogenetic studies. 5. The skull and the gasbladder capsule of the Cobitidae. Proceedings of the National Institute of Sciences of India, 19:323–347.

Ramaswami, L. S. 1957. Skeleton of cyprinoid fishes in relation to phylogenetic studies. 8. The skull and weberian ossicles of Catostomidae. Proceedings of the Zoological Society, Calcutta, Mookerjee Memorial:293–303.

Raney, E. C., AND E. A. Lachner. 1946. Age and growth of the rustyside Sucker, *Thoburnia rhothoeca* (Thoburn). American Midland Naturalist, 36(3):675–681.

Rohlf, F. J. 1998. On applications of geometric morphometrics to studies of ontogeny and phylogeny. Systematic Biology, 47(1):147–158.

Rohlf, F. J. 2010. tpsDig (computer program), Department of Ecology and Evolution, State University of New York, Stony Brook.

Rohlf, F. J. 2016. tpsUtil32 (computer program), Department of Ecology and Evolution, State University of New York, Stony Brook.

Ronquist, F., M. Teslenko, P. Van Der Mark, D. L. Ayres, A. Darling, S. Höhna, B. Larget, L. Liu, M. A. Suchard, AND J. P. Huelsenbeck. 2012. MrBayes 3.2: Efficient Bayesian Phylogenetic Inference and Model Choice Across a Large Model Space. Systematic Biology, 61(3):539–542.

Rupprecht, R. J., AND L. A. Jahn. 1980. Biological notes on blue suckers in the Mississippi River. Transactions of the American Fisheries Society, 109(3):323–326.

Russell, D. E., AND R.-J. Zhai. 1987. The Paleogene of Asia: Mammals and Stratigraphy. Museum National d'Histoire Naturelle, Paries, 488 p.

Russell, L. S. 1954. Mammalian fauna of the Kishenehn Formation, southeastern British Columbia. Bulletin of the National Museum of Canada, 132:92–111.

Sagemehl, M. 1885. Beiträge zur vergleichenden Anatomie der Fische.III. Das Cranium der Characiniden nebst allgemeinen Bemerkungen über die mit einen Weber'schen Apparat versehenen Physostomenfamilien. Morphologisches Jahrbuch, x:1–119.

Saitoh, K., T. Sado, M. H. Doosey, H. L. Bart Jr, J. G. Inoue, M. Nishida, R. L. Mayden, AND M. Miya. 2011. Evidence from mitochondrial genomics supports the lower Mesozoic of South Asia as the time and place of basal divergence of cypriniform fishes (Actinopterygii: Ostariophysi). Zoological Journal of the Linnean Society, 161(3):633–662.

Saitoh, K., T. Sado, R. L. Mayden, N. Hanzawa, K. Nakamura, M. Nishida, AND M. Miya. 2006. Mitogenomic evolution and interrelationships of the Cypriniformes (Actinopterygii : Ostariophysi): The first evidence toward resolution of higher-level relationships of the world's largest freshwater fish clade based on 59 whole mitogenome sequences. Journal of Molecular Evolution, 63(6):826–841.

Sanders, M. 1934. Die fossilen Fische der alttertiaren Susswasserablagerungen aus Mittel-Sumatra. Verhandelingen van het geologisch-mijnbouwkundig genoostschap voor Nedeland en kolonien. Geologische Serie, 11:1–44.

Sawada, Y. 1982. Phylogeny and zoogeography of the superfamily Cobitoidea (Cyprinoidei Cypriniformes). Memoirs of the Faculty of Fisheries Hokkaido University, 28(2):65–224.

Schultze, H.-P., AND G. Arratia. 2013. The caudal skeleton of basal teleosts, its conventions, and some of its major evolutionary novelties in a temporal dimension, p. 187–246. *In* G.

Arratia, H.-P. Schultze, and M. V. H. Wilson (eds.), Mesozoic Fishes 5 – Global Diversity and Evolution. Verlag Dr. Friedrich Pfeil, München.

Shen, W. 2000. Culture of American Bigmouse Buffalo fish. Fisheries Science & Technology Information, 27(2):186–187.

Shockley, F. W., AND D. Greenwalt. 2013. *Ptenidium kishenehnicum* (Coleoptera: Ptiliidae), a new fossil described from the Kishenehn oil shales, with a checklist of previously known fossil ptiliids. Proceedings of the Entomological Society of Washington, 115(2):173–181.

Siebert, D. J. 1987. Interrelationships among families of the order Cypriniformes (Teleostei), City University of New York, New York, 354 p.

Simon, T. P. 2006. Biodiversity of fishes in the Wabash River: Status, indicators, and threats. Proceedings of the Indiana Academy of Science, 115(2):136–148.

Simons, A., AND N. Gidmark. 2010. Systematics and phylogenetic relationships of Cypriniformes, p. 409–440, Gonorynchiformes and Ostariophysan Relationships. Science Publishers, Enfield.

Šlechtová, V., J. Bohlen, J. Freyhof, AND P. Rab. 2006. Molecular phylogeny of the Southeast Asian freshwater fish family Botiidae (Teleostei : Cobitoldea) and the origin of polyploidy in their evolution. Molecular Phylogenetics and Evolution, 39(2):529–541.

Šlechtová, V., J. Bohlen, AND H. H. Tan. 2007. Families of Cobitoidea (Teleostei; Cypriniformes) as revealed from nuclear genetic data and the position of the mysterious genera *Barbucca, Psilorhynchus, Serpenticobitis* and *Vaillantella*. Molecular Phylogenetics and Evolution, 44(3):1358–1365.

Smith, G. R. 1966. Distribution and evolution of the North American catostomid fishes of the

subgenus *Pantosteus*. genus *Catostomus*. Miscellaneous publications / University of Michigan, Museum of Zoology, 129:1–133.

Smith, G. R. 1975. Fishes of the Pliocene Glenns Ferry Formation, Southwest Idaho; Fishes of the Miocene–Pliocene Deer Butte Formation, Southeast Oregon Claude W. Hibbard Memorial Volume V, p. 1–34. Museum of Paleontology, The University of Michigan, Michigan.

Smith, G. R. 1981. Late Cenozoic freshwater fishes of North America. Annual Review of Ecology and Systematics, 1981(12):163–193.

Smith, G. R. 1985. Paleontology of Hidden cave: fish, p. 171–178. *In* D. H. Thomas (ed.), The archaeology of Hidden Cave, Nevada. Volume 61 part 1, New York.

Smith, G. R. 1992. Phylogeny and biogeography of the Catostomidae, freshwater fishes of North America and Asia, p. 778–826. *In* R. L. Mayden (ed.), Systematics, Historical Ecology, and North American Freshwater Fishes. Stanford University Press, Stanford.

Smith, G. R., AND R. K. Koehn. 1971. Phenetic and cladistic studies of biochemical and morphological characteristics of *Catostomus*. Systematic Zoology, 20(3):282–297.

Smith, G. R., N. Morgan, AND E. Gustafson. 2000. Fishes of the Mio-Pliocene Ringold Formation, Washington: Pliocene capture of the Snake River by the Columbia River. Museum of Paleontology, The University of Michigan, Michigan, 32, 1–47 p.

Smith, G. R., W. L. Stokes, AND K. F. Horn. 1968. Some Late Pleistocene Fishes of Lake Bonneville. Copeia, 1968(4):807–816.

Staab, K. L., L. A. Ferry, AND L. P. Hernandez. 2012a. Comparative kinematics of cypriniform premaxillary protrusion. Zoology, 115(2):65–77.

Staab, K. L., AND L. P. Hernandez. 2010. Development of the cypriniform protrusible jaw

complex in *Danio rerio*: constructional insights for evolution. Journal of Morphology, 271(7):814–825.

Staab, K. L., R. Holzman, L. P. Hernandez, AND P. C. Wainwright. 2012b. Independently evolved upper jaw protrusion mechanisms show convergent hydrodynamic function in teleost fishes. Journal of Experimental Biology, 215(9):1456–1463.

Su, D.-Z. 2011. A new cyprinid fish from Paleogene of northern Xinjiang, China. Vertebrata PalAsiatica, 49(2):141–154.

Sun, Y.-H., W. Wang, S.-Y. Liu, S.-P. He, X.-L. Shao, Z.-X. Xie, F.-J. Deng, Y. Liu, J.-G. Tong, AND Q.-J. Wu. 2002. Genetic diversity analysis of mitochondrial D-loop region of Chinese sucker (*Myxocyprinus asiaticus*). Acta Genetica Sinica, 29(9):787–790.

Sun, Y. H., C. X. Xie, W. M. Wang, S. Y. Liu, T. Treer, AND M. M. Chang. 2007. The genetic variation and biogeography of catostomid fishes based on mitochondrial and nucleic DNA sequences. Journal of Fish Biology, 70:291–309.

Swofford, D. L. 2002. PAUP* phylogenetic analysis using parsimony and other methods. Version 4, Sinauer Assoc., Sunderland, Massachusetts.

Swofford, D. L. 2003. PAUP*. Phylogenetic Analysis Using Parsimony (*and Other Methods). Sinauer Associates, Sunderland, Massachusetts.

Sytchevskaya, E. K. 1986. Palaeogene freshwater fish fauna of the USSR and Mongolia. Hayka Publishing House, Moscow, Transactions, vol. 29, 1–154 p.

Takeuchi, H., K. Tokuda, N. Kanagawa, AND K. Hosoya. 2011. Cephalic lateral line canal system of the golden venus chub, Hemigrammocypris rasborella (Teleostei: Cypriniformes). Ichthyological Research, 58:175–179.

Tang, Q. Y., H. Z. Liu, R. Mayden, AND B. X. Xiong. 2006. Comparison of evolutionary rates

in the mitochondrial DNA cytochrome b gene and control region and their implications for phylogeny of the Cobitoidea (Teleostei : Cypriniformes). Molecular Phylogenetics and Evolution, 39(2):347–357.

Tang, T., Y. Xue, Y. Zhou, W. Yang, AND Q. Zang. 1980. The characteristics of carbonate rocks and their sedimentary environment of the Lower Tertiary Buxin Group in Sanshui Basin, Guandong. Acta Geologica Sinica, 54(4):249–258.

Tang, X. 1959. A new cyprnid species from Linli, Hunan. Paleovertebrata Et Paleoanthropologia, 1(4):4.

Tang, X., AND B. Liang. 1965. The "Red Bed" at Bushin of Sanshui District, in Kwangtung Province. Acta Geologica Sinica, 45(4):358–370.

Tseng, Z. J., AND X. Wang. 2011. Do convergent ecomorphs evolve through convergent morphological pathways? Cranial shape evolution in fossil hyaenids and borophagine canids (Carnivora, Mammalia). Paleobiology, 37(3):470–489.

Unmack, P. J., T. E. Dowling, N. J. Laitinen, C. L. Secor, R. L. Mayden, D. K. Shiozawa, AND G. R. Smith. 2014. Influence of introgression and geological processes on phylogenetic relationships of western North American Mountain Suckers (*Pantosteus*, Catostomidae). Plos One, 9(3):e90061.

Valenciennes, A. 1844. Suite du livre dix-huitième. Cyprinoïdes. P. Bertrand, Paris, Tome dix-septième, 497 p.

Wang, B., AND W. Zhang. 1997. Mammalian fossils from Sanshui Basin, Guangdong, China. Vertebrata PalAsiatica, 35(1):44–48.

Wang, J., G. Li, AND J. Wang. 1981. The early Tertiary fossil fishes from Sanshui and its adjacent basin, Guangdong., 22, 90 p.

Wang, M., G. Mayr, J. Zhang, AND Z. Zhou. 2012. New bird remains from the Middle Eocene of Guangdong, China. Acta Palaeontologica Polonica, 57(3):519–526.

Wang, Y., Y. Tong, AND Q. Li. 2011. Chinese Continental Paleocene-Eocene Boundary and Its Correlation. Acta Geologica Sinica-English Edition, 85(2):443–451.

Weisel, G. F. 1960. The osteocranium of the catostomid fish, *Catostomus macrocheilus*. A study in adaptation and natural relationship. Journal of Morphology, 106((1)):109–129.

Weisel, G. F. 1967. The pharyngeal teeth of larval and juvenile suckers (*Catostomus*). Copeia, 1967(1):50–54.

Weitzman, S. H. 1962. The osteology of Brycon meeki, a generalized characid fish, with an osteological definition of the family. Stanford Ichthyological Bulletin, 8:1–77.

Welcomme, R. L. 1988. International introductions of inland aquatic species. FAO Fisheries Technical Paper, 294:1‑318.

Whipple, J. W. 1992. Geologic map of Glacier National Park, Montana, Miscellaneous Investigations Series Map U.S. Geological Survey.

Wiens, J. J. 1998. Does adding characters with missing data increase or decrease phylogenetic accuracy? Systematic Biology, 47(4):625–640.

Wiens, J. J., AND M. C. Morrill. 2011. Missing data in phylogenetic analysis: reconciling results from simulations and empirical data. Systematic Biology, 60(5):719–731.

Wiens, J. J., AND T. W. Reeder. 1995. Combining data sets with different numbers of taxa for phylogenetic analysis. Systematic Biology, 44(4):548–558.

Willink, P. W. 2002. Function and variation of gill rakers in the fish family Catostomidae, with comments on phylogenetic tests of natural selection, University of Michigan, Ann Arbor, 318 p.

Wilson, M. V. H. 1974. Fossil fishes of the Tertiary of British Columbia, University of Toronto, Tronto, 680 p.

Wilson, M. V. H. 1977a. Middle Eocene freshwater fishes from British Columbia. Life Science Contribution Royal Ontario Museum, 113:1–61.

Wilson, M. V. H. 1977b. Paleoecology of Eocene lacustrine varves at Horsefly, British Columbia. Canadian Journal of Earth Sciences, 14(5):953–962.

Wilson, M. V. H. 1980a. Eocene lake environments: Depth and distance-from-shore variation in fish, insect, and plant assemblages. Palaeogeography, Palaeoclimatology, Palaeoecology, 32:21–44.

Wilson, M. V. H. 1980b. Oldest Known Esox (Pisces, Esocidae), Part of a New Paleocene Teleost Fauna from Western Canada. Canadian Journal of Earth Sciences, 17(3):307–312.

Wilson, M. V. H. 1980c. Oldest known *Esox* (Pisces: Esocidae), part of a new Paleocene Teleost fauna from Western Canada. Canadian Journal of Earth Sciences, 17:307–312.

Wilson, M. V. H. 1984. Year classes and sexual dimorphism in the Eocene catostomid fish *Amyzon aggregatum*. Journal of Vertebrate Paleontology, 3(3):137–142.

Wilson, M. V. H. 1996. The Eocene fishes of Republic, Washington. Washington Geology, 24(2):30–31.

Woodburne, M. O., G. F. Gunnell, AND R. K. Stucky. 2009. Climate directly influences Eocene mammal faunal dynamics in North America. Proceedings of the National Academy of Sciences, 106(32):13399–13403.

Wu, G., Y. Liu, Z. Wang, AND D. Yang. 1990. The age and growth of *Myxocyprinus asiaticus* at Yichang region of Changjiang River below Gezhou Dam. Freshwater Fisheries:3–8.

Wu, H.-W., Y. Y. Chen, X. G. Chen, AND J. X. Chen. 1981. A taxonomical system and phylogenetic relationship of the families of the suborder Cyprinoidei (Pisces). Scientia Sinica, 24(4):563–572.

Wu, H.-W., Y.-L. Lo, AND J.-T. Lin. 1979. Phylogenetic relationship and systematic position of *Gyrinocheilus* (Gyrinocheilidae, Pisces). Acta Zootaxonomica Sinica, 4(4):307–311.

Young, C.-C. 1944. Note on the first Eocene mammal from south China. American Museum Novitates, 1944(1268):1–2.

Yue, P., AND Editoral-Committee. 2000. Cypriniformes III. Sciences Press, Beijing, 661 p.

Zachos, J., M. Pagani, L. Sloan, E. Thomas, AND K. Billups. 2001. Trends, rhythms, and aberrations in global climate 65 Ma to present. Science, 292(5517):686–693.

Zachos, J. C., G. R. Dickens, AND R. E. Zeebe. 2008. An Early Cenozoic Perspective on Greenhouse Warming and Carbon-cycle Dynamics. Nature, 451(7176):279–283.

Zelditch, M. L., D. L. Swiderski, H. D. Sheets, AND W. L. Fink. 2004. Geometric Morphometrics for Biologists: A Primer. Elsevier Academic Press, New York and London, 437 p.

Zeng, Y., AND H.-Z. Liu. 2009. Morphological variation of pharyngeal bones and teeth in the subfamily Gobioninae (Cypriniformes: Cyprinidae) and its functional adaptations. Zoological Research, 30(6):699–706.

Zhang, J.-Y. 2003. First *Phareodus* (Osteoglossomorpha: Osteoglossidae) from China Vertebrata PalAsiatica, 41(4):5.

Zhang, X.-Q., G. Li, R.-L. Yang, AND H.-M. Li. 2008. Palaeogene ostracods from the Sanshui Basin of Guangdong. Acta Micropalaeontologica Sinica, 25(3):235–265.

Zhao, T., G. Mayr, M. Wang, AND W. Wang. 2015. A trogon-like arboreal bird from the early

Eocene of China. Alcheringa, 39(2):287–294.

Zhou, H., L. Xiao, Y. Dong, C. Wang, F. Wang, AND P. Ni. 2009. Geochemical and geochronological study of the Sanshui basin bimodal volcanic rock suite, China: Implications for basin dynamics in southeastern China. Journal of Asian Earth Sciences, 34(2):178–189.

Zhou, J. 1990. The Cyprinidae fossils from Middle Miocene of Shanwang Basin Vertebrata PalAsiatica, 28(2):95–127.

Zhou, L. 1995. Cuture and breeding of Rouge Fish. Freshwater Fisheries, 25(1):31‑32.

General Appendix I. Institutional abbreviations

AMNH, American Museum of Natural History, New York, USA;

CMN, Canadian Museum of Nature, Ottawa, Canada;

FMNH, Field Museum of Natural History, Chicago, USA;

GMC, The Geological Museum of China, Beijing, China;

IHEP, Institute of High Energy Physics, Chinese Academy of Sciences, Beijing, China;

IVPP, Institute of Vertebrate Paleontology and Paleoanthropology, Chinese Academy of Sciences, Beijing, China;

KU, University of Kansas, Kansas, USA;

LUC, Loyola University Chicago, Chicago, USA;

NHM, Natural History Museum, London, UK;

ROM, Royal Ontario Museum, Ontario, Canada;

UA, University of Alberta, Canada;

UALVP, University of Alberta Laboratory for Vertebrate Paleontology, Alberta, Canada;

UAMZ, University of Alberta Museum of Zoology, Alberta, Canada.

USNM, National Museum of Natural History, Washington D.C., USA.

General Appendix II. Specimen list for morphology study and comparison:

Fossils:

Catostomidae:

Amyzon aggregatum **Wilson, 1977**

UALVP collection: UALVP 12185, 12186, 12189, 12197–12203, 12205, 12206, 12208, 12212, 12213, 12216, 12218, 12223–12238, 12240–12247, 12249, 12251–12278, 12280–12284, 12289, 12290, 12292–12306, 12310, 13209, 13214, 13218, 13224, 13226, 13228, 13242, 13243, 13245, 13247, 13252, 13253, 13258, 13263, 13264, 13450, 13451, 14721–14725, 14740, 15820–15840, 15842–15884, 15886–15888, 15892, 15894, 15898–15904, 15916, 15918–15920, 7394, 17450–17486, 17489, 17742–17744, 19540, 22871–22875, 22877, 22893–22914, 22921–22924, 22926–22936, 23443–23478, 24209–24225, 27125–27128, 31086–31135, 31137–31158, 31160, 31161, 31165, 31166, 31169–31174, 31543, 32032, 32033, 32035, 32930–32934, 33013–33016, 33036–33055, 33060, 33064, 33072–33074, 33076–33081, 33085, 33087–33091, 33094, 33096–33099, 33101, 33102, 33107, 33111, 33113–33118, 33121–33124, 33127, 33129, 33135, 33141, 33157, 33198, 33199, 33204, 33205, 33207–33210, 33272, 33283, 33285, 33289, 33291–33294, 33296–33315, 33392, 33394–33401, 40761–40788, 40790–40795, 40797–40847, 40851–40888, 40890–40950, 40957–40979, 40981–41009, 41012, 41013, 41015–41150, 41164, 41166–41169, 41171–41176, 41178–41191, 41193–41211, 41219, 41220, 45156 (in total 956 specimens).

ROM collection: holotype ROM 11019; topotypes ROM 11001–11025, 11027–11038, 11040–11061, and 11063–11098; ROM 11006, 11108, 11110, 11125, 11126, 11129, 11131, 11139, 11142, 11143, 11145, 11146, 11201–11226, 11228, 11229, 11231–11236, 11238,

11239, 11241, 11242, 11244, 11247–11249, 11251, 11252, 11254–11257, 11259–11264, 11266, 11269, 11270, 11272–11282, 11284–11288, 11291–11296, 11299, 11302–11304, 11307, 11308, 11310, 11312, 11313, 11314–11318, 11320–11322, 11325, 11327, 11329, 11332–11342, 11348, 11351–11360, 11362, 11363, 11365, and 55314 (selected specimens for photographing or meristic and morphometric).

FMNH collection: FMNH PF 12343, 12344, 12999, 123000, 13451, 13562–12365, 14319, 14325–14328.

CMN collection: pleisotype CMNFV 6190; CMNFV 6191, 125904, 34496–34502, 34505, 34851, 34853–34863, 34865–34871, 34880–34882. This list includes the referred materials in Wilson (1977) NMC 6191 A–D , 9891 A–L, 9891 L and 9891 S, which were re-catalogued with the number of CMN.

"NewGenus" *brevipinne* **(Cope), 1895**

CMN collection: holotype CMNFV 6189, CMNFV 2042, 2046, 2050, 2054, 2055, 2057, 2066, 2068, 2069, 2071–2074, 2090, 2092, 2097, 2099, 2104, 34480–34492, 34509, 34820, 34821, 348883, 34885, 34888, 34891, 34893–34899, 41745, and 41746 (selected specimens for photographing or meristic and morphometric). Specimens listed under NMC 3132 in Wilson (1977) is re-catalogued within   CMNFV 34480–34899.

UALVP collection: UALVP 12104, 12133, 12159, 12462–12464, 12480, 12481, 12483, 12487, 12496, 12509, 12512, 12514–12517, 12519–12521, 12525–12529, 12532–12534, 12537–12539, 12541, 12542, 12545–12547, 12549, 12553–12556, 12558, 12561, 12563–12566, 12568–12570, 12572–12577, 12580, 12583, 12584, 12586–12589, 12591, 12593,

12595, 12597–12599, 12601, 12602, 12605, 12606, 2610–12613, 12616, 12617, 12619, 12621–112626, 126311–12636,12638, 12639, 12641–12645, 12647, 12651–12654, 12658, 12661–12680, 12682–12684, 12686–12689, 12691–12698, 12700–12708, 12710, 12711, 12714–12716, 12719–12729, 12731, 12733–12736, 12743–12746, 12750, 12754, 12757, 12762, 12763, 12767, 12768, 12770–12772, 12775, 12777–12779, 12783–12785, 12787–12790, 12794–12798, 12800–12804, 12806, 12807, 12810, 12812, 12813, 12819, 12820, 12825–12828, 12830, 12831, 12835, 1283712843, 12845–12847, 12850, 12854–12858, 12850–12864, 12866, 12867, 12869, 12878, 12879, 12884, 12888, 12889, 12893–12904, 12906, 12907, 12910, 12912–12921, 12923, 12957, 12969, 12978, 12981, 12987, 12989, 12991, 12992, 13006, 13008, 13012, 13019, 13021, 13037, 13054, 13071, 13072, 13078, 13085, 13089, 13097, 13114–13126, 13129, 13131–13135, 13137–13144, 13146, 13147, 13149, 13150, 13152–13174, 13177, 13182, 13184, 13187, 13435, 14730, 14731, 14735, 14737, 14738, 14745–14748, 14754, 14755, 14759, 14760, 15912–15915, 17836, 21262–21339, and 27140.

ROM collection: ROM 11160–11164, 11166, 11167, 11169–11171, 11179, 11182, 11370, 11377, 11379, 11382, 11387, 11389, 11461, 11468, and 19420 (selected specimens for photographing or meristic and morphometric).

Amyzon commune Cope, 1875

FMNH PF 116, 117;

UALVP 14253 and 14254.

AMNH FF 2579, 2925–2927, 2937–2950, 8068, 8069, and 8437.

Amyzon gosiutense (Grande et al), 1981

FMNH collection: paratype FMNH PF 10425–10428 (previous UMVP 6500–6504), FMNH PF 10429–10431 (previous UMVP 6505–6507), 10552–10559, 10561–10563, 10565–10568, 10570–10575, 10577–10581, and 9895.

UALVP collection: UALVP14723, 71425.

AMNH collection: paratype AMNH FF 10460; AMNH FF 10401, 10402, 19094, 10904, and 10905.

Amyzon hunanense (Cheng), 1962

IVPP V 1102, a nearly complete fish lacking caudal fin, the holotype of the species described by Cheng (1962); IVPP V 12571.1–6, complete fishes; IVPP V 17906.1–53, complete fish preserved on slab and disarticulated bones.

Amyzon kishenehnicum Liu et al., 2016

holotype UALVP 55260; paratype UALVP 24137, 24140, 24147, 24148, 24149, 24152, and 24154; UALVP 23943, 24131–24134, 24138, 24139, 24141–24146, 24150, 24151, 24153, 24155–24199, 24226, 38728–38788, 38792–38807, 38876, 38877, 38881–38920, 38922–38958, 38962–39039, 52373 (in total 303 specimens).

Amyzon mentale Cope, 1872

UALVP13407, latex peel of the original specimen that Cope described.

Plesiomyxocyprinus arratiae **Liu et Chang, 2009**

The holotype IVPP V 12572.1 (nearly complete fish),   and disarticulated bones IVPP V 12572.2–72 and IVPP V 15711.1–39.

Catostomdae indet. from Eocene Ulan Shireh Fm., Inner Mongolia, China, described by Hussakof (1932)

AMNH 8442, and 10344.

Catostomidae indet. from Urdyn Obo Fm. Close to the boundary between China and Mongolia, 150km northwest of Shalamulun, Inner Mongolia, China.

AMNH FF 6278.

Jianghanichthyidae:

Jianghanichthys hubeiensis **(Lei), 1977**:

GMC collection: lectotype GMC V1810-1; paralectotype GMC V1810-2;

IVPP collection: IVPP V 12163.1− 65, IVPP V 15712.1−3, and IVPP V 18858.1 − 2;

FMNH collection: FMNH PF 14317 and 14318.

ROM collection: ROM 47696.

All the above fossil specimens are preserved with the bone in place and articulated.

Extant fish:

Specimens that are Clearing and staining specimens labeled with 'C&S' in following

brackets; Ethanol preserved specimens are labeled with "Et" in brackets; without denotation, the specimens are dry skeletons.

(I) Cypriniformes:

i) Catostomidae:

Carpiodes carpio: KU 12732, AMNH I-21808;

Carpiodes cyprinus: UAMZ 4431 (C&S), CMNFI 77-0183, AMNH I-90212;

Carpiodes sp.: AMNH I-21694;

Catostomus bernardini: AMNH I-77910;

Catostomus cahita: AMNH I-51303 (paratopotype);

Catostomus catostomus: AMNH I-41156 (C&S), I-47712, I-47724;

Catostomus commersoni: UAMZ F3835.6 (C&S), UAMZ F8422, UAMZ F7341, AMNH I-55944, I-55897;

Catostomus discobolus: KU 11902;

Catostomus fumeiventris: AMNH I-47015;

Catostomus latipinnis: AMNH I-47080;

Catostomus leopoldi: AMNH I-50708 (paratopotype):

Catostomus macrocheilus: IVPP OP 327, KU 11867, AMNH I-47148;

Catostomus occidentalis: AMNH I-46002;

Catostomus platyrhynchus: IVPP OP 328, AMNH I-46185, I-46186;

Catostomus (Pantosteus) plebeius: AMNH I-56172;

Catostomus rimiculus: AMNH I-47731;

Catostomus santaanae: AMNH I-47027, I-47028;

Catostomus snyderi: AMNH I-47775;

Catostomus tahoensis: AMNH I-47050;

Catostomus wigginsi: AMNH I-77911;

Chasmistes brevirostris: AMNH I- 47030;

Chasmistes liorus: IVPP OP 329, KU 12456.

Cycleptus elongatus: IVPP OP 330, AMNH I-94810, AMNH I-77906;

Deltistes luxatus: IVPP OP 333, KU 12424, AMNH I-46205;

Erimyzon oblongus: AMNH I-88732;

Hypentelium nigricans, ROM R 5871; AMNH I-55993;

Ictiobus bubalus: IVPP OP 331, AMNH I-88699, 216489;

Ictiobus cyprinellus: KU 15337, AMNH I-56459;

Ictiobus meridionalis: AMNH I-28077;

Ictiobus niger: KU 13047;

Minytrema melanops: ROM R6701;

Moxostoma aureolum: AMNH I-35463;

Moxostoma carinatum: AMNH I-94813;

*Moxostoma erythrurum***:** AMNH I-49309;

Moxostoma macrolepidotum: IVPP OP 332, UAMZ 6731 (C&S), ROM R7377, KU12718;

Moxostoma poecilurum: AMNH I-94811;

Myxocyprinus asiaticus: IHB 79iv001–79iv003, IVPP OP 320; IVPP OP 321 and 322 (Et), IVPP OP 323 and 324 (C&S), AMNH I-22437.

Xyrauchen texanus: AMNH I-30848;

ii) Cobitidae:

Chromobotia macracanthus: UAMZ F8748;

Cobitis taenia: AMNH I-10412 (C&S).

iii) Cyprinidae:

Barbus sp.: AMNH I-21657;

Carassius auratus: AMNH I-21689;

Cyprinus carpio: UAMZ F8464, AMNH 10147, AMNH I 49088 (C&S);

Hypophthalmichthys nobilis: UAMZ F8749;

Osteochilus sp., AMNH I-94472, AMNH I-94473.

iv) Gyrinocheilidae:

Gyrinocheilus aymonieri: UAMZ 5109, AMNH I-77898 (C&S).

(II) Gonorynchiformes:

Chanidae:

Chanos chanos: UAMZ F3523 (C&S), UAMZ F8463, AMNH I-30837, AMNH-I 89719 through 89724, AMNH I-95424, AMNH I-95415, AMNH I-95573.

(III) Characiformes:

Citharinidae:

Citharinus congicus: CMNFI 81-0190 (C&S);

Distichodus lusosso: ROM R6940.